UNIVERSITÄT ZU LÜBECK

From the
Research Center Borstel – Leibniz Lung Center
Priority Research Area Infections
Division of Cellular Microbiology

Hematopoietic Stem Cells as a Niche for *Mycobacterium tuberculosis*: Mechanisms of Internalization and Permissiveness

Dissertation for
Fulfilment of Requirements
for the Doctoral Degree of the
University of Lübeck

from the Department of Natural Sciences

Submitted by
Pit Engling
from Stuttgart

Lübeck 2025

First referee: Prof. Dr. rer. nat. Ulrich E. Schaible

Second referee: Prof. Dr. rer. nat. Christian Karsten

Rapporteur: Prof. Dr. rer. nat. Stefan Taube

Date of oral examination: 28.07.2025

Approved for printing: Lübeck, 30.07.2025

Für Doreen

Abstract

Hematopoietic stem cells are the multipotent progenitors of all immune cells. They play an indispensable role in maintaining immune competence through their differentiation into mature lymphoid and myeloid effector cells, which mediate host protection against infections. The manipulation of the hematopoietic system by infectious agents can, therefore, disrupt protective immune function, facilitating pathogen persistence and exacerbating disease. *Mycobacterium* (*M.*) *tuberculosis*, the etiological agent of tuberculosis, is a paradigm of pathogen persistence. Currently infecting an estimated quarter of the global population, it continues to prevail as the predominant bacterial pathogen on a global scale, underscoring the incapacity of the human immune system to eradicate *M. tuberculosis* infections. Given that pathogen persistence necessitates a compromised immune resistance, the recent discovery of mycobacterial DNA within hematopoietic stem cells, suggested a potential but yet undefined strategy by which *M. tuberculosis* may directly target the source of immune cell generation to persist in the host.

However, hematopoietic stem cells are canonically considered non-phagocytic and resistant to bacterial infections, raising critical questions about how *M. tuberculosis* infects these cells. Our study aimed to elucidate the mechanisms of *M. tuberculosis* infection in hematopoietic stem cells and identify the factors that render these typically resistant cells permissive to infection. Through this investigation, we seek to provide novel insights into the pathogenesis of tuberculosis and strategies of mycobacterial persistence.

To investigate these aspects, we developed an in vitro model to study hematopoietic stem cell infection of both, murine and human origin. The intracellular localization of *M. tuberculosis* within immunophenotypically defined hematopoietic stem cell populations was demonstrated using confocal microscopy. We observed membrane ruffling directed toward surface attached mycobacteria, focal actin polymerisation at sites of mycobacterial attachment and also enwrapping intracellular mycobacteria. Additionally, we demonstrated that actin-polymerisation inhibitors prevent bacterial uptake, proving that *M. tuberculosis* internalization into hematopoietic stem cells is as an active, actin-dependent process. Using distinct inhibitors, we ruled out classical macropinocytosis, as well as opsonic and non-opsonic phagocytosis, as potential uptake pathways. Instead, our data indicate that *M. tuberculosis* internalization involves CD36 binding, a class B scavenger receptor, and clathrin-dependent interactions. Consistent with our observations, CD36 ligation induces

membrane ruffling morphologically reminiscent, yet molecularly distinct, from canonical macropinocytosis pathways. Thus, we propose that *M. tuberculosis* binds the cell surface receptor CD36, which leads to macropinocytosis-like mechanisms, facilitating internalization by the host cell.

We further explored how hematopoietic stem cells become permissive to *M. tuberculosis*. The slow kinetics of mycobacterial uptake in hematopoietic stem cells compared to professional phagocytes and our observation that hematopoietic stem cells of neonatal origin are non-permissive to *M. tuberculosis* indicated that hematopoietic stem cell permissiveness is not an innate inherent trait but develops in response to yet undefined signals. Exposure to *M. tuberculosis*-derived pathogen-associated molecular patterns had only marginal effects on hematopoietic stem cell permissiveness. Instead, our findings suggest that the development of permissiveness requires viable, metabolically active bacteria. Preliminary evidence supports the notion that this process may be cytokine-mediated, although further investigation is required to elucidate the precise signalling pathways involved.

In conclusion, a comprehensive understanding of the mechanisms underlying *M. tuberculosis* infection in hematopoietic stem cells promises insights into the complex pathogenesis of tuberculosis. While the repertoire of described non-canonical host cells harboring mycobacteria has expanded in recent years, little is known about the specific roles these non-phagocytic cells play in immune modulation, immune evasion, and pathogen persistence. Identifying the pathways of *M. tuberculosis* internalization and delineating the signals that drive hematopoietic stem cell permissiveness may uncover novel targets for host-directed therapies aimed at restoring the host's natural immunity.

Zusammenfassung

Hämatopoetische Stammzellen sind die Quelle aller Immunzellen und essenziell für die Aufrechterhaltung der immunologischen Homöostase. Durch ihre Differenzierung in reife lymphoide und myeloide Effektorzellen schützen sie den Organismus vor Infektionen. Eine Manipulation des hämatopoetischen Systems kann folglich diesen Schutz beeinträchtigen und zur Persistenz von Krankheitserregern sowie zur Verschlechterung des Krankheitsverlaufs führen. Die Tuberkulose, hervorgerufen durch *Mycobacterium* (*M.*) *tuberculosis*, ist ein Paradebeispiel für die Persistenz eines Pathogens und stellt die weltweit häufigste Todesursache aller bakteriellen Infektionen dar. Derzeit ist schätzungsweise ein Viertel der Weltbevölkerung mit *M. tuberculosis* infiziert, was die Unzulänglichkeit des menschlichen Immunsystems bei der Bekämpfung dieser Infektion verdeutlicht. Bekanntermaßen setzt die Persistenz von Krankheitserregern eine beeinträchtigte Immunkompetenz voraus. So stellt die jüngst nachgewiesene Präsenz mykobakterieller DNS in hämatopoetischen Stammzellen eine potenzielle, aber noch unzureichend definierte Persistenzstrategie dar, bei der *M. tuberculosis* die Quelle aller Immunzellen infiziert und sie so manipulieren könnte.

Traditionell sind hämatopoetische Stammzellen resistent gegenüber bakteriellen Infektionen und gelten als nicht-phagozytisch, der normale Aufnahmemechanismus für Mykobakterien. Dies wirft die Frage auf, wie *M. tuberculosis* hämatopoetische Stammzellen infizieren kann. Ziel unserer Studie war es daher, die Mechanismen der Internalisierung von *M. tuberculosis* in hämatopoetische Stammzellen aufzuklären und jene Faktoren zu identifizieren, die diese sonst nicht permissiven Zellen anfällig für eine Infektion machen. Unsere Untersuchungen zielen daher darauf ab, neue Erkenntnisse über die Pathogenese der Tuberkulose und die Strategien mykobakterieller Persistenz zu gewinnen.

Um diese Aspekte zu untersuchen, etablierten wir ein murines und humanes in vitro Modell zur Analyse der Infektion hämatopoetischer Stammzellen. Die intrazelluläre Lokalisation von *M. tuberculosis* in immunphänotypisch definierten hämatopoetischen Stammzellpopulationen wurde mittels konfokaler Mikroskopie nachgewiesen. Mikroskopische Analysen offenbarten Membranausstülpungen, die in Richtung der mit der Zelloberfläche in Kontakt stehenden Bakterien ausgebildet wurden. In diesen Regionen konnte eine fokale Polymerisation von F-Aktin nachgewiesen werden, die ebenfalls um intrazelluläre, also internalisierte, Mykobakterien beobachtet wurde. Des Weiteren zeigten wir, dass die Internalisierung der Bakterien durch Inhibitoren der Aktinpolymerisation

blockiert wird, was zeigt, dass es sich um einen aktiven, Aktin-abhängigen Aufnahmeprozess handelt. Durch den Einsatz verschiedener Inhibitoren konnten wir klassische Makropinozytose sowie Phagozytose als potenzielle Aufnahmemechanismen ausschließen. Unsere Daten deuten stattdessen darauf hin, dass die Internalisierung durch einen Mechanismus erfolgt, der durch die Bindung an CD36, einen Klasse-B-Scavenger-Rezeptor ausgelöst wird und Clathrin-abhängige Interaktionen erfordert. Übereinstimmend mit unseren Ergebnissen, induziert die Bindung an CD36 Membranausstülpungen, die morphologisch den bei der klassischen Makropinozytose gebildeten Ausstülpungen ähneln, sich jedoch in ihren zugrundeliegenden molekularen Signalwegen unterscheiden. Deshalb wird die Internalisierung auch nicht durch Makropinozytoseinhibitoren beeinflusst. Unsere Daten legen somit nahe, dass *M. tuberculosis*, CD36, einen Oberflächenrezeptor bindet, was einen Mechanismus ähnlich der Makropinozytose auslöst, um so von der Wirtszelle aufgenommen zu werden.

Zusätzlich untersuchten wir, wie hämatopoetische Stammzellen permissiv für *M. tuberculosis* werden. Die langsame Kinetik der Internalisierung in hämatopoetischen Stammzellen im Vergleich zu professionellen Phagozyten, und unsere Beobachtung, dass hämatopoetische Stammzellen neonatalen Ursprungs nicht permissiv sind, legen nahe, dass die Permissivität nicht angeboren ist, sondern sich erst als Antwort auf noch zu definierende Signale entwickelt. Als potenzielle Signale, zeigten Pathogen-assoziierte molekulare Muster von *M. tuberculosis* nur marginale Effekte auf die Permissivität von hämatopoetischen Stammzellen. Unsere Ergebnisse deuten stattdessen darauf hin, dass die Entwicklung der Permissivität lebende, metabolisch aktive Bakterien erfordert. Vorläufige Daten legen nahe, dass dieser Prozess durch Zytokine vermittelt werden könnte, wobei weitere Untersuchungen notwendig sind, um die zugrundeliegenden Signalwege zu klären.

Zusammenfasend geben unsere grundlegenden Analysen der Infektion hämatopoetischer Stammzellen durch *M. tuberculosis* neue Einblicke in die komplexe Pathogenese der Tuberkulose. In den letzten Jahren wurde das Spektrum beschriebener nicht-kanonischer Wirtszellen, die Mykobakterien beherbergen, erweitert. Dennoch bleiben die spezifischen Rollen dieser nicht-phagozytischen Zellen bei der Immunmodulation und der Persistenz der Pathogene weitgehend unerforscht. Die Identifizierung der von *M. tuberculosis* genutzten Internalisierungswege und die Aufklärung der Signale, die die Permissivität der hämatopoetischen Stammzellen steuern, könnten neue therapeutische Ansätze aufzeigen, um die Immunkompetenz des Wirts wiederherzustellen und zu erhalten.

Table of Contents

Abbreviations

aDNA – Ancient DNA

ANG1 – Angiopoietin-1

AM – Alveolar macrophage

AP – Adaptor protein complex

AP180 – Assembly protein 180

aPB – Adult peripheral blood

APC – Antigen-presenting cell

ARF6 – ADP-ribosylation factor 6

ARP – Actin related protein complex

AU – Airy Unit

BCG – Bacillus Calmette Guerin

C/EBPβ – CCAAT-enhancer-binding protein β

C3b – Complement component 3 b

Cas –Crk-associated substrate

Cat. Nr – Catalogue number

CD – Cluster of differentiation

Cdc42 – Cell division cycle 42

CDK – Cyclin-dependent kinase

CDKI – Cyclin-dependent kinase inhibitor

CFP – Culture-filtrate proteins

CFU – Colony-forming unit

CLP – Common lymphoid progenitor

CME – Clathrin-mediated endocytosis

CMP – Common myeloid progenitor

CNS – Central nervous system

CR – Complement receptor

CR1 – Complement receptor 1

CR3 – Complement receptor 3

CSF – Colony stimulating factor

CXCL – Chemokine (C-X-C motif) ligand

DAMP – Danger-associated molecular pattern

DAPI – 4,6-Diamidino-2-phenylindole

DC – Dendritic Cell

DC-SIGN – Dendritic cell-specific intercellular adhesion molecule-3-grabbing non-integrin

DMSO – Dimethyl sulfoxide

EDTA – Ethylenediaminetetraacetic acid

ESAT6 – Early secretory antigenic target 6

ESX – ESAT6 secretion

FACS – Fluorescence-activated cell sorting

FAT – Fatty acid translocase

FCS – Fetal calf serum

FFA – Free fatty acid

FSC-A – Forward scatter (area)

FSC-H – Forward scatter (height)

GAP – GTPase activating protein

G-CSF – Granulocyte-colony stimulating factor

GEF – Guanine exchange factor

GMP – Granulocyte macrophage progenitor

HIP1R – Huntington-interacting protein-1

HIV – Human immunodeficiency virus

HSC – Hematopoietic stem cell

HSPC – Hematopoietic stem and progenitor cell

hu – Human

IFN – Interferon

IgG – Immunoglobulin G

IL – Interleukin

IT-HSC – Intermediate-term hematopoietic stem cell

IVC – Individually ventilated cage

JAK – Janus kinase

JNK – C-Jun NH2-terminal kinase

LAG3 – Lymphocyte-activation gene 3

LAM – Lipoarabinomannan

LCFA – Long-chain fatty acids

LD – Lipid droplet

LDL – Low density lipoproteins

Lin – Lineage

LKS – Lineage, c-kit, Sca-1

LMPP – Lympho-myeloid primed progenitor

LPS – Lipopolysaccharide

LTA – Lipoteichoic acid

LTBI – Latent tuberculosis infection

LT-HSC – Long-term hematopoietic stem cell

ly-bi-HSC – Lymphoid-biased hematopoietic stem cell

M. – Mycobacterium

MACS – Magnetic-activated cell separation

MAMP – Microbe-associated molecular pattern

ManLAM – Mannose-capped lipoarabinomannan

MAPK – Mitogen-activated protein kinase

MARCO – Macrophage receptor with collagenous structure

MBL – Mannose-binding lectin

MDR-TB – Multidrug-resistant tuberculosis

MEP – Megakaryocyte-erythroid progenitor

MFI – Mean fluorescence intensity

MHC-II – Major histocompatibility complex class II

MMR – Macrophage mannose receptor

MNC – Mononuclear Cell

MOI – Multiplicity of infection

MPP – Multipotent progenitor

ms – Mouse

my-bi-HSC – Myeloid-biased hematopoietic stem cell

MyE – Myeloerythroid progenitor

NF-κB – Nuclear factor 'kappa-light-chain-enhancer' of activated B-cells

NO – Nitric oxides

NOD – Nucleotide binding oligomerization domain

NOS2 – Inducible nitric oxide synthase

NPF – Nucleation promoting factor

OADC – Oleic acid, albumin, dextrose, catalase

OD – Optical density

oxLDL – Oxidized low density lipoprotein

PAMP – Pathogen-associated molecular pattern

PBMC – Peripheral blood mononuclear cell

PBS – Phosphate buffered saline

PCR – Polymerase chain reaction

PD1 – Programmed death-1

PDL1 – Programmed death ligand-1

PFA – Paraformaldehyde

PG – Peptidoglycan

PI3K – Phosphatidylinositol 3 kinase

PIM – Phosphatidyl-myoinositol mannosides

PPAR-γ – Peroxisome proliferator-activated receptor gamma

PPD – purified protein derivative

PRR – Pattern recognition receptor

RD1 – Region of difference 1

Ref. – Reference

ROS – Reactive oxygen species

RR-TB – Rifampicin-resistant tuberculosis

SCAR-B3 – Scavenger receptor class B member 3

SCF – Stem cell factor

SCFA – Short-chain fatty acid

SFK – Src-family kinase

SLAM – Signalling lymphocytic activation molecule

SNX9 – Sorting nexin 9

SP-A – Surfactant protein A

SP-B – Surfactant protein B

SR-B1 – Scavenger receptor B1

SSC-A – Sideward scatter (area)

SSO – Sulfo-N-succinimidyl oleate

STAT3 – Signal transducer and activator of transcription 3

ST-HSC – Short-term hematopoietic stem cell

T7SS – Type VII secretion system

TAG – Triacylglycerol

TB – Tuberculosis

TDM – Trehalose dimycolate

T_{H1} – T helper 1

TIM3 – T-cell immunoglobulin and mucin-domain containg-3

TLR – Toll-like receptor

TNF – Tumor necrosis factor

TPO – Thrombopoietin

T_{regs} – Regulatory T cells

UCB – Umbilical cord blood

Vav-GEF – Vav-family guanine nucleotide exchange factors

WASP – Wiskott-Aldrich syndrome protein

n-WASP – Neuronal Wiskott-Aldrich syndrome protein

WHO – World Health Organization

XDR-TB – Extensively drug-resistant tuberculosis

A. Introduction

1. Tuberculosis

A longstanding medical enigma, persisting for over two millennia, found resolution when Robert Koch concluded his ground laying work, and finally introduced humanity to its most deadly pathogen: *Mycobacterium (M.) tuberculosis*, the causative agent of tuberculosis.

M. tuberculosis is a human companion for 15,000-20,000 years, with its ancestors extending even further into our common past, highlighting a continuous co-evolution [1-3]. The earliest pathognomonic skeletal evidence, aDNA specimen and written records documenting tuberculosis, such as Hippokrates' aphorisms or the hinduistic Atharvaveda, trace back 2000-4000 years across Asia, America, Africa, and Europe [4-8]. Tuberculosis reoccurred and challenged physicians throughout medical history, ranging from Hippokrates' (460 - 370 BC) delineation of phthisis, to Johann Schönlein coining the term of tuberculosis and Robert Koch's fundamental contributions to modern bacteriology [8,9].

Now, in the 21st century, tuberculosis stands as even a bigger challenge to global health than ever before and persists as the most prevalent infectious disease, caused by a single pathogen species, humanity encounters. Advances in therapy, medical stewardship and research reduced the incidence rates globally. Nevertheless, the lack of promising preventive measures in the face of the looming antimicrobial resistance crisis, with *M. tuberculosis* as the most important drug-resistant pathogen, predicts an exponential increase in global annual deaths by 2050 [10-12]. Consequently, novel approaches and a better understanding of the pathogen and the disease it causes are necessary to eventually control *M. tuberculosis* and reassess Robert Koch's prediction [13].

"According to the experiments carried out so far,
however, there does not appear to be much prospect of
finding therapeutic agents that will control the parasites
in the patient's body."

– Robert Koch –

1.1 *Mycobacterium tuberculosis* – A Global Health Threat

Since the era of Robert Koch our comprehension of tuberculosis (TB) grew considerably. It is now established that tuberculosis does not reflect a monomicrobial disease but is indeed caused by various species within the genus *Mycobacterium*. These species constitute the *M. tuberculosis* complex, encompassing *M. tuberculosis*, *M. africanum*, and predominantly zoonotic species such as *M. bovis*, *M. canettii*, *M. caprae*, *M. microti*, *M. mungi*, *M. orygis*, *M. pinnipedii* and *M. suricattae* [14]. The *M. tuberculosis* complex bacteria represent prime examples of genetic homogeneity sharing 99.9% genetic identity and are recognized as rod shaped, nonmotile, aerobic, facultative intracellular bacteria [2]. Among them, *M. tuberculosis* continues to prevail as the predominant bacterial pathogen in humans on a global scale [10]. Typical symptoms include cough, chest pain, bloody sputum, night sweat, fever, fatigue and weight loss. Despite primarily being a pulmonary pathogen, *M. tuberculosis* can also infect other tissues, leading to extrapulmonary manifestations, which can affect bones, central nervous system, digestive tract, and skin, shaping a diverse spectrum comprising tuberculosis disease [15]. A unique scenario is observed in tuberculosis-infected infants, where primary tuberculosis meningitis displaces secondary lung tuberculosis as the predominant manifestation displaying a top ten cause of death in under the age of 5 mortality [16,17]. According to the global tuberculosis report – published by the WHO annually – an estimate of approximately 2 billion people, a quarter of the world's population is currently infected, and 10.8 million people fell ill with tuberculosis in 2023 [10]. With 1.25 million deaths attributed to tuberculosis, the disease displays the top cause of death from a single infectious agent. Despite these unmatched prevalence figures, *M. tuberculosis* is not a highly contagious pathogen *per se*. A single infectious individual, left untreated, might only infect 10 - 15 individuals per year. In contrast, in a highly contagious disease like measles, a single individual can infect 12-18 people within a mere 8-day period (assuming a susceptible population) [18]. The key to understand tuberculosis' apparently paradoxical success lies in the duration of infectiousness, coupled with an often indefinite or subclinical disease phenotype [19-21]. Particularly in high-burden settings where diagnostic and treatment coverage are limited, average duration of infectiousness often exceeds one year [22].

The burden of tuberculosis does not exhibit a homogenous pattern. Geographically, in 2023, the WHO regions with the most cases were South-East Asia (45%), Africa (24%) and the Western Pacific (17%) **(Fig. 1)** [10]. On a demographic level, tuberculosis is presented with a significant male bias, with a male to female ratio of 1.9 ± 0.6 for notified cases of pulmonary

TB [10,23,24]. While established immunocompromising risk factors, particularly human immunodeficiency virus (HIV) co-infection, immunosuppressive treatments against autoimmunity disorders, or type 2 diabetes mellitus, unequivocally demonstrate causal links to tuberculosis susceptibility, the primary driver of the global pandemic is of different nature [25-27]. Despite the limitations of such analyses to prove causality, empirical evidence clearly indicates that paramount determinants are rather rooted in socio-economic factors, encompassing adverse economic conditions, urbanicity, indoor air quality and household crowding at both individual and collective levels [10,28-30]. The attribution of malnutrition and air pollution to 27% respectively 22% of tuberculosis cases, underscores the evident association between poverty and disease [31]. This highlights the imperative for a paradigm shift away from a predominantly biomedically oriented anti-tuberculosis strategy towards an interdisciplinary approach integrating researchers, economical- and political stakeholders equally [10].

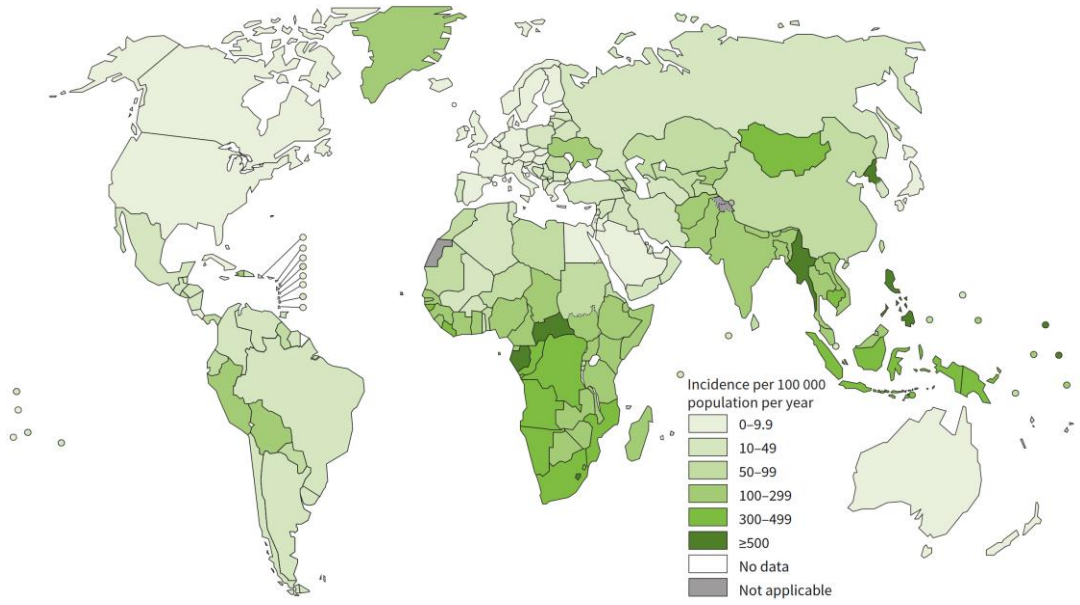

Figure 1: Estimated global tuberculosis incidence rates, 2023. National tuberculosis incidence rates (new cases) per 100 000 population per year. [10].

1.2 Treatment of Mycobacterial Infections

While socio-economic strategies promise the strongest leverage for the global efforts to sustainably reach the set targets of the WHO's 'End TB'-Strategy, the emergence of drug resistance is of major concern and could put a halt to the positive development of recent years. Discovery of antibiotics and introduction into clinic against tuberculosis was quickly followed by the emergence of drug-resistant strains within 10 years [32]. Current standard treatment for drug-susceptible tuberculosis includes four antibiotics, namely rifampicin

(RIF), isoniazid (INH), pyrazinamide (PZA) and ethambutol (EMB). While treatment for drug-susceptible tuberculosis already requires the administration of those first line drugs over a course of 4-7 months, treatment of multidrug-resistant tuberculosis (MDR-TB) or extensively drug-resistant tuberculosis (XDR-TB) requires treatment from 9 up to 24 months [33]. While on a global scale only 3.2% of newly diagnosed and 16% of recently treated cases were identified as MDR-TB or rifampicin-resistant tuberculosis (RR-TB), prevalence varies strongly on a regional scale. The highest proportion of resistance is found in the Russian Federation where over 20% of all new cases are resistant to either rifampicin alone, or both rifampicin and isoniazid [10]. Rifampicin-resistant *M. tuberculosis* strains already account for a quarter of all deaths due to antimicrobial resistance worldwide. Primary drivers of this development are low compliance to therapy – partially due to significant adverse effects – in combination with costs and a receding incentive for drug development in the for-profit sector. Although, novel drugs, like bedaquiline and pretomanid, and repurposed drugs, such as linezolid, clofazimine and cycloserine, are expected to improve treatment outcome, severe adverse effect associated with the use of second line regimen aggravates therapy adherence and thus promote emerging resistances even further [34]. In addition, only three new drugs were approved for treatment within the last decade: Bedaquiline and the two nitroimidazole derivates delamanid and pretomanid, marking the first anti-tuberculosis drugs with a distinct mode of action for 50 years [35].

1.3 Advances and Strategies in Tuberculosis Vaccination

The first vaccine against tuberculosis was already discovered in 1921: an attenuated relative of *M. tuberculosis*, and a derivative of the cattle-tuberculosis agent, *M. bovis*, termed Bacillus Calmette Guerin (BCG) [36,37]. Despite the history of BCG-vaccination, tuberculosis is still the top cause of death from a single infectious agent [38]. While acknowledging the limited efficacy in adults, BCG immunization still provides protection in infants and young children against primary pulmonary tuberculosis and its disseminated forms [39,40]. Hence, the vaccine is not inherently devoid of any protective efficacy, but rather secondary factors impair the efficacy in adults. Especially in latitudes exceeding 40°, regions with traditionally low mycobacterial burden, vaccine effectiveness markedly increases [41]. Furthermore, assessed protection is significantly higher when purified protein derivative (PPD)-positive individuals - indicative of prior mycobacterial exposure - are excluded from study cohorts. Together, these findings align with the scientific consensus that prior exposure to mycobacteria (including environmental) species interferes with the subsequent generation of

adaptive immunity post vaccination [42]. Given that BCG is a live vaccine, bacteria can replicate or persist after administration. This replication contributes to a more pronounced inflammation and might be pivotal to mount a robust adaptive immune response. In cases where immune memory and resistance pre-exists from prior mycobacterial exposure, this beneficial replication might be limited [43].

To increase vaccine efficacy in the adult population regardless of pre-exposure, current tuberculosis vaccine research aims to decipher the prerequisites of a robust, long-lasting, and protective immune response. In the center: T cells and the balance between the spectrum of subpopulations of primed antigen specific $CD4^+$ T Cells. To elicit an optimal vaccine response that balances tissue-resident effector cells with a lymphoid reservoir of memory cells, varying antigen compositions, modified administration routes and novel adjuvant formulations make up the current candidate vaccine pipeline [44]. Unfortunately, their real protective efficacy in humans is only assessed at advanced stages of clinical development. Due to the limitations of animal models, which do not fully replicate secondary tuberculosis in humans, and the absence of adequate immune correlates of protection in humans, clinical stage 3 trials still represent the first real validation of a new vaccine candidate [44,45]. With industrial shareholders increasingly outsourcing this crucial translational research to an underfunded academic sector, the identification of predictive immune correlates is critical to validate vaccine candidates earlier in development and accelerate the process of finding effective tuberculosis vaccines.

1.4 Host-Directed Therapy – An Emerging Strategy Against Tuberculosis

While antibiotic treatment aims to cure the disease and vaccination to prevent it, host-directed therapy aims to support the host's own immunity and prohibit detrimental immunopathology, working in conjunction with conventional antibiotic therapy. By targeting host factors that are hijacked by the pathogen for replication and immune evasion, by direct immune activation, or by immunopathology control, host-directed therapy aids to resolve the infection indirectly [46]. A prime example for a conjunctive application of host-directed therapy is to modulate granuloma vascularization, thereby improving drug delivery to the site of mycobacterial persistence [47]. After prolonged periods of disease, especially after MDR-TB, most individuals suffer from the sequelae of immunopathology and are left with pulmonary cavitation and fibrosis leading to chronic lung impairment even after successful

treatment [48,49]. In these individuals, interventions targeting neutrophil degranulation could limit immunopathology [50]. Host-directed therapy could also serve as a mediator between vaccination and treatment, allowing vaccines with blunted regulatory T cell responses and thus stronger protective immunity that otherwise could not be used for their adverse immunopathological side effects [51]. Thus, host-directed therapy might be the key to redefine a multilateral anti-tuberculosis strategy by equally addressing pathogen clearance and the concurrent prevention of tissue damage. To facilitate such a multilateral approach, one must understand the delicate intricacies of the interplay between pathogenic and protective immune responses throughout the distinct stages of tuberculosis disease.

2. Mycobacterial Latency - A Strategy of Success

Both the epidemiological success and the lack of adequate treatment against *M. tuberculosis* originates from its pathogenesis and especially from its ability to cause latent infections. Latency is defined as a state of pathogen persistence in the absence of clinical symptoms. While one quarter of the global population is estimated to be infected with *M. tuberculosis,* bearing the potential risk of developing active disease, only 10% fall ill during their lifetime [52]. The more common outcome of an infection is an equilibrium of bacterial persistence and host immunological control. This is because tuberculosis is a near perfect paradigm of the host-pathogen relationship. *M. tuberculosis*, with its exclusive human tropism and lack of an environmental reservoir, faces continuous selective pressure to adapt to its host. Since the emergence of the *M. tuberculosis* complex 70,000 years ago, this co-evolutionary trajectory led to a balance between persisting populations in asymptomatic carriers while retaining sufficient virulence to facilitate transmission in active disease [3,53,54]. For nearly five decades, this understanding shaped the binary clinical paradigm, stratifying individuals as either having latent tuberculosis infection (LTBI) with dormant mycobacteria or contagious active disease [55,56]. However, this binary paradigm is challenged by observations of sporadic loss of quiescence and resulting growth of *M. tuberculosis* during 'latent' infection [19]. Furthermore, over a quarter of culture-positive individuals lack clinical symptoms but are still contagious [20,21]. Thus, 'classical' LTBI might rather represent a spectrum of disease states ranging from infection without symptoms nor macroscopic pathology to the transition towards active tuberculosis, where infectiousness and clinical symptoms are not necessarily linked. To address this spectrum, a new classification has been proposed that separately evaluates these two factors, replacing the traditional binary LTBI stratification **(Fig. 2)** [19]. Although it does not strictly align with the definition of true latency, for simplification,

the term ‘latent tuberculosis’ will be used to summarize all disease stages between sterilization and active disease in this study.

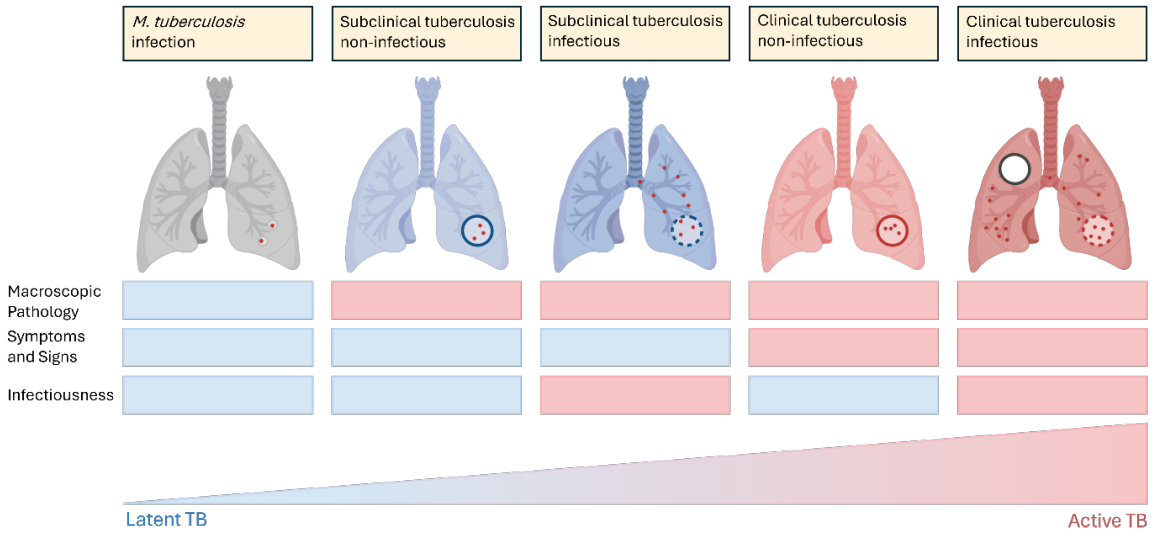

Figure 2: Classification of tuberculosis states. Disease phenotypes between latency and active tuberculosis are classified based on macroscopic pathology, clinical symptoms and infectiousness of the patient. Disease with both macroscopic pathology and symptoms is classified as clinical tuberculosis and further delineated between non-infectious and infectious disease. Instead, disease with only macroscopic pathology but no symptoms is classified as subclinical tuberculosis and further delineated between non-infectious and infectious disease. Detection of *M. tuberculosis* with neither macroscopic pathology, symptoms, nor infectiousness is classified as *M. tuberculosis* infection. Adapted from [19].

Within this continuum of disease phenotypes, factors that promote progression towards active disease stem from the disruption of the homeostasis between bacterial persistence and host immunological control. These disruptions lead to microbial (re-)activation and subsequent manifestations of clinical symptoms. Notably, the underlying events are not well understood and extend beyond immune impairments such as co-morbidities (like HIV) or immuno-suppressive treatment [57]. Conversely, exacerbated immune responses, can also lead to disease (re-)activation. This ambiguity originates from the niche in which *M. tuberculosis* persists within the host: The Granuloma.

2.1 The Granuloma – A Host-Pathogen Compromise

Granulomas are the product of ten-thousands of years of co-evolution and might represent the *opus magnum* of host-pathogen interactions. They are tissue reactions, respectively organized aggregations of macrophages and other cell types, orchestrated by the immune system to sequester invading mycobacteria through specific immune reactions. To this day there is no consensus whether granulomas in tuberculosis serve as a protective immune mechanism or another pathogenicity trait in the life cycle of the *M. tuberculosis* [59]. As an immune reaction associated with protection during LTBI, granulomas were traditionally

believed to successfully 'wall off' persisting bacteria from disseminating into neighbouring tissue, thus restricting tissue damage by focussing collateral immunopathology to preserve surrounding lung function [60,61]. Notably, experimental models and clinical manifestations with phenotypical impairments of granuloma formation all correlate with detrimental disease outcome [62-65].

This exclusive host-centric view was challenged by new methods revealing the dynamic nature of granuloma biology, leading to a more integrated view on tuberculosis pathogenesis. Rather than being a static bacterial 'prison', the granuloma, especially in its early stages, is a niche of continuous immune cell recruitment and egress. The steady supply of susceptible host cells that fail to kill *M. tuberculosis* promotes mycobacterial replication and dissemination, as infected macrophages leaving the primary site of infection can seed new secondary granulomas [66]. Although these dynamics are slowed during later stages of the infection, due to improved macrophage activation by the adaptive immune system and the firmer segregation by the fibrotic and calcified rim, seeding of new granulomatous lesions still occasionally occurs, even under apparent immunological control [67,68]. Hence, from the bacterial perspective, *M. tuberculosis* shapes its own host niche in favor of an ever-regenerating reservoir of host cells.

Integrating both perspectives into a mutual concept characterizes the granuloma as an immunological compromise reflecting a '*damned if you do and damned if you don't'* scenario. A recurring scenario that is commonly recognized in a plethora of immune responses against tuberculosis and represents both a hurdle but also an intervention opportunity for host-directed therapy interventions [46,69,70]. Despite the complexities surrounding the classification of granulomas on a host-pathogen axis, the immunological processes leading to their formation are, at least in parts, well understood.

2.2 Pathogenesis of Tuberculosis: From Inhalation to Transmission

The primary route of tuberculosis airborne transmission involves aerosol particles laden with *M. tuberculosis* **(Fig. 3)**. While coughing significantly contributes to transmission in symptomatic patients, it is not essential in a subclinical context where mere breathing alone can sufficiently generate infectious aerosols [71]. Upon inhalation and translocation to the lower respiratory tract, the first immune cells that *M. tuberculosis* encounters are the alveolar macrophages (AMs). These tissue-resident macrophages inhabit the luminal surface of the

alveolar space and quickly phagocytose the mycobacteria [72]. It is assumed that in most cases this will lead to the immediate clearance of the pathogen. However, at this crucial stage of pathogenesis, *M. tuberculosis* can evade elimination by inhibiting phagosome-lysosome fusion and may even escape into the host cell cytosol through disruption of the phagosomal membrane (via its ESX-1 system) [73-75]. After overcoming this initial barrier, *M. tuberculosis* establishes a primary infection in the lung interstitium. It remains unclear whether crossing of the epithelial barrier is primarily mediated through the transmigration of infected macrophages or through microfold cell transcytosis [72,76,77]. Activation of epithelial cells and *M. tuberculosis* import into the lung interstitium, triggers a pro-inflammatory response. This yet exclusively innate response is characterized by cytokine and chemokine release, mainly tumor necrosis factor alpha (TNFα), Interleukin-1α/β (IL-1α/β) and IL-6 by alveolar macrophages, IL-8 by epithelial cells, and small lipid mediators such as leukotriene B_4 and prostaglandins [63,78-80]. Their concerted action, especially IL-8 (i.e. CXCL8), recruits increasing numbers of immune cells, primarily polymorphonuclear neutrophils, monocytes, dendritic cells, and fibroblasts to the site of infection [81]. This initial focal accumulation of mononuclear cells represents the first stage of nascent granulomas and is exclusively orchestrated by the innate immune system. However, nascent granulomas fail to restrict mycobacterial replication and, while studies report proceeding granuloma formation even in the absence of specific immunity, only additional activation by T helper 1 (T_{H1}) cytokines, primarily IFN-γ, allows granulomas to reach their full protective potential [62,63,67,82,83].

To activate the adaptive immune system either dendritic cells or inflammatory monocytes need to migrate to the draining pulmonary lymph nodes (Ghon complex) for antigen cross-presentation. The following T cell priming predominantly leads to the differentiation into $CD4^+$ T helper 1, T helper 17 as well as $CD8^+$ cytotoxic effector-cells, the canonical response against intracellular pathogens [84-86]. With the involvement of both the innate and adaptive immune system, the initial focal granulomatous lesion becomes more and more organized, marking a critical juncture in disease progression. In rare cases, there is an immediate transition to active disease (primary tuberculosis), typically seen in immunocompromised individuals, especially young children, with severe genetic risk factors or in patients with co-infections. In these individuals, initial granuloma formation fails to control the infection. The result is the immediate infiltration of the lung by disseminated replicating mycobacteria that seed new lesions [87]. In most infected individuals, however, the maturing granuloma, consisting of a centre of activated macrophages surrounded by a rim of lymphocytes, effectively contains the infection and prevents further dissemination. As a result, more than

90% of those latently infected will never develop active tuberculosis in their lifetime [52]. Over the course of time, the integrity of the granuloma is safeguarded by continuous cellular recruitment as well as tissue repair, leading to the highly vascularized follicle-like structures seen in advanced LTBI [68,88]. In the remaining 10%, alterations in the host's immune status may disturb the delicate balance of immunological control and eventually reactivate tuberculosis, leading to active disease (secondary tuberculosis).

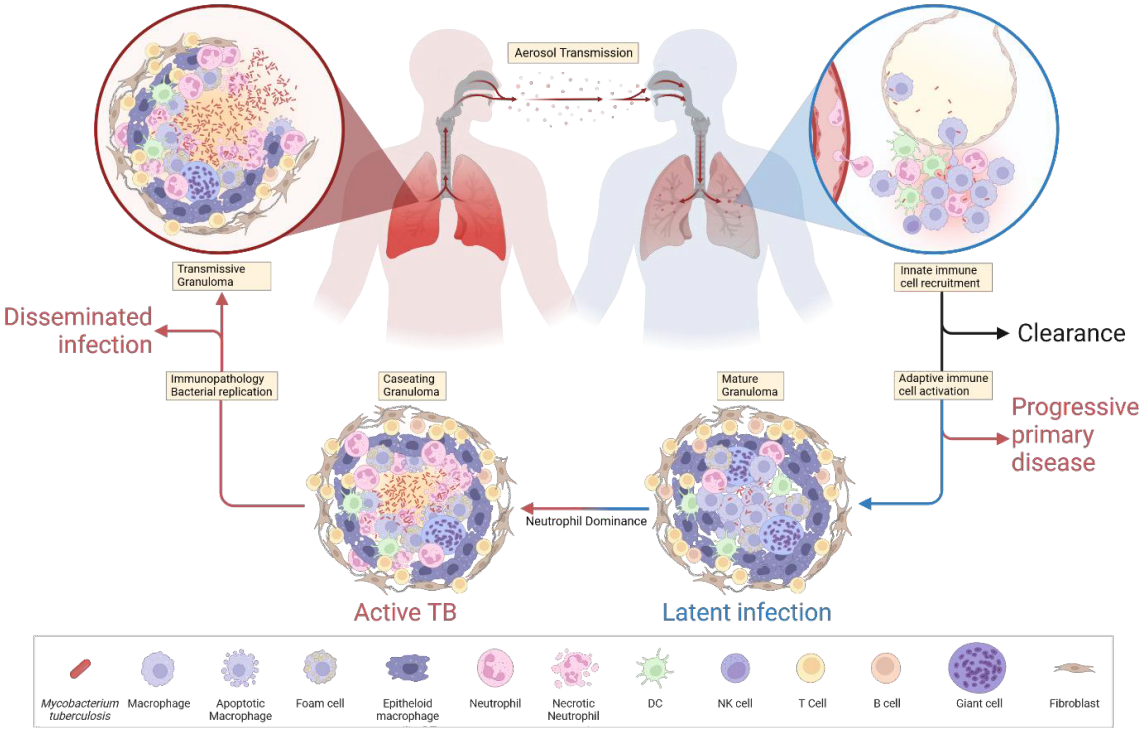

Figure 3: Life cycle of *Mycobacterium tuberculosis*. Transmission occurs via inhalation of mycobacterium-laden aerosols from an individual with active pulmonary disease. The first immune cells *M. tuberculosis* encounters are alveolar macrophages on the luminal surface of the alveolar space. Either via transmigration of infected macrophages or through microfold cell transcytosis, mycobacteria cross the epithelial barrier into the lung interstitium, where a variety of innate immune cells are recruited. When innate immune mechanisms fail to clear the initial infection, antigen-presenting cells (APCs) migrate to the draining lymph node to prime T cells and initiate adaptive immune responses. Activated T cells return to the focal accumulation of innate immune cells and coordinate the formation of a granuloma which – in ~90-95% of infected individuals – effectively sequesters *M. tuberculosis* and prevents further disease progression. In cases where innate and adaptive immune responses are insufficient, mycobacteria replicate and disseminate unhindered resulting in progressive primary disease. Furthermore, even after initial control, during latent tuberculosis infection, disruptions of immune homeostasis – often associated with neutrophil dominance – can lead to mycobacterial reactivation and progression to active disease. In these cases, immunopathology and mycobacterial replication damage the granuloma's structural integrity allowing mycobacterial dissemination, which renders the individual infectious, thus completing the life cycle of *M. tuberculosis*.

2.3 Transition from Latent Infection to Active Disease

Latent tuberculosis infection is characterized by bacterial persistence and immunological control. The equilibrium within the granuloma thus necessitates a finely tuned immune response to sustainably counter microbial replication and host cell death while minimizing collateral tissue destruction. Consequently, both transiently exacerbated and impaired

immune responses shift the balance, irreversibly compromising the granuloma's integrity [79,89]. On one side, in scenarios of impaired immune responses, as clinically most often observed during anti-TNFα treatment, the granuloma becomes permissive due to the lack of phagocyte activation and the resulting *M. tuberculosis* regrowth [27,90]. In scenarios of hyper-immunity on the other side, the granuloma does not merely resolve due to inflammation but metaphorically collapses under its own immunopathology. The initial chain of events, however, is not clearly understood yet and may stem from signals produced by hypersensitive $CD4^+$ T cells [79]. Irrespective of the uncertainty of those triggers, their result is a phenotype that is commonly recognized in active tuberculosis: the recruitment of neutrophils to the granuloma. Abundance of neutrophils is a common factor recognized in active tuberculosis progression and negatively correlates with lung pathology, disease outcome and promotes transmission [91-93]. While macrophages, as the primary phagocytic cell type during steady state and mycobacterial control, play a beneficial role in the immune response, neutrophils have a detrimental one [94,95]. Activated infected macrophages eventually undergo apoptosis, a tightly regulated programmed form of cell death. This ensures that intracellular mycobacteria and other cellular remains are taken up as apoptotic bodies by other phagocytic cells. This process, termed efferocytosis, prevents uncontrolled pathogen dissemination after host cell disintegration and limits danger associated molecular patterns (DAMP)-induced immunopathology and promotes antigen cross presentation [96-98]. Neutrophils fail to control *M. tuberculosis* after initial internalization, which contrasts with other microorganisms [95,99]. Instead, they quickly succumb to a necrotic cell death due to the mycobacteria-induced production of reactive oxygen species [94,95]. This does not only facilitate mycobacterial escape from elimination but also initiates a cascade of detrimental events. Unlike apoptotic macrophages, where mycobacteria become enwrapped in apoptotic blebs, in necrotic neutrophils mycobacteria are loosely associated with the necrotic cell debris. Necrotic neutrophils are removed by macrophages through a process termed necrophorocytosis in contrast to removal of apoptotic cells via efferocytosis [94]. Different to uptake of apoptotic bodies, phagocytosis of necrotic neutrophils drives macrophages into necrotic cell death [100]. Whether macrophage activation by T_H1 cell-derived cytokines rescues this phenotype is currently investigated. While the underlying mechanism is obscure, it is likely to involve distinct interactions between neutrophil-derived danger-associated molecular patterns (DAMPs), mycobacterial virulence factors such as the type VII secretion system (T7SS), ESX-1, or the phagolysosome fusion inhibiting cell wall lipid trehalose dimycolate (TDM), and the macrophage’s phagosomal membranes. The interaction

initiates a vicious cycle of phagocyte necrosis at the granuloma's core that is further increased by the abundance of neutrophil effectors released by degranulation. However, clinical evidence suggests that hypersensitive reactions of $CD4^+$ T cells leading to exacerbated IFN-γ or IL-4/IL-13 responses are also requisite for subsequent central necrosis and caseation [79]. As central granuloma necrosis progresses, the granuloma may eventually burst open, disseminating *M. tuberculosis* into the surrounding tissue. At this stage, extra-granulomatous mycobacterial replication, biofilm formation, attraction of even more neutrophils and monocyte-derived macrophages followed by severed pulmonary symptoms including cough, facilitate infection of a new host via aerosol particles, completing the cycle of tuberculosis transmission **(Fig. 3).** In conclusion, granulomas rather represent an immunological compromise of an immune system in which other antimicrobial mechanisms fail to control the infection.

2.4 Immune Impairment as a Driver of Persistence

Insufficient immune resistance mechanisms are key drivers of pathogen persistence during tuberculosis [101,102]. Only in individuals where alveolar macrophages or the initial recruitment of myeloid cells fail to resolve the primary infection, granuloma formation becomes necessary to restrict further propagation. However, this in turn also establishes the niche for mycobacterial persistence. Furthermore, in LTBI, both sustained mycobacterial survival and the transition to active disease result from an incompetent immune system at the site of infection that fails to eliminate the pathogen without concomitantly causing immunopathology, which negates protection [79]. Hence, the immune system repeatedly fails to control the infection as the disease progresses.

This persistence occurs because *M. tuberculosis* subverts antimicrobial defence mechanisms at multiple levels to prevent regular immune function and survive in the hostile host environment. The mechanisms affected by *M. tuberculosis* include intracellular trafficking pathways, phagosome acidification, phagosome-lysosome fusion, apoptosis, autophagy, immune recognition, antigen presentation and inflammasome activation [103]. For instance, only by undermining lysosomal trafficking pathways via protein and lipid effectors, *M. tuberculosis* establishes its myeloid cell niche [104,105]. While these pathways represent sufficient targets for immediate host evasion on a small scale, we are also beginning to understand more systemic mechanisms of immune impairment, such as the

reprogramming of myeloid cells by epigenetic modifications or the emerging field of immunometabolism [106,107].

Nevertheless, the myeloid cells in the focus of those studies, share one common inherent characteristic that may significantly limit their potential to mediate the immune impairment required for long-term persistence: their life span. Neutrophils have a half-life between 6-10 hours in circulation before undergoing apoptosis [108,109]. Although, inflammatory signals, such as certain cytokines, can delay spontaneous apoptosis of neutrophils to some extent, their life span remains limited to a maximum of two to three days at most [110]. Recruited monocyte derived macrophages life spans might eminently exceed the neutrophils ones but are still relatively short-lived in granulomas, being replaced within an order of days as well [111-113]. Due to these short immune cell lifespans, immunological impairments imposed on the respective immune cell populations will only be transient until the perturbated cell is replaced by a new one. Given their post-mitotic nature, their replacement is realized through *de novo* generation from potentially unperturbed progenitors. Tissue-resident alveolar macrophages may present an exception in this context. Their extended lifespans and mitotic self-maintenance, without necessarily relying on external hematopoietic replacement, could hypothetically allow for a stable pool of perturbated cells, where epigenetic or metabolic priming is transferred across generations [114]. However, in the context of tuberculosis, the relevance of alveolar macrophages beyond primary host cells upon initial lung colonization is limited, without a significant role during latent disease [72,115]. The central role of lymphocytes with respect to myeloid cell activation and immune response orchestration makes them a near perfect target for mycobacterial immune modulation. In addition, their clonal proliferation capacities paired with the presence of memory cell subsets would allow life-long propagation of imprinting. However, the late mobilization of bacteria to the lung lymph nodes to prime naïve T cells, delays specific immune responses to a stage where the primary infection site is already established [84].

In conclusion, the overwhelming proportion of cell types that are and could hypothetically be subject to *M. tuberculosis*' immune modulatory properties, only possess one of the two required characteristics for sustained immune impairment. The first is, to be an integral part along all checkpoints of tuberculosis disease progression, from initial infection up to active disease transition. The second is, to have an extended lifetime and being self-renewing, so that immunological priming is transferred to daughter cell generations.

One cell type, which has long been neglected in tuberculosis research, combines the two characteristics, and thus potentially represents the missing link to integrate both early and life-long impairments to immunity. The respective cell type is the foundation of both the innate and adaptive immune system and has already been shown to interact with *M. tuberculosis*, the hematopoietic stem cell.

3. Hematopoietic Stem Cells

Hematopoietic stem cells (HSCs) are the multipotent cells at the apex of hematopoiesis, a process generating over one million cells per second in adult humans [116]. As stem cells, they possess two key properties: Self-renewal and multilineage differentiation. Thereby, they give rise to all blood cell types, including erythrocytes, megakaryocytes, their platelet progeny, as well as all immune cells of the myeloid and lymphoid lineages throughout the organism's lifespan **(Fig. 4)** [117]. Due to this ability, a single HSC can reconstitute the entire hematopoietic system in lethally irradiated mice [118-121].

HSCs initially appear in the aorto-gonado-mesonephros region during early embryogenesis [122,123]. They subsequently migrate to liver and spleen for transient embryonic hematopoiesis after two to three months and eventually relocate to the bone marrow five months after gestation, where they establish their final niche for their definitive function as progenitors of hematopoiesis [124]. In the bone marrow, HSCs are rare, comprising only 1 in 10,000 cells, and share the limited space with more differentiated hematopoietic cells and stromal (non-hematopoietic) cells [125,126]. The specific composition of hematopoietic and stromal cell populations and spatial distribution in relation to sinusoids and arteries creates distinct microenvironments in the bone marrow that uniquely regulate HSC and hematopoietic progenitor physiology [127-130]. Especially in the hypoxic microenvironments near the endosteum, HSCs are often found in a quiescent, non-replicative state, maintaining a life-long reservoir [131-133]. During steady-state conditions, more than 95% of the stem cell pool remains quiescent, cycles infrequently and primarily rests outside the cell cycle in the G0 phase [133]. Instead, blood cell maintenance predominantly calls upon the successive recruitment of lineage-committed progenitors rather than the multipotent stem cell reservoir [134,135]. Only under haematological stress, such as trauma, blood loss or infection, HSCs exit quiescence to proceed into proliferation and differentiation [136]. To increase peripheral leukocyte numbers, HSCs can switch from renewing symmetric division to asymmetric

division or even symmetric commitment giving rise to differentiated progeny of all lineages [137].

Genetic, functional, and phenotypic characterization of cell populations capable of reconstituting all hematopoietic lineages has enabled the identification of distinct populations with varying degrees of self-renewal **(Fig. 4)** [138,139]. Notably, this classification is still arbitrary and represents a mere snapshot within a continuous spectrum of differentiation stages [140,141]. Among the multipotent cells, only those with the ability to sustain long-term reconstitution across serial transplants are classified as bona fide HSCs. Cells that exhibit more limited or non-serial reconstitution potential are instead categorized as multipotent progenitors (MPPs), which are further divided into subgroups 1-4 based on their predominant lineage output [142]. While HSCs possess multilineage differentiation potential, it appears that a fraction already exhibits a degree of lineage bias and cell type specific trajectories [143]. This suggests that definitive lineage fate decision may already be encoded in transcriptional and (epi-)genetic programs within multipotent and self-renewing HSCs [143,144]. These programs are not inherently hardwired, and a certain degree of lineage plasticity allows the hematopoietic system to flexibly adapt its output in response to exogenous factors, such as cytokines [145]. Hence, the current concept of HSCs represents similar but not functional and phenotypic identical cells.

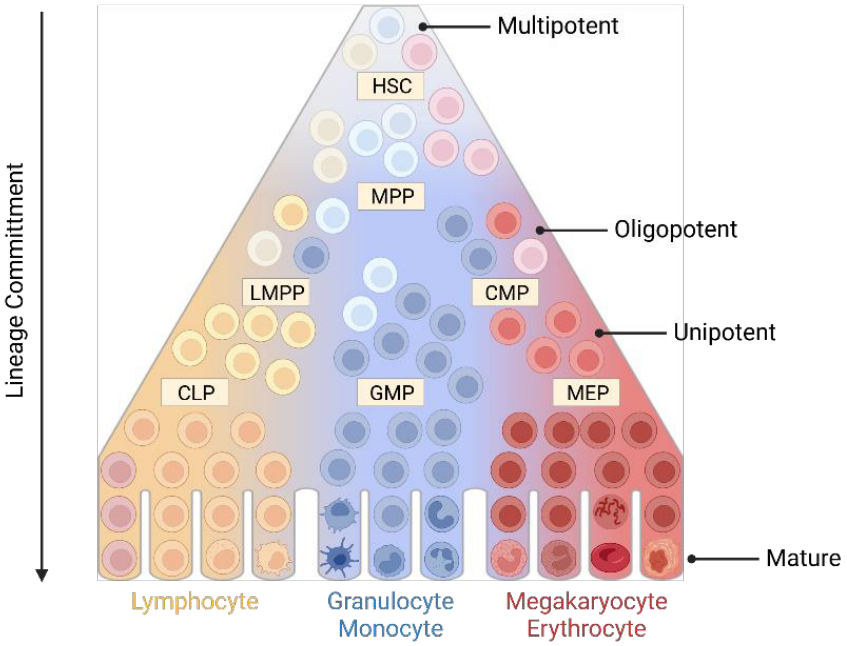

Figure 4: The 'continuum' model of hematopoiesis. Without discrete transition steps, hematopoietic stem cells (HSCs) differentiate into their mature progeny of all hematopoietic lineages. During differentiation, cells possess variable degrees of lineage bias – indicated by colour – in a continuous process of differentiation. Lineage commitment increases during differentiation, while a certain degree of plasticity remains. HSC = hematopoietic stem cell; MPP = multipotent progenitor; LMPP = lympho-myeloid primed progenitor; CMP = common myeloid progenitor; CLP = common lymphoid progenitor; GMP = granulocyte-monocyte progenitor; MEP = megakaryocyte-erythroid progenitor. Adapted from [146].

Despite, the inherent simplification of immunophenotyping, it still represents the state-of-the-art approach to distinguish HSCs and MPPs from more committed progenitors in experimental approaches, where transcriptional and functional characterization is not feasible. As HSCs and MPPs lack a uniquely expressed marker, current research focuses to find better phenotypic correlates of the underlying functional heterogeneity. Several multiparameter identification schemes have so far been developed, each with varying specificity and composition in the identified populations [142]. In most studies two HSC subpopulations are recognized: long-term HSCs (LT-HSCs) and short-term HSCs (ST-HSCs). In the following and for the rest of this study, however, we decided to adhere to an updated classification recognizing only, the formerly called, LT-HSCs as bona fide HSCs but ST-HSC as MPP1s, due to their limited serial reconstitution capacity [142].

3.1 Crosstalk Between Immunity and Hematopoiesis

The innate immune system relies completely on mostly post-mitotic cells and their continuous replenishment from hematopoietic stem and progenitor cells (HSPCs) in the bone marrow. However, steady state regeneration of the myeloid cell pool is insufficient to compensate for the depletion of these crucial and short-lived populations during infection and requires increased *de novo* generation instead [136,147]. For instance, during tuberculosis, neutrophil migration to granulomas which accompanies the transition from latency to active disease, also requires increased granulopoiesis and egress of granulocytes from the bone marrow [147-150].

In response to the increased demand for innate defence cells, HSCs, hematopoietic progenitors, mature immune cells and bone marrow stromal cells are intricately linked with canonical immune response pathways to accelerate myelopoiesis during infection. This integration is most pronounced in the mechanism termed ‘emergency hematopoiesis’ [136]. This multifaceted response involves the cell-cycle entry and biased expansion of the quiescent HSC reservoir towards the myeloid lineage at the expense of erythroid and lymphoid committed progenitors and is driven by concomitant metabolic and transcriptional changes as well as epigenetic priming [147,151,152].

HSCs play a pivotal role in this response, primarily integrating pathogen sensing through indirect pathways **(Fig. 5)**. Cytokines, particularly type I and II interferons (IFN-α, IFN-γ), IL-1β, and colony stimulating factors (CSFs) are key mediators in HSC signalling [153-158]. Notably, most studies focus on hematopoietic progenitors in general and observe an extended array

of cytokines involved in emergency hematopoiesis beyond HSCs. Stromal cells and immune cells, predominantly activated T cells, are the primary sources of these signals, underscoring the bone marrow's hybrid function as both a primary and secondary lymphoid organ, [136,159,160]. Antigen presentation to bone marrow T lymphocytes involves antigen-presenting cells (APCs) like macrophages and dendritic cells, which either capture antigens in peripheral tissues and migrate to the bone marrow or acquire antigens within the bone marrow following vascular pathogen dissemination [160-164]. Notably, even in the absence of inflammatory signalling, the loss of myeloid cells alone, triggers G-CSF-dependent and -independent progenitor proliferation in the bone marrow indicating redundant mechanisms to adapt hematopoiesis independent of cytokine signalling [150]. While the repertoire of pattern recognition receptors in early hematopoietic progenitors has yet-to-be comprehensively characterized, stimulation with lipopolysaccharides (LPS) induces NF-κB activation in subsets of MPPs and a small fraction of HSC, indicating a potential involvement in direct pathogen sensing and immune surveillance [165]. Lastly, HSC may also directly interact with bacterial pathogens. Responses following infection instead of exogeneous signalling or surface recognition of pathogen-associated molecular patterns (PAMPs), and the resulting pathways could also be involved in hematopoietic adaptations and will be discussed in the next section.

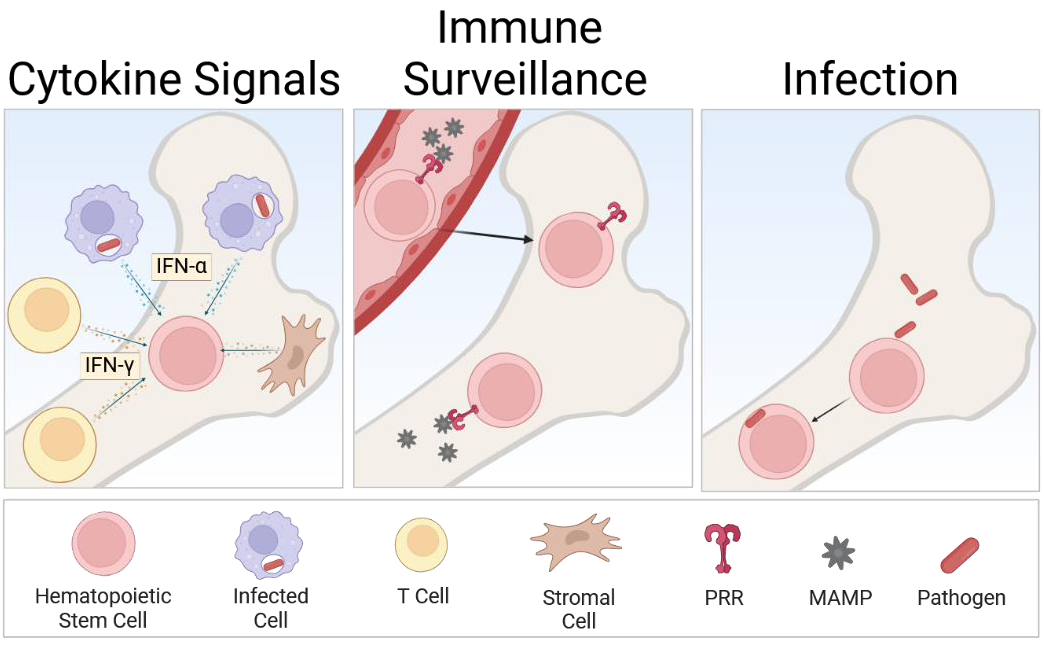

Figure 5: Crosstalk between immunity and hematopoietic stem cells. To adapt to the increased demand of myeloid cells during infection, hematopoietic stem cells (HSCs) are indirectly and directly involved in pathogen sensing. During inflammatory responses, cytokines – produced systemically or within the bone marrow – can directly induce proliferation and differentiation in HSCs. Particularly type II interferons (IFN-II), IL-1β, interferon-alpha (IFN-α) and colony stimulating factors (CSFs) are recognized as key mediators in HSC signalling. HSCs have also been indicated to directly sense pathogens through pattern recognition receptors (PRRs) in an immune surveillance manner. Recent reports also suggest direct infection as a source of interaction. Adapted from [166].

Mycobacterial infections are of special importance in the context of emergency hematopoiesis and HSC responses. Despite sharing 99.9% genetic identity, the hematopoietic adaptations to infection differ tremendously between the non-virulent and virulent mycobacterial species [158,167-169]. Type II interferons (IFN-II) play a well-established protective role during mycobacterial infections, whereas type I interferon (IFN-I) signatures are rather associated with host susceptibility and active disease [170-173]. During microbial control, as observed with non-virulent strains, like *M. bovis* BCG or *M. tuberculosis ΔRD1*, IFN-γ signalling promotes myelopoiesis and trained immunity in the monocyte progeny, offering protection against infection [158,169]. Conversely, during disease caused by virulent *M. tuberculosis*, IFN-I overwrites the protective IFN-γ signatures in HSCs, supressing myelopoiesis and impairing trained immunity [158]. Due to the lack of adequate models of LTBI, our understanding of HSC responses beyond acute infection and how this influences mycobacterial control within the granuloma during latency, is extremely limited.

In summary, HSCs are subject to a complex interplay between pathogen virulence and immunity. This crosstalk allows the hematopoietic system to finely tune the immune cell output to meet the demands of protective immunity. However, given the central role of HSCs in immunity, this interplay also risks opportunities for pathogen-mediated host manipulation.

4. Hijacking the Hematopoietic System

The bone marrow's unique role, combining both primary and secondary lymphoid features, makes it an attractive target for host manipulation. The regulatory crosstalk between immune responses and hematopoiesis requires the exchange of antigen presenting cells, e.g. macrophages, and dendritic cells between peripheral tissue and the bone marrow [160-164]. While granulomas effectively sequester mycobacteria during latency and restrict the dissemination of free bacteria, infected macrophages still occasionally egress and may enter the bone marrow bringing *M. tuberculosis* in close contact to hematopoietic progenitors and the site of hematopoiesis [174,175].

Early myeloid progenitors were suspected as a niche for viable mycobacteria since tuberculosis transmission was observed following bone marrow transplantation to culture-negative recipients [176-179]. Disease resuscitation after deceptively successful treatment of tuberculosis (meeting the WHO-guidelines for clinical treatment endpoints) was traced back to a viable bone marrow reservoir within $CD271^+$ $CD45^-$ mesenchymal stem cells that persisted through treatment [180-182,184,185]. Later, the presence and persistence of bone

marrow-dwelling mycobacteria was also confirmed in murine experimental tuberculosis [182]. Interactions of *M. tuberculosis* within the bone marrow are described to cause long-term impairments to the host's immune competence [158]. Macrophages derived from *M. tuberculosis*-infected donors fail to control growth of a secondary challenge both in vitro and in vivo. This impairment persists for at least one year after pathogen clearance and originates from epigenetically imprinted HSCs [158]. However, these studies predominantly focused on indirect signalling of anti-mycobacterial immune responses on HSCs and omitted a comprehensive characterization of possible direct interactions between *M. tuberculosis* and HSCs, leaving the source of this imprinting incompletely defined [158,169,186].

4.1 HSCs as a *M. tuberculosis* Niche

The recent discovery of *M. tuberculosis* DNA within human and murine HSCs, and preliminary image-based evidence of intact mycobacterial cells suggests host interactions between *M. tuberculosis* and HSCs beyond indirect immune signalling [187]. For the first time Tornack et al. identified a bacterial pathogen in the most upstream progenitors of hematopoiesis [187]. Even more striking, this observation is not a phenomenon of exacerbated active tuberculosis with systemic dissemination and bacteremia but is present in clinical cohorts of LTBI as well [187]. Hence, the quarter of the human population that is estimated to be latently infected with *M. tuberculosis* is prone to carry bacteria in their ultimate immune cell source. The role that infected HSCs play during distinct stages of tuberculosis progression - from initial infection, through latency, to active disease transition, remains largely unclear. HSCs may also provide the definitive reservoir in the bone marrow, acting as the protective niche for *M. tuberculosis* during antimicrobial treatment, which may lead to treatment failure and eventual disease resuscitation. Adoptive transfer of infected HSCs to susceptible hosts – deficient in inducible nitric oxide synthase ($Nos2^{-/-}$) – propagates tuberculosis, successfully demonstrating HSCs as a potential reservoir of viable bacteria and a source of disease resuscitation [188].

Of note, less than 1% of the HSC population harbors mycobacterial DNA in vivo, explaining why HSC infection by *M. tuberculosis* has not been documented earlier [187]. Furthermore, HSCs are traditionally regarded resistant to bacterial infection with archetypical Gram-negative and Gram-positive invasive pathogens, such as *Salmonella enterica* and *Listeria monocytogenes*, being unable to enter these cells [189]. Multiple reports on mycobacteria themselves also conflict, as to whether HSCs are permissive to infection by *M. tuberculosis*

and non-tuberculous mycobacteria. In vitro infection of murine bone marrow cells with *M. tuberculosis* failed to reproduce infection of Lin$^-$ c-Kit$^+$ Sca-1$^+$ hematopoietic progenitors, including HSCs [158]. Additionally, despite confirmed presence in the bone marrow after intravenous administration, cells harboring *M. bovis* BCG were limited to mature cells, and no mycobacteria were found in the Lin$^-$ c-Kit$^+$ Sca-1$^+$ hematopoietic progenitor population [169]. Resistance to infection has so far been attributed to a lack of essential pathways involved in pathogen recognition, internalization and processing. Intracellular pathogens are usually either internalized passively by professional phagocytic cells through phagocytosis (like *M. tuberculosis*) or actively induce their internalization by non-phagocytic cells through induction of membrane ruffles and macropinocytosis (like *Salmonella enterica*) [190,191]. To this point HSCs were not observed to engage in either of the two mechanisms [189]. Nevertheless, HSCs have been described to engage in immune surveillance and can cross-present antigens via MHC-II complexes, requiring at least fundamental pathways of antigen uptake and processing [192,193].

Taken together, the susceptibility of HSCs to *M. tuberculosis* infection is subject to ongoing discussions. The apparent discrepancies in HSC permissiveness to mycobacterial infection between various studies highlights the urgent need for a detailed characterization approach of *M. tuberculosis* internalization. The identification of determining factors of permissiveness and resistance might thus help to explain the observed variance in experimental outcomes. Furthermore, understanding the implications of mycobacterial presence in HSCs is crucial. Identifying the source of the described host impairments that eventually support pathogen persistence is pivotal to restore and protect immune competence of the hosts.

5. Objectives

Tuberculosis is a paradigm of latent disease in which the immune system continuously fails to ultimately clear the mycobacterial infection. Persistence of any pathogen necessitates an impairment of the host's immune competence. HSCs have recently been identified as targets to integrate long-lasting, detrimental immune modulations during tuberculosis [158]. These modulations impair the antimicrobial capacities of their macrophage progeny to fight the mycobacterial infection [158]. The discovery of *M. tuberculosis* DNA and intact mycobacterial cells within murine and human HSCs, might represent a crucial factor in mediating this impairment within the origin of the host's immune system [187].

However, traditionally HSCs are regarded non-phagocytic cells, and other studies failed to reproduce HSC infection in vitro [158,189]. Thus, the central aim of our study is to verify HSCs as definitive host cells of *M. tuberculosis* and to characterize the involved host-pathogen interactions facilitating internalization.

The key questions of this study were:

I) Can HSCs serve as host cells for *M. tuberculosis*?

II) How does *M. tuberculosis* gain access to the intracellular niche in HSCs?

III) Which factors determine HSC permissiveness to *M. tuberculosis*?

B. Materials

1. Chemicals and Reagents

Table 1: Chemicals and reagents used in this study.

Chemical / Reagent	Supplier	Cat. Nr.
Ammonium chloride (NH_4Cl)	Roth	K298.1
Albumin bovine Fraktion V, Protease-free	Serva	9048-46-8
Alexa Fluor® 488 Phalloidin	Thermo Fisher (Invitrogen)	A12379
Aqua destilata (Aq. dest.)	B. Braun	0082479E
BBL Middlebrook OADC Enrichment	BD Biosciences	21186
BD Cytofix™ Buffer	BD Biosciences	554655
BD™ Phosflow Perm Buffer III	BD Biosciences	558050
BD DIFCO™ Asparagine	BD Biosciences	214410
BD DIFCO™ Glycerol	BD Biosciences	228220
Bovine Serum Albumin	Sigma-Aldrich	A8806-1G
β-Mercaptoethanol 50 mM	Gibco	31350-010
CASYton Cellpak	Sysmex	83400116
4,6-Diamidino-2-Phenylindole (DAPI)	Invitrogen	D1306
Difco Middlebrook 7H9 Medium	BD Biosciences	262710
Difco 7H11 Agar	BD Biosciences	212203
Dimethyl sufloxide (DMSO)	Carl Roth	D2650
Dulbecco's Phosphate Buffered Saline (d-PBS)	Pan Biotech	P04-36500
Ethylenediaminetetraacetic acid (EDTA)	AppliChem	A2937,0500
Fatty Acid Supplement	Sigma	F6050
Fetal calf serum (FCS)	PAN Biotech	P30-3306
FITC Streptavadin	Biolegend	405201
Goat Serum*	Sigma-Aldrich	G9023
Hank's balanced salts solution (HBSS)	PAN Biotech	P04-49505
Human Transferrin	Sigma	T8158
Hygromycin B	PAN Biotech	P06-08020
Immersion oil for microscopy	Carl Roth	X8991
L-Glutamin (200mM)	PAN Biotech	P04-80100
Methanol*	Thermo Fisher	325740025
Milli-Q water	In-house	n.a
MEM non ess. Amino Acids 100x	Gibco	11140-035
Normal Goat Serum (NGS)	PAN Biotech	P30-1001
Pancoll human, Density: 1.077 g/ml	PAN Biotech	04-60500
Paraformaldehyde (PFA)	Carl Roth	0335.3
Paraformaldehyde (PFA)*	Electron Microscopy Sciences	15710
Penicillin-Streptomycin	PAN Biotech	P06-07100
Phosphate Buffered Saline (PBS)*	Gibco	10010-049
Potassium Hydrogen Carbonate ($KHCO_3$)	Roth	298-14-6
RPMI 1640 w/o L-Glutamine	PAN Biotech	P04-17500
RPMI 1640 w/ L-Glutamine*	Gibco	11875-119

Sodium Azide (NaN_3)	Merck	8223350
Tween 20/80	Sigma-Aldrich	P9416/-P8074
TRI Reagent	Zymo Research	R2050-1-200
Triton X-100	Carl Roth	3052.3
Trypan blue	Carl Roth	1680.1

*: Experiments performed at the CCHMC.

1.2 Treatment Agents

Table 2: Inhibitors, cytokines, stimulants and pathogen-associated molecular patterns (PAMPs) used as treatment agents in this study.

Compound	Supplier	Cat. Nr.
Inhibitors:		
Cytochalasin D	Sigma	C2618
Imipramine hydrochloride	Sigma-Aldrich	I7379
Mannan from *S. cerevisiae*	Sigma-Aldrich	M7504
Pitstop 2	Sigma-Aldrich	SML1169
Sulfo-N-succinimidyl oleate (SSO)	Sigma-Aldrich	SML2148
Cytokines/Stimulants:		
Angiopoetin 1, human recombinant	Peprotech	130-06
M-CSF, human recombinant	Biolegend	574802
IL-6, human recombinant	Peprotech	200-06
SCF, murine recombinant	Peprotech	250-03
TPO, murine recombinant	Peprotech	315-14
PAMPs:		
Cell wall fraction[*1,2]	BEI Resources[*3,4]	NR-14828
Cell membrane fraction[*1,2]	BEI Resources[*3,4]	NR-14831
Culture filtrate proteins[*1,2]	BEI Resources[*3,4]	NR-14825
Gamma-irradiated whole cells[*1,2]	BEI Resources[*3]	NR-49098
Lipopolysaccharide (from *S. Minnesota* R595)	Alexis Biochemicals	581-008-L002
Purified peptidoglycan[*1,2]	BEI Resources[*4]	NR-14853
Purified trehalose dimycolate (TDM) [*1,2]	BEI Resources[*3,4]	NR-14844
Total lipids[*1,2]	BEI Resources[*3,4]	NR-14837
Whole cell lysate[*1,2]	BEI Resources[*3,4]	NR-14822

[*1]: From *Mycobacterium tuberculosis*, Strain H37Rv
[*2]: The reagent was obtained through BEI Resources, NIAID, NIH
[*3]: Manufacturer: Colorado State University, Fort Collins, Colorado, USA (Karen Dobos)
[*4]: Manufacturer: NIH – TB Vaccine Testing and Research Materials Contract

2. Consumables

Table 3: Consumables used in this study.

Consumable	Supplier	Cat. Nr.
25 mL serological pipettes	Corning	4489

10 mL serological pipettes	Corning	4488
5 mL serological pipettes	Corning	4487
1000 µL Biosphere filter tips	Sarstedt AG & Co. KG	70.762.211
200 µL Biosphere filter tips	Sarstedt AG & Co. KG	70.1130.210
20 µL ART barrier tips	Thermo Scientific	2149P-HR
20 mL syringes	BD Discardit II	300296
10 mL syringes	BD Discardit II	309110
5 mL syringes	BD Discardit II	309050
0,1 mm Neubauer-counting chamber	Marienfeld GmbH&Co.KG	06 400 10
50 mL syringes	BD Plastipak	300865
1 mL syringes	BD Plastipak	303172
27G 3/4" needles	BD Biosciences	302200
26G 3/8” needles	BD Biosciences	300300
Micro sample tube Serum Gel CAT, 1.1ml	Sarstedt AG & Co. KG	41.1378.005
50 /15 mL tubes	Sarstedt AG & Co. KG	62.547.254
15 mL tubes	Sarstedt AG & Co. KG	62.554.502
2 mL micro tubes	Sarstedt AG & Co. KG	73.694.006
1 mL micro tubes	Sarstedt AG & Co. KG	73.692.005
0,5 mL micro tubes	Sarstedt AG & Co. KG	73.730.006
Teflon bags	Crosstex	
TC Flask T25, Standard, Filter cap	Sarstedt AG & Co. KG	83.3910.002
0,20 µm syringe pre-filter	BD Biosciences	83.1826.102
70 µm cell strainer	BD Biosciences	431751
100 µm cell strainer	BD Biosciences	352360
24 flat well cell culture plates	Corning	3526
12 flat well cell culture plates	Corning	3513
6 flat well cell culture plates	Corning	3516
92 x 16 mm Petri dishes	Sarstedt AG &Co. KG	82.1472
10 x 4 x 5 mm polystyrene cuvettes	Sarstedt AG &Co.	67.742
5 mL polystyrene round-bottom tube (FACS tube)	Corning	352054
SepMate™-50 (IVD) *	StemCell	85450
LD Columns	Miltenyi Biotec	130-042-901
LS Columns	Miltenyi Biotec	130-042-401
Parafilm M All-purpose laboratory film	Bemis	PM996

3. Buffers, Solutions and Media

Table 4: Buffers, Solutions and Media used in this study.

Buffer / Solution / Medium	Composition
4 % PFA	4 % (w/v) Paraformaldehyde *In PBS*
7H11 Agar medium	1.9 % (w/v) 7H11 Agar 0.5 % (v/v) Glycerine 0.1 % (w/v) BD DIFCO™ Asparagine *In Milli Q water*

7H9 liquid medium	0.05 % (v/v) Tween 80 0.47 % (w/v) 7H9 Agar 10 % (v/v) OADC medium prior to use *In Milli Q water*
Blocking buffer	10 % (v/v) Normal Goat Serum 0.01 % (v/v) Triton X-100 *In PBS*
Elutriation medium	0.1 % (v/v) BSA *In HBSS*
FACS buffer	0.1 (v/v) % FCS 0.01 (w/v) % NaN_3 2 mM EDTA *In PBS*
FACS Sorting buffer	0.1 % (v/v) FCS 2 mM (w/v) EDTA *In PBS*
Fc receptor-blocking buffer (human)	10 % (v/v) autologous donor serum *In FACS buffer*
Fc receptor-blocking buffer (murine)	1 % (v/v) Rat serum 1:50 (v/v) anti-CD16/32 *In FACS buffer*
MACS buffer	0.5 % (v/v) BSA 2 mM EDTA *In PBS*
Macrophage differentiation medium	10 % autologus serum 1 % (v/v) L-Glutamine (200 mM) 1 % (v/v) Pen-Strep 10 ng/mL M-CSF *In RPMI1640*
Macrophage medium	10 % (v/v) FCS 1 % (v/v) L-Glutamine (200 mM) 10 ng/mL M-CSF *In RPMI1640*
Erythrocyte lysis buffer	155 mM NH_4Cl 0.1 mM EDTA 10 mM $KHCO_3$ *In Aqua dest. (pH 7.2-7.4)*
Complete RPMI (cRPMI)	10 % (v/v) FCS 1 % (v/v) L-Glutamine (200 mM) *In RPMI 1640 w/o L-Glutamine*
KM-IMDM *(serum-free)*[*1]	0.1 % (v/v) β-Mercaptoethanol 50 mM 1 % (v/v) MEM non ess. Amino Acids 100X 0.005 % (v/v) Fatty Acid Supplement 1 % (w/v) Bovine Serum Albumin (delipified) 0.1 % (v/v) human Transferrin (10 mg / mL in PBS) 20 ng/mL murine recombinant SCF 20 ng/mL human recombinant IL-6 20 ng/mL murine recombinant TPO 20 ng/mL human recombinant Angiopoetin 1 *In IMDM medium*

[*1]: Composition of the medium kindly provided by Dr. Peter Jani (German Rheumatism Research Center Berlin).

4. Kits

Table 5: Kits used in this study.

Kit	Supplier	Cat. Nr.
Lineage Cell Depletion Kit, mouse	Miltenyi Biotec	130-110-470
CD34 MicroBead Kit UltraPure, human	Miltenyi Biotec	130-100-453
LIVE/DEAD® Fixable Near-IR Dead Cell Stain Kit*	Thermo Scientific	L34976
Zombie NIR™ Fixable Viability Kit	Biolegend	423105
Zombie Green™ Fixable Viability Kit	Biolegend	423111

*: Experiments performed at the CCHMC.

5. Antibodies

Table 6: Antibodies used for immunofluorescence staining in this study.

Antigen	Conjugate	Host	Clone	Supplier	Cat. Nr.
CD3*	APC/Fire 750	ms	17A2	Biolegend	100247
CD16/32	-	ms	93	Biolegend	101302
CD34	BV421	hu	561	Biolegend	343609
CD34	PE	ms	SA376A4	Biolegend	152203
CD36	FITC	hu	5-271	Biolegend	336203
CD38	PE/Cy7	hu	HIT2	Biolegend	303515
CD41*	AF647	ms	MWReg30	Biolegend	133933
CD45RA	APC/Cy7	hu	HI100	Biolegend	304127
CD48*	AF488	ms	HM48-1	Biolegend	103414
CD48	APC-Cy7	ms	HM48-1	Biolegend	103431
CD90	BV510	hu	5E10	Biolegend	328125
CD127	PE-Cy7	ms	A7R34	Biolegend	135013
CD150	BV421	ms	TC15-12F12.2	Biolegend	115925
CD150	PerCp/Cy5.5	ms	TC15-12F12.2	Biolegend	115921
CD150	BV650	ms	TC15-12F12.2	Biolegend	115931
c-Kit	BV421	ms	2B8	Biolegend	105827
c-Kit*	BV480	ms	2B8	Thermo Fisher	414-1171-82
ESAM*	PE	ms	1G8/ESAM	Biolegend	136203
Lineage, human[*1]	APC	hu	*1	Biolegend	348703
Lineage, murine[*2]	Biotin	ms	*2	Biolegend	133307
MMR	AF488	hu	15-2	Biolegend	321113
Sca-1	APC	ms	D7	Biolegend	108111
pStat3	AF488	hu	4/P-STAT3	BD Biosciences	557714
TLR2	FITC	hu	W15145C	Biolegend	392307
TLR4	Biotin	hu	HTA125	Biolegend	312804
TLR9	FITC	hu	S16013D	Biolegend	394809

[*1]: Antigens: CD3, CD14, CD19, CD20, CD56; Clones: UCHT1, HCD14, HIB19,2H7, HCD56
[*2]: Antigens: CD3, Gr-1, CD11b, CD45R/B220, Ter-119; Clones: 145-2C11; RB6-8C5; M1/70 RA3-B2; Ter119

6. Equipment

Table 7: Laboratory Equipment used in this study.

Equipment	Supplier
Avanti J-26S XP centrifuge	Beckman Coulter
BD FACSCanto™ II	BD Biosciences
BD LSRFortessa™	BD Biosciences
BD FACSymphony™ A3	BD Biosciences
BD FACSAria™ IIIu	BD Biosciences
Branson sonicator cell disrupter W450	Thermo Scientific
CASY Cell Counter	Schaerfe Systems
Hera cell 240 incubator	Thermo Scientific
Heraeus multifugue 3SR+	Thermo Scientific
Jenway™ 6320D visible spectrophotometer	Thermo Scientific
Leica TCS SP5	Leica
Masterflex L/S elutriation pump	Masterflex
MSC-Advantage™ class II biological safety cabinet	Thermo Scientific
Nikon AXR inverted confocal microscope	Nikon
Nikon SMZ1500 stereomicroscope	Nikon
Nikon Eclipse TS100 inverse microscope	Nikon
AP224W analytical balance	Shimadzu
QTUM000EX quantum EX polishing cartridge for Mill-Q system	Merck Chemicals GmbH
Thermo Scientific™ multifuge X4 Pro	Thermo Scientific

7. Software

Table 8: Software used in this study.

Software	Publisher
BD FACSDiva™ software v.9	BD Biosciences
BioRender 2024*	BioRender
FlowJo™ v10.10	BD Biosciences
GraphPad Prism version v10.3.0	GraphPad Software, Inc. (La Jolla, U.S.A)
Imaris v10.2	Bitplane
Leica Application Suite X software v.1.4.6.28433	Leica Microsystems
Luminar Neo v1.20.0[*1]	Skylum
Mendeley Desktop v.2.119.0	Elsevier (London, UK)
Microsoft 365[*1]	Microsoft
NIS-Elements software v5.30.03	Nikon
pyRAT System v4.2-323	Scionics Computer Innovation GmbH (Dresden, DE)

*: Except Fig. 1, all figures in this study were created with biorender.com

8. Bacterial Strains

Table 9: Bacterial Strains used in this study.

Strain	Genotype	Antibiotics	Source
Mycobacterium tuberculosis H37Rv	Wild type	-	Albert Einstein College of Medicine, New York, USA (W.R. Jacobs)
Mycobacterium tuberculosis H37Rv DsRed	pSMT3-S (P_{smyc}'::*Ds*Red, Hyg^R	Hygromycin (50 µg/ml)	Queen Mary University of London, London, England (T. Parish)
Mycobacterium tuberculosis H37Rv ΔRD1 mCherry	ΔRD1, pCherry27 (pSMT3-S) (P_{smyc}'::mCherry, Hyg^R)	Hygromycin (50 µg/ml)	Suzanne M. Hingley-Wilson, William R. Jacobs

9. Murine Strains

Table 10: Murine Strains used in this study.

Strain	Genotype	Health Status	Breeder
C57Bl/6J	wt	SPF	Animal facility, Research Center Borstel
C57Bl/6J	wt	SPF	Animal facility, Cincinnati Children's Hospital Medical Center

C. Methods

1. Serum, Cell and Organ Isolation

1.1 Ethical Statements

Animal handling and all animal experimental procedures at the Research Center Borstel (Borstel, Germany) were performed in strict accordance with protocols approved by the Ethics Committee for Animal Experiments of the Ministry of Energy, Agriculture, Environment, Nature and Digitalization, State of Schleswig-Holstein, Germany, under license number A60. Euthanasia was conducted via lethal CO_2 inhalation under CO_2-induced anaesthesia, in compliance with Paragraph §2(2) of the German 'Tierschutz-Versuchstier Verordnung' (TierSchVerV).

Animal handling and all animal experimental protocols at Cincinnati Children's Hospital Medical Center (Cincinnati, OH, USA) were conducted under approval by the University of Cincinnati Institutional Review Board under protocol number 2022–0049 ex 11–2025. Euthanasia was performed via lethal CO_2 inhalation under CO_2-induced anaesthesia.

All animal experimental work adhered to the 3R-principle (replacement, reduction, refinement) [194,195].

The experimental procedures involving the isolation of human blood cells from adult donors at the Research Center Borstel (Borstel, Germany) were approved by the Ethics Committee of the University of Lübeck, Germany (number 22-202A). Informed consent and authorization were obtained from each individual donor.

Similarly, the isolation of human blood cells from neonatal umbilical cord blood at the Research Center Borstel was conducted with the approval of the Ethics Committee of the University of Lübeck, Germany (number 21-071). Consent and authorization were obtained from the legal guardians of each individual.

1.2 Preparation of Murine Samples

1.2.1 Euthanasia of Mice

Individual mice were anesthetized via a slow gradual increase of CO_2 inhalation before a lethal concentration of CO_2 in the air was achieved. Death was confirmed by cessation of both heartbeat and respiration, as well as the absence of corneal and toe pinch reflexes. Subsequently, cervical dislocation was performed to ensure euthanasia, and the mice were sterilized using 70 % ethanol. For the collection of organs, bones and blood the abdominal cavity or the thorax were aseptically opened.

1.2.2 Preparation of Murine Autologous Serum

Murine blood was collected from the *vena cava* of euthanized animals using a 1mL syringe with a 27G needle and subsequently transferred into Serum Gel micro tubes, which were immediately stored on ice. The tubes were then centrifuged at 4000 rcf, at 4 °C, for 10 min. Following centrifugation, the serum supernatant was aspirated from the top of the gel layer and was stored at – 80 °C until further use.

1.2.3 Isolation and Preparation of Murine Bone Marrow Cells

Murine Bone marrow was isolated from femur and tibia. The hind legs were dissected, and excess soft and connecting tissue was removed using tissue cloth and scissors. The epiphyses were excised and preserved in a 70 µm cell strainer that was used for subsequent bone flushing. The strainer was placed on a 50 mL conical tube, and each bone was gently flushed through the strainer with 10 mL cRPMI1640 using a syringe fitted with a 28G needle. The epiphyses were cut into smaller pieces and superficially flushed with cRPMI1640 (4 °C) while concurrently crushing the pieces with the syringe plunger until a total volume of 50 mL was reached. The bone marrow sample was centrifuged at 500 rcf at 4 °C for 5 min. and resuspended in 3 mL erythrocyte lysis buffer at room temperature. Lysis was terminated by the addition of 20 mL cRPMI1640 (4 °C) and the sample was centrifuged again at 500 rcf at 4 °C for 5 min. The resulting pellet was resuspended in either 1 mL cRPMI1640 (37 °C) for cell culture **(section C.3)** or 1 mL PBS (4 °C) for subsequent magnetic-activated cell separation

(MACS) **(section C.1.2.4)**. The final cell count was determined using a light microscope and a counting chamber, with a 1:100 dilution in PBS.

1.2.4 Enrichment of Hematopoietic Progenitors from Murine Bone Marrow Cells

To enrich the proportion of hematopoietic progenitor cells in murine bone marrow samples **(section C.1.2.3)**, lineage-positive cells ($CD3^+$, $CD45R^+$ (B220), $CD11b^+$, $Gr\text{-}1^+$ (Ly-6G/C), and $Ter\text{-}119^+$) were depleted using magnetic cell separation via the 'direct lineage cell depletion Kit - mouse' (Miltenyi Biotec), following the manufacturer's instructions. Isolated murine bone marrow cells were transferred into a 15 mL conical tube and centrifuged (500 rcf, 4 °C, 5 min.). The pellet was resuspended in an appropriate volume of MACS buffer, to which magnetic bead-coupled antibodies were added. Lineage-positive cells were retained in a LS Column (Miltenyi Biotec), while untouched lineage-negative hematopoietic progenitors were collected in the flow-through. After a wash step (500 rcf, 4 °C, 5 min.), the cells of the flow-through were resuspended in cRPMI1640. The cell count was determined using a light microscope and a counting chamber, with a 1:10 dilution in PBS. The enriched progenitor cells were then seeded for cell culture **(section C.3)**.

1.3 Preparation of Human Samples

1.3.1 Preparation of Mononucleated Cells from Adult Human Peripheral Blood

Peripheral blood (300 – 400 mL) from adult mixed sex, healthy donors between the age of 18 to 65 was collected. Blood was diluted 1:1 with PBS (37 °C). Carefully, 10 mL Pancoll (37 °C), was overlaid with 40 mL blood in 50 mL conical tubes. After centrifugation (500 rcf, RT, 45 min.) without breaks, mononucleated cells were aspirated from the Pancoll-PBS interface layer and transferred to new tubes on ice. Cells were washed once (500 rcf, 4 °C, 5 min.), unified and resuspended in 20 mL PBS (4 °C). Platelets were depleted by centrifugation (300 rcf, 4 °C, 10 min.) and supernatants, containing most platelets, were carefully aspirated. The pellet was resuspended in either cRPMI1640 (37 °C) for immediate use as a mononuclear cell (MNC) culture **(section C.3.1)**, in elutriation medium for elutriation and macrophage differentiation (C.1.3.5), or in PBS (4 °C) for further enrichment by MACS **(C.1.3.3)**. For either

use, the final cell count was determined by cell counting in a light microscope, using a counting chamber with a 1:1000 dilution in PBS.

1.3.2 Preparation of Mononucleated Cells from Neonatal Human Umbilical Cord Blood

Pregnant women aged 18 to 36 scheduled for non-emergency caesarean sections were enrolled in the study. Immunologically relevant exclusion criteria included antenatal antibiotic administration 2 – 14 days before delivery, HIV-positivity, heritable autoimmune diseases and fever exceeding 38 °C. The status of BCG vaccination or prior *M. tuberculosis* infection was assessed through patient notification.

Neonatal umbilical cord blood (5 – 10 mL) was collected via puncture of the *vena umbilicalis impar* immediately after umbilical cord disconnection. The umbilical cord blood was diluted 1:1 with PBS (37 °C). 10 mL Pancoll, (37 °C), was carefully overlaid with 10-20 mL of the diluted blood sample in 50 mL conical tubes. Following centrifugation (500 rcf, RT, 45 min.) without breaks, mononucleated cells were aspirated from the Pancoll-PBS interface layer and transferred to new tubes on ice. The cells were then washed once by centrifugation (500 rcf, 4 °C, 5 min.), unified, and resuspended in 20 mL PBS (4 °C). Platelets were depleted by centrifugation (300 rfc, 4 °C, 10 min.) and the supernatant, containing most platelets, was carefully aspirated. The pellet was resuspended in PBS (4 °C) for subsequent enrichment through magnetic cell separation (MACS) **(section C.1.3.3)**. The final cell count was determined using a light microscope and using a counting chamber, with a 1:1000 dilution in PBS.

1.3.3 Enrichment of Hematopoietic Progenitors from Human Mononucleated Peripheral Blood Cells

Human hematopoietic stem and progenitor cells (HSPCs) from peripheral blood were enriched using magnetic cell separation with the 'CD34 MicroBead Kit UltraPure, human' (Miltenyi Biotec) in accordance with the manufacturer's instructions. Briefly, isolated mononucleated cells from human blood were transferred into a 15 mL conical tube and centrifuged (500 rcf, 4°C, 5 min.). The resulting pellet was resuspended in an appropriate volume of MACS buffer, and magnetic bead-conjugated antibodies were added. A LS-column (Miltenyi Biotiec) was used to retain labelled $CD34^+$ cells, while non-target cells were

discarded with the flow-through. After removing the column from the magnetic separator, it was eluted to collect the $CD34^+$-enriched hematopoietic progenitors. Following a wash step (500 rcf, 4°C, 5 min.), the cells were resuspended in cRPMI1640. The cell count was determined using a light microscope and a counting chamber, with 1:10 dilution in PBS. The enriched cells were then seeded for further cell culture **(section C.3)**.

1.3.4 Preparation of Adult Human Autologous Serum

To prepare human autologous serum for the opsonization of mycobacteria or to use as a component of the Fc receptor-blocking buffer, 1 mL of donor blood was collected into a Serum Gel micro tube, prior to initial 1:1 PBS dilution, and immediately placed on ice. Tubes were centrifuged (4000 rcf, 4°C, 10 min.) before the serum supernatant was aspirated from the top of the gel layer and was stored at – 80 °C until use.

1.3.5 Elutriation and Differentiation of Human Monocyte-Derived Macrophages

For elutriation cell numbers were quantified using the CASY 2 cell counter. The cell suspension was mixed 1:1 with CASYton cellpak and measured with the following setup:

Table 11: CASY 2 cell counter setup.

Setup number	18	Name	Macrophage
Capillary	150 µm	X-axis	30 µm
Sample volume	400 µl	Cycles	3
Dilution	1.000e+0.3		
Y-axis	Auto		
Eval. cursor	8.25 – 25.58 µm		
Norm. cursor	5.25 – 30.00 µm		
% calucation	% via	Debris	On
Aggr. correction	Off	P. vol	0.000e+00 fl
Interface	Par	P. feed	Off
Print mode	Manual	Graphic	On

Before elutriation, the centrifuge was cooled to 4 °C, the tubing system was flushed with 200 mL 70 % ethanol, 300 mL sterile double distilled water and 200 mL elutriation medium. The pump speed was set to 1.8 mL/min. and 50 mL of the prepared MNC cell suspension **(section C.1.3.1)** was loaded. The valve was changed, and the elutriation buffer was led through the tubing system. Flow-through was collected in a sterile glass cylinder. After 200 mL elutriation

volume, the speed was set to 2 mL/min. After another 50 mL elutriation volume, the speed was to 2.2 mL/min. and gradually increased for every 50 mL of elutriation volume, up to a maximum of 2.7 mL/min. Elutriated cells were counted using the CASY 2 cell counter and at 2.7 mL/min. and around 80 % monocyte purity, centrifugation was stopped. 50 mL were subsequently collected in a sterile tube. Final cell counting yielded monocyte purity of around 90 % on average. The cell suspension was centrifuged (500 rcf, RT, 10 min.), the supernatant was discarded, and the pellet was resuspended in 1 mL cRPMI1640 medium. To differentiate monocytes into monocyte-derived macrophages, 25 – 30 million monocytes were diluted in 50 mL macrophage differentiation medium (10 ng/mL M-CSF) and incubated in a sterile polytetrafluoroethylene-coated plastic bag for 6-7 days at 37 °C and 5 % CO_2. After incubation, the plastic bag was pulled along an edge and the cell suspension was transferred to a 50 mL conical tube. Following centrifugation (500 rcf, 4°C, 10 min.), the supernatant was discarded, and the macrophage cell pellet was resuspended in 1 mL macrophage medium. Cells count and viability was determined via Trypan blue staining using a light microscope and a counting chamber. Cells were seeded at the desired concentration in KM-IMDM (serum free) and used for STAT3 activation controls **(section C. 3.3)**.

2. Microbiological Techniques

2.1 Cultivation of *M. tuberculosis*

For most in vitro cell culture infections, a genetically modified strain of *Mycobacterium tuberculosis* H37Rv NY, constitutively expressing a DsRed vector was used. A wildtype strain was used for non-fluorescent controls or lysate preparations when indicated.

Frozen stocks were thawed and cultured at a 1:5 ratio in Middlebrook 7H9 liquid medium, supplemented with 10 % (v/v) OADC (Oleic acid, Albumin, Dextrose, Catalase). For fluorescent strains, the appropriate antibiotic was added to the medium **(section B.8)**. After incubation at 37 °C for 3 – 4 days in a humidified chamber, a 1:10 subculture was passaged into fresh medium. For in vitro infections, only bacteria from passages 2 – 4 were used.

2.2 Isolation of Single Cell Suspensions of *M. tuberculosis*

To obtain single cell suspensions, mycobacteria from passages 2 – 4 were transferred into 15 mL conical tubes. Bacteria were washed twice with 10 mL PBS (4000 rcf, 4 °C, 10 min.) and

subsequently resuspended in 1 mL PBS. To separate cell aggregates bacterial suspensions were passed 5 times though a 27G blunt end needle attached to a 1 mL syringe. The bacterial concentration was determined by measuring the optical density (OD) at 580 nm. For this purpose, the bacterial suspension was transferred into polystyrene cuvettes at a 1:10 dilution in 4 % PFA. The following equation was used to estimate the number of bacteria per mL:

$$\text{Bacteria / mL} = OD_{580\ nm} \times (5 \times 10^8)_{\text{[conversion factor]}} \times 10_{\text{[dilution factor]}}$$

2.3 Colony-Forming Unit Enumeration Assay

To quantify viable mycobacteria in vitro, 100 µl of the prepared *M. tuberculosis* lysates **(section C.3.2)** were plated onto Middlebrook 7H11 agar plates, supplemented with 10% (w/v) OADC, in triplicates. Colonies were counted after 21 – 28 days of incubation at 37 °C in a humified chamber.

3. Cultivation of Primary Cells and Cell Culture Assays

3.1 In Vitro Infection of Murine and Human Primary Cells

Following the isolation of murine and human mononucleated cells or enriched hematopoietic progenitor cells (**sections C.1.2 & C.1.3)**, the cells were seeded at a concentration of 2.5 x 10^5 cells/mL in cRPMI1640 for most experiments, unless otherwise specified. For human cell cultures designated for subsequent measurement of intracellular phosphorylation of signal transducers and transcription factors **(section C.4.4)**, cells were cultured in serum-free KM-IMDM medium instead. For in vitro infection, single-cell suspensions of *M. tuberculosis* (**section C.2.2)** were inoculated at multiplicities of infection (MOIs) of 1, 3, 5 or 10, immediately after seeding the primary cells. All cultures were incubated at 37 °C and 5 % CO_2 in humified chambers for 20 hours post infection, unless other timepoints are specified.

3.2 Characterization of Internalization Pathways

Cells were treated with inhibitors of the respective internalization pathways 2 hours prior to the infection, where indicated. **Table 12** provides a summary of the inhibitors used, their final concentration in the cell culture and their diluents.

Table 12: Internalization pathway inhibitors used in hematopoietic stem and progenitor cells and their application specificities.

Inhibitor	Final concentration	Diluent
Cytochalasin D	2 µg / mL	DMSO
Pitstop II	20 µM	DMSO
Imipramine Hydrochloride	5 µM	Water
Sulfo-N-succinimidyl oleate (SSO)	200 µM	DMSO
Mannan from *S. cerevisiae*	1 µg / mL – 10 mg / mL	Water

For all inhibitor-treated conditions, single-cell suspensions of *My. tuberculosis* **(section C.2.2)** were inoculated at a MOI of 10, following the pre-treatment period. Cultures were incubated at 37 °C and 5 % CO_2 in humified chambers for 20 hours post-infection.

To assess the influence of opsonic phagocytosis, *M. tuberculosis* single cell suspensions were incubated at a ratio of 1:1 with autologous donor serum **(sections C.1.2.2 & C.1.3.4)** for 30 min. prior to infection at room temperature. Subsequently, opsonized *M. tuberculosis* **(section C.2.2)** were inoculated at a MOI of 10, immediately after seeding of primary cells. Cultures were incubated at 37 °C and 5 % CO_2 in humified chambers for 20 hours post-infection.

After incubation, the infection frequency in all conditions was determined by fluorescence-activated cell sorting (FACS) **(section C.4.3)**.

3.2 Pre-Stimulation with Lysates and Pathogen-Associated Molecular Patterns

For lysate pretreatment, a single-cell suspension of wildtype *Mycobacterium tuberculosis* wildtype with a known concentration was obtained **(section C.2.2)** and subjected to 12 cycles of sonication (10 seconds sonification, 5 seconds pause, Branson Sonicator Cell Disrupter W450). Successful lysis was confirmed by CFU analysis of an undiluted sample **(section C.2.3)**. The cell culture was pre-treated with the lysate at a concentration equivalent to a MOI of 10 for 18 hours at 37 °C and 5 % CO_2. Following this treatment, the cell culture was inoculated with viable *M. tuberculosis* DsRed at a MOI of 10 for 2 hours. Post-incubation, the infection frequency was determined by FACS **(section C.4.3)**.

For the characterization of responses to specific mycobacterial PAMPs, cell cultures of enriched hematopoietic progenitors were incubated with purified *M. tuberculosis*-derived

PAMPs, lipopolysaccharide (LPS) or Interluekin-6 (IL-6) for 20 hours at 37 °C ad 5 % CO_2. The proportion of $CD36^+$ HSCs, as a proxy for permissiveness, was quantified by FACS **(section C.4)**. **Table 13** lists the specific molecules, their final concentration in cell culture and their respective diluents.

Table 13: Pathogen-associated molecular patterns (PAMPs) used for stimulation of hematopoietic stem and progenitor cells and their application specificities.

PAMP	Final Concentration	Diluent
Gamma-Irradiated Whole Cells	20 µg / mL	PBS
Whole Cell Lysate	20 µg / mL	PBS
Cell Membrane Fraction	20 µg / mL	PBS
Cell Wall Fraction	20 µg / mL	PBS
Total Lipids	20 µg / mL	DMSO
Purified Peptidoglycan	20 µg / mL	50 % Methanol
Culture Filtrate Proteins	20 µg / mL	PBS
Purified Trehalose Dimycolate	20 µg / mL	DMSO
Controls:		
LPS	100 ng / mL	PBS
IL-6, human recombinant	200 ng / mL	PBS

3.3 Stimulation of Monocyte-Derived Macrophages for Phosphoprotein Analysis

Following the differentiation into human monocyte-derived macrophages **(section C.1.3.5)**, macrophages were seeded at a concentration of 1 x 10^6 cells/mL in KM-IMDM (serum free). As a positive-control for STAT3 activation, IL-6 was added to a final concentration of 200 ng/mL. Cultures were incubated at 37 °C and 5 % CO_2 in humified chambers for 15 min. After incubation, stimulated macrophages were collected and used for phosphoprotein analysis of STAT3 activation **(section C.4.4)**.

4. Phenotypic Analysis of Cell Populations Using FACS

4.1 Immunofluorescence Staining of Surface Antigens

For in vitro phenotypic analysis or sorting for confocal laser scanning microscopy, cell cultures were transferred to FACS tubes for immunofluorescence staining at indicated time points post-infection. Cells were centrifuged (500 rcf, 4 °C, 5 min.) and the supernatant was

discarded. For optional cell viability determination, either the 'Zombie NIR™ Fixable Viability'-Kit (Biolegend) or the 'Zombie Green™ Fixable Viability'-Kit (Biolegend) were used, according to the manufacturer's instructions. Briefly, the cell pellet was washed with PBS (500 rcf, 4 °C, 5 min.) and resuspended in 200 µl of a 1:1000 diluted dye solution in PBS. Samples were incubated for 30 min. at room temperature, centrifuged (500 rcf, 4 °C, 5 min.) and the supernatants were discarded. Cells were then resuspended in 100 µl Fc receptor-blocking buffer to prevent unspecific binding. For staining protocols without cell viability determination, cells were immediately resuspended in 100 µl Fc receptor-blocking buffer after initial transfer and centrifugation of the cell culture. Following incubation on ice for 15 min., 100 µl of antibodies diluted in FACS buffer (Lin-antibodies: 20 µl / 10^6 cells; other antibodies: 5 µl / 10^6 cells) were added, and cells were further incubated on ice for 15 min. The specific antibody panels used can be found in **section C.4.2**. Post-incubation, cells were centrifuged (500 rcf, 4 °C, 5 min.) and resuspended in 4% PFA in PBS for overnight fixation at 4 °C. Prior to FACS, the cell were centrifuged (500 rcf, 4 °C, 5 min.) again and resuspended in either 300 µl FACS buffer for flow cytometric analysis, or 500 µl MACS buffer for flow cytometric sorting.

4.2 Panel Design for Multi-Parameter Flow Cytometry

The following flow cytometry staining panels **(Tables 14-17)** were utilized to identify murine and human HSPCs using flow cytometric analysers (BD FACSCanto™ II, BD LSRFortessa™ and BD FACSymphony™ A3) or flow cytometric sorters (BD FACSAria™ IIIU). To mitigate potential epitope interference, a distinct α-human CD34 antibody (561) was employed, recognizing an epitope different from that recognized by the α-human CD34 antibody (QBEND/10) included in the 'CD34 MicroBead Kit UltraPure, human' (Miltenyi Biotec).

Table 14: FACS-panel used for flow cytometric analysis in a BD FACSCanto™ II.

Laser	Filter	Fluorochrome	Murine HSPCs	Human HSPCs
405 nm	450/40	BV421	c-Kit	CD34
	510/50	BV510	Lineage*1	-
488 nm	530/30	FITC/AF488	-	*Refer to Tab. S*
	585/42	DsRed/mCherry	*Refer to C.5.3*	*Refer to C.5.3*
	670/LP	PerCP-Cy5.5	CD150	CD90
	780/60	PE-Cy7	CD127	CD38
633 nm	660/20	APC	Sca-1	Lineage*2
	780/60	APC-Cy7	CD48	CD45RA

Table 15: FACS-panel used for flow cytometric analysis in a BD LSRFortessa™.

Laser	Filter	Fluorochrome	Human HSPCs
405 nm	450/50	BV421	CD34
488 nm	530/30 694/40	FITC PerCP-Cy5.5	*Refer to Tab. S* CD90
561 nm	780/60	PE-Cy7	CD38
633 nm	670/14 780/60	APC APC-Cy7 Zombie NIR™	Lineage[*2] CD45RA LIVE/DEAD[*3]

Table 16: FACS-panel used for flow cytometric analysis in a BD FACSymphony™ A3.

Laser	Filter	Fluorochrome	Human HSPCs
405 nm	431/28	BV421	CD34
488 nm	710/50	PerCP-Cy5.5	CD90
561 nm	586/15 780/60	DsRed PE-Cy7	*Refer to C.5.3* CD38
633 nm	670/30 780/60	APC APC-Cy7 Zombie-NIR™	Lineage[*2] CD45RA LIVE/DEAD[*3]

Table 17: FACS-panel used for flow cytometric sorting in a BD FACSAria™ IIIu.

Laser	Filter	Fluorochrome	Murine HSPCs I	Murine HSPCs II	Human HSPCs
405 nm	450/40 525/50 661/20	BV421 BV510 BV650	c-Kit Lineage*1 -	c-Kit Lineage*1 CD150	CD34 - -
488 nm	695/40	PerCP-Cy5.5	CD150	-	CD90
561 nm	582/15 780/60	DsRed PE-Cy7	*Refer to C.5.3* CD127	*Refer to C.5.3* CD127	*Refer to C.5.3* CD38
633 nm	660/20 780/60	APC APC-Cy7	Sca-1 CD48	Sca-1 CD48	Lineage[*2] CD45RA

[*1]: The murine Lineage-antigens include: CD3, Gr-1, CD11b, CD45R/B220, Ter-119
[*2]: The human Lineage-antigens include: CD3, CD14, CD19, CD20, CD56
[*3]: The Zombie NIR™ Fixable Viability Kit was only used where indicated

Additional surface and intracellular antigens were analyzed using FITC or AF488-conjugated antibodies or molecules **(Tab. 18)** in the panels described above.

Table 18: Additional surface and intracellular antigens analyzed for phenotypic characterization of hematopoietic stem and progenitor cells.

Antigen	Fluorochrome
CD36	FITC
MMR (CD206)	FITC
pSTAT3 (pY705)	AF488
TLR2	FITC
TLR4	FITC (Biotin – Streptavidin)
TLR9	FITC
Zombie Green™ Fixable Viability Kit	Zombie Green™ dye[*1]

[*1]: Excitation and Emission (Ex./Em. 488 nm/515 nm) comparable to FITC/AF488.

4.3 Identification of Infected Cells and Quantification of Infection Frequency

Infected murine and human HSPCs were identified by DsRed and mCherry, which are expressed by genetically modified *Mycobacterium tuberculosis* strains. To identify infected $DsRed^+$/$mCherry^+$-cells by FACS the following flow cytometers were utilized: BD FACSCanto™ II, BD LSRFortessa™, BD FACSymphony™ A3, BD FACSAria™ IIIu. Positive signals for DsRed and mCherry were distinguished from background fluorescence and gated accordingly by employing samples infected with a non-fluorescent wildtype *M. tuberculosis* strain, as fluorescence minus one (FMO) control. The cytometers were operated with BD FACSDiva™ software, and final data analysis was performed using FlowJo™ (BD Biosciences, v10.10).

4.4 Intracellular Single Cell Phosphoprotein Analysis Via FACS

Immunofluorescence staining of surface antigens was performed as outlined in **section C.4.1**. Instead of fixation with 4 % PFA, cells were resuspended in 500 µl of preheated (37 °C) BD Cytofix fixation buffer (BD Biosciences) and incubated at 37 °C for 10 min. Following incubation, cells were centrifuged (500 rcf, 6 min.) and the supernatant was discarded. For alcoholic permeabilization, the pellet was resuspended 1 mL prechilled (-20 °C) BD Phosflow Perm buffer III (BD Biosciences) and incubated on ice for 15 min. After permeabilization, cells were washed twice (600 rcf, 5 min, 4 °C) with 500 µl FACS buffer. After the second wash, the pellet was resuspended in 100 µl fluorochrome-conjugated antibodies, appropriately diluted

in FACS buffer. After a 30 min. incubation at room temperature, cells were centrifuged (600 rcf, 5 min., 4 °C) and the supernatant was discarded. The pellet was resuspended in 300 µl FACS buffer for fluorescent activated cell sorting and quantification of pSTAT3 (pY705).

4.5 Sorting of HSCs for Microscopic Analysis

HSC populations were sorted for microscopic analysis following immunofluorescence staining **(section C.4.1)**. To remove aggregates and debris, a 70 µm nylon cell strainer was placed over a 50 ml conical tube and rinsed with 1 mL MACS buffer. The cell suspension was poured over the strainer, and the flow-through was collected in a new 50 mL conical tube. The strainer was washed with 1 mL MACS buffer, and the residual liquid from the bottom of the strainer was collected and added to the same tube. The cell suspension was sorted using a BD FACSAria™ IIIu cytometer with purity sort settings and a 100 µm nozzle into 5 mL FACS tubes containing 500 µl PBS. Sorted murine cell populations were centrifuged (500 rcf, 4 °C, 5 min.), and the supernatant was carefully aspirated, leaving a residual volume of approximately 40 µl. Cells were then transferred into a µ-Slide VI 0.4 (ibidi) for subsequent confocal laser scanning microscopy **(section C.5.3.1)**. Sorted human cell populations were centrifuged (500 rcf, 5 min.). The supernatant was discarded, and the pellets were resuspended in 200 µl phalloidin staining solution (66 nM phalloidin-AF488, 1% (v/v) normal goat serum (NGS) in PBS) for 20 min. at room temperature. The samples were washed once with 200 µl PBS (500 rcf, 5 min.), centrifuged (500 rcf, 5 min.) again and the supernatant was discarded. The samples were eventually resuspended in 40 µl PBS and transferred into a µ-Slide VI 0.4 (ibidi) for subsequent confocal laser scanning microscopy **(section C.5.3)**.

5. Microscopic Analyses

5.1 Immunofluorescence Staining for Intracellular Actin Imaging

After successful sorting, PBS was completely aspirated after centrifugation (500 rcf, 4 °C, 5 min.) and sorted cells were permeabilized with 300 µl 0.1 % (v/v) Triton X-100 in PBS for 3 min. at room temperature. Permeabilization was halted by adding 2 mL PBS. The cells were washed once with 200 µl PBS (500 rcf, 5 min.) and centrifuged (500 rcf, 5 min.) again. The supernatant was discarded, and the pellets were resuspended in 200 µl phalloidin staining

solution (66 nM phalloidin-AF488, 1% (v/v) normal goat serum (NGS) in PBS) for 20 min. at room temperature. The samples were washed once with 200 µl Milli-Q water (500 rcf, 5 min.), and centrifuged (500 rcf, 5 min.) again. The supernatant was discarded, and the pellets were resuspended in 200 µl 1:1000 DAPI in Milli-Q water for 7 min. at room temperature. The samples were washed once with 200 µl PBS (500 rcf, 5 min.), centrifuged (500 rcf, 5 min.) again and the supernatant was discarded. The samples were eventually resuspended in 40 µl PBS and transferred into a µ-Slide VI 0.4 (ibidi) for subsequent confocal laser scanning microscopy **(section C.5.3)**.

5.2 Immunofluorescence Staining for Murine Whole-Mount Bone Marrow Microscopy

C57Bl6/J wildtype mice were sacrificed. The bodies were sterilized with 70 % ethanol, and the thorax was opened via an incision below the sternum. Sterna were dissected, cleared of soft and connective tissue, and sectioned at the 3rd, 4th and 5th articular facets to collect the two central segments. The bone marrow within each sternal segment was exposed by sectioning along the coronal plane under a dissecting microscope. Each sternal segment half was immediately fixed in 150 µl 4 % (w/v) PFA in PBS on ice for 3 hours. The segments were then carefully washed three times for 10 min. each with 200 µl PBS and blocked with 150 µl 10% (v/v) goat serum in PBS at 4 °C for 2 hours. The blocking solution was carefully aspirated, and fluorochrome-conjugated antibodies **(Tab. 19)** were added in 2 % (v/v) goat serum in PBS for overnight staining at 4 °C.

Table 19: Multi-parameter Immunofluorescence Panel for murine whole-mount bone marrow microscopy.

Antigen	Fluorochrome
CD3	APC/Fire 750
CD117 (c-Kit)	BV480
CD41	AF647
CD48	AF488
CD150	BV421
ESAM	PE

After staining, the sternal segments were washed three times with PBS for 10 min. and transferred to microscopic slides for imaging in a Nikon AXR Inverted Confocal Microscope **(section C.5.3.2)**.

5.3 Confocal Laser Scanning Microscopy

5.3.1 Confocal Laser Scanning Microscopy of Single Cell Suspensions of Human and Murine HSCs

Confocal imaging of sorted human and murine HSCs was performed in a Leica TCS SP5 confocal microscope. The system was equipped with solid-state diode laser at 405 nm and 561 nm, as well as 488 nm argon and 633 nm helium-neon gas lasers. Detection of fluorescence emission was facilitated by Leica HyD high-quantum efficiency, low noise hybrid detectors, paired with acousto-optical tuneable filters allowing detection across a spectrum of 400 – 780 nm. Super-resolution imaging was achieved with a HC PL APO CS2 63.0x/1.40 UV oil-immersion objective (Leica Microsystems), incorporating 4X line averaging, at a resolution of 2024 x 2024 pixels, with 120 – 240 nm Z-step intervals, using a galvanometric scanner, and a pinhole of 1 AU. This configuration yielded an average voxel size of 60 x 60 x 180 nm, suitable for subsequent lightning deconvolution.

5.3.2 Confocal Laser Scanning Microscopy of Whole-Mount Murine Bone Marrow

Confocal imaging of murine whole-mount sternum segments was performed in a Nikon AXR Inverted Confocal Microscope. The system was equipped with solid-state diode lasers at 405 nm, 445 nm, 488 nm, 514 nm, 561 nm, 594 nm, 640 nm, and 730 nm. Fluorescence emission across the spectrum of 400 – 820 nm was detected via one high-quantum efficiency, low-noise Hamamatsu photomultiplier tube and three high-quantum efficiency gallium arsenide phosphide photomultiplier tubes (GaAsp-PMTs). Images of single sections were acquired using a Plan Apo 20x/0.75 DIC N2 oil-immersion objective (Nikon), incorporating 4X line averaging, at a resolution of 2048 x 2048 pixels, with 1.5 – 2 µm Z-step intervals using a resonant scanner, and a pinhole of 1.6 airy units (AU). This configuration yielded an average voxel size of 0.426 x 0.426 x 0.954-3.61 µm.

5.4 Image Processing

Images of single cell suspension were deconvoluted using the lightning module of the Leica Application Suite X software (Leica Microsystems, version 3.5.2).

Images of single sections of murine whole mount sternum segments were stitched together and denoised by a built-in gaussian denoise algorithm using the Imaris software (Bitplane, version 10.1 to 10.2).

6. Data Analysis and Statistical Tests

Numerical data were exported to GraphPad Prism® (GraphPad Software, version v10.3.0) for statistical analysis and graphical display and are presented as mean values ± standard deviation. Statistical analysis between two groups of normally distributed data at a single timepoint was performed using student's t-test for paired samples, if not specified otherwise. Human data, with underlying donor variability were analysed with ratio-paired t-tests. Differences between data groups were considered statistically significant at a p-value < 0.05. P-values are displayed in graphs with blank space or 'ns' for p-values ≥0.05, '*' for p-values < 0.05, '**' for p-values < 0.005, and '***' for p-values < 0.0005.

D. Results

The permissiveness of HSCs to *M. tuberculosis* infection remains a subject of debate. While HSCs have traditionally been considered non-phagocytic cells, recent reports demonstrated the presence of mycobacterial DNA within these cells [187]. To address this discrepancy, we analyzed the permissiveness of murine and human HSCs as host cells for *M. tuberculosis,* **(section D.1)**, delineated events from pathogen recognition to internalization **(section D.2)** and identified factors contributing to the permissiveness of these cells to infection **(section D.3)**. Building on these studies, we started to adapt novel methods for future studies to characterize *M. tuberculosis* in vivo niches in bone marrow **(section D.5)**.

1. HSCs Are Host Cells of *M. tuberculosis*

The controversy whether HSCs can be host cells for *M. tuberculosis* arose from conflicting results in the literature, about the permissiveness of HSCs to infection. Additionally, *M. tuberculosis*-infected cells were identified by DNA detection, an error prone method rather than imaging-based approaches. Therefore, direct detection of *M. tuberculosis* harboring HSCs is crucial for all subsequent analyses.

1.1 Reliable Infection of HSCs

In murine models of experimental tuberculosis and in human patient cohorts with latent tuberculosis infection, less than 1 % of analysed HSCs harbored *M. tuberculosis* DNA [187]. To increase the frequency of infected HSCs for experimental applications and to create a more controllable and manipulable environment than a whole host organism, we established a method to infect HSCs in vitro. As the bone marrow is the prime reservoir of HSCs in vivo, we isolated mononucleated cells from the bone marrow of C57Bl/6J mice. Since sustained in vitro proliferation of HSCs was not required for our experiments, we cultured cells in supplemented RPMI1640 medium. To allow quantification of infected HSCs by fluorescence-activated cell sorting (FACS), we employed a fluorescent *M. tuberculosis* H37Rv strain expressing DsRed. Hematopoietic progenitors were identified by the lineage, c-Kit and Sca-1 (LKS) markers. In combination with signalling lymphocytic activation molecule (SLAM) family receptor expression (CD150 and CD48), four sub-populations highly enriched in multilineage reconstituting cells were distinguished, based on the studies of Kiel et al. 2005 and Pietras at

al. 2015 [138,197]. HSCs were identified by FACS as Lin$^-$ Sca-1$^+$ c-Kit$^+$ (LKS$^+$) CD150$^+$ CD48$^-$, MPP1 as LKS$^+$ CD150$^-$ CD48$^-$, MPP2 as LKS$^+$ CD150$^+$ CD48$^+$ and a heterogenous population of MPP3 and MPP4 as LKS$^+$ CD150$^-$ CD48$^+$ **(Fig. 6A&B)**. In former studies, the MPP1 population was referred to as short-term HSC (ST-HSC) and the HSC population as long-term HSC (LT-HSC). Recent data on the serial reconstitution capacity of the 'ST-HSC' population rather suggest their classification as MPP1, so that only Lin$^-$ Sca-1$^+$ c-Kit$^+$ (LKS$^+$) CD150$^+$ CD48$^-$ 'LT-HSCs' are bona fide HSCs abandoning the older binary LT-HSC-ST-HSC stratification [142]. While only the population of HSCs comprise serial long-term multilineage reconstituting cells, we also included the other early and multipotent progenitors sharing common characteristics in our analyses. Within these distinct populations, infected cells were distinguished from uninfected cells by DsRed fluorescence **(Fig. 6C)**.

A

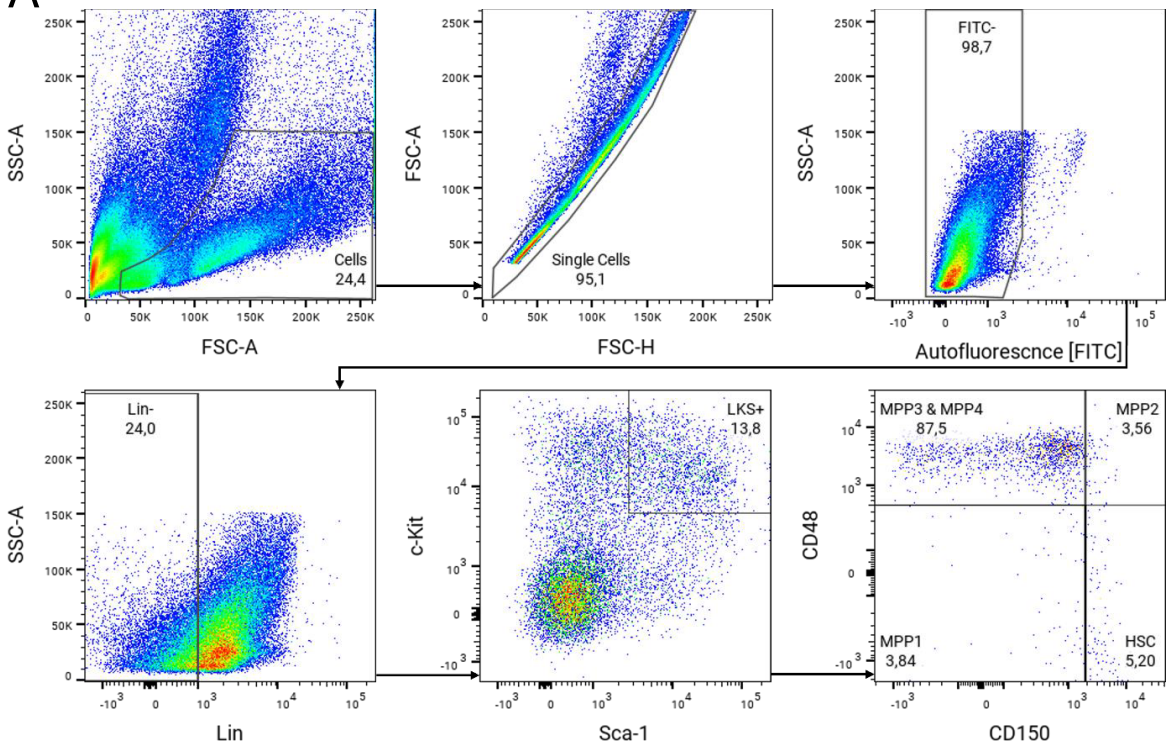

B

Population	Immunophenotype
HSC	Lin$^-$ c-Kit$^+$ Sca-1$^+$ CD150$^+$ CD48$^-$
MPP1	Lin$^-$ c-Kit$^+$ Sca-1$^+$ CD150$^-$ CD48$^-$
MPP2	Lin$^-$ c-Kit$^+$ Sca-1$^+$ CD150$^+$ CD48$^+$
MPP3/MPP4	Lin$^-$ c-Kit$^+$ Sca-1$^+$ CD150$^-$ CD48$^+$

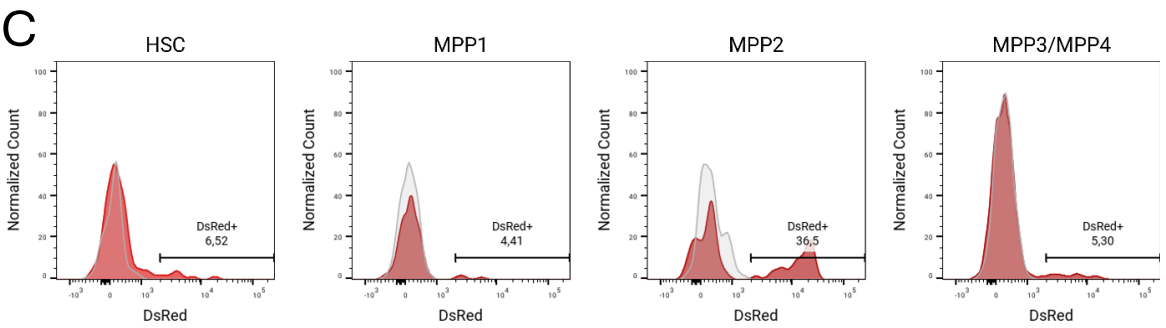

Figure 6: Representative gating scheme to immunophenotypically identify infected murine hematopoietic stem cells and multipotent progenitors. The gating scheme for murine hematopoietic stem and progenitor cell (HSPC) populations was adapted from Pietras et al. 2015 and Kiel et al. 2005. Representative gating is shown for a Lin$^+$-depleted murine bone marrow culture, infected with *M. tuberculosis* DsRed at a MOI of 10 for 24 hours. **A)** Cells are gated in FSC-A against SSC-A. Following doublet-exclusion using FSC-H against FSC-A and autofluorescence-exclusion using FITC, distinct subpopulations of primitive hematopoietic progenitors are then identified by LKS-SLAM multiparameter phenotyping: HSC: Lin$^-$ c-Kit$^+$ Sca-1$^+$ CD150$^+$ CD48$^-$; MPP1: Lin$^-$ c-Kit$^+$ Sca-1$^+$ CD150$^-$ CD48$^-$; MPP2: Lin$^-$ c-Kit$^+$ Sca-1$^+$ CD150$^+$ CD48$^+$; MPP3/MPP4: Lin$^-$ c-Kit$^+$ Sca-1$^+$ CD150$^-$ CD48$^+$. **B)** Immunophenotypes of murine HSPC populations. **C)** Cells infected with fluorescent *M. tuberculosis* H37Rv DsRed are distinguished by DsRed fluorescence from uninfected cells. HSPC populations (HSCs, MPP1, MPP2, MPP3/MPP4) from uninfected cultures (grey) are plotted in comparison to HSPC populations from infected cultures (red).

To optimize the bacterial load necessary to achieve a sufficient frequency of infected hematopoietic stem and progenitor cells (HSPCs), we infected murine bone marrow mononucleated cell cultures with *M. tuberculosis* at increasing multiplicities of infection (MOIs) for 20 hours. Following immunofluorescence staining the frequency of infected HSPCs was quantified by FACS **(Fig. 7)**. After in vitro infection at an MOI of 10, the earliest progenitor population, the HSCs, were identified as the population with the lowest mean mycobacterial burden of 4.3 ± 1.8 % DsRed$^+$ cells. The MPP1 population demonstrated a comparable mean frequency with 4.5 ± 3.0 % under the same conditions. The highest mycobacterial burden was observed in the myeloid-biased MPP2 population with 30.6 ± 21.5 % DsRed$^+$ cells, while the MPP3/MPP4 population of myeloid and lymphoid biased cells exhibited a frequency of infection of 12.3 ± 8.8 % at the highest MOI. For all progenitor populations, except MPP2, the observed infection frequency significantly correlated with the concentration of the bacterial inoculum in a dose dependent manner, as demonstrated by the calculated Pearson correlation coefficients: HSC: r = 0.678, p = 0.023; MPP1: r = 0.750, p = 0.01; MPP2: r = 0.538, p = 0.0674; MPP3/MPP4: r = 0.699, p = 0.018. However, due to the low frequencies of the respective progenitor populations within the infected cultures, the absolute number of cells available was insufficient for quantitative phenotyping in downstream analyses. Hence, further refinement of the conditions underlying the in vitro infection of HSCs by *M. tuberculosis* was required.

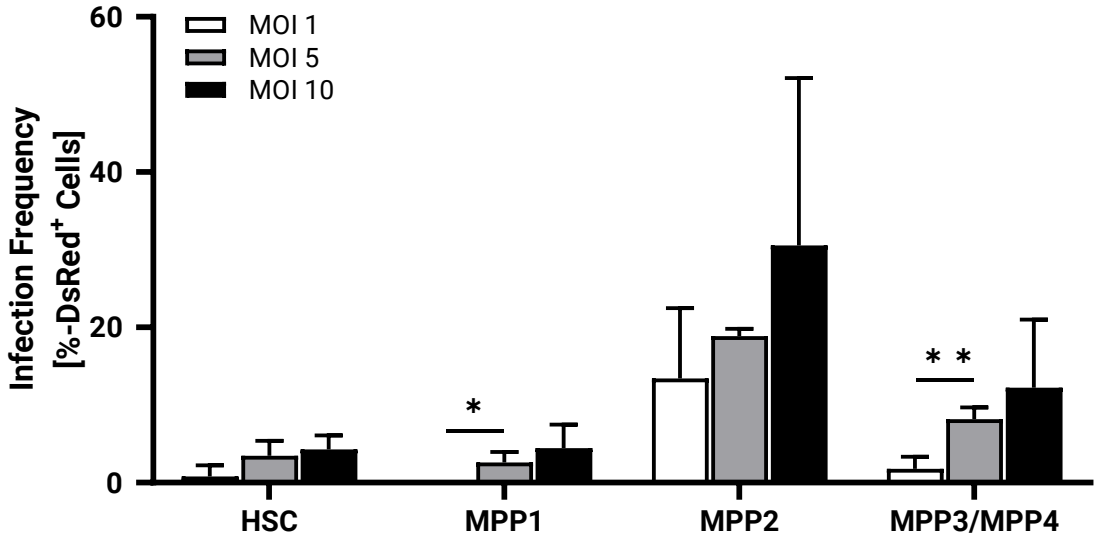

Figure 7: Dose dependent frequency of *M. tuberculosis*-infected hematopoietic stem and progenitor cells in vitro. Bone marrow cells from C57Bl/6J mice were collected and infected with *M. tuberculosis* H37Rv DsRed at MOIs of 1, 5 and 10 for 24 hours. The frequency of infected hematopoietic stem and progenitor cells (HSPCs) was quantified using FACS (HSC: Lin$^-$ c-Kit$^+$ Sca-1$^+$ CD150$^+$ CD48$^-$ DsRed$^+$; MPP1: Lin$^-$ c-Kit$^+$ Sca-1$^+$ CD150$^-$ CD48$^-$ DsRed$^+$; MPP2: Lin$^-$ c-Kit$^+$ Sca-1$^+$ CD150$^+$ CD48$^+$ DsRed$^+$; MPP3/MPP4: Lin$^-$ c-Kit$^+$ Sca-1$^+$ CD150$^-$ CD48$^+$ DsRed$^+$). Bars represent the mean ± SD [n=3]. Statistical significance is determined by paired one-tailed t-test. Asterisks indicate p-values (*p ≤ 0.05; ns p > 0.05). Pearson correlation coefficients are computed between MOI and infected cell frequency: HSC: r = 0.678, p = 0.023; MPP1: r = 0.750, p = 0.01; MPP2: r = 0.538, p = 0.0674; MPP3/MPP4: r = 0.699, p = 0.018.

Bone marrow mononuclear cell cultures contain mature hematopoietic cells including professional phagocytes that take up *M. tuberculosis*. We thus hypothesized that depleting these cells prior to infection could significantly increase the HSC infection frequency in vitro. Additionally, increasing the HSC to *M.* tuberculosis ratio was expected to elevate the likelihood of HSCs to encounter *M. tuberculosis*, thereby increasing the frequency of infection further. To evaluate this hypothesis, lineage-positive (Lin$^+$) cells, including CD3$^+$ T cells, Gr-1$^+$ granulocytes, CD11b$^+$ monocytes, CD45R/B220$^+$ B cells, Ter-119$^+$ erythroid cells and their respective committed precursors, were selectively depleted prior to infection with *M. tuberculosis*. Comparing the DsRed$^+$ frequency of HSPCs between Lin$^+$-depleted and naïve bone marrow cultures after in vitro infection, no significant differences were detected **(Fig. 8A)**. However, prior Lin$^+$-depletion led to an approximately ninefold increase in the relative population sizes of HSCs (0.03 ± 0.02 % to 0.32 ± 0.24 %), MPP1 (0.16 ± 0.03 % to 0.54 ± 0.60 %), MPP2 (0.05 ± 0.02 % to 0.65 ± 0.84 %) and MPP3/MPP4 (0.74 ± 0.30 % to 8.09 ± 9.04 %) suggesting enrichment of Lin$^-$ cells as a feasible approach to increase the absolute counts of infected HSCs for downstream analyses **(Fig. 8B)**. Prior Lin$^+$-depletion did not lead to a significant difference of the Lin$^-$ population size (39.8 ± 16.1 % vs. 45.9 ± 38.1 %). This was not a contradiction as the Lin$^+$ populations comprises mostly professional phagocytes, which

succumb to death after infection with *M. tuberculosis*, when missing proper activation. Hence, they were similarly reduced in non-depleted cultures as well.

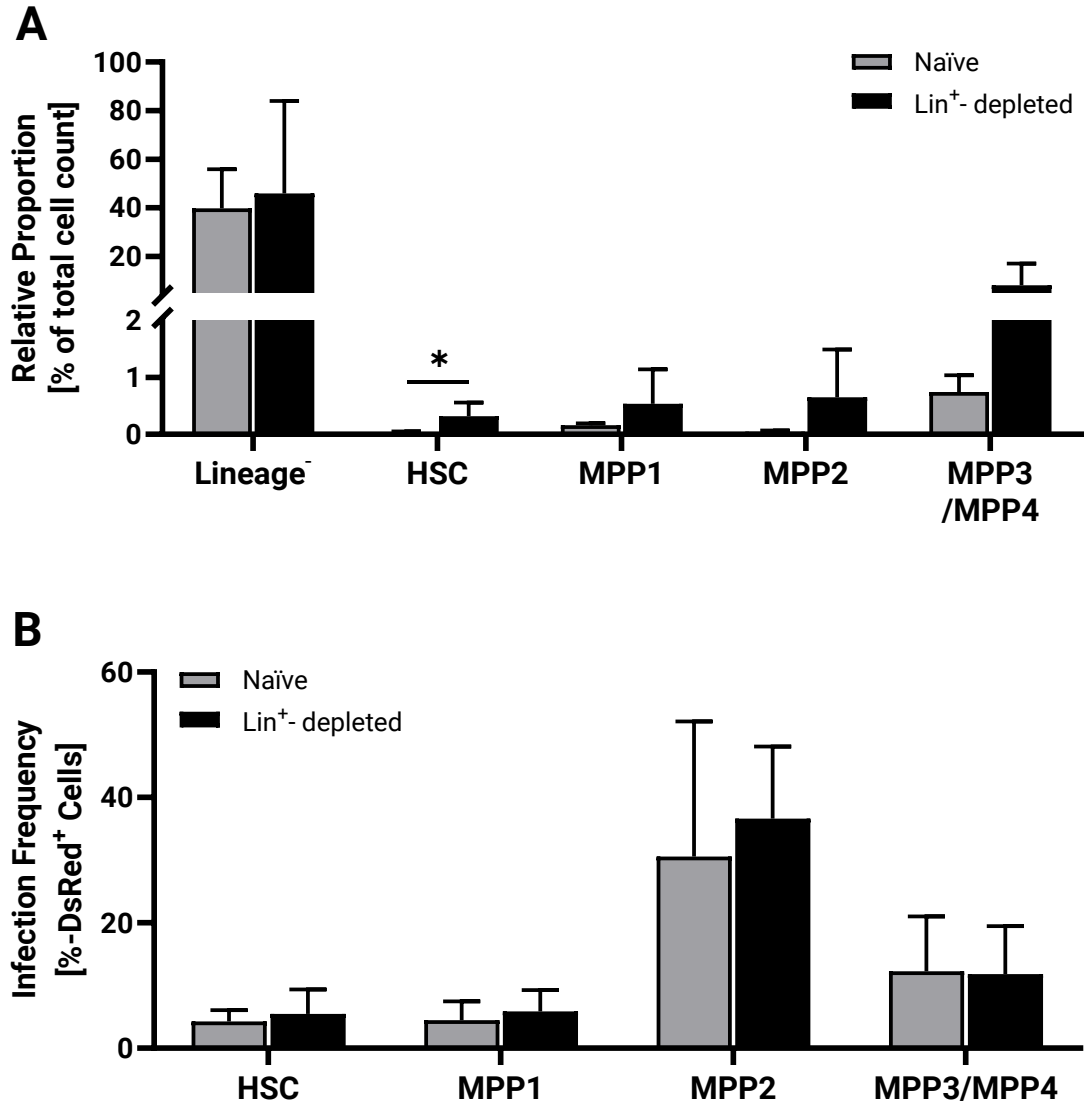

Figure 8: Influence of the depletion of Lin$^+$ cells in murine bone marrow cultures prior to infection with *M. tuberculosis*. Bone marrow cells from C57Bl/6J mice were collected and Lin$^+$-cells were depleted. Progenitor-enriched cultures were infected with *M. tuberculosis* H37Rv DsRed at MOI 10 for 24 hours. **A)** Influence of Lin$^+$ depletion on the relative hematopoietic stem and progenitor cell (HSPC) population sizes. The relative proportion of the indicated cell populations was quantified using FACS (Lineage$^-$; HSC: Lin$^-$ c-Kit$^+$ Sca-1$^+$ CD150$^+$ CD48$^-$; MPP1: Lin$^-$ c-Kit$^+$ Sca-1$^+$ CD150$^-$ CD48$^-$; MPP2: Lin$^-$ c-Kit$^+$ Sca-1$^+$ CD150$^+$ CD48$^+$; MPP3/MPP4: Lin$^-$ c-Kit$^+$ Sca-1$^+$ CD150$^-$ CD48$^+$) and calculated as n [HSPCs] / n [total cells]. **B)** Influence of Lin$^+$ depletion on the *M. tuberculosis* infection frequency of HSPC populations. The frequency of infected HSCs, MPP1, MPP2, and MPP3/MPP4 was quantified using FACS (HSC: Lin$^-$ c-Kit$^+$ Sca-1$^+$ CD150$^+$ CD48$^-$ DsRed$^+$; MPP1: Lin$^-$ c-Kit$^+$ Sca-1$^+$ CD150$^-$ CD48$^-$ DsRed$^+$; MPP2: Lin$^-$ c-Kit$^+$ Sca-1$^+$ CD150$^+$ CD48$^+$ DsRed$^+$; MPP3/MPP4: Lin$^-$ c-Kit$^+$ Sca-1$^+$ CD150$^-$ CD48$^+$ DsRed$^+$) and compared to cells within non-Lin$^+$-depleted cell cultures. Bars represent the mean ± SD [two experiments: n=3 (naïve) & n=6 (Lin$^+$-depleted)]. Statistical significance is determined by unpaired one-tailed t-test. Asterisks indicate p-values (*p ≤ 0.05; ns p > 0.05).

In most studies, in vitro infection of canonical host cells by *M. tuberculosis*, such as macrophages or polymorphonuclear neutrophils, is analyzed between two and eight hours after initial infection, a timeframe during which nearly all permissive cells become infected. However, it was unclear whether HSPCs exhibit infection kinetics comparable to those of

professional phagocytes and if they achieve the infection frequencies observed in overnight cultures within a shorter incubation period already. To potentially reduce the exposure to in vitro conditions following isolation and infection, we characterized the kinetics of HSPC infection. Lin^+-depleted bone marrow cultures were infected with *M. tuberculosis* DsRed, and the frequency of $DsRed^+$ HSCs and MPPs was quantified by FACS 8-, 12-, and 24-hours post-infection **(Fig. 9)**. The frequency of infection significantly increased over time and correlated with the incubation period for HSCs [r = 0.683; p = 0.004], MPP1 [r = 0.729; p=0.002], MPP2 [r = 0.912; p<0.0001] and MPP3/MPP4 [r = 0.739; p=0.001]. Furthermore, a significantly higher mean proportion of HSPCs became infected between 12- and 24-hours post-infection (HSC: 4.2 %; MPP1: 4.2 %; MPP2 32.8 %; MPP3/MPP4: 9.3 %), compared to the first 12 hours post-infection (HSC: 1.2 % %; MPP1: 1.7 % %; MPP2: 3.9 %; MPP3/MPP4: 2.5 %). These infection kinetics suggest an underlying mechanism in HSCs that requires a longer period to achieve proper infection beyond the first 12 hours of incubation and successively increase HSC permissiveness in overnight cell cultures. Consequently, due to these slow kinetics, an overnight incubation of 20 hours post-infection remained the standard for all subsequent analyses.

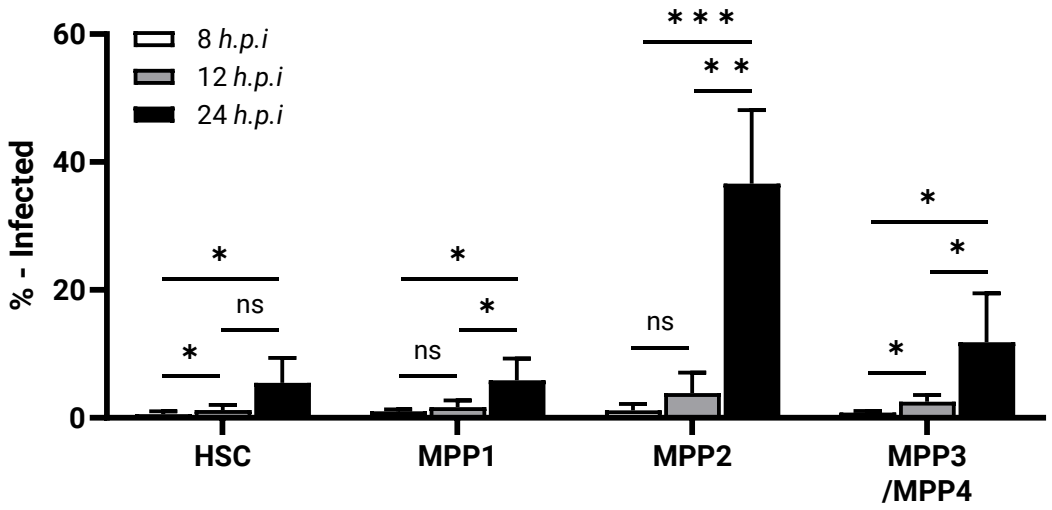

Figure 9: Kinetics of in vitro infection of hematopoietic stem and progenitor cells with *M. tuberculosis*. Bone marrow cells from C57Bl/6J mice were collected and Lin^+-cells were depleted. Progenitor-enriched cultures were infected with *M. tuberculosis* H37Rv DsRed at a MOI of 10. The frequency of infected hematopoietic stem and progenitor cells (HSPCs) was quantified at indicated time points using FACS (HSC: Lin^- c-Kit^+ $Sca\text{-}1^+$ $CD150^+$ $CD48^-$ $DsRed^+$; MPP1: Lin^- c-Kit^+ $Sca\text{-}1^+$ $CD150^-$ $CD48^-$ $DsRed^+$; MPP2: Lin^- c-Kit^+ $Sca\text{-}1^+$ $CD150^+$ $CD48^+$ $DsRed^+$; MPP3/MPP4: Lin^- c-Kit^+ $Sca\text{-}1^+$ $CD150^-$ $CD48^+$ $DsRed^+$). Bars represent the mean ± SD [8 *h.p.i*: n = 4; 12 *h.p.i:* n = 4; 24 *h.p.i:* n = 6]. Statistical significance is determined by unpaired and paired one-tailed t-test. Asterisks indicate p-values (*p ≤ 0.05; **p ≤ 0.005; ***p ≤ 0.0005; ns p > 0.05). Pearson correlation coefficients are calculated between time post infection and infected cell frequency: HSCs [r = 0.683; p = 0.004], MPP1 [r = 0.729; p=0.002], MPP2 [r = 0.912; p<0.0001] and MPP3/MPP4 [r = 0.739; p=0.001].

As *M. tuberculosis* is a human pathogen, analyses carried out in human cells are of greater clinical relevance in the context of tuberculosis. We therefore translated the established in vitro infection system to primary cells of human origin. Instead of bone marrow, primary

human cells were sourced from peripheral blood, as a small fraction of HSCs regularly leaves the bone marrow to enter circulation. Peripheral blood mononuclear cells (PBMCs) were isolated and $CD34^+$ cells, enriched in hematopoietic progenitors, were cultured in supplemented RPMI1640. Enriched $CD34^+$ cell cultures were infected with fluorescent *M. tuberculosis* H37Rv DsRed. Human HSCs were identified by FACS as $CD34^+$ $CD45RA^-$ Lin^- $CD38^{-/low}$ $CD90^+$ cells according to Majeti et al. 2007 [198]. A heterogenous population that comprises hematopoietic progenitors equivalent to the murine MPP1 (the former ST-HSC) population and other multipotent progenitors, is further on categorized as MPPs, and was identified as the $CD34^+$ $CD45RA^-$ Lin^- $CD38^{-/low}$ $CD90^-$ population **(Fig. 10)**.

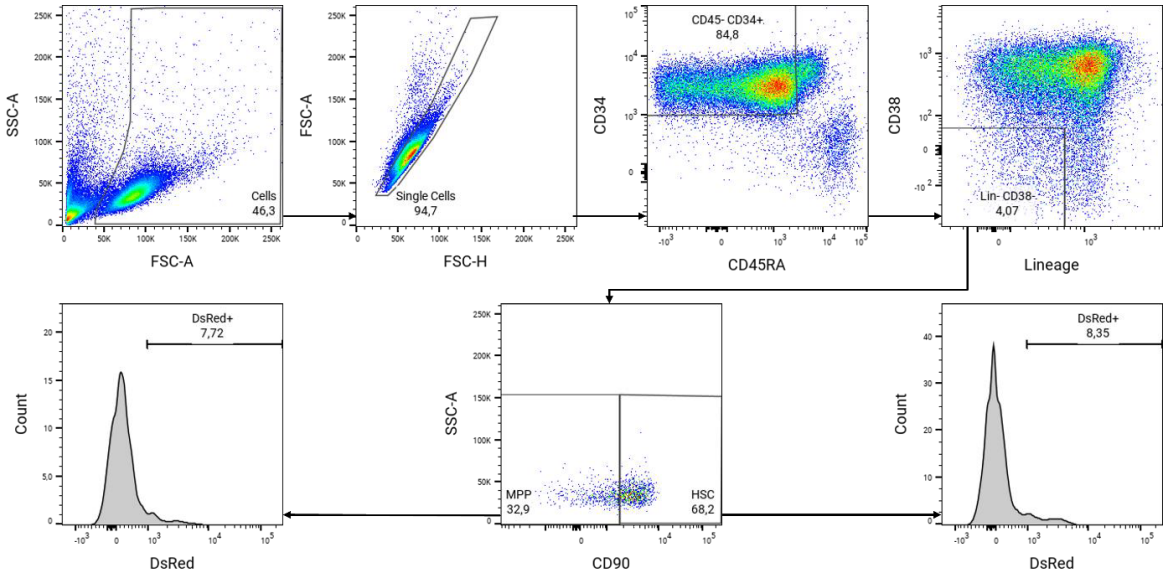

Population	Immunophenotype
HSC	$CD34^+$ $CD45RA^-$ Lin^- $CD38^{-/low}$ $CD90^+$
MPP	$CD34^+$ $CD45RA^-$ Lin^- $CD38^{-/low}$ $CD90^-$

Figure 10: Representative gating strategy to immunophenotypically identify human hematopoietic stem cells and multilineage potential progenitors. Cells are gated in FSC-A against SSC-A. Following doublet-exclusion using FSC-H against FSC-A, human hematopoietic stem cells (HSCs) are identified as $CD34^+$ $CD45RA^-$ Lin^- $CD38^{-/low}$ $CD90^+$ cells. Human multipotent progenitors (MPPs) are identified as $CD34^+$ $CD45RA^-$ Lin^- $CD38^{-/low}$ $CD90^-$ cells. Cells infected with fluorescent *M. tuberculosis* DsRed are identified as the respective subsets of $DsRed^+$ HSC and $DsRed^+$ MPP. Representative gating is shown for a $CD34^+$-enriched human peripheral blood culture, infected with *M. tuberculosis* DsRed at a MOI of 10 for 20 hours.

To evaluate the adapted human in vitro system for HSPC infection, we compared infection frequencies of HSCs and MPPs between murine and human cultures **(Fig. 11A)**. Of note, the heterogenous murine MPP1 and the human MPP population may comprise differently committed hematopoietic progenitors. Data from multiple experiments, in which progenitor populations were infected with *M. tuberculosis* at a MOI of 10 under normalized conditions were summarized. Human and murine populations of MPPs did not show significant

differences in mycobacterial burden carried (human: 5.9 ± 3.4 % vs. murine: 4.4 ± 4.0 %). In contrast, HSCs from human origin had a significantly increased infection frequency compared to those from murine origin (human: 21.3 ± 20.1 % vs. murine: 4.4 ± 4.0 %). The elevated infection frequency in human HSCs was driven by a subset of donors who exhibited significantly ($p < 0.0001$) greater permissiveness to *M. tuberculosis* infection. The two donor subgroups, categorized as 'permissive' and 'resistant' based on unsupervised k-means clustering (k = 2), demonstrated a mean frequency of 51.2 ± 9.8 % DsRed$^+$ HSCs in 'permissive' donors compared to 10.2 ± 6.6 % DsRed$^+$ HSC in 'resistant' donors **(Fig. 11B)**. Notably, only 'permissive' donors showed a significant increase in infected HSCs compared to their murine counterparts but not 'resistant' donors. These results demonstrate both host-species-specific differences but also intra-species donor heterogeneity.

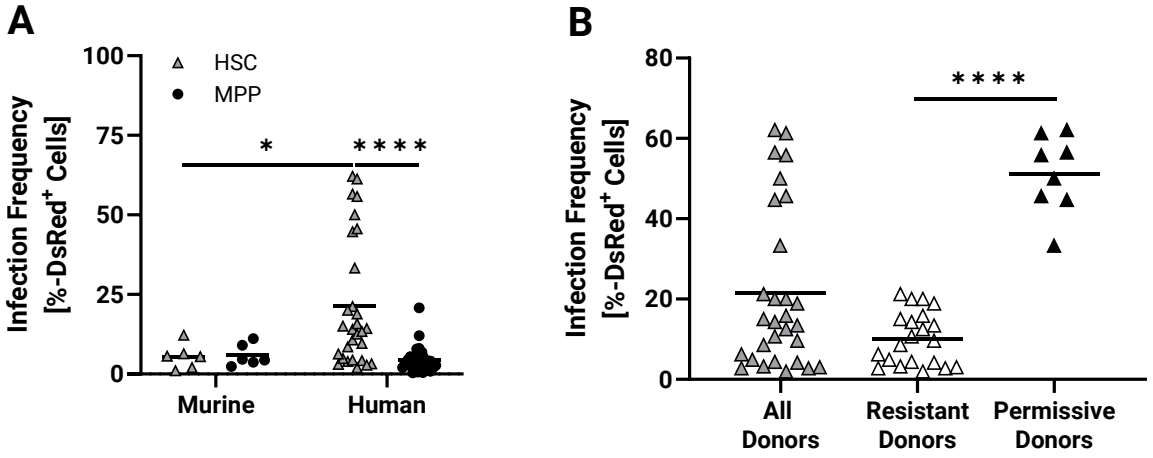

Figure 11: Host-specific differences and donor variances in the frequencies of *M.* tuberculosis-infected hematopoietic stem cells. Bone marrow cells from C57Bl/6J mice were collected and Lin$^+$-cells were depleted. Peripheral blood mononuclear cells from adult human donors were collected and CD34$^+$-cells were enriched. Progenitor-enriched cultures were infected with *M. tuberculosis* H37Rv DsRed at a MOI of 10. **A)** Frequency of *M. tuberculosis*-infected murine and human hematopoietic stem cell (HSC) and multipotent progenitor (MPP) populations. The frequency of infected murine and human HSCs and MPPs was quantified 20 hours post-infection using FACS (murine HSC: Lin$^-$ c-Kit$^+$ Sca-1$^+$ CD150$^+$ CD48$^-$ DsRed$^+$; murine MPP1: Lin$^-$ c-Kit$^+$ Sca-1$^+$ CD150$^-$ CD48$^-$ DsRed$^+$; human HSC: CD34$^+$ CD45RA$^-$ Lin$^-$ CD38$^{-/low}$ CD90$^+$ DsRed$^+$; human MPP: CD34$^+$ CD45RA$^-$ Lin$^-$ CD38$^{-/low}$ CD90$^-$ DsRed$^+$). Individual data points are shown with mean [murine data n=6; human data summarized from 10 experiments n_{total}=29]. **B)** Stratification of human donors based on the permissiveness of HSCs to *M. tuberculosis* infection. Donors were stratified into two subsets based on unsupervised k-means clustering (k = 2). Statistical significance is determined by unpaired two-tailed t-test. Asterisks indicate p-values (*p ≤ 0.05; **p ≤ 0.005; ***p ≤ 0.0005; ****p ≤ 0.00005; ns p > 0.05).

Overall, the in vitro systems established for HSC infection successfully compensate the rarity of these cells in both, host tissues and cell cultures through the extended incubation period and the prior enrichment of progenitor target cells. The systems yield sufficient quantities of *M*. tuberculosis-infected HSCs for further analyses under controlled experimental conditions.

1.2 Intracellular Localization of *M. tuberculosis*

A significant limitation in the initial study by Tornack et al. was the potential for misidentifying surface-adherent mycobacteria as intracellular infections. The polymerase chain reaction (PCR)-based approach used in the study critically depended on the effective removal of extracellular mycobacteria. Due to the tendency of mycobacteria to adhere to surfaces and form aggregates or biofilms, an imaging-based method was necessary to definitively confirm the intracellular localization of *M. tuberculosis* in infected HSCs. To facilitate this, we infected hematopoietic progenitor cultures (murine Lin^- and human $CD34^+$ cells) with fluorescent *M. tuberculosis* H37Rv DsRed at an MOI of 10 for 20 hours. Given that some surface antigens used for immunophenotyping of HSCs by FACS are not sufficiently expressed for detection through multiparameter immunofluorescence microscopy alone, we isolated HSCs prior to imaging by FACS and sorted the HSC population for subsequent microscopy **(Fig. 12)**. The murine MPP1 and the human MPP population represent heterogeneous populations including cells of varying characteristics. We thus focused our microscopic studies of intracellular bacteria on the more homogenous population of HSCs.

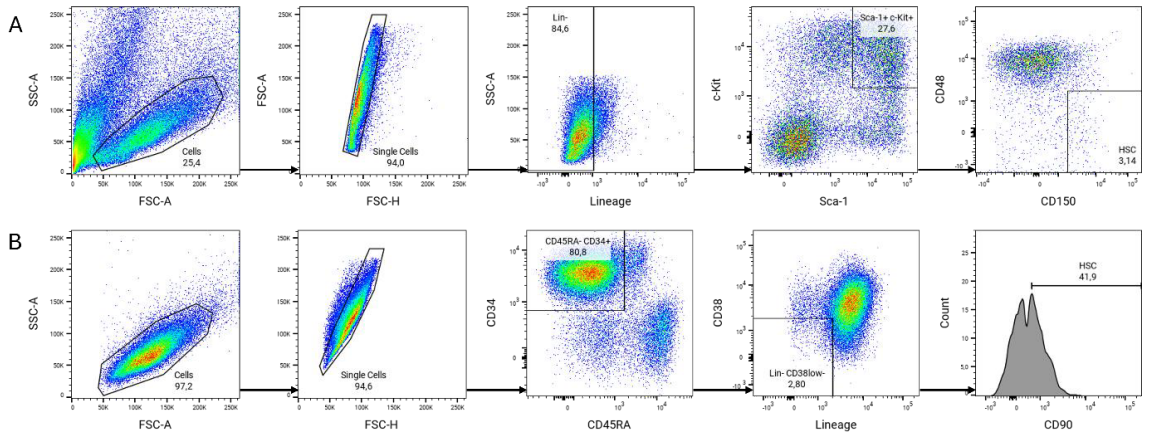

Figure 12: Sorting of murine and human hematopoietic stem cells for confocal laser scanning microscopy. Hematopoietic progenitor cell cultures from murine bone marrow or human peripheral blood were infected with *M. tuberculosis* H37Rv DsRed at a MOI of 10. 20 hours post-infection immunofluorescence staining for surface antigens was performed and cells were sorted. Cells are gated in FSC-A against SSC-A. Following doublet-exclusion using FSC-H against FSC-A, murine hematopoietic stem cells (HSCs) are identified as Lin^- $Sca\text{-}1^+$ $c\text{-}Kit^+$ $CD150^+$ $CD48^-$ cells, and human HSC are identified as $CD34^+$ $CD45RA^-$ Lin^- $CD38^{-/low}$ $CD90^+$ cells. **A)** FACS-plots representing the isolation of murine HSCs for samples displayed in **Fig. 13A**. **B)** FACS-plots representing the isolation of human HSCs for samples displayed in **Fig. 13B-F**.

Confocal imaging was performed at a single optical plane within the cell centre, with a pinhole size of 1 to 1.6 AU, to exclude the possibility to falsely detect surface-adherent mycobacteria above and below the optical plane **(Fig. 13)**. The cell surface was used as a boundary to distinguish intracellular from extracellular spaces. In murine HSCs **(Fig. 13A)**, the cell surface (green) was detected using α-Sca-1-APC. In human HSCs **(Fig. 13B-F)**, we

observed phalloidin-AF488, without additional permeabilization, to stain the cell boundaries, either by accessing sub-membranous actin or unspecific binding to the surface. *M. tuberculosis* (red) was identified by DsRed fluorescence, appearing as rod-shaped bacteria of 0.2-0.5 µm width and 2-5 µm length. Intracellular DsRed$^+$ bacteria were detected in murine **(Fig. 13A)** and human HSCs **(Fig. 13B-F)**. Surface-adherent *M. tuberculosis* were only observed as rare events. Infected HSCs were found to mostly harbor multiple mycobacteria. HSCs, infected with only a single bacterium, were not detected. Most infected HSCs exhibited no visual signs of membrane damage, necrosis, or cell death. However, some cells showed atypical membrane formations, which may have resulted from the pressure applied during sorting or could be artifacts of PFA fixation.

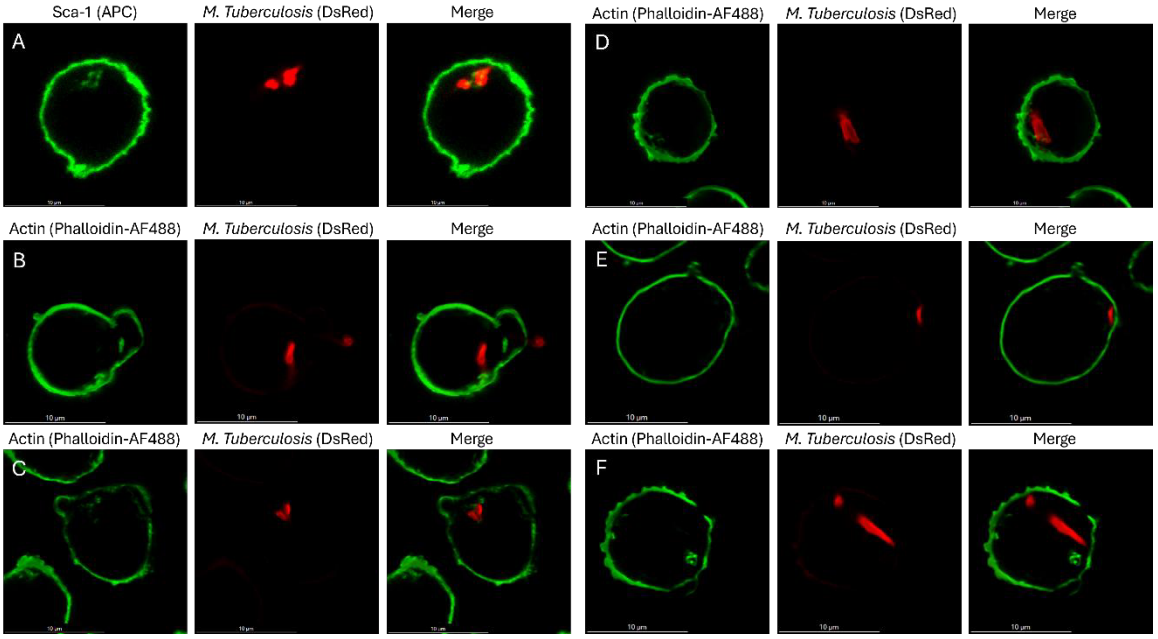

Figure 13: Intracellular localization of *M. tuberculosis* in hematopoietic stem cells as demonstrated by confocal laser scanning microscopy. Hematopoietic progenitor cell cultures from murine bone marrow or human peripheral blood were infected with *M. tuberculosis* H37Rv DsRed at a MOI of 10. 20 hours post-infection hematopoietic stem cells (HSCs) (murine HSC: Lin$^-$ Sca-1$^+$ c-Kit$^+$ CD150$^+$ CD48$^-$; human HSC: CD34$^+$ CD45RA$^-$ Lin$^-$ CD38$^{-/low}$ CD90$^+$) were sorted and imaged using a Leica TCS SP5 confocal microscope. The cell surface (green) of murine HSC was detected by α-Sca1-APC ($\lambda_{Ex.}$ = 651 nm $\lambda_{Em.}$ = 660 nm; Laser = 633 nm; Filter = 640-700 nm). The cell surface (green) of human HSC was detected by phalloidin-AF488 ($\lambda_{Ex.}$ = 494 nm / $\lambda_{Em.}$ = 517 nm; Laser = 488 nm; Filter = 500-545 nm). *M. tuberculosis* (red) was detected through DsRed ($\lambda_{Ex.}$ = 558 nm / $\lambda_{Em.}$ =583 nm; Laser = 488 nm / 561 nm; Filter = 590-625 nm / 621-718 nm). **A)** Murine HSC. **B-F)** Human HSCs from a single donor. All Images were processed using adaptive LIGHTNING deconvolution and automatic LUT-adjustment.

In conclusion, we pivotally show *M. tuberculosis* bacteria within HSCs, demonstrating that HSC are permissive to *M. tuberculosis* in vitro. Furthermore, the rarity of surface-adherent *M. tuberculosis* in our observations supports the validity of FACS-driven analysis as a reliable method using DsRed signals to quantify HSC infection. In summary, our in vitro HSC infection system provides a robust platform for studying the process of HSC infection under controlled conditions, with proven intracellular presence of *M. tuberculosis*.

2. Molecular Factors Involved in HSC Infection

M. tuberculosis is known to use distinct host internalization pathways for infection, such as phagocytosis in professional phagocytes (macrophages, dendritic cells and neutrophils) and macropinocytosis in non-phagocytic host cells (microfold cells, epithelial cells and adipocytes) [199,200]. However, the specific mechanisms by which *M. tuberculosis* infects HSCs remain entirely unknown. HSCs are considered non-phagocytic cells, with phagocytosis and macropinocytosis pathways only emerging during later stages of myeloid differentiation [189]. Given our results that HSCs definitively serve as host cells for *M. tuberculosis* in vitro, we aimed to characterize the internalization pathways facilitating bacterial uptake in HSCs and to identify the receptors involved in the initial recognition and internalization of *M. tuberculosis*.

2.1 Internalization Requires Actin-Cytoskeleton Dynamics

Internalization of larger particles through both phagocytic and non-phagocytic pathways necessitates the remodelling of the host cell's actin cytoskeleton. This remodelling generates the membrane protrusions, invaginations, or incisions that facilitate uptake [201]. Based on this, we hypothesized that if HSCs internalize *M. tuberculosis* in an active manner, the internalization will be influenced or reduced by agents that disrupt actin polymerisation. To test this hypothesis, we infected hematopoietic progenitor cultures from murine bone marrow with *M. tuberculosis* in the presence of 2 µg/mL cytochalasin D **(Fig. 14)**. Cytochalasin D is a cell-permeable toxin that binds to F-actin polymers and prevents further polymerization, thereby arresting actin cytoskeleton dynamics. Comparison between untreated and cytochalasin D-treated cultures revealed a significant reduction in the frequency of infected MPP1, which decreased tenfold (3.5 ± 1.0 % to 0.3 ± 0.5 %), and MPP2, which decreased twofold (42.3 ± 13.5 % to 21.2 ± 8.7 %). Reduction in infection frequency was also observed in HSC (4.3 ± 2.9 to 2.8 ± 0.3 %) and MPP3/MPP4 (6.0 ± 2.3 % to 3.2 ± 0.4 %), although this reduction did not reach statistical significance (HSC: $p = 0.237$; MPP3/MPP4: $p = 0.098$). These findings demonstrate that *M. tuberculosis* infects HSCs and MPPs in an active internalization process that requires actin cytoskeleton dynamics. However, further studies are necessary to statistically support this finding in the most upstream progenitors, the HSCs, as well.

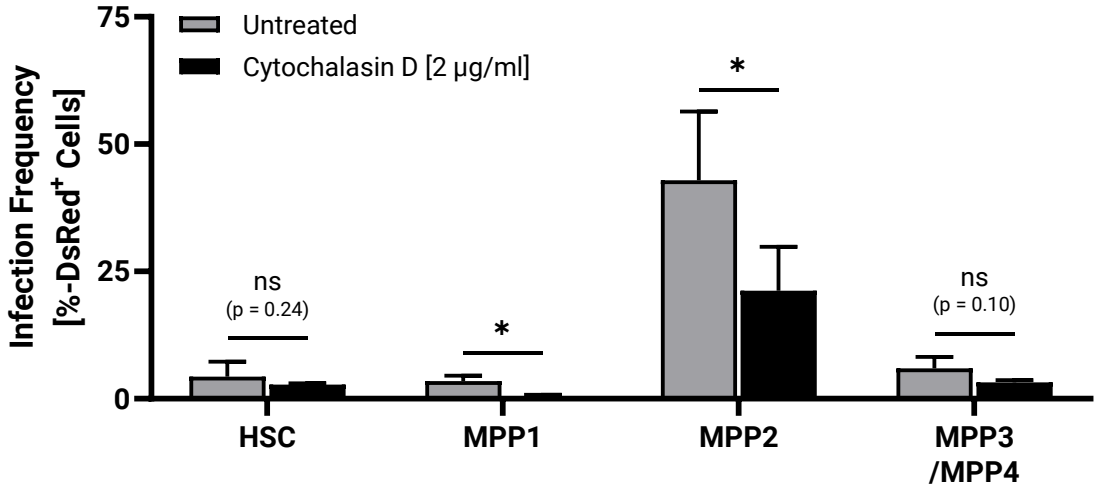

Figure 14: Inhibition of actin-polymerisation in hematopoietic stem and progenitor cells through cytochalasin D during *M. tuberculosis* in vitro infection. Bone marrow cells from C57Bl/6J mice were collected and Lin$^+$-cells were depleted. Progenitor-enriched cultures were treated with cytochalasin D [2 µg/mL] for 2 hours and infected with *M. tuberculosis* H37Rv DsRed at a MOI of 10 without removing cytochalasin D. The frequency of infected hematopoietic stem and progenitor cells (HSPCs) was quantified 20 hours post-infection using FACS (HSC: Lin$^-$ c-Kit$^+$ Sca-1$^+$ CD150$^+$ CD48$^-$ DsRed$^+$; MPP1: Lin$^-$ c-Kit$^+$ Sca-1$^+$ CD150$^-$ CD48$^-$ DsRed$^+$; MPP2: Lin$^-$ c-Kit$^+$ Sca-1$^+$ CD150$^+$ CD48$^+$ DsRed$^+$; MPP3/MPP4: Lin$^-$ c-Kit$^+$ Sca-1$^+$ CD150$^-$ CD48$^+$ DsRed$^+$). Bars represent the mean ± SD [n=3]. Statistical significance is determined by paired one-tailed t-test. Asterisks indicate p-values (*p ≤ 0.05; ns p > 0.05).

To further elucidate the role of actin cytoskeleton dynamics and membrane remodelling in the uptake of *M. tuberculosis* in HSCs, we hypothesized that phenotypic signs thereof might be detectable through immunofluorescence imaging of HSCs interacting with surface-adherent *M. tuberculosis*. To test this, we reanalysed previously sorted suspensions of murine and human HSCs. These samples had been infected with fluorescent *M. tuberculosis* DsRed, followed by cell-sorting to obtain homogenous populations of HSCs **(Fig. 12)**. In murine HSCs, the host cell surface was labelled with α-Sca-1-APC, while in human HSCs, phalloidin-AF488 was used without additional extensive permeabilization to either binding sub-membranous actin or surface molecules in a non-specific manner.

We employed confocal laser scanning microscopy to identify HSCs with surface-adherent *M. tuberculosis* DsRed (red) **(Fig. 15)**. Although most *M. tuberculosis*-associated HSCs are infected, as previously described, we also identified surface-adherent mycobacteria in murine **(Fig. 15A)**, and humane HSC **(Fig. 15B-D)**. Notably, *M. tuberculosis* was consistently found in close proximity to the host cells. Bacteria not associated with HSCs were not observed.

We frequently observed membrane protrusions, morphological signs of membrane ruffling, (indicated by arrows) extending towards extracellular bacteria. Membrane protrusions reminiscent of filopodia or lamellipodia were not observed. In multiple instances, *M.*

tuberculosis was observed crossing the host cell membrane adjacent to a membrane protrusion **(Fig. 15C&D)**. In these cases, the fluorescence signal from membrane labelling was absent at the site of bacterial entry, indicating either lack of the cell membrane or inaccessibility to the phalloidin dye.

In summary, our findings demonstrate that murine and human HSCs exhibit a morphological phenotype reminiscent of membrane ruffling in response to surface-adherent *M. tuberculosis*, providing further evidence that an active, actin-driven internalization mechanism and membrane remodelling facilitate the infection of HSCs by *M. tuberculosis*.

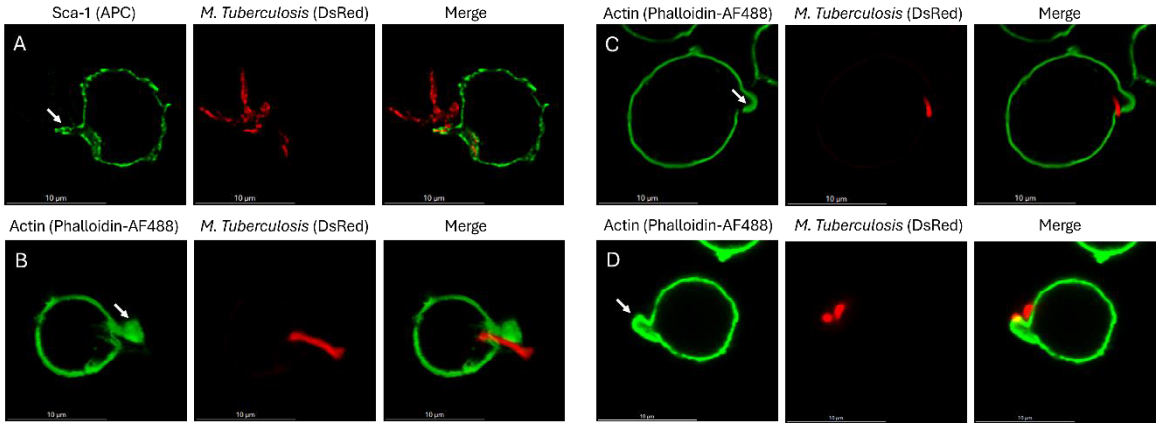

Figure 15: Morphological analysis of hematopoietic stem cells by confocal laser scanning microscopy following *M. tuberculosis* in vitro infection. Hematopoietic progenitor cell cultures from murine bone marrow or human peripheral blood were infected with *M. tuberculosis* H37Rv DsRed at a MOI of 10. 20 hours post-infection hematopoietic stem cells (HSCs) were sorted and imaged using a Leica TCS SP5 confocal microscope. The cell surface (green) of murine HSCs is detected by α-Sca1-APC ($\lambda_{Ex.}$ = 651 nm $\lambda_{Em.}$ = 660 nm; Laser = 633 nm; Filter = 640-700 nm). The cell surface (green) of human HSCs is detected by phalloidin-AF488 ($\lambda_{Ex.}$ = 494 nm / $\lambda_{Em.}$ = 517 nm; Laser = 488 nm; Filter = 500-545 nm). *M. tuberculosis* (red]) is detected through DsRed ($\lambda_{Ex.}$ = 558 nm / $\lambda_{Em.}$ = 583 nm; Laser = 488 nm / 561 nm; Filter = 590-625 nm / 621-718 nm). **A)** Murine HSC. **B-D)** Human HSCs from a single donor. Arrows indicate membrane protrusions extending towards extracellular bacteria. Images were processed using adaptive LIGHTNING deconvolution and automatic LUT-adjustment.

To further delineate the pathways utilized by *M. tuberculosis* to infect HSCs and to confirm the involvement of actin cytoskeletal dynamics, we aimed to visualize actin polymerisation during and after *M. tuberculosis* internalization. The force generated by actin-polymerisation pushes the cell membrane around the particle and is thus typically associated with membrane protrusions and internalized membrane compartments after uptake [203]. Our objective was to detect these focal accumulations of actin in infected HSCs by immunofluorescence imaging.

Human $CD34^+$-enriched cell cultures were infected with fluorescent *M. tuberculosis* H37Rv DsRed, followed by cell sorting to isolate a homogeneous population of HSCs **(Fig. S1)**. To visualize the actin cytoskeleton phalloidin-AF488 was used to detect F-actin polymers in permeabilized cells. Additionally, DNA was detected using 4,6-Diamidino-2-Phenylindole

(DAPI). After immunofluorescence staining, HSCs were imaged using confocal laser scanning microscopy **(Fig. 16)**.

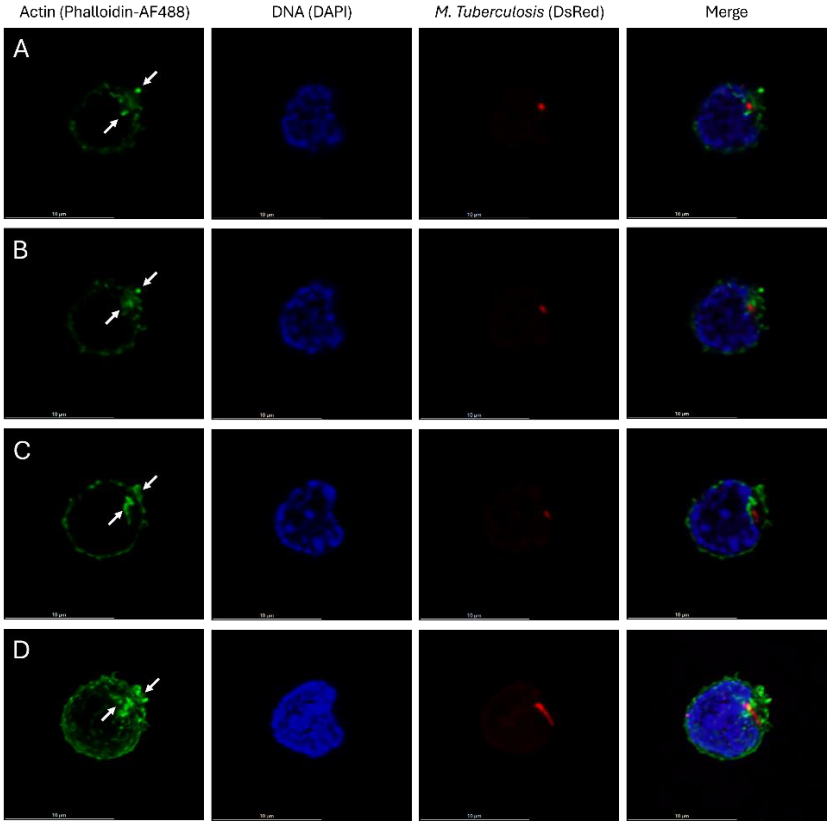

Figure 16: Detection of intracellular F-actin polymers by confocal laser scanning microscopy following *M. tuberculosis* in vitro infection. A hematopoietic progenitor cell culture from human peripheral blood was infected with *M. tuberculosis* H37Rv DsRed at a MOI of 10. 20 hours post-infection human hematopoietic stem cells (HSCs) were sorted and imaged using a Leica TCS SP5 confocal microscope. F-actin (green) is detected through phalloidin-AF488 ($\lambda_{Ex.}$ = 494 nm / $\lambda_{Em.}$ = 517 nm; Laser = 488 nm; Filter = 506-555 nm). DNA (blue) is detected through DAPI ($\lambda_{Ex.}$ = 359 nm / $\lambda_{Em.}$ = 457 nm; Laser = 405 nm; Filter = 420-490 nm). *M. tuberculosis* (red) is detected through DsRed ($\lambda_{Ex.}$ = 558 nm / $\lambda_{Em.}$ = 583 nm; Laser = 561 nm; Filter = 566-614 nm). **A)** Z-stack at 3.13 µm. **B)** Z-stack at 3.55 µm. **C)** Z-stack at 4.3 µm. **D)** Maximum projection image of 200 z-stacks from 0 µm to 8.35 µm. Arrows indicate membrane F-actin polymers surrounding intracellular bacteria and at the site of entry. Images were processed using adaptive LIGHTNING deconvolution and automatic LUT-adjustment.

We found that an accumulation of actin polymers enwrapped intracellular bacteria (upward arrows, first column). Actin polymers were also detected associated with the host cell plasma membrane where membrane protrusions exhibited intensified actin-signals (downward arrows) compared to adjacent structures. Therefore, our microscopic results demonstrate actin polymerization in both the initial (membrane remodeling) and final stages (particle internalization) of bacterial uptake in HSCs.

In summary, our quantitative and qualitative findings show *M. tuberculosis* infection in HSCs as an actin-dependent process. We found actin polymerization to be involved on both a molecular level, through Cytochalasin D-inhibition, and a morphological level, as shown through association between membrane protrusions and intracellular mycobacteria with the actin cytoskeleton.

2.2 HSC Infection Involves neither Phagocytosis nor Macropinocytosis

Bacterial internalization recognizes two major categories of uptake, namely phagocytosis and pinocytosis. They are differentiated by receptor engagement, membrane dynamics, and distinct molecular signalling pathways. Phagocytosis, exclusive to innate immune cells of myeloid origin, involves the uptake of large particles, whereas pinocytosis is primarily a fluid intake process that is co-opted by pathogens for cellular invasion. Pinocytosis occurs in almost all cell types and is further categorizes into macropinocytosis, clathrin-mediated endocytosis, caveolin-mediated endocytosis, and clathrin-and-caveolin-independent endocytosis.

Phagocytosis:

To elucidate the mechanism of HSC infection by *M. tuberculosis,* we sought to determine the specific pathway involved. Phagocytosis is the principal mechanism by which *M. tuberculosis* is taken up by professional phagocytes and is predominantly mediated by opsonic receptors, particularly complement receptors (CRs) following opsonization, and non-opsonic receptors such as the C-type lectins, macrophage mannose receptor (MMR/CD206) on macrophages and dendritic cell-specific intercellular adhesion molecule-3-grabbing non-integrin (DC-SIGN/CD209) on dendritic cells. Non-opsonic receptors primarily recognize mannose-capped lipoarabinomannan (ManLAM) and other similar saccharide motifs of the mycobacterial cell wall [204]. Consequently, our objective was to assess the involvement of both opsonic- and non-opsonic phagocytosis in the process of infection of HSCs by *M. tuberculosis*.

To investigate the role of opsonic phagocytosis, *M. tuberculosis* H37Rv DsRed was pre-incubated with autologous donor serum to facilitate the deposition of opsonins, such as C3b, on the bacterial surface prior to infection. Human hematopoietic progenitor cultures were then infected with either opsonized or non-opsonized *M. tuberculosis*. Following infection, the frequency of infected HSCs was quantified using FACS after immunofluorescence staining **(Fig. 17)**. Prior opsonization resulted in a slight reduction in the frequency of infected HSCs (9.2 ± 6.0 % vs. 6.0 ± 4.1 %) and MPPs (6.9 ± 5.6 % vs. 5.4 ± 4.6 %) compared to the untreated group. However, these differences did not achieve statistical significance (p_{HSC} = 0.133; p_{MPP} = 0.231). As opsonization did not increase infection frequency in HSCs, opsonic-phagocytosis is not involved in HSC infection.

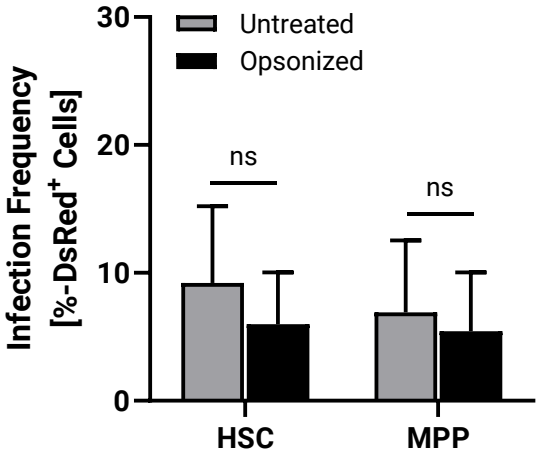

Figure 17: Influence of prior *M. tuberculosis* opsonisation on the infection frequency of hematopoietic stem and progenitor cells in vitro. Peripheral blood cells together with autologous sera from adult human donors were collected and $CD34^+$-cells were enriched. *M. tuberculosis* H37Rv DsRed was incubated 1:1 with autologous donor serum for 30 min. at room temperature. Progenitor-enriched cultures were infected with opsonized *M. tuberculosis* at a MOI of 10. The frequency of infected hematopoietic stem cells (HSCs) and multipotent progenitors (MPP) was quantified 20 hours post-infection using FACS (HSC: $CD34^+$ $CD45RA^-$ Lin^- $CD38^{-/low}$ $CD90^+$ $DsRed^+$; MPP: $CD34^+$ $CD45RA^-$ Lin^- $CD38^{-/low}$ $CD90^-$ $DsRed^+$). Bars represent the mean ± SD [n=3]. Statistical significance is determined by paired two-tailed t-test. Asterisks indicate p-values (*$p \leq 0.05$; ns $p > 0.05$).

To assess the role of non-opsonic phagocytosis in the infection of HSCs by *M. tuberculosis*, we investigated the involvement of non-opsonic receptors that recognize ManLAM, a key component of the mycobacterial cell wall. We hypothesized that competitive inhibition of these receptors with mannose-polymers, as described in earlier studies, could reduce HSC infection [205,206]. To evaluate this hypothesis, we infected human hematopoietic progenitors with *M. tuberculosis* H37Rv DsRed in the presence of mannan at varying concentrations. Following infection, the frequency of infected HSCs in untreated versus mannan-treated cultures was quantified by FACS **(Fig. 18)**.

We observed no significant differences by mannan treatment in the frequency of infected HSC (17.6 ± 19.9 % vs. 18.9 ± 28.0 % [10 mg/mL mannan]) or MPPs (9.0 ± 10.2 % vs. 4.5 ± 3.0 % [10 mg/mL mannan]) compared to untreated controls. Mannan, intended to competitively inhibit mannose binding C-type lectins had no observable influence on HSC infection. Hence, carbohydrate recognition by C-type lectins is also not involved in *M. tuberculosis* internalization by HSCs.

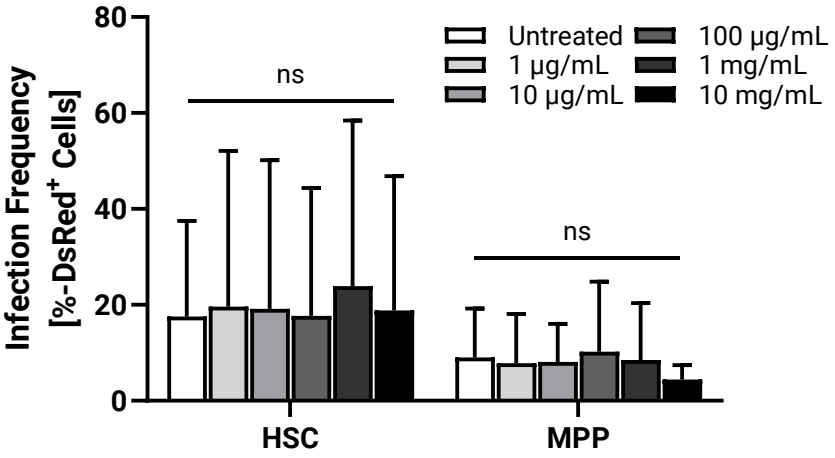

Figure 18: Influence of competitive inhibition of mannose binding C-type lectins through mannan on *M. tuberculosis* in vitro infection of hematopoietic stem and progenitor cells. Peripheral blood cells from adult human donors were collected and $CD34^+$-cells were enriched. Progenitor-enriched cultures were incubated with Mannan from *S. cerevisiae* at indicated concentrations and infected with *M. tuberculosis* H37Rv DsRed at a MOI of 10. The frequency of infected hematopoietic stem cells (HSCs) and multipotent progenitors (MPP) was quantified 20 hours post-infection using FACS (HSC: $CD34^+$ $CD45RA^-$ Lin^- $CD38^{-/low}$ $CD90^+$ $DsRed^+$; MPP: $CD34^+$ $CD45RA^-$ Lin^- $CD38^{-/low}$ $CD90^-$ $DsRed^+$). Bars represent the mean ± SD [n=3]. Statistical significance is determined by paired two-tailed t-test. Asterisks indicate p-values (*$p \leq 0.05$; ns $p > 0.05$).

In summary, our data shows neither opsonic nor non-opsonic phagocytosis to be involved in the infection of HSCs and MPPs by *M. tuberculosis*. Instead, induced internalization pathways, which mediate infection of non-phagocytic cells, are speculated to be responsible.

Macropinocytosis:

Macropinocytosis is the earliest internalization pathway to emerge during myeloid differentiation, involves membrane ruffling, and was shown to facilitate *M. tuberculosis* internalization by non-phagocytic cells other than HSCs [189]. We hypothesized that HSC infection may also depend on this pathway, and thus, inhibition of macropinocytosis would reduce the frequency of infection [189]. Due to the strong fluorescence of amiloride, a well-established inhibitor of macropinocytosis, we instead employed imipramine, a repurposed drug discovered to inhibit macropinocytosis without affecting other internalization pathways [208].

Human hematopoietic progenitor cultures were treated with 5 µM imipramine and subsequently infected with *M. tuberculosis* H37Rv DsRed. Following immunofluorescence staining, the frequency of infected HSCs in untreated versus imipramine-treated cultures was quantified by FACS **(Fig. 19)**. A refined gating strategy was applied to exclude non-viable but intact HSCs **(Fig. S2)**. No significant differences in infection frequency were observed between untreated and treated groups for HSCs (31.8 ± 18.2 % vs. 29.8 ± 17.1 %) and MPPs

(4.1 ± 0.4 % vs. 4.6 ± 0.7 %). These results show that classical macropinocytosis pathways are not involved in the infection of HSCs by *M. tuberculosis*.

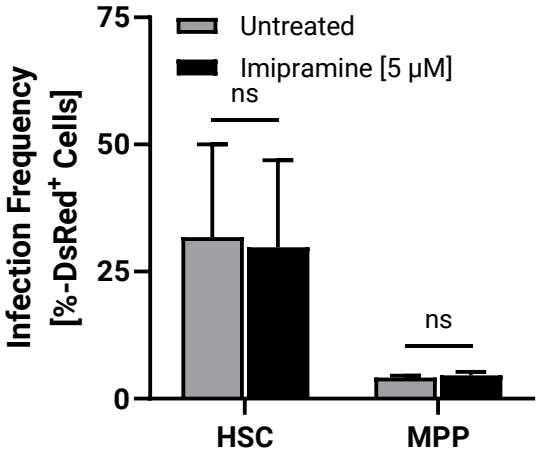

Figure 19: Inhibition of macropinocytosis during *M. tuberculosis* in vitro infection of hematopoietic stem and progenitor cells. Peripheral blood cells from adult human donors were collected and $CD34^+$-cells were enriched. Progenitor-enriched cultures were incubated with imipramine hydrochloride [5 µM] and infected with *M. tuberculosis* H37Rv DsRed at a MOI of 10. The frequency of infected hematopoietic stem cells (HSCs) and multipotent progenitors (MPPs) was quantified 20 hours post-infection using FACS (HSC: $CD34^+$ $CD45RA^-$ Lin^- $CD38^{-/low}$ $CD90^+$ $DsRed^+$; MPP: $CD34^+$ $CD45RA^-$ Lin^- $CD38^{-/low}$ $CD90^-$ $DsRed^+$). Bars represent the mean ± SD [n=2]. Statistical significance is determined by paired one-tailed t-test. Asterisks indicate p-values (*$p \leq 0.05$; ns $p > 0.05$).

Clathrin-mediated internalization:

Clathrin can function as a hub for the complex spatiotemporal recruitment of proteins during particle internalization. Beyond its established role in receptor-mediated endocytosis of small particles, clathrin also orchestrates actin network regulation during uptake of larger particles such as bacteria [191,209]. Unlike clathrin-coated pits observed during viral uptake, bacterial internalization involves clathrin plagues on the cytoplasmic face of the plasma membrane, which have been implicated to function as scaffolds coordinating the interaction of key regulators of the actin cytoskeleton [209]. Demonstrating that *M. tuberculosis* internalization by HSCs is non-phagocytic, we aimed to investigate whether internalization may involve clathrin, similar to induced bacterial internalization in other non-phagocytic cells. We thus hypothesized that interference with clathrin function would impair the infection frequency of HSCs if clathrin played a role in uptake.

To test this hypothesis, we employed Pitstop II, an inhibitor of clathrin-mediated endocytosis that targets the N-terminal domain of the clathrin heavy chain, blocking the interaction with clathrin-box-motif-containing peptides in downstream pathways [210]. Human hematopoietic progenitor cultures were cultured with 20 µM Pitstop II and subsequently infected with *M. tuberculosis* H37Rv DsRed. The frequency of infected HSCs in untreated

versus Pitstop II-treated cultures was quantified using FACS **(Fig. 20, Fig. S2)**. Treatment with Pitstop II resulted in a significant reduction in the frequency of infected HSCs, decreasing to 57.0 % of the untreated level (52.3 ± 9.1 % vs. 29.8 ± 20.9 %). No significant difference was observed in the frequency of infected MPPs (2.9 ± 0.7 % vs. 4.4 ± 1.2 %) between untreated and treated groups. The reduction in HSC infection frequency achieved with Pitstop II treatment – comparable to the reduction observed with cytochalasin D treatment in HSPCs **(Fig. 14)** – demonstrates that clathrin is involved in the internalization of *M. tuberculosis* by HSCs.

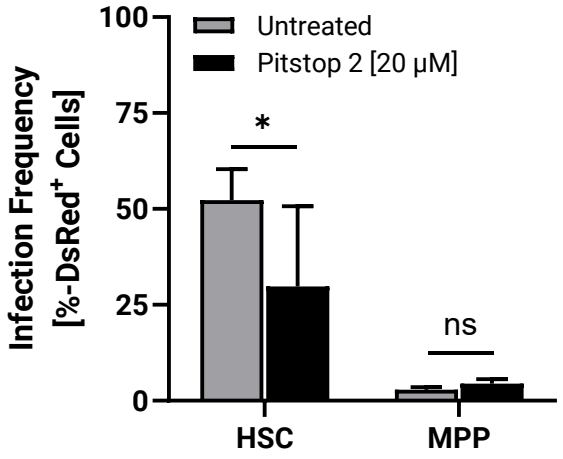

Figure 20: Inhibition of Clathrin-mediated endocytosis through Pitstop 2 during hematopoietic stem and progenitor cell in vitro infection with *M. tuberculosis*. Peripheral blood cells from adult human donors were collected and $CD34^+$-cells were enriched. Progenitor-enriched cultures were incubated with Pitstop 2 [20 µM] and infected with *M. tuberculosis* H37Rv DsRed at a MOI of 10. The frequency of infected hematopoietic stem cells (HSCs) and multipotent progenitors (MPPs) was quantified 20 hours post-infection using FACS (HSC: $CD34^+$ $CD45RA^-$ Lin^- $CD38^{-/low}$ $CD90^+$ $DsRed^+$; MPP: $CD34^+$ $CD45RA^-$ Lin^- $CD38^{-/low}$ $CD90^-$ $DsRed^+$). Bars represent the mean ± SD [n=3]. Statistical significance is determined by paired one-tailed t-test. Asterisks indicate p-values (*$p \leq 0.05$; ns $p > 0.05$).

2.3 Internalization of *M. tuberculosis* by HSCs Involves CD36 Engagement

Following the identification of clathrin interactions and both non-phagocytic and non-macropinocytic membrane ruffling, as underlying mechanisms of mycobacterial uptake in HSCs, our next objective was to identify the receptor responsible for initiating internalization of *M. tuberculosis*. Since our data showed no involvement of carbohydrate recognition by C-type lectins or opsonin recognition by opsonic receptors, we explored the role of scavenger receptors recognizing lipid motifs on *M. tuberculosis*.

Among potential candidates, we focused on scavenger receptor class B member 3 (SCAR-B3), also known as CD36 or fatty acid translocase (FAT). CD36 is known for its role in

facilitating free fatty acid uptake in HSCs during emergency hematopoiesis [151]. Furthermore, its analogue, scavenger receptor B1 (SR-B1) has been implicated in the invasion of non-phagocytic cells, such as airway microfold cells and mesenchymal stem cells by *M. tuberculosis* [211,212]. Given these findings, we sought to investigate the involvement of CD36 in the infection of HSCs by *M. tuberculosis*. We aimed to quantify the surface expression of CD36 on HSCs, and to analyze whether CD36 expression correlates with infection frequency and might thereby represent a determinant for permissiveness.

Human hematopoietic progenitor cultures were infected with *M. tuberculosis* H37Rv DsRed. Following infection, immunofluorescence staining was performed for subsequent identification of HSCs and MPPs. The presence of CD36 was quantified using α-CD36-FITC and the frequency of $CD36^+$ HSCs ($CD34^+$ $CD45RA^-$ Lin^- $CD38^{-/low}$ $CD90^+$ $CD36^+$) and $CD36^+$ MPPs ($CD34^+$ $CD45RA^-$ Lin^- $CD38^{-/low}$ $CD90^-$ $CD36^+$) was quantified by FACS **(Fig. 21A; Fig. S3)**. We found that 91.1 ± 4.1 % of all HSCs and 77.4 ± 17.8 % of all MPPs expressed CD36 on their surface. Hence, the scavenger receptor CD36 is present on human HSCs.

To determine whether CD36 is enriched among infected HSCs and may represent a determinant for HSC permissiveness, we quantified the subsets of $CD36^+$ $DsRed^-$ HSCs versus $CD36^+$ $DsRed^+$ HSCs **(Fig. 21B)**. CD36 was neither enriched nor reduced in infected cells, as no significant difference in the ratio of $CD36^+$ cells in uninfected versus infected HSCs (90.1 ± 6.4 % vs. 90.0 ± 7.1 %) and MPPs (74.6 ± 22.2 % vs. 82.3 ± 19.8 %) was observed. Additionally, the frequency of $CD36^+$ HSC did not correlate with variations in infection frequency among donors ($r = 0.5758$ $p = 0.1159$). Substantially more HSCs were found to be $CD36^+$ (HSC: 91.1 ± 4.1 %; MPP: 77.4 ± 17.8 %) than $DsRed^+$ (HSC: 4.0 ± 1.1 %; MPP: 3.8 ± 0.5 %). Although CD36 may be involved in *M. tuberculosis* uptake by HSCs, it is not the only receptor responsible for determining permissiveness of HSCs to *M. tuberculosis* infection.

In summary, our data pivotally demonstrate surface expression of CD36, a known receptor to recognize *M. tuberculosis*, in HSCs.

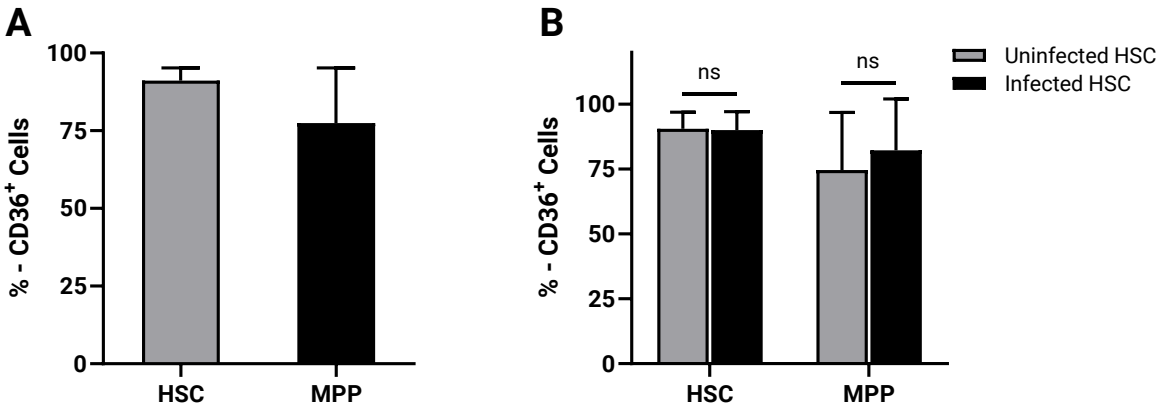

Figure 21: Surface expression of the class B type scavenger receptor CD36 in naïve human hematopoietic stem and progenitor cells and following *M. tuberculosis* in vitro infection. Peripheral blood cells from adult human donors were collected and $CD34^+$-cells were enriched. **A)** After 20 hours, the frequency of $CD36^+$ hematopoietic stem cells (HSCs) and multipotent progenitors (MPPs) was quantified using FACS (HSC: $CD34^+$ $CD45RA^-$ Lin^- $CD38^{-/low}$ $CD90^+$ $CD36^+$; MPP: $CD34^+$ $CD45RA^-$ Lin^- $CD38^{-/low}$ $CD90^-$ $CD36^+$). **B)** Progenitor-enriched cultures were infected with *M. tuberculosis* H37Rv DsRed at a MOI of 10. After 20 hours, the frequency of CD36-positive cells among infected versus uninfected HSCs and MPPs was quantified using FACS. Pearson correlation coefficients were computed between the frequency of $CD36^+$ HSCs and the frequency of infection: r = 0.5758 p = 0.1159. Bars represent the mean ± SD [n = 3]. Statistical significance is determined by paired two-tailed t-test. Asterisks indicate p-values (*p ≤ 0.05; ns p > 0.05).

To validate the role of CD36 in mediating *M. tuberculosis* uptake by HSCs, we employed sulfo-N-succinimidyl oleate (SSO), a described inhibitor of CD36 binding. SSO binds irreversibly to lysine 164 within the hydrophobic binding pocket of CD36, thereby preventing the access of fatty acids and oxidized low-density lipoproteins (oxLDLs) [213]. We hypothesized that inhibiting ligand recognition by CD36 would lead to a decrease in the frequency of infected HSCs if the receptor played a pivotal role in *M. tuberculosis* internalization.

To test this hypothesis, human hematopoietic progenitor cultures were treated with 200 µM SSO prior to infection with *M. tuberculosis* H37Rv DsRed. Following immunofluorescence staining, the frequency of infected HSCs in untreated versus SSO-treated cultures was quantified via FACS **(Fig. 22, Fig. S2)**. SSO treatment led to a significant reduction in the frequency of infected HSC, decreasing it to 22.7 % of the untreated control (13.0 ± 0.6 % vs. 2.9 ± 4.2 %). A slight reduction in the infection frequency of MPPs was also observed (5.7 ± 3.3 % vs. 3.6 ± 5.0 %) but not in a statistically significant manner. With the observed reduction of infection frequency in HSCs following CD36 inhibition, these results show that CD36-mediated recognition is involved in *M. tuberculosis* internalization by HSCs.

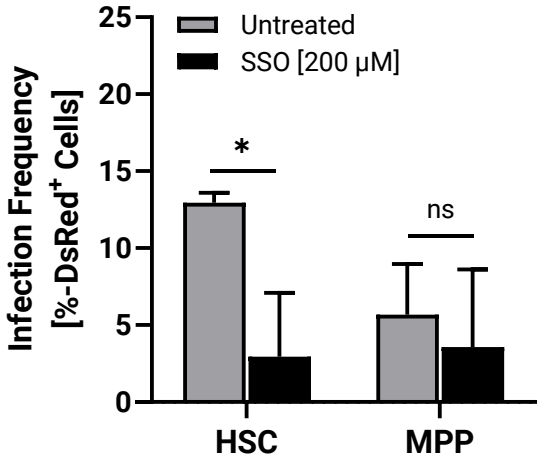

Figure 22: Inhibition of the class B type scavenger receptor CD36 through Sulfo-N-succinimidyl oleate during hematopoietic stem and progenitor cell in vitro infection with *M. tuberculosis*. Peripheral blood cells from adult human donors were collected and $CD34^+$-cells were enriched. Progenitor-enriched cultures were incubated with Sulfo-N-succinimidyl oleate (SSO) [200 µM] and infected with *M. tuberculosis* H37Rv DsRed at a MOI of 10. The frequency of infected hematopoietic stem cells (HSCs) and multipotent progenitors (MPPs) was quantified 20 hours post-infection using FACS (HSC: $CD34^+$ $CD45RA^-$ Lin^- $CD38^{-/low}$ $CD90^+$ $DsRed^+$; MPP: $CD34^+$ $CD45RA^-$ Lin^- $CD38^{-/low}$ $CD90^-$ $DsRed^+$). Bars represent the mean ± SD [n=2]. Statistical significance is determined by paired one-tailed t-test. Asterisks indicate p-values (*$p \leq 0.05$; ns $p > 0.05$).

2.4 The RD1-Locus is Not Crucial for HSC infection

The closely related class B scavenger receptor, SR-B1, has been shown to facilitate entry of *M. tuberculosis* into another type of non-phagocytic cell, airway microfold cells. EsxA/ESAT-6, a protein secreted by a mycobacterial T7SS, was identified as the ligand to initiate this process [211]. Given the homology between SR-B1 and CD36 within the conserved CD36 binding domain, we sought to determine whether EsxA or other Esx-T7SS-secreted factors are similarly required for HSC infection by *M. tuberculosis*. The T7SS machinery, and its secreted effectors are encoded by the region of difference 1 (RD1) [214]. Consequently, we aimed to assess whether deletion of the RD1 locus impacts the ability of *M. tuberculosis* to infect HSCs.

To test this, we infected human hematopoietic progenitor cultures with either a wildtype RD1 strain, *M. tuberculosis* H37Rv DsRed, or an RD1-deletion strain, *M. tuberculosis* H37Rv ΔRD1 mCherry. Following immunofluorescence staining, the frequency of infected HSCs was quantified using FACS **(Fig. 23)**. Deletion of RD1 did not significantly affect the frequency of infected HSCs (3.1 ± 1.2 % vs 4.6 ± 4.9 %) and MPPs (2.4 ± 0.2 % vs. 3.8 ± 0.5 %). These findings show that HSC infection by *M. tuberculosis* is independent of T7SS-associated, RD1-encoded factors. This indicates that bacterial recognition and internalization by HSCs involves mechanisms and interactions other than those active in airway microfold cells.

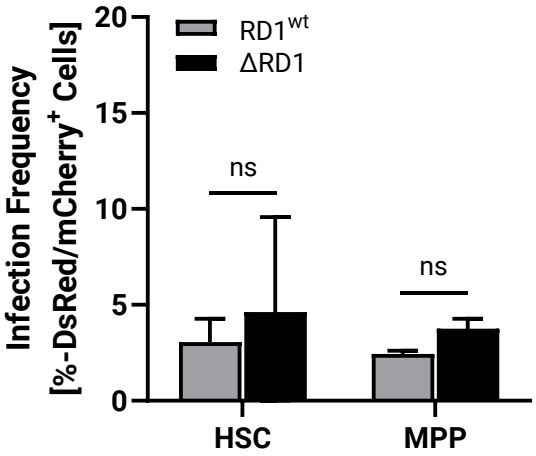

Figure 23: In vitro hematopoietic stem and progenitor cell infection with a RD1-locus deletion mutant of *M. tuberculosis*. Peripheral blood cells from adult human donors were collected and $CD34^+$-cells were enriched. Progenitor-enriched cultures were either infected with *M. tuberculosis* H37Rv DsRed or *M. tuberculosis* H37Rv ΔRD1 mCherry at a MOI of 10. The frequency of infected hematopoietic stem cells (HSCs) and multipotent progenitors (MPPs) was quantified 20 hours post-infection using FACS (HSC: $CD34^+$ $CD45RA^-$ Lin^- $CD38^{-/low}$ $CD90^+$ $DsRed^+/mCherry^+$; MPP: $CD34^+$ $CD45RA^-$ Lin^- $CD38^{-/low}$ $CD90^-$ $DsRed^+/mCherry^+$). Bars represent the mean ± SD [n=2]. Statistical significance is determined by paired two-tailed t-test. Asterisks indicate p-values (*$p \leq 0.05$; ns $p > 0.05$).

In conclusion, we found CD36 to be expressed by most HSCs and that *M. tuberculosis* infection can be fundamentally reduced by inhibiting CD36 binding. Furthermore, molecular characterization of the underlying pathways using Cytochalasin D and Pitstop II identified actin cytoskeleton dynamics and clathrin interactions as key molecular factors of *M. tuberculosis* internalization. Lastly, morphological observations with confocal laser scanning microscopy identified membrane structures reminiscent of membrane ruffles towards surface adherent mycobacteria. Co-localization of actin-polymers with both, the membrane protrusions and intracellular *M. tuberculosis* after successful internalization demonstrated the engagement of actin as the final step of the signalling cascade.

3. Naïve HSCs Are Rendered Permissive to Infection by Unknown Stimuli

The observed slow kinetics of HSC infection in vitro **(section D.1.1)** led us to hypothesize that specific stimuli may render those otherwise non-permissive cells permissive to *M. tuberculosis*. We speculated that this change in permissiveness could be induced by microbial stimuli. Accordingly, our objective was to identify these stimuli and to elucidate underlying mechanisms that promote HSC permissiveness to infection.

3.1 HSCs of Neonatal Origin Are Non-Permissiveness to *M. tuberculosis* Infection

We hypothesized that HSCs permissiveness is a result of atypical genetic programs in HSCs arising from the cumulative impact of microbial exposure during an individual's life. To elucidate the mechanisms underlying HSC permissiveness to infection, we initially focused on neonatal HSCs. Neonatal HSCs, which have not been exposed to any microbial stimuli yet, were selected as an ideal model to test this hypothesis. Unlike adult-derived HSCs, which have been exposed to a history of infections and repeating exposure to microbiome-derived microbe-associated molecular patterns (MAMPs), neonatal HSCs offer a unique opportunity to examine the effects of initial exposure to *M. tuberculosis* as their first encounter with bacterial antigens.

Human hematopoietic progenitor cultures isolated from neonatal umbilical cord blood were infected with *M. tuberculosis* H37Rv DsRed. Following immunofluorescence staining, the frequency of infected HSCs was quantified using FACS. Infection frequency of umbilical cord blood HSCs was compared to that of adult HSCs, infected under standardized conditions across multiple experiments **(Fig. 24)**. HSC infection frequencies were significantly lower in HSCs (0.6 ± 0.2 % vs. 21.3 ± 20.1 %) and MPPs (0.3 ± 0.4 % vs. 4.5 ± 4.0 %) derived from umbilical cord blood compared to adult peripheral blood. Umbilical cord blood HSCs and MPPs were almost entirely non-permissive to infection under conditions in which adult peripheral blood HSCs and MPPs are permissive. Hence, HSCs of equal immunophenotypes exhibit distinct host-specific functional characteristics in the acquisition of permissiveness to *M. tuberculosis* infection. These results show that the host's age and immunological

background are critical determinants of acquired permissiveness to *M. tuberculosis* infection.

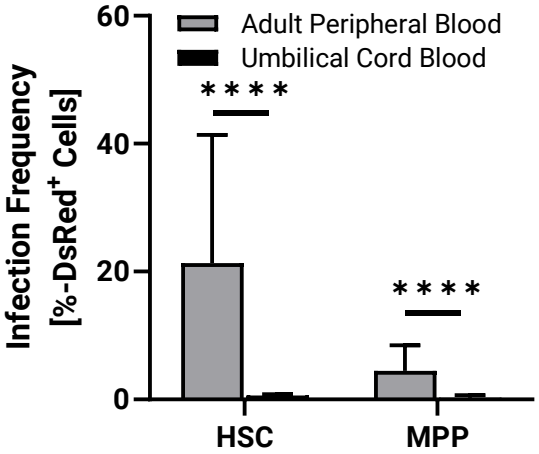

Figure 24: Comparison of *M. tuberculosis* in vitro infection between hematopoietic stem and progenitor cells derived from neonatal umbilical cord blood and adult peripheral blood. Peripheral blood cells from adult human donors and umbilical cord blood cells from neonates was collected and $CD34^+$-cells were enriched. Progenitor-enriched cultures were infected with *M. tuberculosis* H37Rv DsRed at a MOI of 10. The frequency of infected hematopoietic stem cells (HSCs) and multipotent progenitors (MPPs) was quantified 20 hours post-infection using FACS (HSC: $CD34^+$ $CD45RA^-$ Lin^- $CD38^{-/low}$ $CD90^+$ $DsRed^+$; MPP: $CD34^+$ $CD45RA^-$ Lin^- $CD38^{-/low}$ $CD90^-$ $DsRed^+$). Bars represent the mean ± SD [Adult Peripheral Blood n=29; Umbilical Cord Blood n=4]. Statistical significance is determined by unpaired one-tailed t-test with Welch's correction. Asterisks indicate p-values (****$p \leq 0.00005$; ns $p > 0.05$).

In accordance with our hypothesis of microbe-induced permissiveness, we sought to determine whether the non-permissiveness of HSCs of neonatal origin is due to a general lack of responsiveness to microbial stimuli. Therefore, we examined the well-described response of emergency hematopoiesis in infected umbilical cord blood cultures. As a hallmark of emergency hematopoiesis, we analysed the expansion of lineage-committed progenitor and leukocyte populations **(Fig. 25)**. Using FACS, we distinguished between early hematopoietic progenitors ($CD45^-$ $CD34^+$), lineage-committed hematopoietic progenitors ($CD45RA^+$ $CD34^+$), and mature leukocytes ($CD45RA^+$ $CD34^-$) **(Fig. 25A&B)**. A comparative analysis of these populations before and after infection revealed significant differences between umbilical cord blood and adult peripheral blood cultures **(Fig. 25C)**. We observed a significant expansion of the committed hematopoietic progenitor population ($CD45RA^+$ $CD34^+$) exclusively in adult peripheral blood cultures (2.2 ± 1.9% vs. 11.7 ± 5.9 %). No comparable change was detected in umbilical cord blood cultures (3.0 ± 0.9 % vs. 1.4 ± 0.3). The expansion of $CD45RA^+$ $CD34^+$ cells appeared to result from a newly emerging population arising from the population of $CD45RA^-$ $CD34^+$ early hematopoietic progenitors **(Fig. 25B)**. It was accompanied by a significant reduction in the $CD45RA^-$ $CD34^+$ population (74.0 ± 14.6 % vs. 64.5 ± 16.9 %), while the $CD45RA^+$ $CD34^-$ population remained unchanged (18.8 ± 10.0 %

vs. 18.7 ± 11.7 %) **(Fig. 25C)**. Additionally, umbilical cord blood cultures exhibited a distinct CD34^{high} population, which is absent in adult peripheral blood cultures. As all HSCs derived from umbilical cord blood were non-permissive we did not further investigate whether heterogeneity in their CD34 expression correlates with permissiveness.

In summary, these findings demonstrate that only hematopoietic progenitor cultures derived from adult peripheral blood respond with the expansion of committed progenitors, whereas umbilical cord blood cultures remained unresponsive to the same stimuli. Consequently, the observed non-permissiveness of HSCs from umbilical cord blood correlates with the absence of committed progenitor expansion during in vitro infection. This indicates that key hematopoietic responses towards microbial stimuli are not yet present in cultures from neonatal origin.

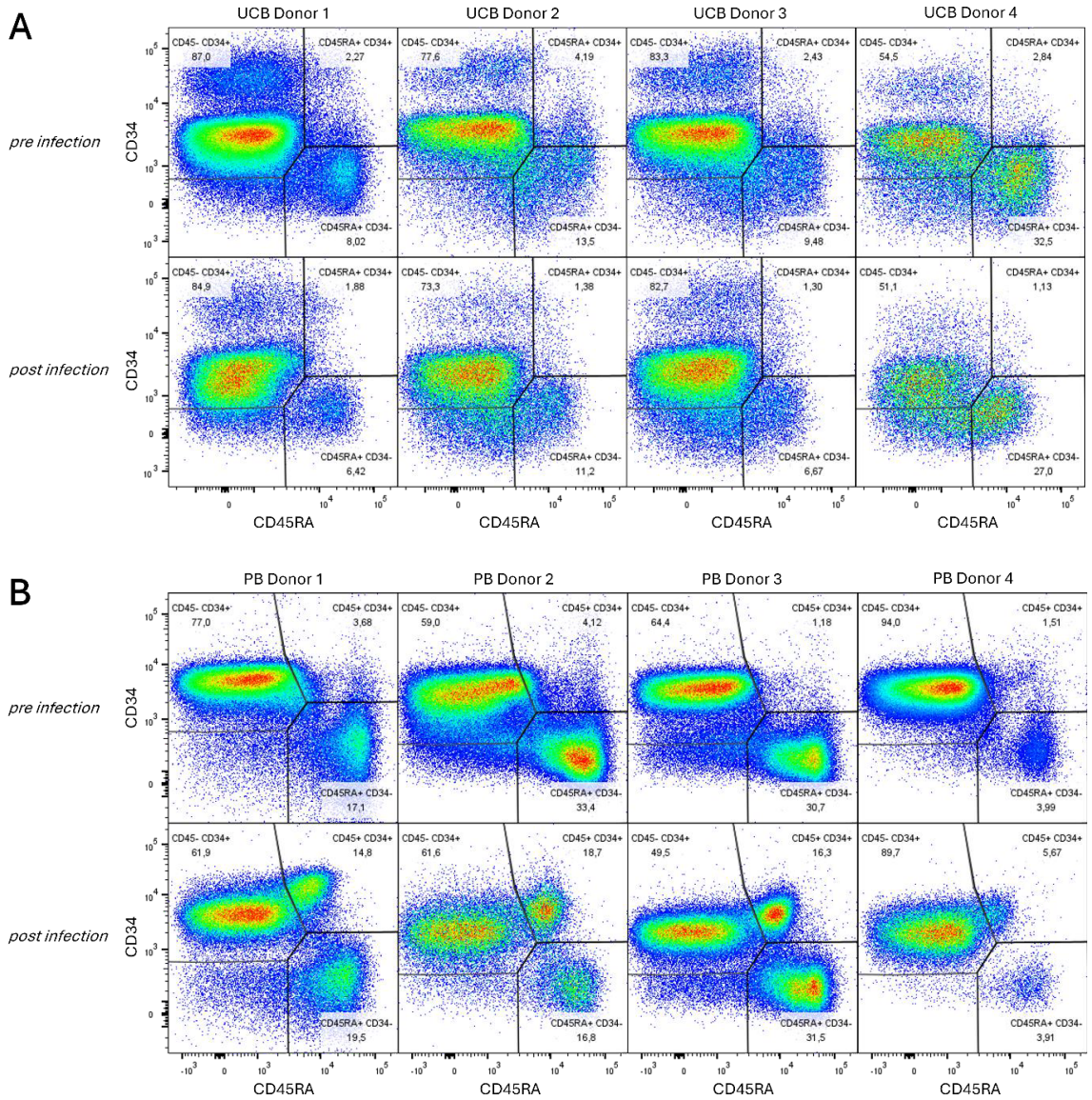

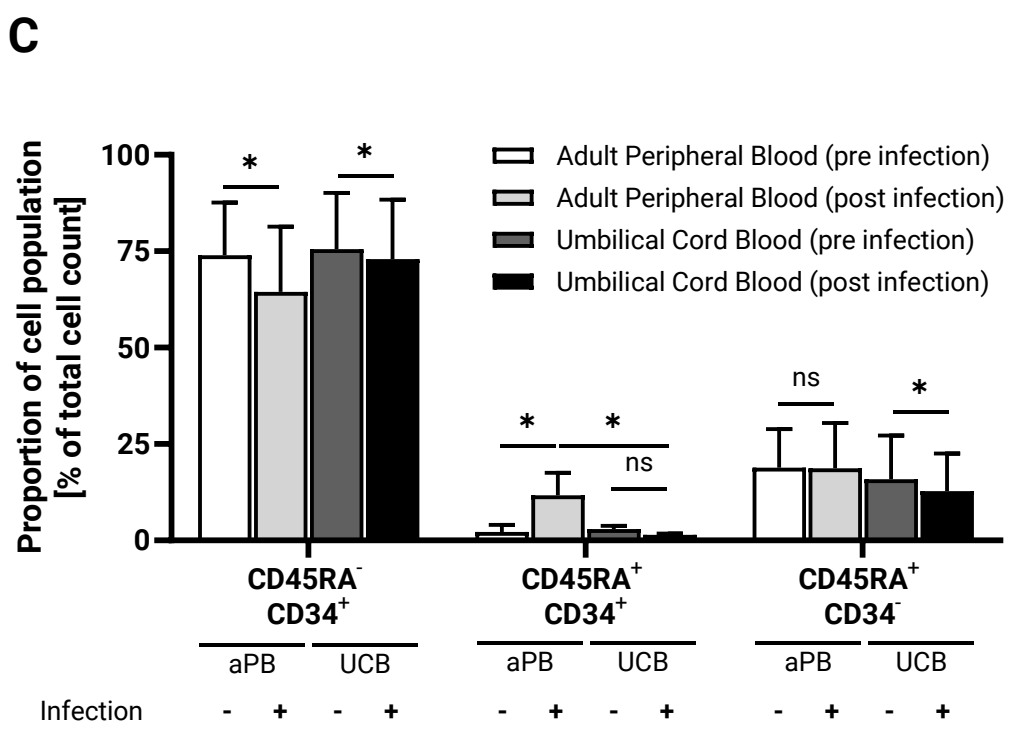

Figure 25: Expansion of the CD45RA$^+$ CD34$^+$ committed progenitor population following *M. tuberculosis* in vitro infection in adult peripheral blood and umbilical cord blood hematopoietic stem and progenitor cell cultures. Peripheral blood cells from adult human donors and umbilical cord blood cells from neonates were collected and CD34$^+$-cells were enriched. The frequency of the indicated populations, distinguished by CD45RA and CD34 expression, was quantified before and 20 hours post infection with *M. tuberculosis* H37Rv DsRed (MOI of 10) using FACS (CD45RA$^-$ CD34$^+$: Early Hematopoietic Progenitors and hematopoietic stem cells (HSCs); CD45RA$^+$ CD34$^+$: Committed Hematopoietic Progenitors; CD45RA$^+$ CD34$^-$: Mature Leukocytes). **A)** FACS-plots of CD45RA and CD34 expression in umbilical cord blood (UCB) cultures. **B)** FACS-plots of CD45RA and CD34 expression in adult peripheral blood (aPB) cultures. **C)** Quantification of the indicated populations between umbilical cord blood (UCB) and adult peripheral blood (aPB) cultures pre- and post-infection. Bars represent the mean ± SD [UCB n=4; aPB n=9]. Statistical significance is determined by paired two-tailed t-test within UCB or aPB-samples and unpaired two-tailed t-test between UCB and aPB-samples. Asterisks indicate p-values (*p ≤ 0.05; ns p > 0.05).

To determine whether the expansion of the CD45RA$^+$ CD34$^+$ population was specifically induced by *M. tuberculosis* or a general consequence of in vitro cultivation, hematopoietic progenitors derived from adult peripheral blood were cultured in the absence of *M. tuberculosis*. These cultures were maintained in either supplemented cRPMI1640 or serum-free KM-IMDM. The latter contains defined cytokines, namely stem cell factor (SCF), IL-6, thrombopoietin (TPO), and angiopoietin (ANG1), excluding potential influences from undefined cytokines and growth factors present in fetal calf serum. Following immunofluorescence staining, we quantified the frequency of CD45RA$^-$ CD34$^+$, CD45RA$^+$ CD34$^+$ and CD45RA$^+$ CD34$^-$ cells by FACS, comparing post-incubation frequences with those measured pre-incubation **(Fig. 26)**.

We observed a significant expansion of the CD45RA$^+$ CD34$^+$ population (2.7 ± 2.1 % vs 17.5 ± 1.7 %) in cRPMI1640 and KM-IMDM cultures (2.7 ± 2.1 % vs. 13.5 ± 1.4 %). These findings show that the expansion of the CD45RA$^+$ CD34$^+$ population is observed independent of *M.*

tuberculosis, as it remained in its absence. Therefore, the expansion is driven by cytokines shared in both media, most likely SCF and IL-6 – or by autocrine or paracrine effects of cytokine produced by the cultured cells.

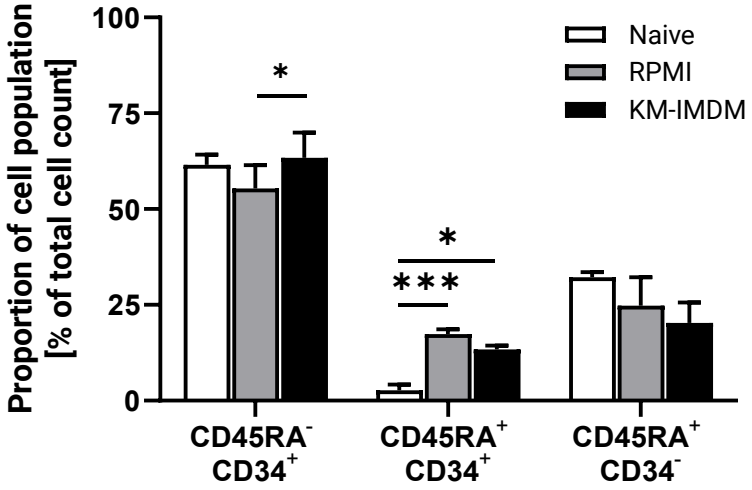

Figure 26: Expansion of the CD45RA$^+$ CD34$^+$ committed progenitor population in serum-free media without *M. tuberculosis* infection. Peripheral blood cells from adult human donors were collected and CD34$^+$-cells were enriched. The frequency of the indicated populations, distinguished by CD45RA and CD34 expression, was quantified before and 21 hours post incubation in either cRPMI1640, containing FCS, or serum-free KM-IMDM (SCF, IL-6, TPO. ANG1) using FACS (CD45RA$^-$ CD34$^+$: Early Hematopoietic Progenitors and hematopoietic stem cells (HSCs); CD45RA$^+$ CD34$^+$: Committed Hematopoietic Progenitors; CD45RA$^+$ CD34$^-$: Mature Leukocytes). Bars represent the mean ± SD [n=3]. Statistical significance is determined by paired two-tailed t-test. Asterisks indicate p-values (*p ≤ 0.05; ns p > 0.05).

Contrary to our initial hypothesis, the expansion of the CD45RA$^+$ CD34$^+$ population was not directly driven by *M. tuberculosis*. It nevertheless emerged as a significant distinction between cultures of ‘primed‘ permissive (adult peripheral blood-derived) and ‘naïve‘ non-permissive (umbilical cord blood-derived) HSCs. Given our hypothesis that certain stimuli might induce atypical (myeloid) genetic programs in HSCs that render them permissive to infection, we sought to determine whether the magnitude of CD45RA$^+$ CD34$^+$ expansion correlates with HSC infection frequency.

To address this question, we calculated the Pearson correlation coefficient between the post-infection frequencies of CD45RA$^+$ CD34$^+$ cells and the frequency of infected HSCs and MPPs from adult donors across multiple experiments with standardized conditions. Data from 18 blood donors were plotted as a linear regression **(Fig. 27)**. No significant correlation between the frequency of CD45RA$^+$ CD34$^+$ cells and infected HSCs ($r = 0.395$; $p = 0.052$) or MPPs ($r = 0.261$; $p = 0.148$) was observed.

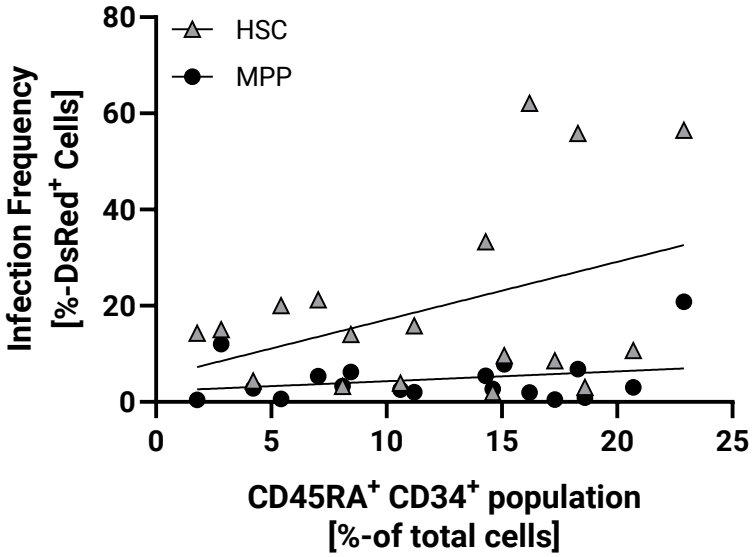

Figure 27: Correlation analysis between the size of the CD45RA+ CD34+ population and the infection frequency of hematopoietic stem cells derived from adult peripheral blood in vitro. Peripheral blood cells from adult human donors were collected and $CD34^+$-cells were enriched. The frequency of the indicated CD45RA+ CD34+ population and infected hematopoietic stem cells (HSCs) and multipotent progenitors (MPPs) was quantified 20 hours post infection with *M. tuberculosis* H37Rv DsRed at a MOI of 10 using FACS (Committed Hematopoietic Progenitors: $CD45RA^+$ $CD34^+$; HSC: $CD34^+$ $CD45RA^-$ Lin^- $CD38^{-/low}$ $CD90^+$ $DsRed^+$; MPP: $CD34^+$ $CD45RA^-$ Lin^- $CD38^{-/low}$ $CD90^-$ $DsRed^+$). A linear regression was calculated for both HSCs and MPPs and Pearson correlation coefficients were determined between the ratio of infected HSCs or MPPs and the ratio of $CD45RA^+$ $CD34^+$ cells. HSC: $r_{Pearson} = 0.395$ $p = 0.0523$; MPP: $r_{Pearson} = 0.2605$ $p= 0.1482$.

Based on these findings, we conclude that the expansion of $CD45RA^+$ $CD34^+$ cells, is not a reliable predictor of HSC permissiveness to *M. tuberculosis*. Instead, differences in permissiveness between umbilical cord blood-derived HSCs and adult peripheral blood-derived HSCs arise from different factors. Nonetheless, the absence of canonical responses of emergency hematopoiesis in umbilical cord blood-derived HSCs provides valuable insights into the nature of possible determinants of HSC permissiveness.

3.2 *M. tuberculosis*-Derived PAMPs Do Not Increase Permissiveness to Infection in HSCs

We pivotally demonstrated that HSCs exhibit slower infection kinetics compared to professional phagocyte, coupled with an exponential increase in the number of infected HSCs over time **(section D.1.1)**. Therefore, we hypothesized that HSCs gradually become more permissive to mycobacterial infection when exposed to pathogen-associated molecular patterns during in vitro culture. To evaluate this hypothesis, we reduced the infection period, but in return pre-exposed HSCs to *M. tuberculosis* lysates prior to infection. The lysates were generated via sonication to preserve the integrity of most three-dimensional PAMP structures while also producing larger particles for optimal recognition. Colony-

forming unit enumeration assays confirmed that no viable mycobacteria remained post-sonication (*data not shown*).

Hematopoietic progenitor cultures, isolated from adult peripheral blood, were treated with either PBS or *M. tuberculosis*-derived lysates, at an equivalent concentration to an MOI of 10 for 18 hours before being infected with live *M. tuberculosis* H37RV DsRed at an MOI of 10 for 2 hours. Following immunofluorescence staining, the frequency of infected HSCs and MPPs was quantified by FACS **(Fig. 28A)**. Our analysis revealed no significant differences in infection frequencies between untreated and lysate-treated conditions for either HSCs (2.1 ± 0.7 % vs. 2.3 ± 0.8 %) or MPPs (0.1 ± 0.3 % vs. 0.3 ± 0.3 %). Moreover, the overall frequency of HSC infection under both conditions was markedly lower than that observed in experiments where HSCs were co-cultured with live *M. tuberculosis* for 20 hours (HSCs: 21.3 ± 20.1 %; MPPs: 4.5 ± 4.0 %) **(Fig. 28B)**. Hence, neither pre-culture infection alone (in PBS), nor the additional exposure to *M. tuberculosis* lysates had a significant effect on the permissiveness of HSC to *M. tuberculosis* infection. These findings show that pre-treatment with *M. tuberculosis*-lysates does not enhance the permissiveness of HSCs to a level that allows for internalization at kinetics comparable to professional phagocytes. Instead, prolonged exposure to live, intact mycobacteria is necessary for efficient infection.

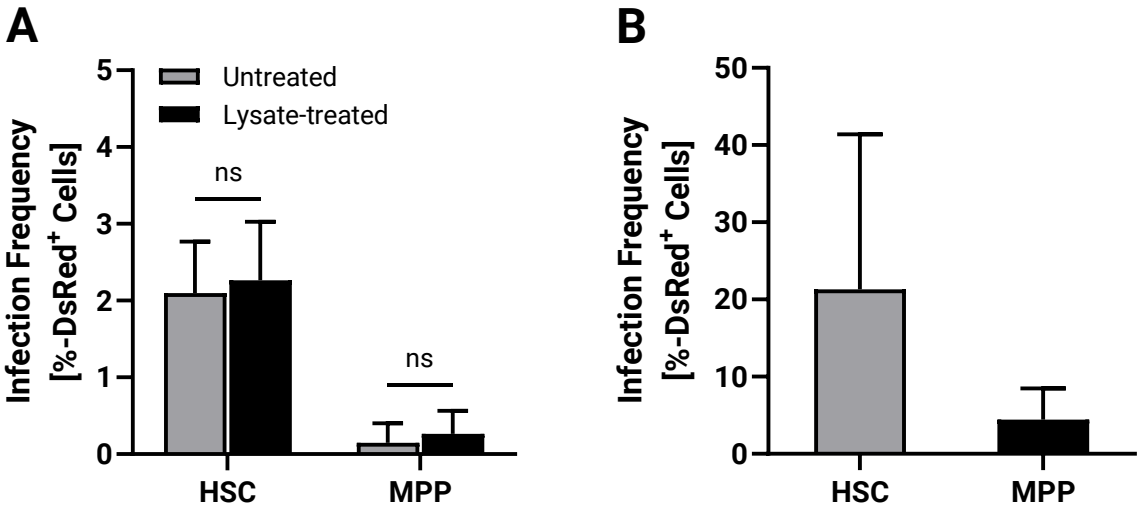

Figure 28: Influence of pre-treatment with *M. tuberculosis*-derived lysate on the infection frequency of hematopoietic stem and progenitor cells in vitro. A) Peripheral blood cells from adult human donors were collected and $CD34^+$-cells were enriched. Progenitor-enriched cultures were incubated with *M. tuberculosis* H37Rv wildtype sonication-lysates at a concentration equivalent to a MOI of 10 or PBS for 18 hours. After treatment cultures were infected with *M. tuberculosis* H37Rv DsRed at a MOI of 10. The frequency of infected hematopoietic stem cells (HSCs) and multipotent progenitors (MPPs) was quantified 2 hours post-infection using FACS (HSC: $CD34^+$ $CD45RA^-$ Lin^- $CD38^{-/low}$ $CD90^+$ $DsRed^+$; MPP: $CD34^+$ $CD45RA^-$ Lin^- $CD38^{-/low}$ $CD90^-$ $DsRed^+$). Bars represent the mean ± SD [n=3]. Statistical significance is determined by paired one-tailed t-test. Asterisks indicate p-values (*$p \leq 0.05$; ns $p > 0.05$). **B)** Mean *M. tuberculosis* infection frequency of HSCs and MPPs after 20 hours of infection across multiple experiments. Peripheral blood from adult human donors was collected and $CD34^+$-cells were enriched. Progenitor-enriched cultures were infected with *M. tuberculosis* H37Rv DsRed at a MOI of 10. The frequency of infected HSCs and MPPs was quantified 20 hours post-infection using FACS (HSC: $CD34^+$ $CD45RA^-$ Lin^- $CD38^{-/low}$ $CD90^+$ $DsRed^+$; MPP: $CD34^+$ $CD45RA^-$ Lin^- $CD38^{-/low}$ $CD90^-$ $DsRed^+$). Bars represent the mean ± SD [n=29].

Although our data did not support the generation of permissiveness in response to *M. tuberculosis* lysates alone, further elucidation of HSC responses to specific *M. tuberculosis*-derived PAMPs may still provide valuable insights into the host pathogen interaction. In initial experiments, we observed high degrees of donor heterogeneity regarding *M. tuberculosis* HSC infection frequencies **(section D.1.1, Fig. 11)**. We also demonstrated that CD36 has an essential role in the uptake of *M. tuberculosis* **(section D.2.3, Fig. 22)**. We thus aimed to further characterize a hypothetical donor-specific heterogeneity in CD36 surface expression. As CD36 surface expression by HSCs was only characterized in a small number of donors at our primary study site before, we aimed to repeat this characterization at a secondary study site with more donors.

When comparing hematopoietic progenitor cultures from our primary site (RCB, Germany) to those from a secondary site (CCHMC, Ohio, USA), we observed a significant reduction in the proportion of $CD36^+$ cells within both HSCs (90.5 ± 6.4% vs. 30.9 ± 20.0) and MPPs (74.9 ± 22.1 % vs. 37.0 ± 25.6 %) **(Fig. 29A)**. Beyond these site-specific discrepancies, we also identified significant inter-donor variability at the CCHMC-study site **(Fig. 29B)**. Stratification of donors via unsupervised k-means clustering (k = 2) identified subgroups with significantly different frequencies of CD36 expression in the HSPC populations, designated 'low $CD36^+$' (HSCs: 6.8 ± 1.5 %; MPPs: 9.2 ± 4.2 %) and 'high $CD36^+$' (HSC: 42.9 ± 10.9 %; MPPs: 50.1 ± 18.6 %).

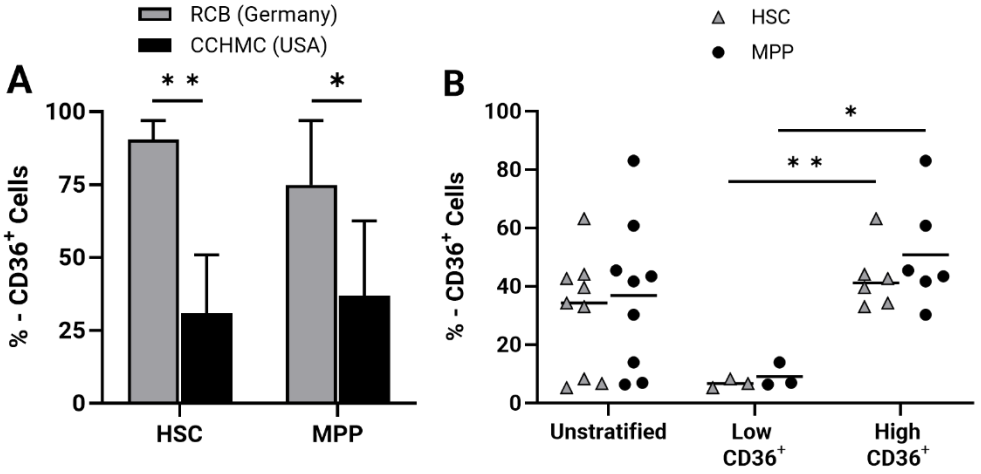

Figure 29: Differences in surface expression of CD36, a class B type scavenger receptor, in hematopoietic stem and progenitor cells isolated at distinct study sites and between individual blood donors. Peripheral blood cells from adult human donors were collected and $CD34^+$-cells were enriched. After incubation for 20 hours, the frequency of $CD36^+$ hematopoietic stem cells (HSCs) and multipotent progenitors (MPPs) was quantified using FACS (HSC: $CD34^+$ $CD45RA^-$ Lin^- $CD38^{-/low}$ $CD90^+$ $CD36^+$; MPP: $CD34^+$ $CD45RA^-$ Lin^- $CD38^{-/low}$ $CD90^-$ $CD36^+$). **A)** Samples collected at the Research Center Borstel (RCB, Germany) and the Cincinnati Children's Hospital Medical Center (CCHMC, USA) were compared in the frequency of $CD36^+$ HSC. **B)** Individual blood samples collected at the Cincinnati Children's Hospital Medical Center (CCHMC, USA) were compared regarding the frequency of $CD36^+$ hematopoietic stem cells (HSCs) and multipotent progenitors (MPPs) and stratified into two subgroups by k-means clustering (k = 2). Bars represent the mean ± SD [RCB n = 3; CCHMC n = 9]. Statistical significance is determined by unpaired two-tailed t-test. Asterisks indicate p-values (*$p \leq 0.05$; **$p \leq 0.005$; ns $p > 0.05$).

The characterization of CD36 expression at a secondary study site demonstrated significant variations both between individual donors and across study sites. These observations show that CD36 expression in HSCs is not as rigidly programmed as initially assumed but rather modulated by host- or external factors such as microbial or pro-inflammatory stimuli. This heterogeneity in CD36 expression led us to further investigate potential cues that regulate this receptor's expression, although *M. tuberculosis*-derived lysates failed to ultimately induce permissiveness in previous experiments. We thus sought to explore whether CD36 surface expression, as a potential determinant of permissiveness, can be influenced by *M. tuberculosis*-derived PAMPs.

We quantified the surface expression of the receptor in response to specific *M. tuberculosis*-derived PAMPs by FACS. Unlike previous experiments that relied solely on whole-cell lysates, we employed a range of defined mycobacterial molecules, each characterized by distinct molecular properties and capable of engaging different host cell pattern recognition receptors. These included culture-filtrate proteins (CFP), trehalose dimycolate (TDM), peptidoglycans (PG), and cell-derived lipids next to enzymatically active but non-viable γ-irradiated cells (whole bacteria), and whole cell lysates (lysate). For additional controls, Il-6 was used as a pro-inflammatory cytokine, while lipopolysaccharide (LPS) was used as a positive control for CD36 induction [151].

Human hematopoietic progenitor cultures were exposed to the indicated molecules for 20 hours. Post-treatment, cells were immunofluorescently stained and the mean fluorescence intensity (MFI) of CD36-FITC was measured across untreated and treated HSC populations to assess changes in CD36 receptor levels in response to these stimuli **(Fig. 30)**. No significant differences in the MFI between untreated and treated groups were observed. Neither *M. tuberculosis*-derived PAMPs, Il-6 nor LPS significantly increased the surface levels of $CD36^+$ on HSCs after in vitro culture. We were not able to acquire sufficient data for every condition to be further stratified into our previously defined categories of 'low $CD36^+$' and 'high $CD36^+$' with enough donors for statistical significance **(Fig. S4)**, leading to a marked influence of donor variability. Based on this, we are also not able to determine whether PAMP treatment may only influence the 'low $CD36^+$' donor subset, reminiscent of a naïve state, but not the 'high $CD36^+$' donor subset.

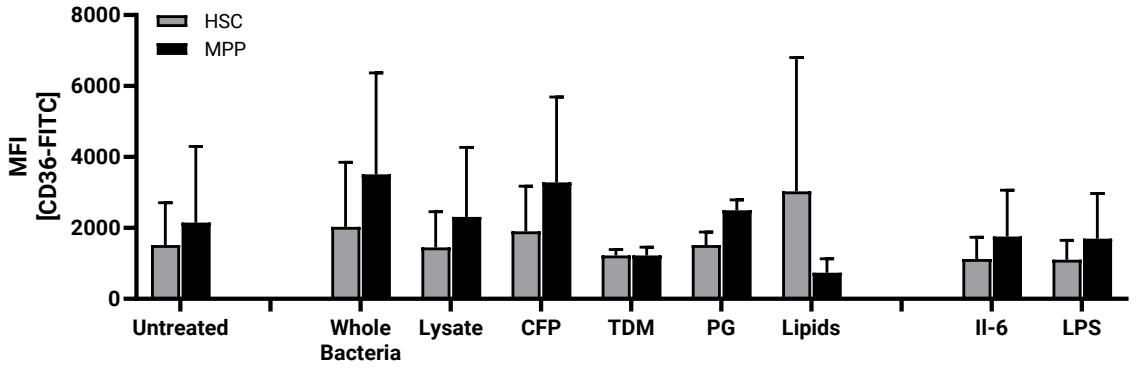

Figure 30: Surface expression of the class B type scavenger receptor CD36 by hematopoietic stem and progenitor cells in response to treatment with *M. tuberculosis*-derived pathogen-associated molecular patterns in vitro. Peripheral blood cells from adult human donors were collected and $CD34^+$-cells were enriched. Progenitor-enriched cultures were incubated *M. tuberculosis* H37Rv-derived pathogen-associated molecular patterns (PAMPs) for 20 hours: Whole Bacteria = γ-irradiated cells [20 µg/mL]; Lysate = Whole Cell Lysates [20 µg/mL]; CFP = Culture filtrate protein [20 µg/mL]; TDM = trehalose dimycolate [20 µg/mL]; PG = Peptidoglycan [20 µg/mL]; Lipids = Lipids [20 µg/mL]; IL-6 = Interleukin-6 [200 ng/mL]; LPS = Lipopolysaccharide (from *S. Minnesota* R595) [100 ng/mL]. The mean fluorescence intensity (MFI) of CD36-FITC, was quantified using FACS (HSC: $CD34^+$ $CD45RA^-$ Lin^- $CD38^{-/low}$ $CD90^+$; MPP: $CD34^+$ $CD45RA^-$ Lin^- $CD38^{-/low}$ $CD90^-$). Bars represent the mean ± SD [n=3]. Statistical significance is determined by paired one-tailed t-test. Asterisks indicate p-values (*$p \leq 0.05$; ns $p > 0.05$).

In conclusion, our findings show that exposure to *M. tuberculosis*-derived PAMPs alone is not sufficient to increase HSC permissiveness. Neither the frequency of infected HSCs nor $CD36^+$ HSCs, the receptor indicated in *M. tuberculosis* internalization by HSCs, was significantly elevated in response to mycobacterial PAMPs. These results demonstrate that factors other than PAMPs must play a role in rendering HSCs permissive to *M. tuberculosis* infection.

To confirm whether HSCs could actually respond to microbial PAMPs, we investigated the presence of specific pattern recognition receptors on HSCs. We analyzed presence of toll-like receptor 2 (TLR2), toll-like receptor 4, toll-like receptor 9 and MMR, all of which have been implicated in influencing myeloid lineage differentiation and thus may induce myeloid genetic programs in HSCs leading to permissiveness [165,189]. We analyzed the surface expression of these receptors on freshly isolated human HSCs using FACS to verify our previous observations that HSCs do not become permissive in response to *M. tuberculosis* PAMPS **(Fig. 31)**. Our results revealed a complete absence of TLR4 and TLR9 HSCs. Only a minor fraction of HSCs expressed TLR2 (1.01 ± 1.17 %) and MMR (0.36 ± 0.63 %). Comparably small fractions of MPPs expressed PRRs (TLR2: 0.08 ± 0.12 %; TLR4: 0.10 ± 0.09 %; TLR9: 0.00 ± 0.00 %; MMR: 0.02 ± 0.01 %). The exceedingly low frequency of PRR^+ HSCs, with fewer than one in a hundred cells expressing these receptors, demonstrates that canonical pattern recognition receptors involved in pathogen sensing are largely absent in HSCs and MPPs. Consequently, these receptors are unlikely to play a direct role in the development of HSC permissiveness to *M. tuberculosis* infection. Our findings that treatment with dead mycobacteria and selected mycobacterial PAMPs had no effect on HSC permissiveness,

instead indicate an inflammatory response towards infection and viable bacteria to be responsible.

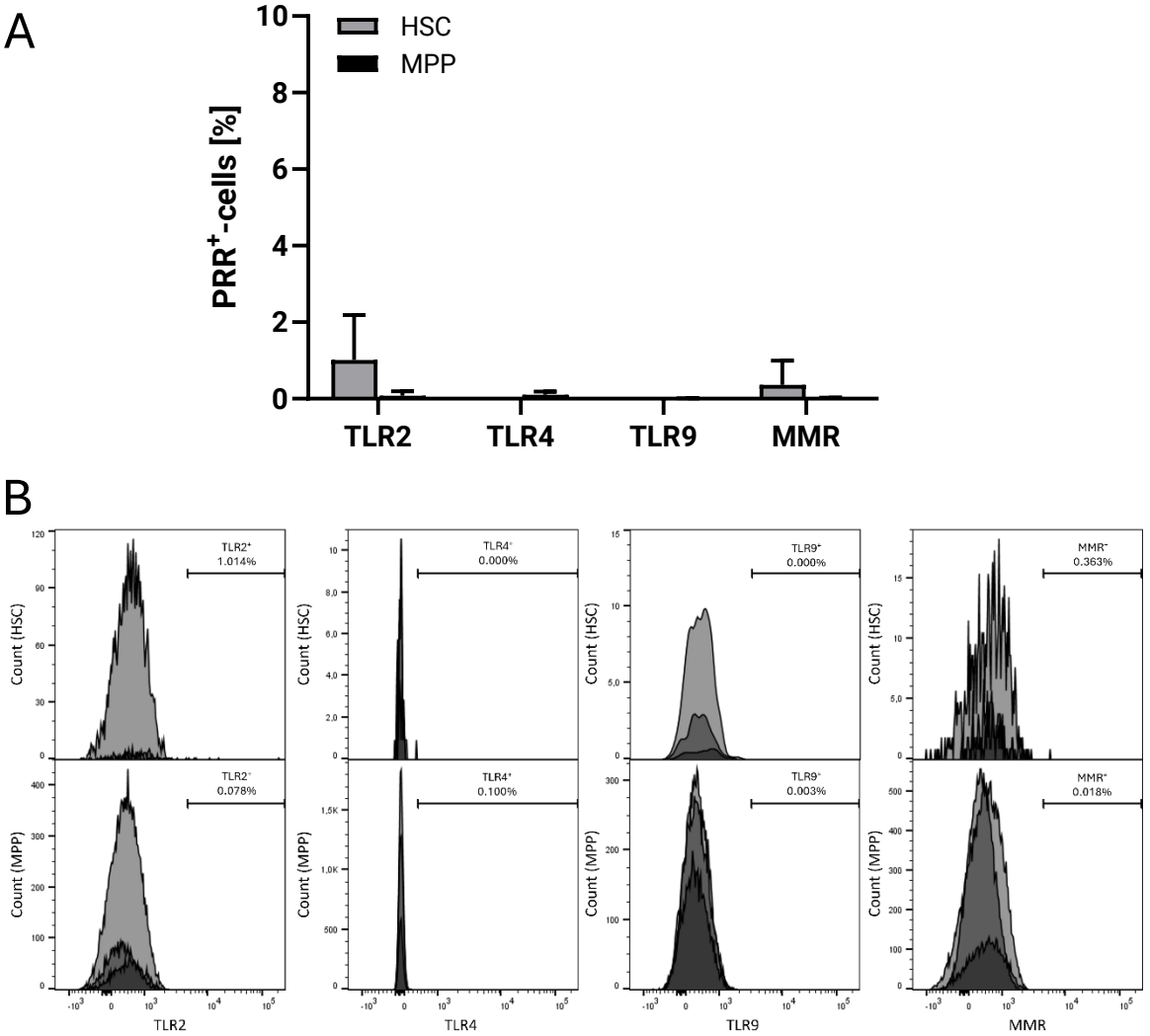

Figure 31: Presence of pattern recognition receptors involved in the potential recognition of *M. tuberculosis* by hematopoietic stem and progenitor cells. Peripheral blood cells from adult human donors were collected and $CD34^+$-cells were enriched. Expression of pattern recognition receptors (PRRs), toll-like receptor 2 (TLR2), TLR4, TLR9 and macrophage mannose receptor (MMR) was quantified in hematopoietic stem cells (HSCs) and multipotent progenitors (MPPs) using FACS (HSC: $CD34^+$ $CD45RA^-$ Lin^- $CD38^{-/low}$ $CD90^+$; MPP: $CD34^+$ $CD45RA^-$ Lin^- $CD38^{-/low}$ $CD90^-$). **A)** Bars represent the mean ± SD [n=3]. **B)** Histograms of surface PRR expression and mean gate frequencies [n=3]. Upper panel: Hematopoietic stem cells (HSCs). Lower panel: multipotent progenitors (MPPs) [n=3]

3.3 Cell Intrinsic Inflammatory Pathways Are Activated Upon Infection in HSCs

To evaluate whether HSCs exhibit responses indicative of pro-inflammatory signalling, we investigated the phosphorylation of signal transducer and activator of transcription 3 (STAT3). Phosphorylation of STAT3 at tyrosine 705, mediated by receptor-associated Janus kinases (JAK), is a critical step that enables its translocation to the nucleus, where it activates target

gene expression. STAT3 is known to play a role in the genetic programs driving myeloid cell differentiation in response to inflammatory stimuli through the induction of CCAAT-enhancer-binding-protein β (C/EBPβ) expression and co-regulation of c-Myc [216].

We thus hypothesized that STAT3 activation may contribute to the induction of certain genetic programs in HSCs, potentially rendering them permissive to *M. tuberculosis* infection. To test this hypothesis, we employed an antibody specific to phosphorylated STAT3 at tyrosine 705 (pY705) to quantify pSTAT3 levels. This approach allowed us to assess the activation of the JAK-STAT3 signaling pathway on a cellular level in response to *M. tuberculosis* infection, thereby providing insights into the molecular mechanisms that might underly HSC permissiveness.

To validate the assay to measure STAT3 activation in our approach, we treated human macrophages with 200 ng/mL Il-6, a well-characterized activator of STAT3 phosphorylation through the Il-6/JAK2/STAT3 signaling axis. Phosphorylated STAT3 (pY705) levels in macrophages were quantitatively assessed using FACS, demonstrating the system's reliability in detecting STAT3 activation **(Fig. 32A)**. Subsequently, naïve human hematopoietic progenitor cultures or those infected with *M. tuberculosis* H37Rv DsRed were investigated **(Fig. 32B)**.

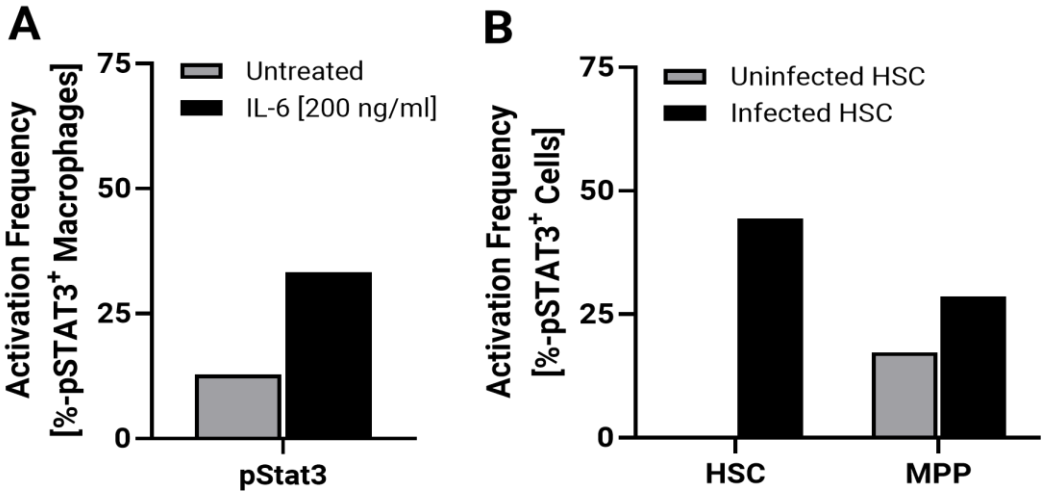

Figure 32: Signal transducer and activator of transcription 3 activation in *M. tuberculosis*-infected hematopoietic stem and progenitor cells. A) Peripheral blood-derived macrophages were incubated with 200 ng/mL human recombinant IL-6 for 15 min. before the frequency of signal transducer and activator of transcription 3 (STAT3) phosphorylation (pSTAT3-AF488$^+$) was quantified using FACS. **B)** Peripheral blood cells from adult human donors were collected and CD34$^+$-cells were enriched. Progenitor-enriched cultures were infected with *M. tuberculosis* H37Rv DsRed at a MOI of 10. The frequency of STAT3 phosphorylation (pSTAT3-AF488$^+$) of infected and uninfected hematopoietic stem cells (HSCs) and multipotent progenitors (MPPs) was quantified 20 hours post-infection using FACS (HSC: CD34$^+$ CD45RA$^-$ Lin$^-$ CD38$^{-/low}$ CD90$^+$ DsRed$^{+/-}$; MPP: CD34$^+$ CD45RA$^-$ Lin$^-$ CD38$^{-/low}$ CD90$^-$ DsRed$^{+/-}$). The graphs represent preliminary data of n = 1.

A greater proportion of pSTAT3^{+} cells was observed in infected HSCs (44.4 %) and MPPs (28.6 %) compared to their uninfected counterparts (HSCs: 0 %; MPPs: 17.3 %). The increased phosphorylation of STAT3 in infected cells shows that inflammatory cytokine signaling in response to viable *M. tuberculosis* correlates with HSC permissiveness to infection. However, given the preliminary nature of these analyses (n=1), which is primarily attributable to cell loss during permeabilization and subpar kit-protocols for HSCs, definitive conclusions cannot yet be drawn in a statistically significant manner.

In conclusion, naïve HSCs derived from neonatal umbilical cord blood are intrinsically non-permissive to *M. tuberculosis* infection, while HSCs sourced from adult peripheral blood are. Our data show that HSCs acquire a degree of priming towards adulthood that allows them to become more permissive during in vitro infection. These differences correlate with an underlying lack of anti-microbial responses as known adaptions of emergency hematopoiesis were absent in umbilical cord blood HSC. The acquisition of permissiveness is not driven by exposure to mere *M. tuberculosis*-derived PAMPs, as no corresponding increase in permissiveness was observed, nor were pattern recognition receptors expressed by HSCs in a significant manner. Instead, preliminary findings point towards a potential role for inflammatory cytokine signalling in response to viable *M. tuberculosis* in the process of becoming permissive. However, further analysis is required to substantiate this hypothesis and fully elucidate the molecular mechanisms underlying the acquisition of a permissive phenotype in HSCs.

4. The Spatial Organization of HSC Microenvironments

M. tuberculosis is suggested to persist during antibiotic treatment by establishing a niche within the marrow [181,185]. Additionally, Tornack et al. reported that *M. tuberculosis* enters a dormant state within infected HSCs [187]. Both findings may be attributed to the spatial organization of HSC niches within the bone marrow, which are predominantly found in the hypoxic microenvironments of the endosteal regions, distant from arterioles and sinusoids [131-133]. To investigate whether *M. tuberculosis* residing in the bone marrow localizes specifically within HSC microenvironments or close to sinusoids, we aimed to develop a whole-mount multiparameter immunofluorescence imaging approach to visualize spatial bone marrow organization following infection with mycobacteria.

The protocol for whole-mount multiparameter immunofluorescence imaging was adapted from Wu et al. 2024, including further parameters to additionally detect T cells [217]. Sternal

segments were excised at the designated timepoint, and the bone marrow cavity was exposed via coronal sectioning prior to immunofluorescence staining. Six markers were selected for the identification of HSCs, endothelial structures, and T cell receptor bearing cells. Sinusoids and arterioles were detected based on their structural characteristics in conjunction with ESAM expression. The following markers were employed for immunophenotyping of hematopoietic progenitors: CD150, c-Kit, CD48, ESAM and CD41 enabling the identification of HSCs (c-Kit$^+$ ESAM$^+$ CD150$^+$ CD48$^-$ CD41$^-$), MPP1 (c-Kit$^+$ ESAM$^+$ CD150$^-$ CD48$^-$ CD41$^-$), MPP2/MyE (c-Kit$^+$ ESAM$^+$ CD150$^+$ CD48$^+$ CD41$^-$), MPP3/MPP4/CMP: c-Kit$^+$ ESAM$^+$ CD150$^-$ CD48$^+$ CD41$^-$), and megakaryocytic progenitors (c-Kit$^+$ ESAM$^+$ CD150$^+$ CD48$^-$ CD41$^+$). CD3 was selected as a marker for T lymphocytes (CD3$^+$). Confocal laser scanning microscopy was subsequently used for whole-mount multiparameter imaging.

Significant challenges were encountered in identifying of hematopoietic progenitors within whole-mount sterna. Although individual markers were reliably detected, multiparameter identification of hematopoietic progenitors was not possible. For instance, the diameters of cells expressing ESAM and CD41, located adjacent to blood vessels **(Fig. 33A)**, were consistent with megakaryocytes (50 – 100 µm) or megakaryocyte progenitors (10 – 20 µm). However, the co-expression of c-Kit in the absence of CD150 excluded these cells as either of these cell types, as megakaryocytes are c-Kit$^-$, while megakaryocyte progenitors are CD150$^+$. Furthermore, neither HSCs nor other early hematopoietic progenitors could be reliably identified, as no c-Kit$^+$ ESAM$^+$ CD41$^-$ cells simultaneously expressed CD150 or CD48 **(Fig. 33B)**. More surprisingly, we did not observe c-Kit expression in any cells of ~10 µm diameter in size identified by CD150 and CD48 as the most abundant cells in bone marrow **(Fig. 33C)**. The underlying reasons for these discrepancies in antigen detection by the employed antibody conjugates remain unclear. Given these challenges, further refinement of the multiparameter immunofluorescence staining protocol is required before this approach can be effectively applied to models of experimental tuberculosis.

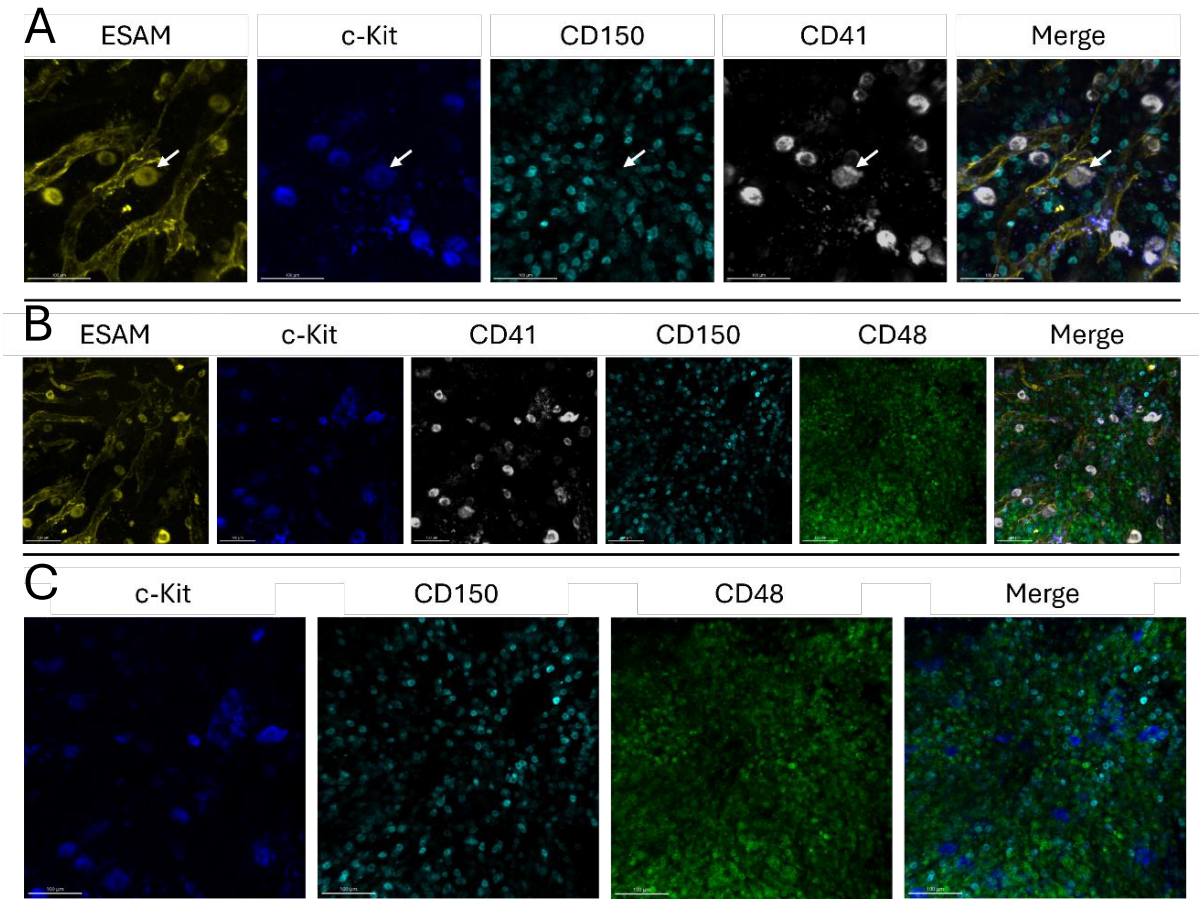

Figure 33: Multiparameter immunofluorescence staining fails to reliably detect hematopoietic progenitors in murine whole-mount bone marrow. SPF female C57Bl6/J mice were sacrificed, and sterna were prepared for whole-mount immunofluorescence imaging. The following antibody-conjugates were used for immunofluorescence staining: ESAM-PE (yellow), c-Kit-BV480 (blue), CD150-BV420 (cyan); CD48-AF488 (green); CD41-AF647 (white), CD3-APC/Fire^{TM}750 (*not shown*). **A)** Empirically and morphologically identified megakaryocytes (c-Kit$^-$ ESAM$^+$ CD150$^-$ CD48$^-$ CD41$^+$, 50-100 µm diameter) or megakaryocyte progenitors (c-Kit$^+$ ESAM$^+$ CD150$^+$ CD48$^-$ CD41$^+$ cells of 10-20 µm diameter) are not reliably detected by immunophenotyping**. B)** Hematopoietic stem cells (HSCs) c-Kit$^+$ ESAM$^+$ CD150$^+$ CD48$^-$ CD41$^-$) and multipotent progenitors (MPPs) (MPP1: c-Kit$^+$ ESAM$^+$ CD150$^-$ CD48$^-$ CD41$^-$, MPP2/MyE: c-Kit$^+$ ESAM$^+$ CD150$^+$ CD48$^+$ CD41$^-$, MPP3/MPP4/CMP: c-Kit$^+$ ESAM$^+$ CD150$^-$ CD48$^+$ CD41$^-$) are not detectable by immunophenotyping**. C)** No cells co-expressing c-Kit and CD150 or CD48 are presents. All panels display representative images of whole-mount sterna from uninfected mice.

E. Discussion

Approximately two billion human beings are estimated to be potent carriers of *M. tuberculosis*. Of those, only 10% fall ill during their lifetime, making *M. tuberculosis* a perfect example of pathogen persistence and host-adaption [52]. The central feature of tuberculosis immune responses is the formation of granulomas, which sequester invading mycobacteria. However, rather than representing an effective containment strategy, granulomas should be perceived as a mere immunological comprise that fails to fully eradicate the pathogen [59]. Far from being a protective 'prison', granulomas serve as dynamic sites of continuous immune cell recruitment in favor of an ever-regenerating reservoir of host cells unable to control *M. tuberculosis*. The lack of mycobacterial control has been linked to impaired immune resistance mechanisms and deficiencies in T cell-mediated immunity alongside immune evasion, particularly in macrophages and neutrophils [106,107,218,219]. Consequently, prior vaccine research has focused on the interactions between *M. tuberculosis* and T cells, with innate immune cells recently emerging as novel targets for host-directed therapy strategies [50,220].

Advances in the fields of trained immunity and HSC imprinting, have suggested that the basis of immune impairment beyond transient effects in mostly – post-mitotic and mature – innate immune cells also originates from imprinted self-renewing and differentiating HSCs [158,169]. During tuberculosis, imprinted HSCs produce macrophage progeny with compromised antimicrobial function [158]. However, the mechanisms by which HSCs get imprinted remain unclear. Reports conflict as to whether HSCs directly interact with *M. tuberculosis* in the context of an infection or only respond to extrinsic trans-signaling [158,187,189]. So far, the scenario of direct infection of HSCs in the bone marrow has been vastly neglected. Given the crucial role of HSCs in immune homeostasis, the potential significance of bone marrow as an extrapulmonary reservoir for *M. tuberculosis*, and possible healthcare consequences for bone marrow transplant recipients, we aimed to characterize the ability of HSCs to internalize *M. tuberculosis*.

Building on a previous report of the detection of mycobacterial DNA in HSCs in vivo, we pivotally demonstrated internalization of *M. tuberculosis* in immunophenotyped HSCs in vitro [187]. Infection of HSCs in vitro prompted us to study the process of infection under controlled conditions and let us reconcile discrepancies between previous reports. We found these were not mutually exclusive. Our results showed that HSCs internalize *M. tuberculosis*

through mechanisms similar to those seen in other non-phagocytic cells, such as epithelial cells, endothelial cells, airway microfold cells, B cells and adipocytes [186,199,211,221,222]. Molecular characterization of the underlying pathways identified interactions with the actin cytoskeleton and clathrin as key molecular factors in the internalization of *M. tuberculosis*. We identified CD36, a member of the class B scavenger receptor family, as a surface receptor, at least partly, facilitating uptake of *M. tuberculosis*. Consistent with described signalling cascades upon CD36 engagement we observed that *M. tuberculosis*-internalization is associated with macropinocytosis-like membrane ruffling, which is insensitive to inhibitors of classical macropinocytosis [223].

As *M. tuberculosis* remains yet the only bacterial pathogen known to infect HSCs, we explored HSC permissiveness to infection. Our findings suggest a link between permissiveness and inflammaging. HSCs derived from neonatal umbilical cord blood were intrinsically non-permissive to *M. tuberculosis* infection, and lacked hematopoietic responses common to adult HSC cultures, indicating the absence of critical signalling pathways of microbial recognition. In HSC cultures from adult donors, permissiveness was neither induced by exposure to *M. tuberculosis*-derived PAMPs, nor did HSCs express common pattern recognition receptors. Instead, our preliminary data indicate trans-signalling by pro-inflammatory cytokine signalling in conferring permissiveness to *M. tuberculosis* internalization.

1. Identification of HSCs as Definitive Host Cells of *M. tuberculosis*

HSCs are multipotent and self-renewing cells at the apex of the hematopoietic system and thus responsible for the generation of every single immune cell in the host organism [117]. Due to their primitive identity, HSCs have long been considered to neither directly interact with pathogens nor take part in immune responses. However, emerging evidence suggests a more relevant role in immune surveillance mechanisms than initially anticipated [224,225]. Detection of *M. tuberculosis* DNA in HSCs further promoted the recent paradigm change [187]. To settle the persisting controversy about the permissiveness of HSCs to *M. tuberculosis* infection, we used an imaging-based approach combined with FACS to determine *M. tuberculosis* intracellular localization.

1.1 The Immunophenotypic Identity of HSCs

Characterization of HSCs as host cells for *M. tuberculosis* critically depends on the precise identification of these cells. Early hematopoietic progenitors exhibit a considerable degree of heterogeneity, encompassing cells with varying potency for multilineage bone marrow reconstitution. Among these progenitors, only those displaying both, multilineage potential and the ability to sustain long-term reconstitution across serial transplants are classified as bona fide HSCs. Cells that exhibit more limited or non-serial reconstitution potential are instead categorized as MPPs [142]. Over recent decades, advances in elucidating immunophenotypic correlates of hematopoietic function have significantly improved the identification of distinct hematopoietic stem and progenitor cell (HSPC) populations. In the absence of a single, uniquely expressed marker, several multiparameter identification schemes have been developed, each with varying specificity and composition in the identified populations [142]. In both, humans and mice, HSCs are now well-characterized immunophenotypically, though a standardized approach to identifying MPPs remains to be established [142,226].

The state-of-the-art identification methods for HSPCs, which were employed in this study **(Tab. 20)**, balance practical applicability and the precise identification of HSCs. These methods have improved the single-cell engraftment efficiency to approximately 50 % for murine cells in vivo and 70 % for human cells in vitro [142,227,228]. The incorporation of dye efflux and additional markers – such as Flk2, CD34, EPCR, CD229, CD244, CD41 in mice, and CD133, CD201, GPI-80 and CD49f in humans – has further enhanced the enrichment of long-term reconstituting cells, leading to even higher rates of single cell engraftment [197,226,227,229]. Nonetheless, the relationship between stemness, steady-state hematopoiesis and engraftment mechanisms remains a subject of ongoing debate. Specifically, it is unclear whether successful reconstitution in vivo is a universal HSC trait or if it is confined to specific HSC subsets [230].

Population	Immunophenotype	Output	Reconstitution
Murine:			
HSC	Lin$^-$ c-Kit$^+$ Sca-1$^+$ CD150$^+$ CD48$^-$	Multilineage	Long-term, serial
MPP1*	Lin$^-$ c-Kit$^+$ Sca-1$^+$ CD150$^-$ CD48$^-$	Multilineage	Long-/ intermediate-term,
MPP2	Lin$^-$ c-Kit$^+$ Sca-1$^+$ CD150$^+$ CD48$^+$	Mk/E, GM > Ly	Intermediate-term / transient
MPP3/MPP4	Lin$^-$ c-Kit$^+$ Sca-1$^+$ CD150$^-$ CD48$^+$	GM > Ly / Ly > GM	Transient
Human:			
HSC	Lin$^-$ CD34$^+$ CD38$^{-/low}$ CD45RA$^-$ CD90$^+$	Multilineage	Long-term, serial
MPP*	Lin$^-$ CD34$^+$ CD38$^{-/low}$ CD45RA$^-$ CD90$^-$	Multilineage	Long-term

***:** Previously referred to as ST-HSC

Table 20: Immunophenotypic identification panels for murine and human hematopoietic stem and progenitor cell populations applied in this study. HSC = Hematopoietic stem cell. MPP1 = Multipotent progenitor cell 1. MPP2 = Multipotent progenitor cell 2. MPP3 = Multipotent progenitor cell 3. MPP4 = Multipotent progenitor cell 4. 'Multilineage' output = Multipotent differentiation into myeloid, erythroid and lymphoid cells. 'MK/E, GM > Ly' output = Multipotent biased differentiation into erythroid and myeloid cells. 'GM > Ly' = Oligopotent biased differentiation into myeloid cells. 'Ly > GM' = Oligopotent biased differentiation into lymphoid cells. Long-term reconstitution = myeloid output for > 16 weeks. Intermediate-term reconstitution = myeloid output for 6-16 weeks. transient reconstitution = myeloid output for < 6 weeks. Serial reconstitution = providing multilineage reconstitution in a secondary recipient. Adapted from [142,227,228].

While bona fide HSCs are classically defined by their capacity for multilineage reconstitution, they do not represent a homogenous population. Emerging evidence indicates that lineage fate decision can occur already within HSCs prior to differentiation [143,144,231]. In murine models, at least four distinct subsets of HSCs, each with unique engraftment capacities, self-renewal potential, and differentiation programs have been identified within the Lin$^-$ c-Kit$^+$ Sca-1$^+$ CD150$^+$ CD48$^-$ HSC population. These subsets are primarily characterized by their lineage bias towards either myeloid (my-bi-HSC) or lymphoid (ly-bi-HSC) fate [232-234]. Although CD150 expression has been proposed to distinguish between CD150^{high} myeloid-biased HSCs, CD150^{low} lymphoid-biased HSCs and CD150^{med} balanced HSCs, this method has not consistently enriched for functionally distinct and pure populations in vitro [232,234]. Furthermore, self-renewing progenitors exhibiting oligo-, bi-, and unipotent megakaryocyte, megakaryocyte-erythroid and myeloid restricted lineage commitment, have been identified within immunophenotypically defined HSC populations [235]. In humans, comparable myeloid-, lymphoid- and megakaryocyte-/erythrocyte-biased HSC with long-term repopulating potential, have been detected in rare CD34$^-$ HSC subsets [236,237].

The underlying causes of HSC heterogeneity remain incompletely understood. Evidence from studies on epigenetic imprinting and transcriptional regulation suggests that intrinsic hardwired differences exist between distinct HSC subsets. However, functional heterogeneity has also been attributed to extrinsic factors, such as microenvironmental influences and the individual cell cycle history [238]. Heterogeneity may therefore represent an acquired, transient functional state rather than being strictly hardwired to allow flexibility in responses to exogenous and endogenous alterations.

It should be noted that the classification of HSCs and their progeny is arbitrary, representing a snapshot within a continuous spectrum of differentiation stages, with no discrete boundaries separating these stages in a strict hematopoietic hierarchy [140,141]. Thus, the current concept of HSCs does not represent a single, well-defined cell type with uniform functional and phenotypic characteristics. Given the challenges in delineating HSPC heterogeneity, conclusions drawn about the interactions between *M. tuberculosis* and bona fide HSCs in this study must be understood as referring to an heterogenous population of HSC subtypes, each instructed by potentially distinct genetic programs. Future advances could redefine certain HSC subsets, possibly reclassifying further HSCs as MPPs, as it was the case when the former terms ‘ST-HSC’ and ‘IT-HSC’ were abandoned [142]. Despite their functional diversity, all primitive hematopoietic progenitors – whether HSCs or MPPs – still play an essential role in the *de novo* generation of immune cells are thus equally relevant targets for potential immune impairments.

1.2 Replicating In Vivo Encounters In Vitro

In vivo, macrophages, neutrophils and dendritic cells in the lung are the prime cells infected with *M. tuberculosis* [239]. In contrast, fewer than one in a hundred HSCs have been shown to harbor *M. tuberculosis* DNA during experimental active tuberculosis in mice or latent tuberculosis infection in humans [187]. To address this limitation, we established in vitro HSC culture models of *M. tuberculosis* infection to significantly enrich the population of infected cells for further studies. Given the ongoing uncertainties regarding the primary site and mechanisms of the encounters between *M. tuberculosis* and HSCs in vivo, it remains unclear whether predominantly bone marrow or circulating HSCs become infected and thus serve as equally representative models for modelling HSC infection in vitro.

While most HSCs reside within bone marrow, a certain number of HSCs continuously egress into circulation under steady-state conditions. During emergency hematopoiesis, this

number is further increased [224,240,241]. Circulating HSCs are thought to play a role in immune surveillance and can serve as localized sources of immune cell proliferation through extramedullary hematopoiesis in peripheral tissues [224,225]. For instance, extramedullary hematopoiesis and tissue-resident HSCs and MPPs have been documented in lung and spleen [242,243]. Reflecting their function, circulating HSCs exhibit enhanced priming for differentiation, adhesion, and immune responses compared to their bone marrow counter parts, while still retaining reconstitution potential [225,244]. Reports conflict as to whether circulating bone marrow derived HSCs regularly home back to bone marrow, in the absence of bone marrow ablation [245-247]. There is also no evidence that HSCs residing in peripheral tissues can re-enter circulation [187]. Hence, the question emerges, how and where bone marrow HSCs encounter *M. tuberculosis* during granulomatous control.

The ability of *M. tuberculosis* to access the bone marrow following aerosol infection, without apparent vascular dissemination of free bacteria, suggests a potential mechanism of APC-mediated transport [158]. Occasional egress of infected macrophages from granulomas, even during latency, suggests that infection of bone marrow HSC is most likely promoted by migrating infected macrophages [174,175]. Antigen transport to bone marrow by macrophages, dendritic cells, and neutrophils has also been documented as a natural immune response mechanism during infections with pathogens other than *M. tuberculosis* [160-164].

In conclusion, considering the HSCs' migration behaviour and known routes of *M. tuberculosis* dissemination in the host, HSCs are most likely to encounter *M. tuberculosis* in bone marrow. Since circulating HSCs typically home back to the bone marrow only under hematopoietic stress, when spatial niche availability permits, the observation of *M. tuberculosis* DNA in bone marrow HSCs in vivo implies that infection likely occurs within bone marrow itself [187,245-247]. *M. tuberculosis* DNA harboring HSCs observed in circulation are more likely the result of infected HSCs entering circulation from bone marrow compared to peripheral sites or even infection in the blood stream itself [187]. Peripheral infection cannot fully be excluded, as extramedullary hematopoiesis shares potential sites of *M. tuberculosis* infection. Namely, the lungs being the primary site of tuberculosis infection and the spleen serving an indirect role by hosting cross-presentation of *M. tuberculosis*-infected APCs to lymphocytes.

Taken together, bone marrow-derived HSCs may provide a more natural model for mimicking HSC infection in vitro. However, due to limited availability of human bone marrow samples,

only murine HSCs were sourced from bone marrow, while human HSCs were derived from peripheral blood for in vitro infection studies. To mitigate the potential confounding influences from the distinct bystander cell populations between bone marrow and peripheral blood cultures, mature myeloid cell populations were removed, although some residual effects cannot be fully excluded.

Using these in vitro models, we mimicked the in vivo situation during *M. tuberculosis* infection and demonstrated that *M. tuberculosis* can indeed infect HSCs. Notably, no significant differences in permissiveness to *M. tuberculosis* between circulating human and bone marrow murine HSCs were observed **(Fig. 11)**. However, further studies with murine circulating and human bone marrow derived HSCs are needed to draw definitive conclusions.

1.3 Preserving HSC Identity In Vitro

A critical question in evaluating our in vitro *M. tuberculosis* infection model is whether isolated HSCs retain their original phenotype and functional properties during the experiments to draw parallels to the situation in vivo. In vivo, HSC self-renewal and quiescence are tightly regulated by a cooperative network of niche-derived factors within their microenvironment **(Fig. 34)** [248,249]. Physical manipulation during HSPC enrichment, transition from hypoxic to normoxic conditions, and loss of essential stromal factors – particularly CXCL-12, transforming growth factor beta (TGF-β), SCF, ANG-1 and Notch ligands – disrupt cell cycle regulation (cyclins, cyclin-dependent kinases (CDKs), cyclin-dependent kinase inhibitors (CDKIs), transcription factors and microRNAs), which leads to a progressive loss of quiescence and favours differentiation in vitro [248,250,251]. The most significant limitation of in vitro HSC models lies in the fact that these functional changes do not necessarily go along phenotypic alterations. Notably, the loss of reconstitution capacity is associated with decreased CD150 or CD90 expression [226]. According to Mayer et al. 2022, these changes become particularly visible during long-term culture in vitro over several weeks but less obvious within the first 24 hours [248]. One rapid response triggered by the transition from hypoxic in vivo to normoxic in vitro conditions leads to metabolic and mitochondrial adaptions in HSCs just within the first 30 minutes ex vivo [251]. However, in the context of host-pathogen interactions, HSC differentiation in vitro generally requires 72 hours to generate cells, which can be infected by bacterial pathogens such as *Listeria monocytogenes*, *Salmonella* Typhimurium, and *Yersinia enterocolitca*, suggesting that in vitro, *M. tuberculosis* infection within 24 hours is unlikely to be driven by differentiation-

mediated acquisition of phagocytosis competence but rather by a HSC intrinsic uptake mechanism [189]. Apart from expansion of hematopoietic progenitor populations we did not observe changes in HSC permissiveness to *M. tuberculosis* infection over the observation time from culture alone **(Fig. 28)**.

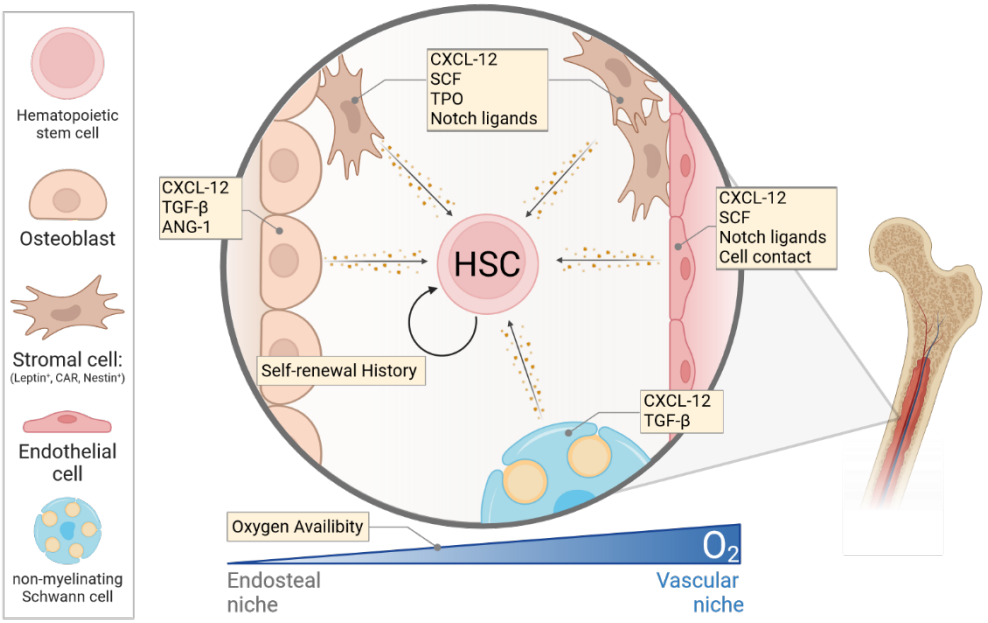

Figure 34: Niche factors in the bone marrow hematopoietic stem cell microenvironments that regulate self-renewal and quiescence. Hematopoietic stem cell (HSC) quiescence and self-renewal during homeostatic conditions is regulated by stromal factors, especially chemokine (C-X-C motif) ligand 12 (CXCL-12), transforming growth factor beta (TGF-β), stem cell factor (SCF), angiopoietin 1 (ANG-1), thrombopoietin (TPO) and Notch ligands. HSCs are also subject to an oxygen gradient between hypoxic conditions in the endosteal niches (most quiescent) and normoxic conditions near the sinusoids and arterioles (least quiescent). Eventually, progressing through repeated cell cycles HSCs successively lose quiescence during aging.

In summary, the in vitro HSC infection models used in here remain indispensable for elucidating the mechanistic interactions between HSCs and *M. tuberculosis*, and to gain critical insights into host-pathogen dynamics in the bone marrow. Still, HSC in vitro culture may not fully replicate the in vivo microenvironment and its associated functional heterogeneity. Although advances in long-term HSC culture techniques have been made, maintaining HSCs in an undifferentiated state remains a challenge. Given the complexities of long-term culture requirements such as maintenance of hypoxic conditions, appropriate cytokine stimulation, and so-called 2.5D co-culture with mesenchymal stem and endothelial cells, we opted for short-term cultivation of freshly isolated primary cells to mitigate long-term culture-induced artifacts [248].

1.4 Permissiveness of HSCs to *M. tuberculosis* Infection

Using the in vitro models for *M. tuberculosis* infection of murine bone marrow and human circulating HSCs, the interaction between pathogen and host HSCs was studied by confocal

laser scanning microscopy. Thereby intracellular mycobacteria were detected in immunophenotypically defined stem cell populations. We detected *M. tuberculosis* within sorted murine Lin^- c-Kit^+ $Sca\text{-}1^+$ $CD150^+$ $CD48^-$ and human Lin^- $CD34^+$ $CD38^-$ $CD45RA^-$ $CD90^+$ HSCs **(Fig. 13)**. Infected HSCs mostly harbored multiple mycobacteria. Given the generation time of *M. tuberculosis* of at least 14 hours in nutrient-rich media and ranging from 21 to over 100 hours in macrophages, it is unlikely that detection of more than one mycobacterium per HSC is due to proliferation [252,253]. Instead, HSCs have likely internalized multiple mycobacteria independently or multicellular bacterial aggregates.

We pivotally demonstrate that HSC can indeed become infected with M. tuberculosis in vitro. While *M. tuberculosis* DNA detection – though specific – cannot distinguish between surface-adherent bacteria or DNA thereof, our imaging-based approach conclusively revealed the intracellular localization of *M. tuberculosis* within immunophenotypically defined HSC populations. Using a DsRed fluorescent *M. tuberculosis* strain as an effective method to quantify HSC infection rate by FACS, in vitro *M. tuberculosis* infection of HSCs provides a robust platform for studying host-pathogen interaction mechanisms under controlled conditions in a quantitative manner.

Other reports suggesting that HSCs are non-permissive to *M. tuberculosis* do not necessarily contradict our findings. Three key studies examined HSCs for the presence of mycobacteria post-infection but failed to detect intracellular bacteria. Khan et al. conducted in vitro *M. tuberculosis* infection experiments in HSCs at a MOI of 3 for four hours after infection [158]. Our data indicate that an incubation period of 12 hours at a higher MOI, is required to achieve detectable infection rates in vitro **(Fig. 7, Fig. 9)**. Moreover, despite studying HSC responses during experimental tuberculosis in mice, Khan et al. did not provide in vivo data from *M. tuberculosis*-infected animals regarding HSC infection in a similar experimental setting to Tornack et al. to corroborate their in vitro observations [158,187].

Two previous studies on HSC permissiveness to mycobacteria were conducted with *M. bovis* BCG and *M. avium*, both of reduced pathogenicity due to the lack of certain virulence factors [254,255]. Moreover, reported non-permissiveness to *M.* avium, was based on sole absence of bacteria in spleens of bone marrow graft recipients 20 weeks post-transplantation, despite the actual presence of mycobacteria in the graft itself [153]. Recent murine models have shown that wildtype graft recipients do not develop tuberculosis after the transfer of *M. tuberculosis*-infected HSCs while immunodeficient *Nos2-/-* recipients, lacking an important anti-mycobacterial defence mechanism, do [188]. This demonstrates that tuberculosis

transmission, through bone marrow transfer to immune competent recipients, fails as a proxy for bone marrow cell permissiveness. Permissiveness of HSCs to *M. bovis* BCG was characterized three days after intravenous injection, as *M. bovis* BCG does not replicate within the host [169]. In contrast, in the study by Tornack et al. animals infected with *M. tuberculosis* were analyzed at 28 days post-infection [187]. Hence, all three studies differ not only in the mycobacterial species studied, but also in the stage of infection.

Thus, the apparent discrepancies in HSC permissiveness to mycobacterial infection are not mutually exclusive but rather highlight species-specific differences in virulence, in vivo growth rates and dissemination that determine HSC tropism and infection kinetics. These findings underscore the importance of considering mycobacterial species variations and experimental conditions when assessing HSC infection by mycobacteria.

2. Characterizing *M. tuberculosis* Internalization in HSCs

Facultative intracellular pathogens generally employ two main strategies for entering host cells. Some pathogens, including *M. tuberculosis*, are passively taken up by professional phagocytic cells but developed strategies to deviate their phagosomal fate by arresting phagosomal maturation [190]. Other pathogens, such as *Salmonella*, actively invade non-phagocytic cells by inducing their own internalization to shield themselves from professional phagocytes and humoral immune responses [191].

HSCs are generally regarded non-phagocytic. Macropinocytosis and phagocytosis pathways which could facilitate pathogen internalization emerge only at later stages of myeloid cell differentiation [189]. It has been assumed that acquisition of phagocytosis is synchronized with the capacity for phagosomal processing machinery, which inherently protects the most primitive progenitors from microbial infection [189,256]. Following our demonstration that HSCs can serve as host cells for *M. tuberculosis*, we investigated the mechanisms of mycobacterial internalization by these cells.

2.1 Actin-Remodelling is Associated with *M. tuberculosis* Internalization by HSCs

The polymerization force generated by the actin cytoskeleton as it pushes the cell membrane around a target particle is fundamental to all forms of particle internalization [203]. During phagocytosis, actin is polymerized to form a structured cup, which progressively extends as

a ring to the distal end of the particle [203]. In contrast, during macropinocytosis – and similarly in complement-triggered phagocytosis – large, actin-rich protrusions envelop particles within a thin membrane veil [257]. While these processes differ in their initiation and signaling pathways, both require actin-remodeling to facilitate particle internalization. The spatiotemporal regulation of upstream regulators of actin polymerization, including Rho GTPases, phosphoinositides and their associated enzymes are prime drivers of the morphological distinctions between these pathways. These regulators integrate signals that ultimately modulate the nucleation-promoting factors (NPFs) Wiskott-Aldrich syndrome protein (WASP) and neuronal WASP (N-WASP), which, in turn, activate the actin related protein 2 and 3 complexes (ARP2/3) [203].

Activation of ARP2/3 by NPFs induces a conformational change, creating a heterodimeric template for nucleation and branching of new actin filaments, forming a dense network of actin filaments ideally suited for force generation [258]. The precise kinetic and spatial organization of the upstream effectors orchestrating distinct modes of actin remodeling remains incompletely understood. Other cytoskeletal components may be engaged as well, as complement-mediated phagocytoses does not critically rely on WASP but involves microtubules instead [203].

In non-phagocytic cells, induced internalization is broadly categorized as either a ‘zipper’ and ‘trigger’ mechanism [259]. The ‘trigger‘ mechanism is defined by actin-cytoskeleton rearrangements – reminiscent of macropinocytosis – initiated by translocated virulence factors that directly interact with Rho-GTPases [191,259]. Conversely, the ‘zipper‘ mechanism resembles phagocytosis and involves direct interaction of particle surface molecules with host transmembrane receptors, such as E-cadherin or β-integrin [260,261]. Binding induces a signalling cascade that activates phosphatidylinositol 3-kinases (PI3Ks) and Rho-GTPases Rac and cell division cycle 42 (Cdc42), leading to a controlled and localized internalization process [259,262].

In our investigation of *M. tuberculosis* internalization, we observed membrane morphology consistent with findings in other non-phagocytic cells [221]. HSCs exhibited morphological characteristics reminiscent of membrane ruffling adjacent to surface-adherent mycobacteria, but neither lamellipodia, filopodia or phagocytic cups were observed **(Fig. 15)**. This suggests that *M. tuberculosis* infection of HSCs shares morphological traits with macropinocytosis. Notably, while internalization of enteroinvasive bacteria in non-phagocytic cells also elicits longer actin projections, such responses were markedly less

pronounced during *M. tuberculosis* infection of B cells observed by García-Pérez et al. and completely absent in HSCs in our study [221]. In both epithelial cells and B cells, membrane ruffling induced by *M. tuberculosis* is associated with actin reorganization at sites of bacterial adhesion and within membrane protrusions [199,221]. In HSCs and MPPs, we identified actin polymers enriched within membrane protrusions and surrounding intracellular bacteria as well **(Fig. 16)**. Furthermore, we found the internalization of *M. tuberculosis* to be at least partially sensitive to inhibitors of actin polymerization, such as Cytochalasin D **(Fig. 14)**. The observed induction of membrane ruffling, coupled with actin reorganization, indicates macropinocytosis as the pathway for *M. tuberculosis* uptake over alternative forms of membrane remodeling facilitating particle uptake. Nevertheless, morphological evidence alone is insufficient for comprehensive characterization, given the intricate crosstalk among pathways associated with canonical macropinocytosis, complement-triggered phagocytosis and 'trigger' mechanism phagocytosis, all of which culminate in membrane ruffling.

2.2 Internalization of *M. tuberculosis* by HSCs Is Not Phagocytic

Phagocytosis constitutes the principal mechanism for the internalization of *M. tuberculosis* by professional phagocytes [263]. Certain subsets of HSCs, which exhibit intrinsic myeloid lineage commitment, may already be predisposed to the associated transcriptional programs underlying phagocytosis pathways [232,235]. Generally, phagocytosis is directed to a ligand spotted surface recognized by cellular receptors. It can be conceptualized as a stepwise process characterized by three key events, each involving multiple simultaneously engaged signalling cascades: I) Ligation of cell-surface phagocytic receptors ii) formation of the phagocytic cup and internalization, and iii) phagosomal maturation [264].

The recognition of *M. tuberculosis* by antigen-presenting cells initially occurs through non-opsonic phagocytosis, which is mediated through the engagement of certain PRRs, although not ubiquitously expressed by all APCs [265,266]. Among the relevant PRRs are transmembrane C-type lectins, recognizing glycoconjugates of the *M. tuberculosis* cell wall, particularly ManLAM [267]. Soluble C-type lectins, such as surfactant protein A (SP-A), SP-B, along with the mannose-binding lectin (MBL), facilitate crosstalk with opsonic phagocytosis by activating the complement cascade, which leads to C3bi-opsonization and subsequent recognition by CR3 [269]. Importantly, in addition to the lectin pathway, both classical and alternative complement cascades contribute to C3b/C3bi opsonization of *M. tuberculosis*

[266]. After initial infection of the host and the onset of adaptive immune responses FcγR binding of immunoglobulin G- (IgG) decorated mycobacteria mediates opsonic-phagocytosis.

In both scenarios of recognition, opsonic and non-opsonic, phagocytosis is achieved through the sequential activation of small GTPases. FcγR-mediated phagocytosis is the most studied form and predominantly relies on Rac1, Cdc42 and WASP, whereas CR3-mediated phagocytosis requires RhoA formin activation, but does neither involve Cdc42 nor WASP [203,270,271]. Upon activation, these GTPases recruit WASP, which in turn recruits the ARP2/3 complex, facilitating subsequent F-actin remodeling and phagosome internalization [264].

Despite recognizing opsonins and mycobacterial lipoglycans as key determinants of *M. tuberculosis* phagocytic uptake, our data did not support the notion that HSCs engage classical non-opsonic or opsonic phagocytosis for the internalization of *M. tuberculosis*. Neither the competitive inhibition of mannan-binding C-type lectins, nor prior opsonization of *M. tuberculosis* with autologous serum compounds significantly altered the frequency of HSC infection **(Fig. 17, Fig. 18)**. This came to no surprise, as HSCs – in contrast to macrophages – lack CR3 and only weakly express opsonic-receptor, such as CD16, CD32, and CD64, on their surface [189]. These results demonstrate that *M. tuberculosis* infects HSCs through induced internalization instead of classical phagocytic pathways. However, the potential compensatory role of non-opsonic recognition in the absence of opsonic recognition, and vice versa, remains unexplored. Notably, in macrophages, receptor-blocking agents targeting either CR3 or C-type lectins did not significantly reduce infection when applied alone but did so in conjunction with αCR1 [272].

2.3 Induced Internalization in HSCs

Among the recognized mechanisms underlying induced internalization by non-phagocytic cells, macropinocytosis is one of two general pathways invasive bacteria primarily exploit [191]. Physiologically, classical macropinocytosis mediates the non-selective uptake of large volumes of extracellular fluids and macromolecules. Nevertheless, the channelling of antigens ingested through macropinocytosis by APCs into MHC-II pathways also implies an inherent role in immune surveillance [264,273]. Macropinocytosis, a constitutive process in many cell types, can also be induced by extracellular signals such as growth factor, cytokine, or scavenger receptor engagement, as well as experimentally by phorbol esters triggering

protein kinase C. These signals activate distinct downstream pathways, thereby distinguishing constitutive from induced macropinocytosis [264,274,275]. Ultimately, all these pathways promote F-actin nucleation through the activation of the ARP2/3 complex, leading to actin-remodelling and subsequent membrane ruffling [264]. However, contrasting phagocytosis, signals inducing macropinocytosis only indirectly activate pathways but do not represent a selective receptor ligand recognition for targeted uptake of a ligand-spotted particle.

Invasive bacteria co-opt these processes by translocating effectors into the host cell cytoplasm that mimic guanine nucleotide exchange factors (GEFs) and GTPase activating proteins (GAPs), thereby modulating the activity of the small GTPases central to macropinocytosis [191,276]. This manipulation triggers focal membrane ruffling at sites of bacterial adhesion. However, unlike the type III secretion systems employed by enteroinvasive pathogens such as *Salmonella*, *M. tuberculosis* expresses a T7SS, which is incapable of transmembrane effector secretion due to its structural constraints [277]. Consequently, outside-in receptor signalling cascades may be of relevance instead **(section E.3)**.

While *M. tuberculosis* is a paradigm of phagocytic uptake and intracellular survival within professional phagocytes, reports exist that *M. tuberculosis* can also infect non-phagocytic cells, including endothelial cells, epithelial cells, airway microfold cells, B cells, and mesenchymal stem cells [186,190,199,211,221,222]. In these non-phagocytic cells, macropinocytotic internalization has previously been implicated for *M. tuberculosis* internalization, as demonstrated by characteristic morphological changes and sensitivity to macropinocytosis inhibitors, such as amiloride [199,221]. Engagement of surface transmembrane receptors by *M. tuberculosis* surface proteins, such as Mce and heparin binding haemagglutinin, induces membrane protrusions in epithelial cells, underscoring a general mechanism for induced macropinocytosis in non-phagocytic cells, despite the absence of transmembrane effector secretion [199].

Microscopic analysis of HSCs during their interaction with *M. tuberculosis* revealed morphological features reminiscent of membrane ruffling **(Fig. 15)**. Yet, uptake was not reduced by macropinocytosis inhibitors **(Fig. 19)**, suggesting that the mechanisms of induced internalization in HSCs may differ from those in other non-phagocytic cells. Notably, instead of amiloride we employed imipramine, a repurposed drug with macropinocytosis inhibitor capacity and no cross-inhibition of other uptake pathways, albeit its precise target remains

unknown [207,208]. Of note, imipramine, as a cationic amphiphilic drug, also interferes with lysosomal lipid metabolism and pH, thus influencing a variety of cellular processes [278]. As the drug's exact mode of macropinocytosis inhibition is yet to be fully characterized, the insensitivity of HSC infection to imipramine does not provide clear information about the underlying signalling pathways beyond independence of canonical macropinocytosis.

While *M. tuberculosis* infection of non-phagocytic cells, such as epithelial cells and B cells, shares similarities regarding the employment of macropinocytosis by other invasive bacteria, our data demonstrate that distinct signalling pathways mediate HSC infection. Key surface receptors and intracellular signalling pathways described so far to be hijacked by invasive bacteria, may be absent in HSCs thus explaining their general resistance to infection and may thus explain why *M. tuberculosis* is uniquely capable of infecting HSCs.

2.4 Clathrin as a Protein Recruitment Hub During HSC Infection by *M. tuberculosis*

Clathrin-mediated endocytosis (CME) in the context of infection has been recognized as a key mechanism of viral entry due to the size constraints of the clathrin triskelion lattice, which forms clathrin-coated pits ranging from 1000 – 2000 Å (100 – 200 nm) in diameter [279]. This classical paradigm is being reconsidered as evidence emerges that clathrin functions as a major hub for the recruitment of proteins during bacterial uptake, orchestrating actin network regulation beyond its established role as a membrane coat for receptor-mediated endocytosis of small particles [191,209]. Notably, clathrin recruitment is critical for the 'zipper mechanism' uptake mode of various invasive bacteria, such as *L. monocytogenes*, *R. conorii* and enteropathogenic *E. coli*, where it precedes actin rearrangements [191,209]. Clathrin plagues on the cytoplasmic face of the plasma membrane, distinct from the classical clathrin-coated pits, have been described as scaffolds coordinating the interaction of key regulators of the actin cytoskeleton during induced phagocytosis [209]. Importantly, clathrin was found to be absent from internalized phagosomes, underscoring its regulatory role rather than direct structural involvement in clathrin-coated vesicle formation during bacterial internalization [209].

In alignment with this emerging understanding that clathrin is involved in induced internalization by non-phagocytic cells, our results demonstrate that *M. tuberculosis* infection of HSCs can be inhibited by CME inhibitors, showing that clathrin-mediated recruitment of downstream regulators plays a pivotal role in mycobacterial internalization

(Fig. 20). Specifically, we utilized Pitstop II, an inhibitor that targets the clathrin terminal domain and disrupts interactions with clathrin box ligands, such as amphiphysin, assembly protein 180 (AP180) and sorting nexin 9 (SNX9), notably without affecting adaptor protein complex 1 (AP-1)- or AP-2-mediated clathrin recruitment to the membrane itself [210]. Therefore, the lower uptake frequency of *M. tuberculosis* by Pitstop II-treated HSCs results from impaired recruitment of clathrin box ligands and their downstream interactions. Among them, dynamin, which is recruited through clathrin box ligands (via Bin/Amphiphysin/Rvs domains), mostly to facilitate membrane fission, is also involved in membrane ruffling during macropinocytotic uptake, via regulation of Rac1 GTPase distribution and is further indicated to influence ARP2/3 recruitment through cortactin or syndapin [280,281,209,264]. Thus, dynamin recruitment to clathrin plagues could present a critical checkpoint bridging clathrin recruitment to membrane ruffling, membrane fission and vesicle internalization following *M. tuberculosis* adhesion. However, not all interaction partners of clathrin bind the terminal domain. For instance, the binding domain of clathrin for Huntington-interacting protein-1 related (HIP1R), which directly binds F-actin, is located outside of the domain targeted by Pitstop II [282]. While putative interactions with HIP1R remaining in Pitstop II-treated cultures did not sufficiently compensate the inhibition, they might still play a role in uptake.

Hence, further investigations are necessary to delineate the extent to which clathrin-box ligands contribute to *M. tuberculosis* internalization in HSCs in cooperation with dynamin and HIP1R recruitment [209]. Exploring the colocalization with F-actin of clathrin, major clathrin-box ligands, dynamin, ARP2/3 and HIP1R at sites of *M. tuberculosis* surface adhesion, might thus provide initial hints towards the complex interplay of regulators during the mechanism of internalization in HSCs.

2.5 The Model of Mycobacterial Internalization by HSCs

Based on our findings, we propose a hypothetical model for induced internalization of *M. tuberculosis* by permissive HSCs, wherein the engagement of host cell surface receptors by *M. tuberculosis* initiates an intracellular signalling cascade **(Fig. 35)**. The specific receptors involved are likely distinct from opsonic receptors, such as Fc receptors and complement receptors, as well as C type lectins and will be discussed in more detail in the next section.

Among several possible pathways, we hypothesize that the triggered signalling cascade activates GTPases and phopshoinositides involved in macropinocytosis-independent membrane ruffling. Additionally, clathrin seems to be focally recruited to form a lattice

structure on the inner face of the plasma membrane, orchestrating the activation of actin-network regulators. The coordinated action of downstream clathrin box ligands, HIP1R, dynamin and clathrin-independently activated GTPases, may then recruit nucleation promoting factors. Their spatiotemporal regulation may then result in the formation of membrane ruffles that enwrap *M. tuberculosis*, leading to its internalization in a membrane vesicle linked to the growing actin network.

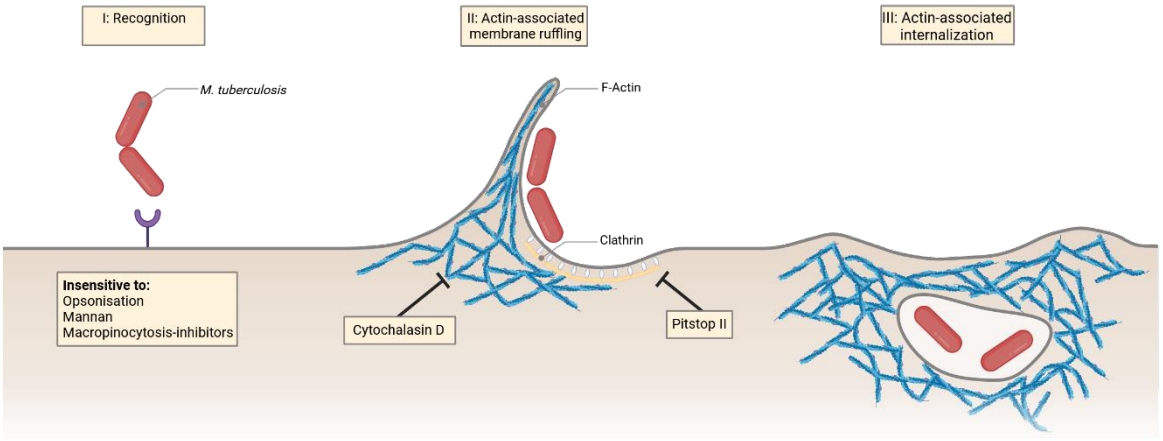

Figure 35: Morphological and molecular observations during *M. tuberculosis* internalization by hematopoietic stem cells within our hypothetical model. Internalization in hematopoietic stem cells (HSCs) deviates from common phagocytosis and macropinocytosis pathways described for phagocytic and non-phagocytic *M. tuberculosis* host cells, regarding recognition and uptake. We demonstrated that internalization of *M. tuberculosis* is not reduced when targeting classical phagocytosis and macropinocytosis pathways **(section D.2.2)**. Nevertheless, following recognition, HSCs exhibited morphological characteristics indicative of membrane ruffling adjacent to surface-adherent mycobacteria **(section D.2.1)**. Actin polymers were enriched within these membrane protrusions **(section D.2.1)**. Furthermore, we found the internalization of *M. tuberculosis* to be targetable by inhibitors of actin polymerization **(section D.2.1)**, such as Cytochalasin D, and clathrin-interactions **(section D.2.2)**, such as Pitstop II, resulting in reduced HSC infection rates. Within infected HSCs, we found intracellular mycobacteria enwrapped by actin polymers **(section D.2.1)**, indicative of the actin-mediated membrane vesicle internalization, as the final step of uptake.

3. CD36 as a Putative *M. tuberculosis* Receptor in HSCs

Bacterial internalization by non-phagocytic cells involves either mimicking endogenous ligands of surface receptors or translocating virulence factors with enzymatic activity into the cytoplasm to manipulate host signalling pathways [191]. *M. tuberculosis* lacks the secretion systems required for cross-membrane protein translocation into the host cell cytosol. Furthermore, our data did not support any involvement of complement receptors, Fc receptors and C type lectins in the recognition of *M. tuberculosis* by HSC. We thus aimed to elucidate the engaged surface receptors and focused on class B scavenger receptors which have already been implicated as receptors of *M. tuberculosis* uptake in other non-phagocytic cells [277].

3.1 Class B Scavenger Receptors in Mycobacterial Recognition

Scavenger receptors exhibit considerable diversity in their structure, function, and ligand repertoire. They are classified into twelve distinct groups based on their molecular structure. Among these, classes A (SR-AI, SR-AII and MARCO), B (SR-B1 and CD36) and E (dectin-1 and MMR) are particularly relevant for interactions with *M. tuberculosis* [265,284]. Expressed on innate immune cells they play crucial roles in recognizing mycobacterial lipids and glycoproteins, thereby integrating pathogen sensing into signalling pathways associated with inflammatory responses, immune metabolism, lysosomal trafficking and phagocytosis [285].

CD36, a member of the class B scavenger receptor family, is an 88 kDa heavily glycosylated transmembrane protein that plays a role in lipid acquisition, metabolic regulation, immune recognition, inflammation and cell adhesion. The receptor is expressed across a variety of immune and non-immune cells [285]. Structurally, CD36 consists of an extracellular ectodomain and two short, C- and N-terminal cytosolic domains [286]. Binding to microbial and endogenous ligands, respectively microbe-associated molecular patterns (MAMPs) and damage-associated molecular patterns (DAMPs), is mediated through the conserved CD36-region, which is shared by other class B scavenger receptors, such as SR-B1 [287]. These ligands include oxidized phospholipid moieties (in oxLDLs and on apoptotic cells), glycated proteins, glycans, long chain fatty acids, lipoteichoic acid (LTA) and lipopolysaccharides (LPS) [286,288]. In the context of *M. tuberculosis* recognition, ManLAM has been identified as the predominant ligand for CD36 recognition, as strains deficient in ManLAM synthesis are not bound by CD36 [285].

In our study, we found that CD36 is expressed by bona fide human HSCs in vitro as well as MPPs **(Fig. 21)**. We observed significant donor-dependent variability in the frequency of $CD36^+$ HSCs, but surface expression was not influenced by inflammatory stimuli such as LPS, IL-6, or *M. tuberculosis*-derived PAMPs **(Fig. 29, Fig. 30)**. We demonstrated that CD36 can facilitate internalization of *M. tuberculosis* into HSCs as specific inhibition of CD36 using SSO, a compound that specifically binds CD36 but not SR-B1 (despite sharing 30% sequence identity), significantly reduced the *M. tuberculosis* infection rate of HSCs in vitro **(Fig. 22)** [213,290]. Notably, CD36 alone is not sufficient for uptake as i) ~10 times more HSCs were $CD36^+$ than *M. tuberculosis* $DsRed^+$ and ii) the frequency of $CD36^+$-HSCs did not correlate with donor variabilities of HSC infection rates. Furthermore, MPP infection frequency was

slightly but not significantly reduced by SSO, highlighting this population's heterogeneity in function and potential receptor recognizing *M. tuberculosis* [197]. These findings demonstrate that while CD36 plays a role in uptake, additional receptors must be involved in *M. tuberculosis* recognition and HSC permissiveness.

3.1 The Role of CD36 in Mycobacterial Recognition

Our findings in HSCs, support the involvement of class B scavenger receptors, particularly CD36 and SR-B1, in the internalization of *M. tuberculosis* in distinct canonical and especially non-canonical host cells. While scavenger receptors play partly redundant roles to other PRRs in phagocytic cells, they are essential in various non-phagocytic cells [265]. For instance, in airway microfold cells, SR-B1 facilitates internalization upon *M. tuberculosis*-derived EsxA ligation, a process critical for translocation through the airway mucosa to initiate infection of the lung [211]. While expression of both, bacterial *exsA* by and host *SR-B*1 were essential for this mechanism, we found that a ΔRD1 mutant strain of *M. tuberculosis*, lacking the *esxA* gene, was still able to infect HSCs, indicating that CD36 recognition of *M. tuberculosis* in HSCs differs from SR-B1 recognition, despite the shared CD36-loop region **(Fig. 23)** [211]. MSCs also express SR-B1 and internalize *M. tuberculosis* in a MARCO- and SR-B1 dependent manner [212]. B cells, which internalize *M. tuberculosis* through induced macropinocytosis also express CD36, among other PRRs, although the specific interaction has not yet been extensively studied [221]. In adipocytes, CD36 likely plays a role in *M. tuberculosis* recognition as well, as binding of OxLDLs, known ligands of CD36, either directly or indirectly inhibits internalization [291]. Most interestingly, transfection of HeLa cells with human CD36 significantly enhances internalization of both Gram-negative and Gram-positive bacteria, underscoring CD36's role in bacterial uptake by non-phagocytic cells [288]. Yet, transfection of HeLa cells promoted bacterial internalization in an unspecific manner whereas our and previous data suggest rather mycobacteria-specific uptake in HSCs. Hence, secondary pathways, distinguishing HeLa cells from HSCs, influence species-specific differences in CD36-mediated uptake.

Since we could not entirely exclude efferocytosis underlying the delayed kinetics of HSC infection in vitro, it remains a possibility that instead of free bacteria, CD36 recognizes host ligands of infected cells or *M. tuberculosis* containing apoptotic bodies. Indeed, invasion of non-phagocytic epithelial cells via CD36-mediated efferocytosis has previously been shown to occur during *Salmonella* infection [292]. However, in the absence of other pathogens

infecting HSCs, efferocytosis seems rather unlikely to be the underlying mechanism. In addition, depletion of mature myeloid cells prior to infection, prime targets of *M. tuberculosis*, did not influence infection frequency of HSCs.

The exact mechanism by which CD36 engagement leads to *M. tuberculosis* internalization in HSCs remains to be elucidated. Interestingly, CD36-mediated uptake resembles macropinocytosis-like morphology but is mechanistically distinct. Compounds described to inhibit classical macropinocytosis do not affect CD36-mediated uptake [223]. This aligns with our observation that imipramine did not inhibit CD36-mediated *M. tuberculosis* infection in HSCs, despite the observation of membrane ruffling reminiscent of macropinocytosis **(Fig. 36)**. While the cytosolic domains of CD36 are essential for particle uptake, neither the cytosolic C- nor N-terminal regions exhibit intrinsic kinase or phosphatase activity [286,293]. Instead, palmitoylation of these cytosolic tails allows CD36 to localize in lipid rafts, where the receptor physically interacts with other signalling proteins [294,295]. Upon ligand binding, CD36 initiates assembly of a signalosome complex, including src-family kinases (SFKs) such as Fyn, Yes, and Lyn as well as the c-Jun NH_2-terminal kinases 1/2 (JNK1/2), activating transcription factors, mitogen-activated protein kinases (MAPKs) and Vav-family guanine nucleotide exchange factors (Vav-GEFs) involved in Rho and Rac GTPases, which are crucial for cytoskeletal reorganization [286,288]. Indeed, CD36 activation has also been linked to Rac GTPases, Cdc42 and ADP-ribosylation factor 6 (Arf6) activation, although the upstream mediators connecting CD36 to these regulators are still obscure [223]. Additionally, CD36 ligation promotes phosphorylation of p130-Crk-associated substrate (Cas) and paxillin, activating the Rac1 exchange factor complex Dock180/Elmo, which facilitates membrane ruffling and lamellipodia formation [296]. Eventually, the signalling cascades result in macropinocytosis-like CD36 receptor-internalization with a bound ligand, which hypothetically could be *M. tuberculosis* [223,285]. However, we have yet to confirm CD36 receptor internalization and vesicular co-localization in infected HSCs. Whether the CD36 signalling pathways observed in HEK293 cells, macrophages, microglia cells and adipocytes are equally present to their full extent in HSCs and thus truly responsible for *M. tuberculosis* internalization by these cells remains an open question.

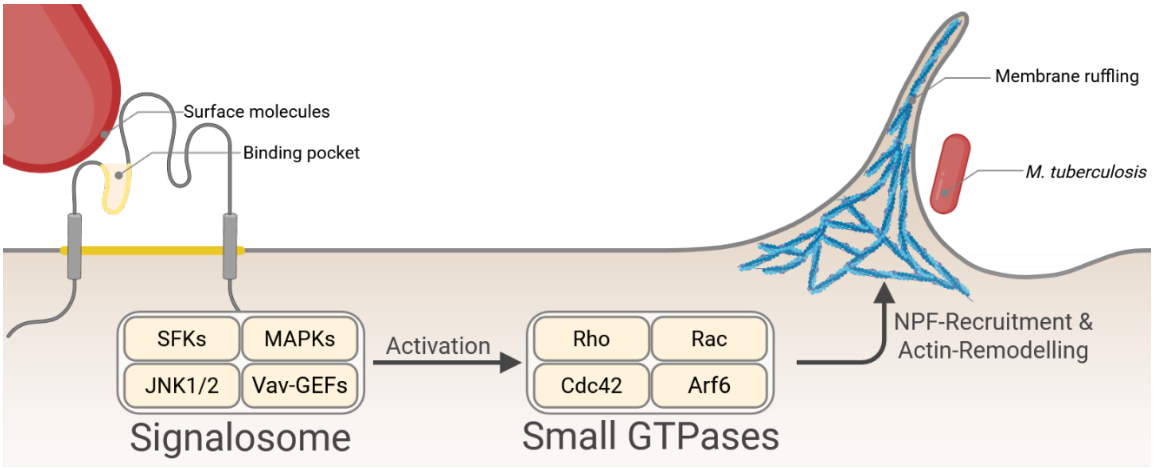

Figure 36: Described CD36 downstream signalling cascades that facilitate membrane ruffling and particle internalization. Ligation of the receptor initiates assembly of a signalosome complex, including src-family kinases (SFKs), c-Jun NH_2-terminal kinases 1/2 (JNK1/2), mitogen-activated protein kinases (MAPKs) and Vav-family guanine nucleotide exchange factors (Vav-GEFs). The signalosome complex activates small GTPases involved in cytoskeletal reorganization, such as Rho GTPases, Rac GTPases, cell division cycle 42 (Cdc42) and ADP-ribosylation factor 6 (Arf6). These small GTPases facilitate nucleation promoting factor (NPF)-recruitment leading to actin polymerisation to form membrane ruffles for particle or fluid internalization.

Beyond its role in microbial internalization, CD36 can also promote inflammatory responses, either autonomously or in conjunction with engagement of TLR2/6 and TLR4/6 heterodimers thereby enhancing cytokine production, such as IL-1β and TNFα [285,297]. Although, the downstream pathways of pro-inflammatory CD36 signalling upon receptor engagement are still not well-defined, CD36 engagement in HSCs might promote the emergency hematopoiesis signalling observed during mycobacterial infections [147,216,285]. In support of this hypothesis and our preliminary data on the phosphorylation status of STAT3 in *M. tuberculosis* infected HSCs in vitro, in vivo studies observe enrichment of Il6/JAK2/STAT3-pathway target genes in HSCs during experimental tuberculosis [158]. Moreover, STAT3 phosphorylation mediates myeloid lineage commitment by activating *Spi1*, *Gfi1*, *Cebpa/b* and *Myc* expression [216,298]. Despite the presence of a CD36/STAT3 signalling axis in metabolic regulation, there is yet no evidence in HSCs that inflammatory pathways are activated in direct response to CD36 signalling [299]. Thus, while CD36 plays a role in *M. tuberculosis* recognition and internalization by HSCs, further research is needed to delineate the exact signalling pathways triggered and the putative participation of other accessory receptors and downstream signalling molecules.

3.2 Exploiting CD-36 mediated Lipid Homeostasis

CD36 plays a multifaceted role during tuberculosis. Next to being a receptor involved in pathogen recognition and internalization, the receptor predominantly functions by mediating host cell lipid uptake and metabolism. Exploitation of CD36-mediated lipid homeostasis

marks an apparently widely spread virulence mechanism of *M. tuberculosis* host-pathogen interaction fostering intracellular survival. Enabling access to nutrients, especially fatty acids and cholesterols is crucial for *M. tuberculosis* growth [300]. *M. tuberculosis* relies on these host lipids to maintain its complex cell wall, to use them as a carbon and energy source, and to store them in the form of intracytoplasmic lipid inclusions for persistence during latent infection [301].

In macrophages, CD36 expression is upregulated during infection, facilitating the uptake of long chain fatty acids (LFCAs) and (oxidized) low density lipoproteins ((ox-)LDLs) due to its hybrid transporter function [301]. Additionally, this process is enhanced by CD36 and TLR2 signalling in an autocrine manner, which synergistically modulate lipid metabolism through peroxisome proliferator-activated receptor gamma (PPAR-γ) and NF-κB dependent pathways. The increase in intake and disruption of intracellular lipid regulatory mechanisms results in the accumulation of triacylglycerols (TAGs) and esterified cholesterol as lipid droplets (LD), leading to a 'foamy' macrophage phenotype that benefits *M. tuberculosis* survival by providing a nutrient-rich environment **(Fig. 37)** [285].

Interestingly, a similar mechanism occurs in HSCs [151]. Under steady state conditions, quiescent HSCs primarily rely on anaerobic glycolysis to maintain their minimal function. However, to compensate for the increased metabolic requirements during emergency hematopoiesis in response to infection and inflammation, they shift to fatty acid β-oxidation to meet the energy demands of cell cycling and proliferation [151]. Similarly to macrophages, this metabolic shift is driven by CD36-mediated uptake of fatty acid, which are readily released by lipolysis from bone marrow adipocytes and contributes to the increased production of myeloid cells during emergency hematopoiesis **(Fig. 37)** [151]. Studies in CD36 knockout mice demonstrate that this process is critical to stem cell and myeloid expansion, and its absence increases mortality during infection [151]. The positive feedback loop between CD36 engagement, PPAR-γ activation and *CD36* expression, might thus provide *M. tuberculosis* with a carbon source after infection of HSCs, further shaping HSCs as a reservoir for persistence. The crosstalk between CD36-mediated pathways for actin-remodelling but also lipid acquisition and metabolism, makes HSCs a useful niche for *M. tuberculosis*, as initial receptor engagement might concomitantly activate the relevant pathways to facilitate a steady supply of energy and building blocks for the mycobacterial cell wall [302]. A potential prime example of host-pathogen interaction where metabolism and infection meet.

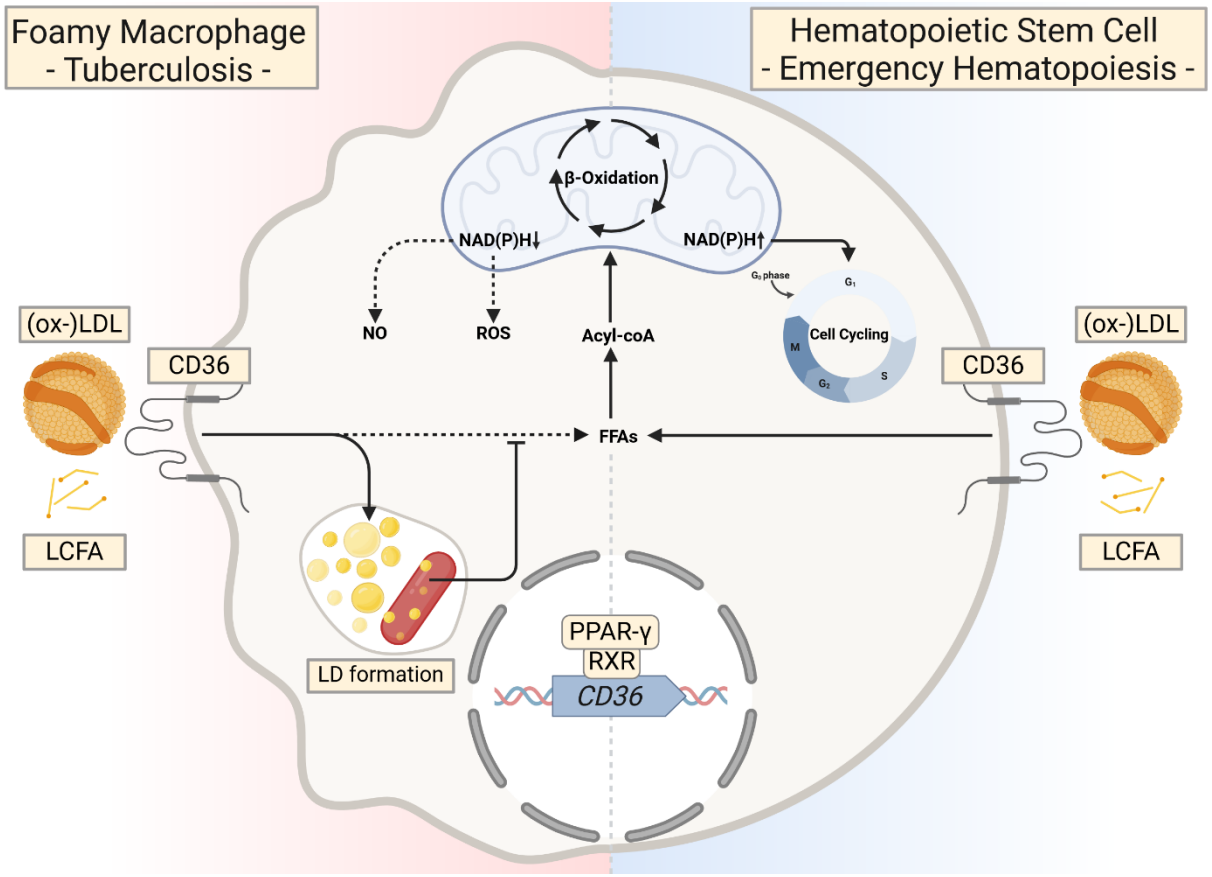

Figure 37: Parallels of lipid metabolism adaptations between *M. tuberculosis* infected macrophages and hematopoietic stem cells during emergency hematopoiesis. In infected macrophages, CD36 expression is upregulated during infection, facilitating the uptake of long-chain fatty acids (LCFAs) and (oxidized) low-density lipoproteins ((ox-)LDLs) through CD36. *M. tuberculosis* interferes with host lipid metabolism leading to the accumulation of these lipids as lipid droplets (LD). This benefits its survival representing a nutrient source and concomitantly reducing NAD(P)H levels for the generation of nitric oxides (NO) and reactive oxygen species (ROS) [303]. In hematopoietic stem cells (HSCs), CD36 expression is upregulated during emergency hematopoiesis facilitating the uptake of LFCAs and (ox-)LDLs. This uptake supports the increased energy demands of differentiation and proliferation and could potentially be exploited by *M. tuberculosis* [151].

In theory, the increase in nutrient availability and metabolic shift to fatty acid β-oxidation of quiescent HSCs during emergency hematopoiesis could re-activate persisting dormant *M. tuberculosis* in infected HSCs upon a secondary acute infection [151]. However, resuscitation of tuberculosis, at least in a clinically relevant context, is not common to secondary acute infections other than HIV. Hence, further studies are required to characterize the extent to which *M. tuberculosis* accesses HSC lipid metabolism and storage.

Persistence of *M. tuberculosis* as facilitated in lipid-rich environments is paralleled in both, phagocytic cells, such as foamy macrophages, as well as non-phagocytic cells such as HSCs. Activated monocyte-derived macrophages that switch to glycolysis can control *M. tuberculosis* more effectively than alveolar macrophages relying on fatty acid metabolism [285,304]. These observations have prompted novel therapeutic strategies focusing on metabolic reprogramming, and CD36 has been proposed as a target for host-directed therapies. However, targeting CD36 might prove challenging. While targeting CD36 could

theoretically improve macrophage-mediated control and protect the HSC reservoir from infection by *M. tuberculosis*, it would likely impair essential hematopoietic processes. Despite identifying the receptor for *M. tuberculosis* internalization in HSCs, CD36 is an unsuitable target to interfere with *M. tuberculosis* pathogenicity.

3.3 Concluding Remarks on CD36

In conclusion, our findings reveal a novel mechanism by which *M. tuberculosis* exploits a CD36-mediated process, canonically involved in the metabolic adaption of HSCs to stress, to facilitate its own entry into these non-phagocytic cells. The capacity of mycobacterial surface molecules to bind CD36, or the capacity of CD36 to also recognize pathogen-derived molecules, represent a prime example of host-pathogen co-evolution. As *M. tuberculosis* remains the only bacterial pathogen known to infect HSCs to this date, this represents a yet unique strategy of host-cell invasion. The molecular resemblance of endogenous ligands by mycobacterial surface molecules might trigger CD36 recognition, initiating an intracellular signalling cascade that leads to actin-remodelling and eventual internalization by a macropinocytosis-like mechanism. As pathogens other than *M. tuberculosis* also target CD36 for host cell invasion, CD36 alone cannot be the sole determinant for *M. tuberculosis* permissiveness in HSCs and secondary pathways are likely involved [288,292].

Despite these insights, several key aspects of this mechanism remain unexplored. The exact molecular pathways linking CD36 ligation to the activation of small GTPases and NPFs require further investigation, particularly how these pathways drive the tightly spatiotemporally regulated cytoskeletal rearrangement critical for bacterial uptake. Additionally, the role of CD36 in the recruitment of clathrin during *M. tuberculosis* internalization is still entirely unclear, as is the degree to which clathrin is essential for this process in general. Future studies are necessary to fully delineate these pathways and to understand the broader implications of CD36 in both host-pathogen interaction and HSC physiology.

4. Developing Permissiveness to Infection in HSCs

The differential susceptibility of HSCs to infection by a certain but not to other pathogens – specifically, their resistance to invasive bacteria such as *Salmonella* and *Listeria* while being permissiveness to *M. tuberculosis* – remains a fundamental question. Elucidating the mechanisms underlying permissiveness will provide valuable insights into protecting the HSC niche against infection during tuberculosis. While receptors such as CD36, along with

other yet-to-be-identified receptors, have been implicated to play an important role in HSC permissiveness, these factor alone cannot fully account for the observed permissiveness. Moreover, our findings indicate that *M. tuberculosis*-induced signalling primes HSCs to become permissive to infection, as we found both, host-specific variability and differential kinetics of in vitro HSC infection by *M. tuberculosis*.

4.1 Inflammaging as a Driver of HSC Permissiveness

In contrast to murine bone marrow HSCs and adult human circulating HSCs, we demonstrate that neonatal umbilical cord blood HSCs are resistant to infection by *M. tuberculosis* **(Fig. 24)**. The observed differences between immunophenotypically identical cells under identical experimental conditions, proof that donor age exerts a more pronounced influence on permissiveness than host species or tissue origin. This heterogeneity led to the hypothesis that HSC subsets acquire age-related modifications over time between birth and adulthood, rendering them increasingly permissive to infection over time. Aging in HSCs is recognized by epigenetic and transcriptional imprinting, increased expression of stress markers and accumulation of DNA damage, resulting in reduced self-renewal capacity, myeloid lineage bias, resistance to apoptosis, impaired autophagy, and disturbed migration [305]. These physiological differences between adult and neonatal HSCs arise from cumulative exposure to inflammatory signals, a process described as 'inflammaging' **(Fig. 38)** [238,306].

Further, the 'generation age hypothesis' postulates that HSC heterogeneity is driven by an individual cell's proliferative history, shaped by repeated inflammatory events that require the cell cycling of the most upstream progenitors [307]. Over time, these cumulative events not only induce intrinsic changes within HSCs but also alter the cellular composition of the HSC pool, leading to the accumulation of myeloid-biased HSCs that replace the predominantly lymphoid biased HSCs present during early stages of life [232]. Key drivers of this progression include interactions with the commensal microbiome and pathogenic agents, which begin influencing the hematopoietic system as early as during embryonal development and are essential for maintaining healthy, steady-state hematopoiesis [305,308]. Microbial translocation from the intestinal lumen into circulation along with chronic exposure to microbiome-derived molecules, sustains pro-inflammatory signalling – particularly through IL-1 and TNF-α pathways – which promote the accumulation of myeloid-biased HSCs expressing *Csf3r*, *Eto*, *Hoxb6* and *Meis2* alongside other aging-related phenotypes [305]. Furthermore, microbiome-derived short-chain fatty acids (SCFAs) have been shown to

modulate HSC commitment by influencing metabolic processes, such as iron availability in the bone marrow [309].

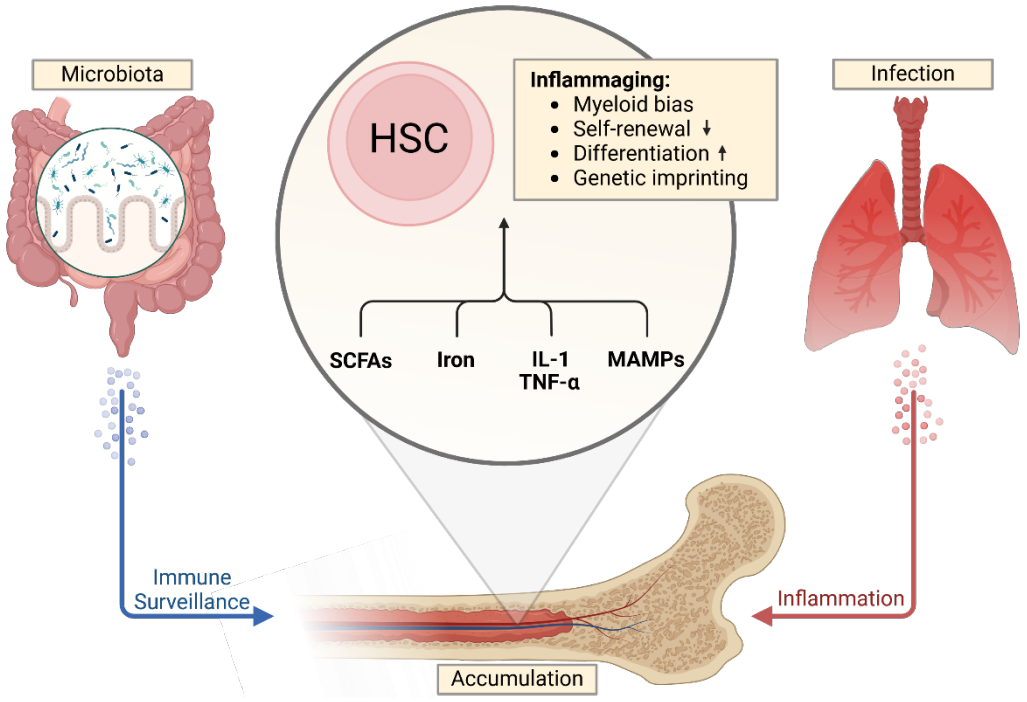

Figure 38: Inflammaging of hematopoietic stem cells. Hematopoietic stem cell (HSC) heterogeneity is shaped by repeated inflammatory events. Chronic exposure to microbiome-derived microbe-associated molecular patterns (MAMPs) and short-chain fatty acids (SCFAs), which affect iron availability, and pro-inflammatory cytokines in response to infections (particularly interleukin 1 (IL-1) and tumor necrosis factor alpha (TNF-α)), promote the accumulation of myeloid-biased HSCs over time. This leads to reduced self-renewal capacities and increased differentiation towards myeloid effector cells, which impairs immune competence of the host [305].

Although we did not directly assess the differentiation potential between neonatal HSCs and *M. tuberculosis*-infected adult HSCs, we hypothesize that the permissive cells observed in adults became enriched in numbers over time forming a subset of myeloid-biased HSCs, which are scarce in neonatal hosts but accumulate with age and exposure to inflammatory signals. This hypothesis could explain the differential infection frequencies, as only myeloid biased HSCs may express the requisite signalling pathways for CD36- and clathrin-mediated internalization of *M. tuberculosis* or may represent a distinct stage of myeloid-biased HSCs. Since reliable immunophenotypic markers to distinguish lineage-biased HSC subsets are not yet established, future research will be required to characterize these subsets in greater detail and validate our hypothesis. Given the wide distribution in CD36 surface expression between study sites and donors **(Fig. 29)**, a substantial influence of inflammaging and donor heterogeneity on the receptor that facilitates *M. tuberculosis* internalization by HSCs is indicated. Evaluation of HSC permissiveness in germ-free mice and CD36 expression in neonatal HSCs might provide initial insights in support of this hypothesis. In summary, we propose that the proliferative history of HSCs and their exposure to various commensal and

pathogenic stimuli not only dictate lineage commitment and stemness but also confer the genetic plasticity required for permissiveness to *M. tuberculosis* infection.

4.2 *M. tuberculosis* Induces Permissiveness in HSCs During In Vitro Culture

In our own observations of in vitro infection of phagocytic macrophages or neutrophils, intracellular localization of *M. tuberculosis* is typically observed within 2 hours, reaching an infection rate of ~100 % at a MOI of 3. In contrast, infection of HSCs progresses markedly slower, with most cells becoming infected between 12- and 24-hours upon inoculation **(Fig. 9)**. These observations cannot solely be explained by differences in cellular motility between the cell types.

We hypothesize that, rather than being inherently permissive, myeloid-biased HSCs acquire a state of priming that predisposes them to become permissive in response to additional stimuli encountered during culture in presence of *M. tuberculosis*. Although in vitro culture alone induced an expansion of $CD34^+$ $CD45RA^+$ hematopoietic progenitors, this expansion did not correlate with increased HSC infection rates **(Fig. 26)**. Moreover, periods of culturing HSCs with mycobacterial PAMPs in the absence of viable *M. tuberculosis* did not enhance permissiveness or accelerated the kinetics of infection after such initial culture **(Fig. 28)**. These findings indicate that permissiveness to *M. tuberculosis* infection is not a mere consequence of in vitro culture and the loss of niche-specific host factors, as has been described in long-term cultured of HSCs, which tend to accumulate myeloid functions [248].

Notably, treatment of HSCs with mycobacterial PAMPs did not induce a permissive phenotype either. Although some studies claim that HSCs express TLRs, allowing them to directly respond to PAMPs, these reports are often misattributed to HSCs. Misleading nomenclature – where murine LKS (Lin^- c-Kit^+ Sca-1^+), or human $CD34^+$ populations are labelled as HSCs – alongside the inaccurate use of HSC and HSPC terms has contributed to an ambiguous literature landscape [166,310-312]. Yet, no study has comprehensively characterized the PRR repertoire in precisely defined HSC populations. In support of our observation that *M. tuberculosis* -derived PAMPs did not induce permissiveness, we found that in our hands HSCs lack TLR2, TLR4, TLR9 and MMR, with CD36 being the only PRR detected on HSCs **(Fig. 31)**. However, the absence of any influence from potential CD36-ligands such as irradiated mycobacteria, whole cell lysates, cell wall fractions, or mannan on HSC infection rate suggest that while CD36 is involved in uptake, its signalling does not

influence permissiveness. However, we cannot completely exclude the possibility of intrinsic PAMP-mediated signalling in HSCs, as not all receptors described to recognize *M. tuberculosis* were included in our analysis, such as C-type lectins other than MMR [313].

Responses of HSCs to non-mycobacterial PAMPs have been shown to be mostly indirectly mediated by cytokine secretion from stromal cells and hematopoietic progenitors [136]. Our findings that neither *M. tuberculosis*-derived PAMPs nor dead whole bacteria induced permissiveness, led us to rather hypothesize that inflammatory mediators secreted in response to infection with viable *M. tuberculosis* are necessary to trigger signalling cascades that gradually render HSCs permissive. Studies on emergency hematopoiesis and HSC imprinting during mycobacterial infections highlight the role of interferons, particularly IFN-γ upon *M. bovis* infection and IFN-α upon *M. tuberculosis* infection, in triggering HSC signalling pathways [158,169]. Gene expression profiling of HSCs from *M. tuberculosis*-infected animals revealed enrichment in pathways related to interferon responses, inflammation and IL-6/JAK2/STAT3 signalling [158]. Consistent with our preliminary findings showing STAT3 activation in infected HSCs, these results suggest that pro-inflammatory signalling may represent the missing link between *M. tuberculosis* and the induction of HSCs permissiveness **(Fig. 32)**.

Most importantly, we found no evidence that permissiveness to *M. tuberculosis* is due to differentiation into myeloid progenitors. Permissiveness to non-mycobacterial pathogens in comparable experimental settings were only observed by Kolb-Mäurer et al. 2002 after three days of culture and was associated with the expression of lineage markers as signs of differentiation [189]. In our study, infected HSCs retained all immunophenotypic markers characteristic of bona fide HSCs throughout the experiments. Nevertheless, it remains possible that HSC permissiveness is a byproduct of myeloid-biased HSCs on the verge of differentiation, driven by cytokine instruction. Unilineage-restricted cells can emerge directly from cytokine-primed, undifferentiated HSC without transitioning through recognizable MPP stages [141,314]. Especially type I and II interferon signatures are both, established key mediators of HSC-signalling, but also define immune protective (IFN-II) versus susceptible pathogenic (IFN-I) host responses during tuberculosis [157,158,169,315,170-173]. Therefore, detailed transcriptional analysis and characterization of the differentiation potential of infected HSCs are crucial to elucidate genetic-based factors of permissiveness.

In summary, our findings suggest that the permissiveness of HSCs to *M. tuberculosis* is not intrinsic but rather a product of extrinsic inflammatory signals, potentially mediated by

cytokines such as interferons I and/or II. Certain HSC subsets might undergo functional changes during culture, rendering them permissive to *M. tuberculosis*. Thus, permissiveness to infection may represent a side-effect, of the HSC's role in immune surveillance and their ability to adapt their hematopoietic function and lineage commitment in response to microbial and inflammatory signals. Future studies should aim to precisely define the molecular mechanisms underlying this phenomenon and the definitive role of lineage-biased HSC subsets.

5. HSCs – Prime Targets for Mycobacterial Persistence

While our study provides a foundational understanding of the key processes leading up to the infection of HSCs, the functional role of infected HSCs – once *M. tuberculosis* successfully establishes this reservoir – remains largely undefined. The bone marrow's unique function, combining both primary and secondary lymphoid features, and the distinct properties of HSCs and their niches, makes it an attractive site for pathogen persistence and host immune system manipulation. Although hematopoietic manifestations of tuberculosis, such as pancytopenia, are observed, they are typically linked to miliary tuberculosis in patients with pre-existing immune impairing comorbidities [316]**.** Moreover, the idea that impaired immune-driven resistance allows pathogen persistence has so far been primarily attributed to systemic signals transferred to bone marrow cells instead of direct interactions of *M. tuberculosis* within the bone marrow environment [158,317,318]. Therefore, our understanding of the interactions within the bone marrow in the context of tuberculosis is still limited.

However, it is important to note that *M. tuberculosis* is not the only pathogen known to infiltrate the bone marrow, as several other pathogens exhibit a tropism for hematopoietic progenitors, albeit not specifically HSCs. Comparison with other infectious diseases in which bone marrow progenitors become infected, may offer valuable insights into the potential consequences of HSC infection during tuberculosis **(Tab. 21)**. Exploring these parallels could elucidate the broader implications of HSC involvement in latent infections and pathogen persistence.

Table 21: Non-viral pathogens infecting bone marrow cells.

Species	Host cell	Role during Infection	*Ref.*
Bacteria*:*			
M. tuberculosis	Mesenchymal Stem Cells, Myeloid Cells, Hematopoietic Stem Cells	Surviving treatment Interference with innate immune training	[158] [186] [187]
M. bovis BCG	Monocytes	Innate immune training	[169]
L. monocytogenes	Macrophages, Myelomonocytic Progenitors	Reservoir with insufficient antimicrobial properties	[319] [320] [321]
B. abortus	Monocytes, Neutrophils, Granulocyte Monocyte Progenitors	Disease Resuscitation	[322] [323] [324]
S. typhi	*Not assessed*	Surviving Treatment	[325]
S. typhimurium	Mature Myeloid Cells, Myeloid Progenitors, B Cells, B plasma cells, B cell precursors	Surviving Treatment Reservoir with insufficient antimicrobial properties	[189] [326]
Protozoa:			
L. infantum, L. donovani & L. major	Hematopoietic Stem Cells, Mesenchymal Stem Cells, Mature Myeloid Cells, Early Myeloid Progenitors (*L. major*)	Surviving Treatment Disease Resuscitation Reservoir with insufficient antimicrobial properties	[327] [328] [329]
Fungi:			
H. capsulatum	Mesenchymal Stem Cells, Hematopoietic Progenitors	Reservoir with insufficient antimicrobial properties	[330] [331]
P. brasiliensis	Mesenchymal Stem Cells	Reservoir with insufficient antimicrobial properties	[332]

Protection against antimicrobial regimen and a source of disease resuscitation

The primary implication of bone marrow infection, common to most pathogens is the establishment of a persisting reservoir throughout immune responses and medical treatment **(Fig. 39)**. This reservoir can serve as a source for disease resuscitation and peripheral dissemination, although in case of tuberculosis, lung granulomas are still assumed to be the primary source of reactivation. Among the unique traits of the bone marrow environment, the impaired efficacy of antimicrobial regimen holds the highest clinical relevance and often led to the initial discovery of bone marrow infections by various pathogens. Relapses after 'successful' treatment of tuberculosis, visceral leishmaniasis, and typhoid fever have been

attributed to a bone marrow reservoir that persists through treatment, causing disease relapses [180-183,187,327]. Although tuberculosis patients may meet the WHO's guidelines for clinical treatment endpoints (e.g., consecutive culture negativity in sputum), viable mycobacteria were still recovered from $CD271^+$ $CD45^-$ mesenchymal stem cells in bone marrow [181,185]. The persistence of bone marrow-dwelling mycobacteria throughout treatment was also confirmed in controlled experimental tuberculosis in mice [182].

The generally lower perfusion of bone marrow compared to other tissues might drive this observation [333]. Perfusion negatively correlates with the distance to the sinusoids and is most pronounced in the endosteal microenvironments, which is the main niche of HSCs [334]. Additionally, *M. tuberculosis* enters a dormant, non-replicative state within the hypoxic endosteal HSC niches, which is indicated by *dosR, c-lat* and *hspX* expression facilitating reduced drug efficacy as most first-line drugs – except pyrazinamide – only target metabolically active bacteria [132,335,336]. The elevated activity of efflux pumps in HSPCs might further reduce intracellular drug concentration and efficacy, lowering the effective intracellular drug concentrations reaching the pathogen [337].

Immune impairment through modulated hematopoiesis:

Since the discovery of trained immunity and HSC imprinting, it has been hypothesized that immune impairment allowing mycobacterial persistence is not only mediated by transient effects in mature post-mitotic immune cells but originates from imprinted self-renewing HSCs [158,169]. Negatively imprinted HSCs are known to cause long-term impairments in the immune system's antimicrobial function **(Fig. 39)** [158]. Macrophages derived from *M. tuberculosis*-infected donors fail to control mycobacterial growth upon a secondary infectious challenge, both in vitro and in vivo. This impairment persists for at least one year after pathogen clearance and originates from epigenetically imprinted HSCs [158]. It has also long been speculated that the lack of natural T cell driven immunity and protection originates from intrinsic reprogramming as well [218,338]. While both *M. bovis* BCG and virulent *M. tuberculosis* induce similar transcriptional changes in HSCs, HSCs exposed to *M. tuberculosis* do not develop trained immunity phenotypes but confer immune impairment in their progeny due to additional activation of type I IFN and heme pathways. These detrimental effects were solely attributed to the paracrine responses of type I IFN production [158]. Given the conflicting reports on the permissiveness of HSCs to *M. tuberculosis* and the incomplete validation in the respective studies, as discussed above **(section E.1.4)**, a contribution of infected HSCs and early progenitors to the phenotypes described should not be entirely

omitted. Particularly the finding that necrotic cell death in myeloid but not other hematopoietic progenitors skews hematopoiesis toward lymphopoiesis, could be explained by *M. tuberculosis* infection, although it remains an open question why necrosis was not observed in HSCs [158]. The distinct outcomes of interactions between *M. tuberculosis* and *M. bovis* BCG with HSCs considering that only *M. tuberculosis* but no other mycobacterial species might be able to infect them, opens the possibility that this difference is a key driver of detrimental imprinting driving *M. tuberculosis* persistence.

In addition to the direct interaction between HSCs and *M. tuberculosis*, the chronic exposure to microbial and pro-inflammatory signals during mycobacterial persistence might further drive immune impairment. Signaling in response to acute infection mediates protective emergency hematopoiesis [147,166,339]. In contrast, the chronic exposure to identical signals as it likely happens in tuberculosis mediates HSC exhaustion in association with long-term impairments in myeloid output [157,340,341]

In conclusion, the immune dysfunction apparent throughout the distinct disease stages of tuberculosis is not only driven by direct interactions between *M. tuberculosis* and immune effector cells at the primary site of infection but also by lasting impairments imposed on the hematopoietic system. To which extent infected MPP populations are also involved in these impairments has yet to be characterized. HSCs may primarily serve as a long-term source of imprinted cells, whereas MPPs could represent the more immediate targets to induce immune impairment, as only during acute inflammation, but unlikely during mycobacterial persistence in latent tuberculosis, HSCs extensively engage in proliferation [342]. This underscores the need for further investigation into the mechanisms underlying HSC infection and its broader implications for long-term immune competence.

Infecting cells with insufficient antimicrobial properties:

The primary hallmark of the bone marrow is the presence of immature immune cells. As a result, cells that lack fully developed downstream processing pathways may internalize pathogens. This concept is supported by the Infection of HSCs by *Leishmania*, the only other non-viral pathogen known to infect HSCs. Unlike IFN-γ-activated macrophages, in which reactive oxygen species and nitric oxide (ROS/NO) production increases upon infection, production declines over time in infeced HSCs, resulting in increasing amastigote burdens [327,343,344]. Similar effects could lead to reduced tuberculocidal activity in *M. tuberculosis*-infected HSCs. Although further experiments are needed to support our observation, deletion of the RD1 region, which attenuates *M. tuberculosis* and is necessary

for macrophage intracellular survival and growth, did not affect the infection frequency in HSCs 20 hours after inoculation **(Fig. 23)** [345,346]. Additionally, myeloid progenitors with inadequate antimicrobial responses undergo delayed apoptosis upon infection compared to activated professional phagocytes, extending the potential period of intracellular replication and delaying immune recognition [189].

Besides intrinsic lack of antimicrobial responses, there is also a lack of exogenous pro-inflammatory signals in the bone marrow to mediate immune protection [347]. The bone marrow contains the highest numbers of $CD4^+$ $CD25^+$ $FoxP3^+$ regulatory T cells (T_{regs}) compared to any other secondary lymphoid organ [348]. These T_{regs} limit inflammation in the stem cell niche through IL-10 production [348,349]. HSCs play a significant role in maintaining this immune privilege by engaging in immune surveillance to prime resident $CD4^+$ T cells via MHC-II-presented endo- and exogenous antigens **(Fig. 39)** [347,350]. While HSCs only weakly express classical co-stimulatory molecules, the co-inhibitory molecule PD-L1 is abundant. When primed by antigen-presenting HSCs, T cells are polarized into a Tr1-like phenotype associated with the expression of IL-10, programmed death-1 (PD1), programmed death ligand-1 (PDL1), lymphocyte-activation gene 3 (LAG3) and T-cell immunoglobulin and mucin-domain containg-3 (TIM3), limiting inflammation [350]. In a similar mechanism, infection of HSCs by *M. tuberculosis* could lead to the cross-presentation of mycobacterial antigens to $CD4^+$ T cells and the subsequent priming and expansion of *M. tuberculosis*-reactive T_{regs} with anti-inflammatory properties. Nevertheless, maintenance of immune privilege during bone marrow infections and how T_{regs} may influence pathogen persistence in HSC microenvironments has yet to be characterized.

Conclusions

The published data on tuberculosis, listeriosis, typhoid fever, and leishmaniasis – where pathogens have been identified within bone marrow – suggest that bone marrow infection is an integral part of the pathogenicity of these facultative intracellular microbes. The infection of HSCs by *M. tuberculosis* particularly highlights how pathogens can hijack the unique features of HSCs and the hematopoietic system. In the light of evolution, the human immune system likely benefitted from HSCs that acquired mechanisms enabling them to take part in immune surveillance. However, the same mechanisms are in danger of being exploited by bacteria, especially by using a receptor for infection, CD36, which is critical for HSC function, so that mutations conferring resistance to infection are unlikely. A perfect example of the arms race that is host-pathogen co-evolution.

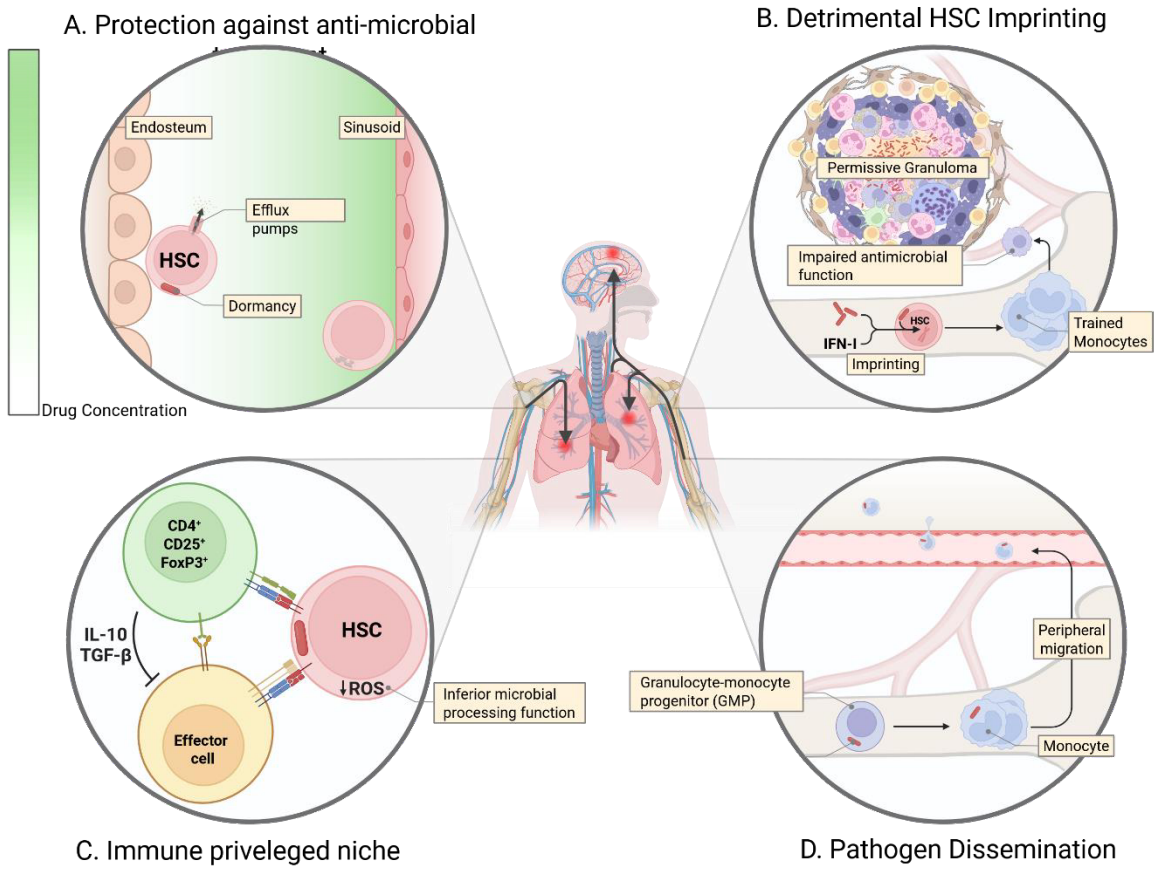

Figure 39: Consequences of bone marrow infection. A) Lower perfusion and sinusoidal distance protect against anti-microbial regimen. Host cells expressing efflux pumps and bacterial dormancy in hypoxic endosteal niches further improve protection. **B)** Hematopoietic stem cells (HSCs) can become detrimentally imprinted by adverse immune responses in bone marrow or interactions with bone marrow dwelling bacteria. Imprinted progeny has impaired antimicrobial function and potentially interfere with bacterial control in the periphery. **C)** The bone marrow is an immune privileged niche and contains the highest numbers of regulatory T cells (T_{regs}) compared to any other secondary lymphoid organ. Dampening pro-inflammatory responses could protect bone marrow bacteria against elimination. Hematopoietic progenitors also possess inferior microbial processing functions compared to their mature counterparts. **D)** The bone marrow can function as a reservoir of infected migrating cells disseminating pathogens into peripheral tissues.

6. How *M. tuberculosis* Infects HSCs – An Outlook

Our findings propose a hypothetical model delineating a sequential cascade of events that ultimately enable *M. tuberculosis* to infect HSCs **(Fig. 40)**. At birth, HSCs exist in their most naïve state, characterized by maximal 'stemness' [306]. With advancing age, HSCs accumulate pro-inflammatory signals that are essential for maintaining healthy steady-state hematopoiesis but also drive a progressive shift toward myeloid-biased HSCs, concomitant with a decline in intrinsic 'stemness' [232]. We hypothesize that specific subsets of HSCs, particularly myeloid-biased subpopulation, may exhibit a genetically primed state that induces key factors required for pathogen internalization in response to *M. tuberculosis*-triggered inflammatory cues.

Engagement of CD36, may initiate signalling cascades leading to cytoskeletal remodelling, engaging clathrin in a yet to define function. This remodelling likely triggers an actin-driven macropinocytosis-like mechanism that, although mechanistically distinct from classical macropinocytosis, generates membrane ruffles leading to *M. tuberculosis* uptake into HSCs. Once infected, HSCs may constitute a critical niche for persistence, contributing to long-term immune dysregulation and serving as a reservoir for disease resuscitation.

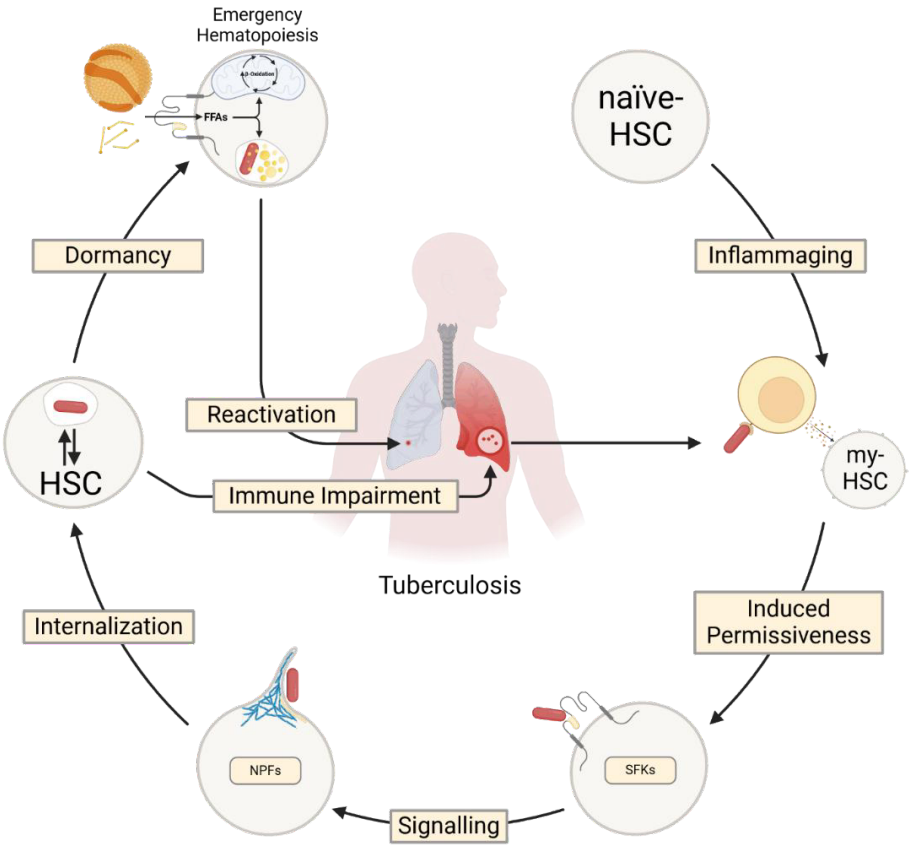

Figure 40: The hypothetical chain of events enabling *M. tuberculosis* to establish a niche in hematopoietic stem cells. Naïve hematopoietic stem cells (HSCs) acquire myeloid bias (my-HSC) through inflammaging and become permissive to *M. tuberculosis* infection by extrinsic signals to viable mycobacteria. This enables *M. tuberculosis* to induce its internalization through CD36-signalling and eventual actin-mediated membrane remodelling. Infected HSCs might represent the source of long-lasting immune impairments and a potential niche for persistence and disease resuscitation.

Several open questions along this cascade of events warrant further investigation, as elaborated in the respective sections. A key question is whether inflammaging and myeloid lineage bias indeed influence differential permissiveness between neonatal and adult-derived HSCs **(section E.4.1)**. Germ-free murine models may provide a suitable system to examine HSCs in the absence of prior microbial exposure and assess their susceptibility to *M. tuberculosis* infection. To further explore CD36 as a putative receptor, investigating its expression in HSCs of neonatal or germ-free origin could elucidate the heterogeneity within the HSC compartment as observed in our study. Given the lack of reliable phenotypic markers for myeloid lineage bias in HSCs, confirming myeloid bias in permissive HSCs subsets

requires functional characterization [232,234]. However, such characterization is challenging, as permissiveness is only then becoming obvious when HSCs internalize *M. tuberculosis*. This interaction may however immediately alter host cell physiology, narrowing the window in which the functional state can be assessed un-biased. Deciphering the molecular pathways mediating internalization could thus offer an indirect means of defining permissiveness to circumvent this limitation.

In this study, we identified CD36 recognition **(section E.3)**, clathrin interactions **(section E.2.4)**, and subsequent actin polymerisation **(section E.2.1)** as key checkpoints of *M. tuberculosis* uptake in HSCs. The involvement of yet-to-be verified SFKs, clathrin-box ligands and NPFs, represents missing mechanistic links between *M. tuberculosis* recognition and cytoskeletal remodelling. Their expression could identify permissiveness-determining genetic programs in HSC subsets. Investigating the spatial co-localization of clathrin (within sub-membranous plagues) and NPFs, such as ARP2/3, at sites of *M. tuberculosis* adherence, along with analyses of downstream signalling, for example through interference with CD36-palmitoylation constitutes a logical next step [209,294].

Moreover, to define the role of HSC infection in *M. tuberculosis* persistence, we propose refining our whole-mount multiparameter immunofluorescence imaging approach to spatially resolve the *M. tuberculosis* reservoir within bone marrow. Potential localization within hypoxic endosteal regions together with spatial transcriptomics of bone marrow cells may inform a dormant bacterial phenotype within quiescent HSCs, conferring protection against both immune clearance and therapeutic interventions **(section E.5)**. Initial analyses in vivo found *M. tuberculosis* in an unculturable state within HSCs, expressing dormancy-related genes [187]. We have yet to investigate whether *M. tuberculosis* shares this phenotype in vitro for future studies. So far, CFU-assays in vitro have been inconclusive due to technical and bio-safety limitations when isolating an infected homogenous HSC population without fixation.

Finally, utilizing our in vitro models to inhibit HSC infection may clarify whether the immune imprinting effects observed by Khan et al. arise from direct intracellular infection or indirect host-pathogen interactions [158].

Understanding the distinct implications of mycobacterial persistence in HSCs within the bone marrow and in peripheral tissue is crucial. Only through an in-depth understanding of these interactions, can we fully recognize the role of HSCs and their infection in tuberculosis and ultimately invent strategies to safeguard the HSC niche against infection.

References

[1] R. Brosch *et al.*, 'A new evolutionary scenario for the Mycobacterium tuberculosis complex', *Proc Natl Acad Sci U S A*, vol. 99, no. 6, pp. 3684–3689, 2002, doi: 10.1073/pnas.052548299.

[2] S. Sreevatsan *et al.*, 'Restricted structural gene polymorphism in the Mycobacterium tuberculosis complex indicates evolutionarily recent global dissemination', *Proc Natl Acad Sci U S A*, vol. 94, no. 18, pp. 9869–9874, 1997, doi: 10.1073/pnas.94.18.9869.

[3] I. Comas *et al.*, 'Out-of-Africa migration and Neolithic co-expansion of Mycobacterium tuberculosis with modern humans', *Nat Genet*, vol. 45, no. 10, pp. 1176–1182, 2014, doi: 10.1038/ng.2744.Out-of-Africa.

[4] M. R. Zimmerman, 'Pulmonary and osseous tuberculosis in an Egyptian mummy.', *Bull N Y Acad Med*, vol. 55, no. 6, pp. 604–8, Jun. 1979.

[5] W. L. Salo, A. C. Aufderheide, J. Buikstra, and T. A. Holcomb, 'Identification of Mycobacterium tuberculosis DNA in a pre-Columbian Peruvian mummy', *Proc Natl Acad Sci U S A*, vol. 91, no. 6, pp. 2091–2094, 1994, doi: 10.1073/pnas.91.6.2091.

[6] H. FUSEGAWA, B.-H. Wang, K. SAKURAI, K. NAGASAWA, M. OKAUCHI, and K. NAGAKURA, 'Outbreak of Tuberculosis in a 2000-Year-Old Chinese Population', *Journal of the Japanese Association for Infectious Diseases*, vol. 77, no. 3, pp. 146–149, 2003, doi: 10.11150/kansenshogakuzasshi1970.77.146.

[7] P. V. V Prasad, 'General medicine in Atharvaveda with special reference to Yaksma (consumption/tuberculosis).', *Bull Indian Inst Hist Med Hyderabad*, vol. 32, no. 1, pp. 1–14, 2002.

[8] Hippocrates, 'Aphorisms'.

[9] R. Koch, 'Die Aetiologie der Tuberculose', *Berliner Klinische Wochenschrift*, 1882.

[10] WHO, 'Global tuberculosis report, 2024', 2024.

[11] IACG, 'No Time to Wait: Securing the Future from Drug-Resistant Infections', *WHO*, 2019.

[12] WHO, *Global tuberculosis report, 2023*. 2023. [Online]. Available: https://iris.who.int/.

[13] W. Genschorek, *Robert Koch. Selbstloser Kampf gegen Seuchen und Infektionskrankheiten*. Leibzig, Deutschland: Hirzel, 1982.

[14] N. H. Smith, R. G. Hewinson, K. Kremer, R. Brosch, and S. V. Gordon, 'Myths and misconceptions: The origin and evolution of Mycobacterium tuberculosis', *Nat Rev Microbiol*, vol. 7, no. 7, pp. 537–544, 2009, doi: 10.1038/nrmicro2165.

[15] I. Smith, 'Mycobacterium tuberculosis pathogenesis and molecular determinants of virulence', *Clin Microbiol Rev*, vol. 16, no. 3, pp. 463–496, 2003, doi: 10.1128/CMR.16.3.463-496.2003.

[16] C. L. Skevaki and D. A. Kafetzis, 'Tuberculosis in Neonates and Infants', *Pediatric Drugs*, vol. 7, no. 4, pp. 219–234, 2005, doi: 10.2165/00148581-200507040-00002.

[17] P. J. Dodd, C. M. Yuen, C. Sismanidis, J. A. Seddon, and H. E. Jenkins, 'The global burden of tuberculosis mortality in children: a mathematical modelling study', *Lancet Glob Health*, vol. 5, no. 9, pp. e898–e906, 2017, doi: 10.1016/S2214-109X(17)30289-9.

[18] F. M. Guerra *et al.*, 'The basic reproduction number (R0) of measles: a systematic review', *Lancet Infect Dis*, vol. 17, no. 12, pp. e420–e428, 2017, doi: 10.1016/S1473-3099(17)30307-9.

[19] A. K. Coussens *et al.*, 'Classification of early tuberculosis states to guide research for improved care and prevention: an international Delphi consensus exercise', *Lancet Respir Med*, vol. 12, no. 6, pp. 484–498, 2024, doi: 10.1016/S2213-2600(24)00028-6.

[20] N. B. Hoa, D. N. Sy, N. V. Nhung, E. W. Tiemersma, M. W. Borgdorff, and F. G. J. Cobelens, 'National survey of tuberculosis prevalence in Viet Nam', *Bull World Health Organ*, vol. 88, no. 4, pp. 273–280, 2010, doi: 10.2471/BLT.09.067801.

[21] D. W. Dowdy, S. Basu, and J. R. Andrews, 'Is passive diagnosis enough? The impact of subclinical disease on diagnostic strategies for tuberculosis', *Am J Respir Crit Care Med*, vol. 187, no. 5, pp. 543–551, 2013, doi: 10.1164/rccm.201207-1217OC.

[22] I. Onozaki, I. Law, C. Sismanidis, M. Zignol, P. Glaziou, and K. Floyd, 'National tuberculosis prevalence surveys in Asia, 1990-2012: An overview of results and lessons learned', *Tropical Medicine and International Health*, vol. 20, no. 9, pp. 1128–1145, 2015, doi: 10.1111/tmi.12534.

[23] G. H. Bothamley, 'Male Sex Bias in Immune Biomarkers for Tuberculosis', *Front Immunol*, vol. 12, no. March, 2021, doi: 10.3389/fimmu.2021.640903.

[24] P. B. Miller *et al.*, 'Association between tuberculosis in men and social network structure in Kampala, Uganda', *BMC Infect Dis*, vol. 21, no. 1, pp. 1–9, 2021, doi: 10.1186/s12879-021-06475-z.

[25] C. Y. Jeon and M. B. Murray, 'Diabetes mellitus increases the risk of active tuberculosis: A systematic review of 13 observational studies', *PLoS Med*, vol. 5, no. 7, pp. 1091–1101, 2008, doi: 10.1371/journal.pmed.0050152.

[26] D. V. Havlir, H. Getahun, I. Sanne, and P. Nunn, 'Opportunities and Challenges for HIV Care in Overlapping HIV and TB Epidemics', *JAMA*, vol. 300, no. 4, p. 423, Jul. 2008, doi: 10.1001/jama.300.4.423.

[27] K. L. Winthrop, 'Risk and prevention of tuberculosis and other serious opportunistic infections associated with the inhibition of tumor necrosis factor', *Nat Clin Pract Rheumatol*, vol. 2, no. 11, pp. 602–610, 2006, doi: 10.1038/ncprheum0336.

[28] J. R. Hargreaves, D. Boccia, C. A. Evans, M. Adato, M. Petticrew, and J. D. H. Porter, 'The Social Determinants of Tuberculosis: From Evidence to Action', *Am J Public Health*, vol. 101, no. 4, pp. 654–662, Apr. 2011, doi: 10.2105/AJPH.2010.199505.

[29] O. Oxlade and M. Murray, 'Tuberculosis and Poverty: Why Are the Poor at Greater Risk in India?', *PLoS One*, vol. 7, no. 11, p. e47533, Nov. 2012, doi: 10.1371/journal.pone.0047533.

[30] G. Harling and M. C. Castro, 'A spatial analysis of social and economic determinants of tuberculosis in Brazil', *Health Place*, vol. 25, pp. 56–67, Jan. 2014, doi: 10.1016/j.healthplace.2013.10.008.

[31] K. Lönnroth *et al.*, 'Tuberculosis control and elimination 2010-50: cure, care, and social development', *The Lancet*, vol. 375, no. 9728, pp. 1814–1829, 2010, doi: 10.1016/S0140-6736(10)60483-7.

[32] M. Daniels and A. B. Hill, 'Chemotherapy of Pulmonary Tuberculosis in Young Adults', *BMJ*, vol. 1, no. 4769, pp. 1162–1168, May 1952, doi: 10.1136/bmj.1.4769.1162.

[33] E. Vanino *et al.*, 'Update of drug-resistant tuberculosis treatment guidelines: A turning point', *International Journal of Infectious Diseases*, vol. 130, pp. S12–S15, 2023, doi: 10.1016/j.ijid.2023.03.013.

[34] I. S. Pradipta, D. Houtsma, J. F. M. van Boven, J. W. C. Alffenaar, and E. Hak, 'Interventions to improve medication adherence in tuberculosis patients: a systematic review of randomized controlled studies', *NPJ Prim Care Respir Med*, vol. 30, no. 1, 2020, doi: 10.1038/s41533-020-0179-x.

[35] T. A. Black and U. K. Buchwald, 'The pipeline of new molecules and regimens against drug-resistant tuberculosis', *J Clin Tuberc Other Mycobact Dis*, vol. 25, p. 100285, 2021, doi: 10.1016/j.jctube.2021.100285.

[36] A. Calmette, C. Guerin, and A. Boquet, 'La vaccination préventive contre la tuberculose par le "BCG"', *Paris: Masson et cie*, 1927.

[37] A. Calmette, 'L'infection bacillaire et la tuberculose chez l'homme et chez les animaux', 1922.

[38] World Health Organization, *Global Tuberculosis Report 2023*. 2023.

[39] M. L. Barreto *et al.*, 'Evidence of an effect of BCG revaccination on incidence of tuberculosis in school-aged children in Brazil: Second report of the BCG-REVAC cluster-randomised trial', *Vaccine*, vol. 29, no. 31, pp. 4875–4877, 2011, doi: 10.1016/j.vaccine.2011.05.023.

[40] Tuberculosis Research Centre (ICMR), 'Fifteen year follow up of trial of BCG vaccines in south India for tuberculosis prevention. 1999.', 2013.

[41] P. Mangtani *et al.*, 'Protection by BCG vaccine against tuberculosis: A systematic review of randomized controlled trials', *Clinical Infectious Diseases*, vol. 58, no. 4, pp. 470–480, 2014, doi: 10.1093/cid/cit790.

[42] P. Andersen and T. M. Doherty, 'The success and failure of BCG-implications for a novel tuberculosis vaccine', *Nat Rev Microbiol*, vol. 3, pp. 656–662, 2005, doi: 10.1016/S0140-6736(13)61482-8.

[43] L. Brandt *et al.*, 'Failure of the Mycobacterium bovis BCG vaccine: Some species of environmental mycobacteria block multiplication of BCG and induction of protective immunity to tuberculosis', *Infect Immun*, vol. 70, no. 2, pp. 672–678, 2002, doi: 10.1128/IAI.70.2.672-678.2002.

[44] P. Andersen and T. J. Scriba, 'Moving tuberculosis vaccines from theory to practice', *Nat Rev Immunol*, vol. 19, no. 9, pp. 550–562, 2019, doi: 10.1038/s41577-019-0174-z.

[45] H. M. Dockrell and S. G. Smith, 'What have we learnt about BCG vaccination in the last 20 years?', *Front Immunol*, vol. 8, no. SEP, pp. 1–10, 2017, doi: 10.3389/fimmu.2017.01134.

[46] S. H. E. Kaufmann, A. Dorhoi, R. S. Hotchkiss, and R. Bartenschlager, 'Host-directed therapies for bacterial and viral infections', *Nat Rev Drug Discov*, vol. 17, no. 1, pp. 35–56, 2018, doi: 10.1038/nrd.2017.162.

[47] M. Datta *et al.*, 'Normalizing granuloma vasculature and matrix improves drug delivery and reduces bacterial burden in tuberculosis-infected rabbits', *Proceedings of the National Academy of Sciences*, vol. 121, no. 14, p. e2321336121, 2024, doi: 10.1073/pnas.

[48] J. Taylor, M. L. Bastos, S. Lachapelle-Chisholm, N. E. Mayo, J. Johnston, and D. Menzies, 'Residual respiratory disability after successful treatment of pulmonary tuberculosis: a systematic review and meta-analysis', *EClinicalMedicine*, vol. 59, p. 101979, 2023, doi: 10.1016/j.eclinm.2023.101979.

[49] A. Bansal *et al.*, 'Surviving Pulmonary Tuberculosis: Navigating the Long Term Respiratory Effects', *Cureus*, vol. 15, no. 5, 2023, doi: 10.7759/cureus.38811.

[50] T. Dallenga and U. E. Schaible, 'Neutrophils in tuberculosis--first line of defence or booster of disease and targets for host-directed therapy?', Apr. 01, 2016. doi: 10.1093/femspd/ftw012.

[51] G. A. W. Rook, K. Dheda, and A. Zumla, 'Immune responses to tuberculosis in developing countries: Implications for new vaccines', *Nat Rev Immunol*, vol. 5, no. 8, pp. 661–667, 2005, doi: 10.1038/nri1666.

[52] E. Vynnycky and P. E. M. Fine, 'Lifetime risks, incubation period, and serial interval of tuberculosis', *Am J Epidemiol*, vol. 152, no. 3, pp. 247–263, 2000, doi: 10.1093/aje/152.3.247.

[53] R. Dawkins and J. R. Krebs, 'Arms races between and within species', *Proc R Soc Lond B Biol Sci.*, vol. 205, no. 1161, pp. 489–511, 1979, doi: 10.1098/rspb.1979.0081.

[54] S. Gagneux, 'Host-pathogen coevolution in human tuberculosis', *Philosophical Transactions of the Royal Society B: Biological Sciences*, vol. 367, no. 1590, pp. 850–859, 2012, doi: 10.1098/rstb.2011.0316.

[55] J. G. Weg, 'Diagnostic standards of tuberculosis--revised', *JAMA*, vol. 235, no. 13, pp. 1329–1330, 1976, doi: 10.1001/jama.235.13.1329.

[56] E. R. Long and F. D. Hopkins, 'History of Diagnostic Standards and Classification of Tuberculosis of the National Tuberculosis Association', *Am Rev Tuberc.*, vol. 65, no. 4, pp. 494–504, 1952, doi: 10.1164/art.1952.65.4.494.

[57] S. Kiazyk and T. Ball, 'Latent tuberculosis infection: An overview', *Canada Communicable Disease Report*, vol. 43, no. 3/4, pp. 62–66, Mar. 2017, doi: 10.14745/ccdr.v43i34a01.

[58] L. Pirofski and A. Casadevall, 'The state of latency in microbial pathogenesis', *Journal of Clinical Investigation*, vol. 130, no. 9, pp. 4525–4531, Aug. 2020, doi: 10.1172/JCI136221.

[59] T. D. Bold and J. D. Ernst, 'Who Benefits from Granulomas, Mycobacteria or Host?', *Cell*, vol. 136, no. 7, pp. 17–19, 2009, doi: 10.1016/j.cell.2008.12.032.

[60] D. O. Adams, 'The Granulomatous Inflammatory Response', *American Journal of Pathology*, vol. 84, no. 1, pp. 164–191, 1976.

[61] J. G. Egen, A. G. Rothfuchs, C. G. Feng, N. Winter, A. Sher, and R. N. Germain, 'Macrophage and T Cell Dynamics during the Development and Disintegration of Mycobacterial Granulomas', *Immunity*, vol. 28, no. 2, pp. 271–284, 2008, doi: 10.1016/j.immuni.2007.12.010.

[62] R. J. North and A. A. Izzo, 'Granuloma formation in severe combined immunodeficient (SCID) mice in response to progressive BCG infection: Tendency not to form granulomas in the lung is associated with faster bacterial growth in this organ', *American Journal of Pathology*, vol. 142, no. 6, pp. 1959–1966, 1993.

[63] D. Smith, H. Hänsch, G. Bancroft, and S. Ehlers, 'T-cell-independent granuloma formation in response to Mycobacterium avium: Role of tumour necrosis factor-α and interferon-γ', *Immunology*, vol. 92, no. 4, pp. 413–421, 1997, doi: 10.1046/j.1365-2567.1997.00384.x.

[64] S. D. Lawn, S. T. Butera, and T. M. Shinnick, 'Tuberculosis unleashed: The impact of human immunodeficiency virus infection on the host granulomatous response to Mycobacterium tuberculosis', *Microbes Infect*, vol. 4, no. 6, pp. 635–646, 2002, doi: 10.1016/S1286-4579(02)01582-4.

[65] I. M. ; C. F. M. Orme, 'Protection Against Mycobacterium Tuberculosis Infection By Adoptive Immunotherapy Requirement for T Cell-deficient Recipients', *Jem*, vol. 158, no. July, pp. 74–83, 1983.

[66] J. M. Davis and L. Ramakrishnan, 'The Role of the Granuloma in Expansion and Dissemination of Early Tuberculous Infection', *Cell*, vol. 136, no. 1, pp. 37–49, 2009, doi: 10.1016/j.cell.2008.11.014.

[67] S. H. E. Kaufmann, 'How can immunology contributed to TB control', *Nat Rev Immunol*, vol. 1, no. October, pp. 20–30, 2001.

[68] P. L. Lin *et al.*, 'Quantitative comparison of active and latent tuberculosis in the cynomolgus macaque model', *Infect Immun*, vol. 77, no. 10, pp. 4631–4642, 2009, doi: 10.1128/IAI.00592-09.

[69] Lúcia Moreira-Teixeira, K. Mayer-Barber, A. Sher, and A. O'Garra, 'Type I interferons in tuberculosis: Foe and occasionally friend', *Journal of Experimental Medicine*, vol. 215, no. 5, pp. 1273–1285, 2018, doi: 10.1084/jem.20180325.

[70] D. X. Ji *et al.*, 'Type I interferon-driven susceptibility to Mycobacterium tuberculosis is mediated by interleukin-1 receptor antagonist IL-1Ra', *Nat Microbiol*, vol. 4, no. 12, pp. 2128–2135, 2019, doi: 10.1038/s41564-019-0578-3.Type.

[71] B. Patterson and R. Wood, 'Is cough really necessary for TB transmission?', *Tuberculosis*, vol. 117, no. January, pp. 31–35, 2019, doi: 10.1016/j.tube.2019.05.003.

[72] S. B. Cohen *et al.*, 'Alveolar Macrophages Provide an Early Mycobacterium tuberculosis Niche and Initiate Dissemination', *Cell Host Microbe*, vol. 24, no. 3, pp. 439-446.e4, 2018, doi: 10.1016/j.chom.2018.08.001.

[73] R. Simeone, L. Majlessi, J. Enninga, and R. Brosch, 'Perspectives on mycobacterial vacuole-to-cytosol translocation: the importance of cytosolic access', *Cell Microbiol*, vol. 18, no. 8, pp. 1070–1077, 2016, doi: 10.1111/cmi.12622.

[74] D. Houben *et al.*, 'ESX-1-mediated translocation to the cytosol controls virulence of mycobacteria', *Cell Microbiol*, vol. 14, no. 8, pp. 1287–1298, 2012, doi: 10.1111/j.1462-5822.2012.01799.x.

[75] D. G. Russell, 'The ins and outs of the Mycobacterium tuberculosis-containing vacuole', *Cell Microbiol*, vol. 18, no. 8, pp. 1065–1069, 2016, doi: 10.1111/cmi.12623.

[76] H. S. Khan *et al.*, 'Identification of scavenger receptor B1 as the airway microfold cell receptor for mycobacterium tuberculosis', *Elife*, vol. 9, pp. 1–20, 2020, doi: 10.7554/eLife.52551.

[77] M. B. Ryndak and S. Laal, 'Mycobacterium tuberculosis Primary Infection and Dissemination: A Critical Role for Alveolar Epithelial Cells', *Front Cell Infect Microbiol*, vol. 9, no. August, 2019, doi: 10.3389/fcimb.2019.00299.

[78] R. Domingo-Gonzalez, O. Prince, A. Cooper, and S. A. Khader, 'Cytokines and chemokines in Mycobacterium tuberculosis infection', *Tuberculosis and the Tubercle Bacillus: Second Edition*, pp. 33–72, 2017, doi: 10.1128/9781555819569.ch2.

[79] S. Ehlers and U. E. Schaible, 'The granuloma in tuberculosis: Dynamics of a host-pathogen collusion', 2012. doi: 10.3389/fimmu.2012.00411.

[80] K. Law, M. Weiden, T. Harkin, K. Tchou-Wong, C. Chi, and W. N. Rom, 'Increased release of interleukin-1 beta, interleukin-6, and tumor necrosis factor-alpha by bronchoalveolar cells lavaged from involved sites in pulmonary tuberculosis.', *Am J Respir Crit Care Med*, vol. 153, no. 2, pp. 799–804, Feb. 1996, doi: 10.1164/ajrccm.153.2.8564135.

[81] S. W. Chensue, 'Chemokines in innate and adaptive granuloma formation', *Front Immunol*, vol. 4, no. FRB, pp. 1–9, 2013, doi: 10.3389/fimmu.2013.00043.

[82] J. M. Davis, H. Clay, J. L. Lewis, N. Ghori, P. Herbomel, and L. Ramakrishnan, 'Real-time visualization of Mycobacterium-macrophage interactions leading to initiation of granuloma formation in zebrafish embryos', *Immunity*, vol. 17, no. 6, pp. 693–702, 2002, doi: 10.1016/S1074-7613(02)00475-2.

[83] H. C. R. Mansch, D. A. Smith, M. E. A. Mielke, H. Hahn, G. J. Bancroft, and S. Ehlers, 'Mechanisms of granuloma formation in murine Mycobacterium avium infection: The contribution of CD4+ T cells', *Int Immunol*, vol. 8, no. 8, pp. 1299–1310, 1996, doi: 10.1093/intimm/8.8.1299.

[84] A. J. Wolf *et al.*, 'Initiation of the adaptive immune response to Mycobacterium tuberculosis depends on antigen production in the local lymph node, not the lungs', *Journal of Experimental Medicine*, vol. 205, no. 1, pp. 105–115, 2008, doi: 10.1084/jem.20071367.

[85] M. Samstein, H. A. Schreiber, I. M. Leiner, B. Sušac, M. S. Glickman, and E. G. Pamer, 'Essential yet limited role for CCR2+ inflammatory monocytes during Mycobacterium tuberculosis-specific T cell priming', *Elife*, vol. 2013, no. 2, pp. 1–10, 2013, doi: 10.7554/eLife.01086.

[86] A. Cooper, 'T cells in mycobacterial infection and disease', *Curr Opin Immunol.*, vol. 21, no. 4, pp. 378–384, 2009, doi: 10.1016/j.coi.2009.06.004.T.

[87] D. P. Maison, 'Tuberculosis pathophysiology and anti-VEGF intervention', *J Clin Tuberc Other Mycobact Dis*, vol. 27, no. January, p. 100300, 2022, doi: 10.1016/j.jctube.2022.100300.

[88] T. Ulrichs and S. H. E. Kaufmann, 'New insights into the function of granulomas in human tuberculosis', *Journal of Pathology*, vol. 208, no. 2, pp. 261–269, 2006, doi: 10.1002/path.1906.

[89] D. M. Tobin *et al.*, 'Host genotype-specific therapies can optimize the inflammatory response to mycobacterial infections', *Cell*, vol. 148, no. 3, pp. 434–446, 2012, doi: 10.1016/j.cell.2011.12.023.

[90] L. Bekker, S. Freeman, P. J. Murray, and B. Ryffel, 'Controls Intracellular Mycobacterial Growth by Both Inducible Nitric Oxide Synthase-Dependent and Inducible Nitric Oxide Synthase- Independent Pathways 1 ', 2001.

[91] S. Y. Eum *et al.*, 'Neutrophils are the predominant infected phagocytic cells in the airways of patients with active pulmonary TB', *Chest*, vol. 137, no. 1, pp. 122–128, 2010, doi: 10.1378/chest.09-0903.

[92] R. Gopal *et al.*, 'S100A8/A9 proteins mediate neutrophilic inflammation and lung pathology during tuberculosis', *Am J Respir Crit Care Med*, vol. 188, no. 9, pp. 1137–1146, 2013, doi: 10.1164/rccm.201304-0803OC.

[93] M. P. R. Berry *et al.*, 'An interferon-inducible neutrophil-driven blood transcriptional signature in human tuberculosis', *Nature*, vol. 466, no. 7309, pp. 973–977, 2010, doi: 10.1038/nature09247.

[94] T. Dallenga *et al.*, 'M. tuberculosis-Induced Necrosis of Infected Neutrophils Promotes Bacterial Growth Following Phagocytosis by Macrophages', *Cell Host Microbe*, vol. 22, no. 4, pp. 519-530.e3, 2017, doi: 10.1016/j.chom.2017.09.003.

[95] B. Corleis, D. Korbel, R. Wilson, J. Bylund, R. Chee, and U. E. Schaible, 'Escape of Mycobacterium tuberculosis from oxidative killing by neutrophils', *Cell Microbiol*, vol. 14, no. 7, pp. 1109–1121, 2012, doi: 10.1111/j.1462-5822.2012.01783.x.

[96] C. J. Martin *et al.*, 'Efferocytosis is an innate antibacterial mechanism', *Cell Host Microbe*, vol. 12, no. 3, pp. 289–300, 2012, doi: 10.1016/j.chom.2012.06.010.

[97] M. L. Hartman and H. Kornfeld, 'Interactions between naïve and infected macrophages reduce Mycobacterium tuberculosis viability', *PLoS One*, vol. 6, no. 11, 2011, doi: 10.1371/journal.pone.0027972.

[98] J. Lee, H. G. Remold, M. H. Ieong, and H. Kornfeld, ' Macrophage Apoptosis in Response to High Intracellular Burden of Mycobacterium tuberculosis Is Mediated by a Novel Caspase-Independent Pathway ', *The Journal of Immunology*, vol. 176, no. 7, pp. 4267–4274, 2006, doi: 10.4049/jimmunol.176.7.4267.

[99] G. Filio-Rodríguez *et al.*, 'In vivo induction of neutrophil extracellular traps by Mycobacterium tuberculosis in a Guinea pig model', *Innate Immun*, vol. 23, no. 7, pp. 625–637, 2017, doi: 10.1177/1753425917732406.

[100] T. Dallenga *et al.*, 'M. tuberculosis-Induced Necrosis of Infected Neutrophils Promotes Bacterial Growth Following Phagocytosis by Macrophages', *Cell Host Microbe*, vol. 22, no. 4, pp. 519-530.e3, 2017, doi: 10.1016/j.chom.2017.09.003.

[101] J. L. Flynn and J. Chan, 'Tuberculosis: latency and reactivation.', *Infect Immun*, vol. 69, no. 7, pp. 4195–201, Jul. 2001, doi: 10.1128/IAI.69.7.4195-4201.2001.

[102] J. Chan and J. Flynn, 'The immunological aspects of latency in tuberculosis', *Clinical Immunology*, vol. 110, no. 1, pp. 2–12, Jan. 2004, doi: 10.1016/S1521-6616(03)00210-9.

[103] S. Upadhyay, E. Mittal, and J. A. Philips, 'Tuberculosis and the art of macrophage manipulation', *Pathog Dis*, vol. 76, no. 4, pp. 1–12, 2018, doi: 10.1093/femspd/fty037.

[104] B. Y. J. A. Armstrong and A. P. D. A. Hart, 'Response of cultured macrophages to Mycobacterium tuberculosis, With observations on fusion of lysosomes with phagosomes', *J Exp Med*, vol. 134, no. 3, pp. 713–740, 1971.

[105] J. Augenstreich and V. Briken, 'Host Cell Targets of Released Lipid and Secreted Protein Effectors of Mycobacterium tuberculosis', *Front Cell Infect Microbiol*, vol. 10, no. October, 2020, doi: 10.3389/fcimb.2020.595029.

[106] N. C. Howard and S. A. Khader, 'Immunometabolism during Mycobacterium tuberculosis Infection', *Trends Microbiol*, vol. 28, no. 10, pp. 832–850, 2020, doi: 10.1016/j.tim.2020.04.010.

[107] A. Khadela, V. P. Chavda, H. Postwala, Y. Shah, P. Mistry, and V. Apostolopoulos, 'Epigenetics in Tuberculosis: Immunomodulation of Host Immune Response', *Vaccines (Basel)*, vol. 10, no. 10, pp. 1–19, 2022, doi: 10.3390/vaccines10101740.

[108] T. Laskay, G. van Zandbergen, and W. Solbach, 'Neutrophil granulocytes as host cells and transport vehicles for intracellular pathogens: Apoptosis as infection-promoting factor', *Immunobiology*, vol. 213, no. 3–4, pp. 183–191, 2008, doi: 10.1016/j.imbio.2007.11.010.

[109] J. S. Savill, A. H. Wyllie, J. E. Henson, M. J. Walport, P. M. Henson, and C. Haslett, 'Macrophage phagocytosis of aging neutrophils in inflammation. Programmed cell death in the neutrophil leads to its recognition by macrophages', *Journal of Clinical Investigation*, vol. 83, no. 3, pp. 865–875, 1989, doi: 10.1172/JCI113970.

[110] U. Koedel *et al.*, 'Apoptosis is essential for neutrophil functional shutdown and determines tissue damage in experimental pneumococcal meningitis', *PLoS Pathog*, vol. 5, no. 5, 2009, doi: 10.1371/journal.ppat.1000461.

[111] R. van Furth and Z. A. Cohn, 'The origin and kinetics of mononuclear phagocytes.', *J Exp Med*, vol. 128, no. 3, pp. 415–435, 1968, doi: 10.1084/jem.128.3.415.

[112] C. M. McClean and D. M. Tobin, 'Macrophage form, function, and phenotype in mycobacterial infection: Lessons from tuberculosis and other diseases', *Pathog Dis*, vol. 74, no. 7, pp. 1–15, 2016, doi: 10.1093/femspd/ftw068.

[113] T. Tsuda, A. M. Danneberg, M. Ando, H. Abbey, and A. R. Corrin, 'Mononuclear Cell Turnover in Chronic Inflammation', *American Journal of Pathology*, vol. 83, no. 2, pp. 255–268, 1976.

[114] E. L. Soucie *et al.*, 'Lineage-specific enhancers activate self-renewal genes in macrophages and embryonic stem cells', *Science (1979)*, vol. 351, no. 6274, 2016, doi: 10.1126/science.aad5510.

[115] F. Ahmad *et al.*, 'Macrophage: A Cell With Many Faces and Functions in Tuberculosis', *Front Immunol*, vol. 13, no. May, pp. 1–18, 2022, doi: 10.3389/fimmu.2022.747799.

[116] M. Ogawa, 'Differentiation and Proliferation of Hematopoietic Stem Cells', *Blood*, vol. 81, no. 11, pp. 2844–2853, Jun. 1993, doi: 10.1182/BLOOD.V81.11.2844.2844.

[117] E. A. Mcculloch and J. E. Till, 'Perspectives on the properties of stem cells', *Nat Med*, vol. 11, pp. 1026–1028, 2005, doi: 10.1038/nm1005-1026.

[118] S. Abramson, R. G. Miller, and R. A. Phillips, 'The identification in adult bone marrow of pluripotent and restricted stem cells of the myeloid and lymphoid systems', *J Exp Med*, vol. 145, no. 6, pp. 1567–1579, 1977.

[119] B. Capel, R. G. Hawley, and B. Mintz, 'Long-and Short-Lived Murine Hematopoietic Stem Cell Clones Individually Identified With Retroviral Integration Markers', 1990.

[120] C. T. Jordan and I. R. Lemischka, 'Clonal and systemic analysis of long-term hematopoiesis in the mouse', *Genes Dev*, vol. 4, no. 2, pp. 220–32, 1990, doi: 10.1101/gad.4.2.220.

[121] G. Keller, C. Paige, E. Gilboa, and E. F. Wagner, 'Expression of a foreign gene in myeloid and lymphoid cells derived from multipotent haematopoietic precursors', *Nature*, vol. 318, no. 6042, pp. 149–54, 1985, doi: 10.1038/318149a0.

[122] A. Ivanovs, S. Rybtsov, L. Welch, R. A. Anderson, M. L. Turner, and A. Medvinsky, 'Highly potent human hematopoietic stem cells first emerge in the intraembryonic aorta-gonad-mesonephros region', *Journal of Experimental Medicine*, vol. 208, no. 12, pp. 2417–2427, Nov. 2011, doi: 10.1084/jem.20111688.

[123] A. Ivanovs, S. Rybtsov, R. A. Anderson, M. L. Turner, and A. Medvinsky, 'Identification of the niche and phenotype of the first human hematopoietic stem cells', *Stem Cell Reports*, vol. 2, no. 4, pp. 449–456, Apr. 2014, doi: 10.1016/j.stemcr.2014.02.004.

[124] A. Medvinsky, S. Rybtsov, and S. Taoudi, 'Embryonic origin of the adult hematopoietic system: Advances and questions', Mar. 2011. doi: 10.1242/dev.040998.

[125] S. J. Szilvassy, R. K. Humphries, P. M. Lansdorp, A. C. Eaves*tt$, and C. J. Eaves, 'Quantitative assay for totipotent reconstituting hematopoietic stem cells by a competitive repopulation strategy', 1990. doi: 10.1073/pnas.87.22.8736.

[126] D. E. Harrison, 'Competitive Repopulation: A New Assay for Long-Term Stem Cell Functional Capacity', 1980.

[127] D. Lucas, 'Structural organization of the bone marrow and its role in hematopoiesis', Jan. 01, 2021, *Lippincott Williams and Wilkins*. doi: 10.1097/MOH.0000000000000621.

[128] K. D. Kokkaliaris *et al.*, 'Adult blood stem cell localization reflects the abundance of reported bone marrow niche cell types and their combinations', *Blood*, vol. 136, no. 20, pp. 2296–2307, 2020, doi: 10.1182/blood.2020006574.

[129] M. May, A. Slaughter, and D. Lucas, 'Dynamic Regulation of Hematopoietic Stem Cells by Bone Marrow Niches', Sep. 01, 2018, *Springer International Publishing*. doi: 10.1007/s40778-018-0132-x.

[130] C. Nombela-Arrieta and M. G. Manz, 'Quantification and three-dimensional microanatomical organization of the bone marrow', *Blood Adv*, vol. 1, no. 6, pp. 407–416, Feb. 2017, doi: 10.1182/bloodadvances.2016003194.

[131] S. J. Morrison and D. T. Scadden, 'The bone marrow niche for haematopoietic stem cells', 2014. doi: 10.1038/nature12984.

[132] C. Nombela-Arrieta *et al.*, 'Quantitative imaging of haematopoietic stem and progenitor cell localization and hypoxic status in the bone marrow microenvironment', *Nat Cell Biol*, vol. 15, no. 5, pp. 533–543, May 2013, doi: 10.1038/ncb2730.

[133] A. Wilson *et al.*, 'Hematopoietic Stem Cells Reversibly Switch from Dormancy to Self-Renewal during Homeostasis and Repair', *Cell*, vol. 135, no. 6, pp. 1118–1129, Dec. 2008, doi: 10.1016/j.cell.2008.10.048.

[134] J. Sun *et al.*, 'Clonal dynamics of native haematopoiesis', *Nature*, vol. 514, no. 7522, pp. 322–327, Oct. 2014, doi: 10.1038/nature13824.

[135] K. B. Schoedel *et al.*, 'The bulk of the hematopoietic stem cell population is dispensable for murine steady-state and stress hematopoiesis', *Blood*, vol. 128, no. 19, pp. 2285–2296, Nov. 2016, doi: 10.1182/blood-2016-03-706010.

[136] H. Takizawa, S. Boettcher, and M. G. Manz, 'Demand-adapted regulation of early hematopoiesis in infection and inflammation', *Blood*, vol. 119, no. 13, pp. 2991–3002, Mar. 2012, doi: 10.1182/blood-2011-12-380113.

[137] M. Wu *et al.*, 'Imaging Hematopoietic Precursor Division in Real Time', *Cell Stem Cell*, vol. 1, no. 5, pp. 541–554, 2006, doi: 10.1016/j.stem.2007.08.009.

[138] M. J. Kiel, Ö. H. Yilmaz, T. Iwashita, O. H. Yilmaz, C. Terhorst, and S. J. Morrison, 'SLAM family receptors distinguish hematopoietic stem and progenitor cells and reveal endothelial niches for stem cells', *Cell*, vol. 121, no. 7, pp. 1109–1121, Jul. 2005, doi: 10.1016/j.cell.2005.05.026.

[139] R. G. Hawley, A. Ramezani, and T. S. Hawley, 'Hematopoietic Stem Cells', *Methods Enzymol*, vol. 419, pp. 149–179, 2006, doi: 10.1016/S0076-6879(06)19007-2.

[140] C. Dussiau *et al.*, 'Hematopoietic differentiation is characterized by a transient peak of entropy at a single-cell level', *BMC Biol*, vol. 20, no. 1, p. 60, Mar. 2022, doi: 10.1186/s12915-022-01264-9.

[141] L. Velten *et al.*, 'Human haematopoietic stem cell lineage commitment is a continuous process', *Nat Cell Biol*, vol. 19, no. 4, pp. 271–281, Apr. 2017, doi: 10.1038/ncb3493.

[142] G. A. Challen, E. M. Pietras, N. C. Wallscheid, and R. A. J. Signer, 'Simplified murine multipotent progenitor isolation scheme: Establishing a consensus approach for multipotent progenitor identification', *Exp Hematol*, vol. 104, pp. 55–63, Dec. 2021, doi: 10.1016/j.exphem.2021.09.007.

[143] E. I. Athanasiadis, J. G. Botthof, H. Andres, L. Ferreira, P. Lio, and A. Cvejic, 'Single-cell RNA-sequencing uncovers transcriptional states and fate decisions in haematopoiesis', *Nat Commun*, vol. 8, no. 1, Dec. 2017, doi: 10.1038/s41467-017-02305-6.

[144] C. P. Rodrigues, M. Shvedunova, and A. Akhtar, 'Epigenetic Regulators as the Gatekeepers of Hematopoiesis', Feb. 01, 2021, *Elsevier Ltd*. doi: 10.1016/j.tig.2020.09.015.

[145] M. Kondo *et al.*, 'Cell-fate conversion of lymphoid-committed progenitors by instructive actions of cytokines', *Nature*, vol. 407, no. 6802, pp. 383–386, Sep. 2000, doi: 10.1038/35030112.

[146] L. A. Liggett and V. G. Sankaran, 'Unraveling Hematopoiesis through the Lens of Genomics', *Cell*, vol. 182, no. 6, pp. 1384–1400, Sep. 2020, doi: 10.1016/j.cell.2020.08.030.

[147] M. G. Manz and S. Boettcher, 'Emergency granulopoiesis', *Nat Rev Immunol*, vol. 14, no. 5, pp. 302–314, May 2014, doi: 10.1038/nri3660.

[148] S. Pokkali and S. D. Das, 'Augmented chemokine levels and chemokine receptor expression on immune cells during pulmonary tuberculosis', *Hum Immunol*, vol. 70, no. 2, pp. 110–115, Feb. 2009, doi: 10.1016/j.humimm.2008.11.003.

[149] R. Lombard *et al.*, 'IL-17RA in Non-Hematopoietic Cells Controls CXCL-1 and 5 Critical to Recruit Neutrophils to the Lung of Mycobacteria-Infected Mice during the Adaptive Immune Response', *PLoS One*, vol. 11, no. 2, p. e0149455, Feb. 2016, doi: 10.1371/journal.pone.0149455.

[150] C. B. Johnson, J. Zhang, and D. Lucas, 'The Role of the Bone Marrow Microenvironment in the Response to Infection', *Front Immunol*, vol. 11, Nov. 2020, doi: 10.3389/fimmu.2020.585402.

[151] J. J. Mistry *et al.*, 'Free fatty-acid transport via CD36 drives β-oxidation-mediated hematopoietic stem cell response to infection', *Nat Commun*, vol. 12, no. 1, Dec. 2021, doi: 10.1038/s41467-021-27460-9.

[152] M. G. Netea *et al.*, 'Defining trained immunity and its role in health and disease', *Nat Rev Immunol*, vol. 20, no. 6, pp. 375–388, Jun. 2020, doi: 10.1038/s41577-020-0285-6.

[153] M. T. Baldridge, K. Y. King, N. C. Boles, D. C. Weksberg, and M. A. Goodell, 'Quiescent haematopoietic stem cells are activated by IFN-γ in response to chronic infection', *Nature*, vol. 465, no. 7299, pp. 793–797, Jun. 2010, doi: 10.1038/nature09135.

[154] T. P. Zanto, K. Hennigan, M. Östberg, W. C. Clapp, and A. Gazzaley, 'Predictive knowledge of stimulus relevance does not influence top-down suppression of irrelevant information in older adults', *Cortex*, vol. 46, no. 4, pp. 564–574, Apr. 2010, doi: 10.1016/j.cortex.2009.08.003.

[155] N. Mossadegh-Keller *et al.*, 'M-CSF instructs myeloid lineage fate in single haematopoietic stem cells', *Nature*, vol. 497, no. 7448, pp. 239–243, May 2013, doi: 10.1038/nature12026.

[156] E. M. Pietras *et al.*, 'Chronic interleukin-1 exposure drives haematopoietic stem cells towards precocious myeloid differentiation at the expense of self-renewal', *Nat Cell Biol*, vol. 18, no. 6, pp. 607–618, Jun. 2016, doi: 10.1038/ncb3346.

[157] M. A. G. Essers *et al.*, 'IFNα activates dormant haematopoietic stem cells in vivo', *Nature*, vol. 458, no. 7240, pp. 904–908, Apr. 2009, doi: 10.1038/nature07815.

[158] N. Khan *et al.*, 'M. tuberculosis Reprograms Hematopoietic Stem Cells to Limit Myelopoiesis and Impair Trained Immunity', *Cell*, vol. 183, no. 3, pp. 752-770.e22, Oct. 2020, doi: 10.1016/j.cell.2020.09.062.

[159] R. A. Tripp, D. J. Topham, S. R. Watson, and P. C. Doherty, 'Bone marrow can function as a lymphoid organ during a primary immune response under conditions of disrupted lymphocyte trafficking.', *J Immunol*, vol. 158, no. 8, pp. 3716–20, 1997.

[160] M. Feuerer *et al.*, 'Bone marrow as a priming site for T-cell responses to blood-borne antigen', *Nat Med*, vol. 9, no. 9, pp. 1151–1157, 2003, doi: 10.1038/nm914.

[161] M. Feuerer *et al.*, 'Bone marrow microenvironment facilitating dendritic cell: CD4 T cell interactions and maintenance of CD4 memory', *Int J Oncol*, vol. 25, no. 4, pp. 867–876, 2004.

[162] D. Duffy *et al.*, 'Neutrophils Transport Antigen from the Dermis to the Bone Marrow, Initiating a Source of Memory CD8+ T Cells', *Immunity*, vol. 37, no. 5, pp. 917–929, 2012, doi: 10.1016/j.immuni.2012.07.015.

[163] L. L. Cavanagh *et al.*, 'Activation of bone-resident memory T cells by circulating, antigen-bearing dendritic cells', *Nat Immunol.*, vol. 6, no. 10, pp. 1029–1037, 2005, doi: 10.1371/journal.pone.0178059.

[164] I. Milo *et al.*, 'Dynamic imaging reveals promiscuous crosspresentation of blood-borne antigens to naïve CD8+ T cells in the bone marrow', *Blood*, vol. 122, no. 2, pp. 193–208, 2013, doi: 10.1182/blood-2012-01-401265.

[165] J. L. Zhao *et al.*, 'Conversion of Danger Signals into Cytokine Signals by Hematopoietic Stem and Progenitor Cells for Regulation of Stress-Induced Hematopoiesis', *Cell Stem Cell*, vol. 14, no. 4, pp. 445–459, Apr. 2014, doi: 10.1016/j.stem.2014.01.007.

[166] A. G. Zaretsky, J. B. Engiles, and C. A. Hunter, 'Infection-Induced Changes in Hematopoiesis', *The Journal of Immunology*, vol. 192, no. 1, pp. 27–33, Jan. 2014, doi: 10.4049/jimmunol.1302061.

[167] S. Sreevatsan *et al.*, 'Restricted structural gene polymorphism in the Mycobacterium tuberculosis complex indicates evolutionarily recent global dissemination', *Proc Natl Acad Sci U S A*, vol. 94, no. 18, pp. 9869–9874, 1997, doi: 10.1073/pnas.94.18.9869.

[168] Lúcia Moreira-Teixeira, K. Mayer-Barber, A. Sher, and A. O'Garra, 'Type I interferons in tuberculosis: Foe and occasionally friend', May 01, 2018, *Rockefeller University Press*. doi: 10.1084/jem.20180325.

[169] E. Kaufmann *et al.*, 'BCG Educates Hematopoietic Stem Cells to Generate Protective Innate Immunity against Tuberculosis', *Cell*, vol. 172, no. 1–2, pp. 176-190.e19, Jan. 2018, doi: 10.1016/j.cell.2017.12.031.

[170] M. P. R. Berry *et al.*, 'An interferon-inducible neutrophil-driven blood transcriptional signature in human tuberculosis', *Nature*, vol. 466, no. 7309, pp. 973–977, Aug. 2010, doi: 10.1038/nature09247.

[171] A. M. Cooper, D. K. Dalton, T. A. Stewart, J. P. Griffin, D. G. Russell, and I. M. Orme, 'Disseminated Tuberculosis in Interferon 7 Gene-disrupted Mice', *J Exp Med*, vol. 178, no. 6, pp. 2243–7, 1993, doi: 10.1084/jem.178.6.2243.

[172] J. L. Flynn, J. Chan, K. J. Triebold, D. K. Dalton, T. A. Stewart, and B. R. Bloom, 'An Essential Role for Interferon 7 in Resistance to Mycobacterium tuberculosis Infection', *J Exp Med*, vol. 178, no. 6, pp. 2249–54, 1993, doi: 10.1084/jem.178.6.2249.

[173] D. I. Kotov *et al.*, 'Early cellular mechanisms of type I interferon-driven susceptibility to tuberculosis', *Cell*, vol. 186, no. 25, pp. 5536-5553.e22, Dec. 2023, doi: 10.1016/j.cell.2023.11.002.

[174] P. J. Cardona and J. Ruiz-Manzano, 'On the nature of Mycobacterium tuberculosis-latent bacilli', *European Respiratory Journal*, vol. 24, no. 6, pp. 1044–1051, Dec. 2004, doi: 10.1183/09031936.04.00072604.

[175] P. J. Cardona, 'A dynamic reinfection hypothesis of latent tuberculosis infection', Apr. 2009. doi: 10.1007/s15010-008-8087-y.

[176] R. L. Russo, F. L. Dulley, L. Suganuma, I. L. França, M. A. S. Yasuda, and S. F. Costa, 'Tuberculosis in hematopoietic stem cell transplant patients: Case report and review of the literature', *International Journal of Infectious Diseases*, vol. 14, no. SUPPL. 3, 2010, doi: 10.1016/j.ijid.2009.08.001.

[177] I. Kerridge, M. Ethell, M. Potter, and H. G. Prentice, 'Mycobacterium tuberculosis infection following allogeneic peripheral blood stem cell transplantation', Dec. 2003. doi: 10.1111/j.1445-5994.2003.00451.x.

[178] T. Kindler, C. Schindel, U. Brass, and T. Fischer, 'Case report Fatal sepsis due to Mycobacterium tuberculosis after allogeneic bone marrow transplantation', 2001. doi: 10.1038/sj.bmt.1702737.

[179] M. Aljurf *et al.*, 'Mycobacterium tuberculosis infection in allogeneic bone marrow transplantation patients', *Bone Marrow Transplant*, vol. 24, pp. 551–554, 1999, doi: 10.1038/sj.bmt.1701930.

[180] L. Dirkx *et al.*, 'Long-term hematopoietic stem cells as a parasite niche during treatment failure in visceral leishmaniasis', *Commun Biol*, vol. 5, no. 1, pp. 1–15, 2022, doi: 10.1038/s42003-022-03591-7.

[181] B. Das *et al.*, 'CD271+ bone marrow mesenchymal stem cells may provide a niche for dormant mycobacterium tuberculosis', *Sci Transl Med*, vol. 5, no. 170, Jan. 2013, doi: 10.1126/scitranslmed.3004912.

[182] G. Beamer, S. Major, B. Das, and A. Campos-Neto, 'Bone marrow mesenchymal stem cells provide an antibiotic-protective niche for persistent viable mycobacterium tuberculosis that survive antibiotic treatment', *American Journal of Pathology*, vol. 184, no. 12, pp. 3170–3175, 2014, doi: 10.1016/j.ajpath.2014.08.024.

[183] B. J. Farooqui, M. Khurshid, M. K. Ashfaq, and M. Ata Khan, 'Comparative yield of Salmonella typhi from blood and bone marrow cultures in patients with fever of unknown origin', *J Clin Pathol*, vol. 44, pp. 258–259, 1991.

[184] V. Singh *et al.*, 'Human mesenchymal stem cell based intracellular dormancy model of *Mycobacterium tuberculosis*', *Microbes and Infection*, vol. 22, no. 9, pp. 423–431, 2020, doi: 10.1016/j.micinf.2020.05.015.

[185] WHO, 'WHO consolidated guidelines on tuberculosis Module 4: Treatment Drug-susceptible tuberculosis treatment', 2022.

[186] B. Das *et al.*, 'CD271+ bone marrow mesenchymal stem cells may provide a niche for dormant mycobacterium tuberculosis', *Sci Transl Med*, vol. 5, no. 170, Jan. 2013, doi: 10.1126/scitranslmed.3004912.

[187] J. Tornack *et al.*, 'Human and mouse hematopoietic stem cells are a depot for dormant mycobacterium tuberculosis', *PLoS One*, vol. 12, no. 1, Jan. 2017, doi: 10.1371/journal.pone.0169119.

[188] S. T. Reece *et al.*, 'Mycobacterium tuberculosis -Infected Hematopoietic Stem and Progenitor Cells Unable to Express Inducible Nitric Oxide Synthase Propagate Tuberculosis in Mice', *Journal of Infectious Diseases*, vol. 217, no. 10, pp. 1667–1671, Apr. 2018, doi: 10.1093/infdis/jiy041.

[189] A. Kolb-Mäurer, M. Wilhelm, F. Weissinger, E. B. Bröcker, and W. Goebel, 'Interaction of human hematopoietic stem cells with bacterial pathogens', *Blood*, vol. 100, no. 10, pp. 3703–3709, Nov. 2002, doi: 10.1182/blood-2002-03-0898.

[190] C. Bussi and M. G. Gutierrez, 'Mycobacterium tuberculosis infection of host cells in space and time', *FEMS Microbiol Rev*, vol. 43, no. 4, pp. 341–361, Jul. 2019, doi: 10.1093/femsre/fuz006.

[191] P. Cossart and C. R. Roy, 'Manipulation of host membrane machinery by bacterial pathogens', *Curr Opin Cell Biol*, vol. 22, no. 4, pp. 547–554, Aug. 2010, doi: 10.1016/j.ceb.2010.05.006.

[192] J. R. Boiko and L. Borghesi, 'Hematopoiesis sculpted by pathogens: Toll-like receptors and inflammatory mediators directly activate stem cells', Jan. 2012. doi: 10.1016/j.cyto.2011.10.005.

[193] P. Hernández-Malmierca *et al.*, 'Antigen presentation safeguards the integrity of the hematopoietic stem cell pool', *Cell Stem Cell*, vol. 29, no. 5, pp. 760-775.e10, May 2022, doi: 10.1016/j.stem.2022.04.007.

[194] R. C. Hubrecht and E. Carter, '*The 3Rs and Humane Experimental Technique: Implementing Change*', *Animals (Basel)*, vol. 9, no. 10, pp. 754, Sep. 2019, doi: 10.3390/ani9100754

[195] W. M. S. Russel and R. K. Burch, *The Principles of Humane Experimental Technique*. London, UK: Methuen & Co Ltd, 1959.

[196] D. Morton and P. Griffiths, 'Guidelines on the recognition of pain, distress and discomfort in experimental animals and an hypothesis for assessment', *Veterinary Record*, vol. 116, no. 16, pp. 431–436, Apr. 1985, doi: 10.1136/vr.116.16.431.

[197] E. M. Pietras *et al.*, 'Functionally Distinct Subsets of Lineage-Biased Multipotent Progenitors Control Blood Production in Normal and Regenerative Conditions.', *Cell Stem Cell*, vol. 17, no. 1, pp. 35–46, Jul. 2015, doi: 10.1016/j.stem.2015.05.003.

[198] R. Majeti, C. Y. Park, and I. L. Weissman, 'Identification of a Hierarchy of Multipotent Hematopoietic Progenitors in Human Cord Blood', *Cell Stem Cell*, vol. 1, no. 6, pp. 635–645, Dec. 2007, doi: 10.1016/j.stem.2007.10.001.

[199] B. E. García-Pérez, R. Mondragón-Flores, and J. Luna-Herrera, 'Internalization of Mycobacterium tuberculosis by macropinocytosis in non-phagocytic cells', *Microb Pathog*, vol. 35, no. 2, pp. 49–55, Aug. 2003, doi: 10.1016/S0882-4010(03)00089-5.

[200] J. Pieters, 'Mycobacterium tuberculosis and the Macrophage: Maintaining a Balance', *Cell Host Microbe*, vol. 3, no. 6, pp. 399–407, Jun. 2008, doi: 10.1016/j.chom.2008.05.006.

[201] O. L. Mooren, B. J. Galletta, and J. A. Cooper, 'Roles for Actin Assembly in Endocytosis', *Annu Rev Biochem*, vol. 81, no. 1, pp. 661–686, Jul. 2012, doi: 10.1146/annurev-biochem-060910-094416.

[202] J. M. Kinchen and K. S. Ravichandran, 'Phagosome maturation: going through the acid test', *Nat Rev Mol Cell Biol*, vol. 9, no. 10, pp. 781–795, Oct. 2008, doi: 10.1038/nrm2515.

[203] P. Rougerie, V. Miskolci, and D. Cox, 'Generation of membrane structures during phagocytosis and chemotaxis of macrophages: role and regulation of the actin cytoskeleton', *Immunol Rev*, vol. 256, no. 1, pp. 222–239, Nov. 2013, doi: 10.1111/imr.12118.

[204] J. Turner and J. B. Torrelles, 'Mannose-capped lipoarabinomannan in Mycobacterium tuberculosis pathogenesis', *Pathog Dis*, vol. 76, no. 4, Jun. 2018, doi: 10.1093/femspd/fty026.

[205] T. E. Wileman, M. R. Lennartz, and P. D. Stahl, 'Identification of the macrophage mannose receptor as a 175-kDa membrane protein.', *Proceedings of the National Academy of Sciences*, vol. 83, no. 8, pp. 2501–2505, Apr. 1986, doi: 10.1073/pnas.83.8.2501.

[206] B. J. Appelmelk *et al.*, 'The mannose cap of mycobacterial lipoarabinomannan does not dominate the Mycobacterium–host interaction', *Cell Microbiol*, vol. 10, no. 4, pp. 930–944, Apr. 2008, doi: 10.1111/j.1462-5822.2007.01097.x.

[207] M. Koivusalo *et al.*, 'Amiloride inhibits macropinocytosis by lowering submembranous pH and preventing Rac1 and Cdc42 signaling', *Journal of Cell Biology*, vol. 188, no. 4, pp. 547–563, Feb. 2010, doi: 10.1083/jcb.200908086.

[208] H. Lin *et al.*, 'Identification of novel macropinocytosis inhibitors using a rational screen of Food and Drug Administration-approved drugs', *Br J Pharmacol*, vol. 175, no. 18, pp. 3640–3655, Sep. 2018, doi: 10.1111/bph.14429.

[209] J. Pizarro-Cerdá, M. Bonazzi, and P. Cossart, 'Clathrin-mediated endocytosis: What works for small, also works for big', *BioEssays*, vol. 32, no. 6, pp. 496–504, Jun. 2010, doi: 10.1002/bies.200900172.

[210] L. von Kleist *et al.*, 'Role of the Clathrin Terminal Domain in Regulating Coated Pit Dynamics Revealed by Small Molecule Inhibition', *Cell*, vol. 146, no. 3, pp. 471–484, Aug. 2011, doi: 10.1016/j.cell.2011.06.025.

[211] H. S. Khan *et al.*, 'Identification of scavenger receptor B1 as the airway microfold cell receptor for mycobacterium tuberculosis', *Elife*, vol. 9, Mar. 2020, doi: 10.7554/eLife.52551.

[212] A. Khan *et al.*, 'Mesenchymal stem cells internalize Mycobacterium tuberculosis through scavenger receptors and restrict bacterial growth through autophagy', *Sci Rep*, vol. 7, no. 1, p. 15010, Nov. 2017, doi: 10.1038/s41598-017-15290-z.

[213] O. Kuda *et al.*, 'Sulfo-N-succinimidyl Oleate (SSO) Inhibits Fatty Acid Uptake and Signaling for Intracellular Calcium via Binding CD36 Lysine 164', *Journal of Biological Chemistry*, vol. 288, no. 22, pp. 15547–15555, May 2013, doi: 10.1074/jbc.M113.473298.

[214] M. A. Behr *et al.*, 'Comparative Genomics of BCG Vaccines by Whole-Genome DNA Microarray', *Science (1979)*, vol. 284, no. 5419, pp. 1520–1523, May 1999, doi: 10.1126/science.284.5419.1520.

[215] M. R. Hughes *et al.*, 'A sticky wicket: Defining molecular functions for CD34 in hematopoietic cells', *Exp Hematol*, vol. 86, pp. 1–14, Jun. 2020, doi: 10.1016/j.exphem.2020.05.004.

[216] H. Zhang, H. Nguyen-Jackson, A. D. Panopoulos, H. S. Li, P. J. Murray, and S. S. Watowich, 'STAT3 controls myeloid progenitor growth during emergency granulopoiesis', *Blood*, vol. 116, no. 14, pp. 2462–2471, Oct. 2010, doi: 10.1182/blood-2009-12-259630.

[217] Q. Wu *et al.*, 'Resilient anatomy and local plasticity of naive and stress haematopoiesis', *Nature*, vol. 627, no. 8005, pp. 839–846, Mar. 2024, doi: 10.1038/s41586-024-07186-6.

[218] D. L. Barber, K. D. Mayer-Barber, C. G. Feng, A. H. Sharpe, and A. Sher, 'CD4 T Cells Promote Rather than Control Tuberculosis in the Absence of PD-1–Mediated Inhibition', *The Journal of Immunology*, vol. 186, no. 3, pp. 1598–1607, Feb. 2011, doi: 10.4049/jimmunol.1003304.

[219] S. Upadhyay, E. Mittal, and J. A. Philips, 'Tuberculosis and the art of macrophage manipulation', Jun. 01, 2018, *Oxford University Press*. doi: 10.1093/femspd/fty037.

[220] S. H. E. Kaufmann, A. Dorhoi, R. S. Hotchkiss, and R. Bartenschlager, 'Host-directed therapies for bacterial and viral infections', Jan. 01, 2018, *Nature Publishing Group*. doi: 10.1038/nrd.2017.162.

[221] B. E. García-Pérez *et al.*, 'Macropinocytosis is responsible for the uptake of pathogenic and non-pathogenic mycobacteria by B lymphocytes (Raji cells)', *BMC Microbiol*, vol. 12, no. 1, p. 246, Dec. 2012, doi: 10.1186/1471-2180-12-246.

[222] B. E. García-Pérez *et al.*, 'Innate response of human endothelial cells infected with mycobacteria', *Immunobiology*, vol. 216, no. 8, pp. 925–935, Aug. 2011, doi: 10.1016/j.imbio.2011.01.004.

[223] R. F. Collins, N. Touret, H. Kuwata, N. N. Tandon, S. Grinstein, and W. S. Trimble, 'Uptake of Oxidized Low Density Lipoprotein by CD36 Occurs by an Actin-dependent Pathway Distinct from Macropinocytosis', *Journal of Biological Chemistry*, vol. 284, no. 44, pp. 30288–30297, Oct. 2009, doi: 10.1074/jbc.M109.045104.

[224] S. Massberg *et al.*, 'Immunosurveillance by Hematopoietic Progenitor Cells Trafficking through Blood, Lymph, and Peripheral Tissues', *Cell*, vol. 131, no. 5, pp. 994–1008, Nov. 2007, doi: 10.1016/j.cell.2007.09.047.

[225] P. Quaranta *et al.*, 'Unveiling the Biological Role of Peripheral Blood Human Circulating Hematopoietic Stem and Progenitor Cells', *Blood*, vol. 140, no. Supplement 1, pp. 1977–1978, Nov. 2022, doi: 10.1182/blood-2022-163251.

[226] I. M. Mayer, A. Hoelbl-Kovacic, V. Sexl, and E. Doma, 'Isolation, Maintenance and Expansion of Adult Hematopoietic Stem/Progenitor Cells and Leukemic Stem Cells', *Cancers (Basel)*, vol. 14, no. 7, p. 1723, Mar. 2022, doi: 10.3390/cancers14071723.

[227] M. J. Kiel, O. H. Yilmaz, T. Iwashita, O. H. Yilmaz, C. Terhorst, and S. J. Morrison, 'SLAM family receptors distinguish hematopoietic stem and progenitor cells and reveal endothelial niches for stem cells.', *Cell*, vol. 121, no. 7, pp. 1109–21, Jul. 2005, doi: 10.1016/j.cell.2005.05.026.

[228] R. Majeti, C. Y. Park, and I. L. Weissman, 'Identification of a Hierarchy of Multipotent Hematopoietic Progenitors in Human Cord Blood.', *Blood*, vol. 110, no. 11, pp. 2237–2237, Nov. 2007, doi: 10.1182/blood.V110.11.2237.2237.

[229] F. Notta, S. Doulatov, E. Laurenti, A. Poeppl, I. Jurisica, and J. E. Dick, 'Isolation of Single Human Hematopoietic Stem Cells Capable of Long-Term Multilineage Engraftment', *Science (1979)*, vol. 333, no. 6039, pp. 218–221, Jul. 2011, doi: 10.1126/science.1201219.

[230] K. W. Christopherson, G. Hangoc, C. R. Mantel, and H. E. Broxmeyer, 'Modulation of Hematopoietic Stem Cell Homing and Engraftment by CD26', *Science (1979)*, vol. 305, no. 5686, pp. 1000–1003, Aug. 2004, doi: 10.1126/science.1097071.

[231] S. J. Loughran, S. Haas, A. C. Wilkinson, A. M. Klein, and M. Brand, 'Lineage commitment of hematopoietic stem cells and progenitors: insights from recent single cell and lineage tracing technologies', *Exp Hematol*, vol. 88, pp. 1–6, Aug. 2020, doi: 10.1016/j.exphem.2020.07.002.

[232] C. E. Muller-Sieburg, H. B. Sieburg, J. M. Bernitz, and G. Cattarossi, 'Stem cell heterogeneity: implications for aging and regenerative medicine', *Blood*, vol. 119, no. 17, pp. 3900–3907, Apr. 2012, doi: 10.1182/blood-2011-12-376749.

[233] H. Ema, Y. Morita, and T. Suda, 'Heterogeneity and hierarchy of hematopoietic stem cells', *Exp Hematol*, vol. 42, no. 2, pp. 74-82.e2, Feb. 2014, doi: 10.1016/j.exphem.2013.11.004.

[234] R. Jurecic, 'Hematopoietic Stem Cell Heterogeneity', 2019, pp. 195–211. doi: 10.1007/978-3-030-24108-7_10.

[235] R. Yamamoto *et al.*, 'Clonal Analysis Unveils Self-Renewing Lineage-Restricted Progenitors Generated Directly from Hematopoietic Stem Cells', *Cell*, vol. 154, no. 5, pp. 1112–1126, Aug. 2013, doi: 10.1016/j.cell.2013.08.007.

[236] K. Sumide *et al.*, 'A revised road map for the commitment of human cord blood CD34-negative hematopoietic stem cells', *Nat Commun*, vol. 9, no. 1, p. 2202, Jun. 2018, doi: 10.1038/s41467-018-04441-z.

[237] Y. Matsuoka *et al.*, 'Human cord blood-derived primitive CD34-negative hematopoietic stem cells (HSCs) are myeloid-biased long-term repopulating HSCs', *Blood Cancer J*, vol. 5, no. 3, pp. e290–e290, Mar. 2015, doi: 10.1038/bcj.2015.22.

[238] S. Haas, A. Trumpp, and M. D. Milsom, 'Causes and Consequences of Hematopoietic Stem Cell Heterogeneity', *Cell Stem Cell*, vol. 22, no. 5, pp. 627–638, May 2018, doi: 10.1016/j.stem.2018.04.003.

[239] S. Y. Eum *et al.*, 'Neutrophils are the predominant infected phagocytic cells in the airways of patients with active pulmonary TB', *Chest*, vol. 137, no. 1, pp. 122–128, Jan. 2010, doi: 10.1378/chest.09-0903.

[240] A. Wilson and A. Trumpp, 'Bone-marrow haematopoietic-stem-cell niches', *Nat Rev Immunol*, vol. 6, no. 2, pp. 93–106, Feb. 2006, doi: 10.1038/nri1779.

[241] P. Bianco, 'Bone and the hematopoietic niche: a tale of two stem cells', *Blood*, vol. 117, no. 20, pp. 5281–5288, May 2011, doi: 10.1182/blood-2011-01-315069.

[242] E. Lefrançais *et al.*, 'The lung is a site of platelet biogenesis and a reservoir for haematopoietic progenitors', *Nature*, vol. 544, no. 7648, pp. 105–109, Apr. 2017, doi: 10.1038/nature21706.

[243] E. Coppin *et al.*, 'Splenic hematopoietic stem cells display a pre-activated phenotype', *Immunol Cell Biol*, vol. 96, no. 7, pp. 772–784, Aug. 2018, doi: 10.1111/imcb.12035.

[244] P. Quaranta *et al.*, 'Circulating hematopoietic stem/progenitor cell subsets contribute to human hematopoietic homeostasis', *Blood*, vol. 143, no. 19, pp. 1937–1952, May 2024, doi: 10.1182/blood.2023022666.

[245] D. E. Wright, A. J. Wagers, A. P. Gulati, F. L. Johnson, and I. L. Weissman, 'Physiological Migration of Hematopoietic Stem and Progenitor Cells', *Science (1979)*, vol. 294, no. 5548, pp. 1933–1936, Nov. 2001, doi: 10.1126/science.1064081.

[246] J. L. Abkowitz, A. E. Robinson, S. Kale, M. W. Long, and J. Chen, 'Mobilization of hematopoietic stem cells during homeostasis and after cytokine exposure', *Blood*, vol. 102, no. 4, pp. 1249–1253, Aug. 2003, doi: 10.1182/blood-2003-01-0318.

[247] S. McKinney-Freeman and M. A. Goodell, 'Circulating hematopoietic stem cells do not efficiently home to bone marrow during homeostasis', *Exp Hematol*, vol. 32, no. 9, pp. 868–876, Sep. 2004, doi: 10.1016/j.exphem.2004.06.010.

[248] I. M. Mayer, A. Hoelbl-Kovacic, V. Sexl, and E. Doma, 'Isolation, Maintenance and Expansion of Adult Hematopoietic Stem/Progenitor Cells and Leukemic Stem Cells', *Cancers (Basel)*, vol. 14, no. 7, p. 1723, Mar. 2022, doi: 10.3390/cancers14071723.

[249] M. A. E. Ali *et al.*, 'Functional dissection of hematopoietic stem cell populations with a stemness-monitoring system based on NS-GFP transgene expression', *Sci Rep*, vol. 7, no. 1, p. 11442, Sep. 2017, doi: 10.1038/s41598-017-11909-3.

[250] T. Kimura *et al.*, 'Impaired stem cell function of CD34+ cells selected by two different immunomagnetic beads systems', *Leukemia*, vol. 18, no. 3, pp. 566–574, Mar. 2004, doi: 10.1038/sj.leu.2403211.

[251] C. R. Mantel *et al.*, 'Enhancing Hematopoietic Stem Cell Transplantation Efficacy by Mitigating Oxygen Shock', *Cell*, vol. 161, no. 7, pp. 1553–1565, Jun. 2015, doi: 10.1016/j.cell.2015.04.054.

[252] D. Mahamed *et al.*, 'Intracellular growth of Mycobacterium tuberculosis after macrophage cell death leads to serial killing of host cells', *Elife*, vol. 6, Jan. 2017, doi: 10.7554/eLife.22028.

[253] B. W. James, A. Williams, and P. D. Marsh, 'The physiology and pathogenicity of Mycobacterium tuberculosis grown under controlled conditions in a defined medium', *J Appl Microbiol*, vol. 88, no. 4, pp. 669–677, Apr. 2000, doi: 10.1046/j.1365-2672.2000.01020.x.

[254] I. Smith, 'Mycobacterium tuberculosis Pathogenesis and Molecular Determinants of Virulence', *Clin Microbiol Rev*, vol. 16, no. 3, pp. 463–496, Jul. 2003, doi: 10.1128/CMR.16.3.463-496.2003.

[255] T. Tran, A. J. Bonham, E. D. Chan, and J. R. Honda, 'A paucity of knowledge regarding nontuberculous mycobacterial lipids compared to the tubercle bacillus', *Tuberculosis*, vol. 115, pp. 96–107, Mar. 2019, doi: 10.1016/j.tube.2019.02.008.

[256] A. Kolb-Mäurer and W. Goebel, 'Susceptibility of hematopoietic stem cells to pathogens: role in virus/bacteria tropism and pathogenesis', *FE;MS Microbiology Letters*, vol. 226, no. 2, pp. 203-207, Sep. 2003, doi: 10.1016/S0378-1097(03)00643-8.

[257] P. C. Patel and R. E. Harrison, 'Membrane Ruffles Capture C3bi-opsonized Particles in Activated Macrophages', *Mol Biol Cell*, vol. 19, no. 11, pp. 4628–4639, Nov. 2008, doi: 10.1091/mbc.e08-02-0223.

[258] E. D. Goley and M. D. Welch, 'The ARP2/3 complex: an actin nucleator comes of age', *Nat Rev Mol Cell Biol*, vol. 7, no. 10, pp. 713–726, Oct. 2006, doi: 10.1038/nrm2026.

[259] K. Rottner, S. Lommel, J. Wehland, and T. E. Stradal, 'Pathogen-induced actin filament rearrangement in infectious diseases', *J Pathol*, vol. 204, no. 4, pp. 396–406, Nov. 2004, doi: 10.1002/path.1638.

[260] P. Dersch, 'A region of the Yersinia pseudotuberculosis invasin protein enhances integrin-mediated uptake into mammalian cells and promotes self-association', *EMBO J*, vol. 18, no. 5, pp. 1199–1213, Mar. 1999, doi: 10.1093/emboj/18.5.1199.

[261] J. Mengaud, H. Ohayon, P. Gounon, R.-M. Mège, and P. Cossart, 'E-Cadherin Is the Receptor for Internalin, a Surface Protein Required for Entry of L. monocytogenes into Epithelial Cells', *Cell*, vol. 84, no. 6, pp. 923–932, Mar. 1996, doi: 10.1016/S0092-8674(00)81070-3.

[262] P. Cossart and P. J. Sansonetti, 'Bacterial Invasion: The Paradigms of Enteroinvasive Pathogens', *Science (1979)*, vol. 304, no. 5668, pp. 242–248, Apr. 2004, doi: 10.1126/science.1090124.

[263] L. E. Bermudez and F. J. Sangari, 'Cellular and molecular mechanisms of internalization of mycobacteria by host cells', *Microbes Infect*, vol. 3, no. 1, pp. 37–42, Jan. 2001, doi: 10.1016/S1286-4579(00)01355-1.

[264] S. Kumari, S. MG, and S. Mayor, 'Endocytosis unplugged: multiple ways to enter the cell', *Cell Res*, vol. 20, no. 3, pp. 256–275, Mar. 2010, doi: 10.1038/cr.2010.19.

[265] G. Schäfer, M. Jacobs, R. J. Wilkinson, and G. D. Brown, 'Non-Opsonic Recognition of Mycobacterium tuberculosis by Phagocytes', *J Innate Immun*, vol. 1, no. 3, pp. 231–243, 2009, doi: 10.1159/000173703.

[266] D. Acharya, X. R. (Lisa) Li, R. E.-S. Heineman, and R. E. Harrison, 'Complement Receptor-Mediated Phagocytosis Induces Proinflammatory Cytokine Production in Murine Macrophages', *Front Immunol*, vol. 10, Jan. 2020, doi: 10.3389/fimmu.2019.03049.

[267] L. S. Schlesinger, S. R. Hull, and T. M. Kaufman, 'Binding of the terminal mannosyl units of lipoarabinomannan from a virulent strain of Mycobacterium tuberculosis to human macrophages.', *J Immunol*, vol. 152, no. 8, pp. 4070–9, Apr. 1994.

[268] J. B. Torrelles, A. K. Azad, and L. S. Schlesinger, 'Fine Discrimination in the Recognition of Individual Species of Phosphatidyl- *myo* -Inositol Mannosides from *Mycobacterium tuberculosis* by C-Type Lectin Pattern Recognition Receptors', *The Journal of Immunology*, vol. 177, no. 3, pp. 1805–1816, Aug. 2006, doi: 10.4049/jimmunol.177.3.1805.

[269] G. Lugo-Villarino, D. Hudrisier, A. Tanne, and O. Neyrolles, 'C-type lectins with a sweet spot for Mycobacterium tuberculosis', *Eur J Microbiol Immunol (Bp)*, vol. 1, no. 1, pp. 25–40, Mar. 2011, doi: 10.1556/EuJMI.1.2011.1.6.

[270] L. A. Allen and A. Aderem, 'Molecular definition of distinct cytoskeletal structures involved in complement- and Fc receptor-mediated phagocytosis in macrophages.', *J Exp Med*, vol. 184, no. 2, pp. 627–637, Aug. 1996, doi: 10.1084/jem.184.2.627.

[271] E. Caron and A. Hall, 'Identification of Two Distinct Mechanisms of Phagocytosis Controlled by Different Rho GTPases', *Science (1979)*, vol. 282, no. 5394, pp. 1717–1721, Nov. 1998, doi: 10.1126/science.282.5394.1717.

[272] S. Zimmerli, S. Edwards, and J. D. Ernst, 'Selective receptor blockade during phagocytosis does not alter the survival and growth of Mycobacterium tuberculosis in human macrophages.', *Am J Respir Cell Mol Biol*, vol. 15, no. 6, pp. 760–770, Dec. 1996, doi: 10.1165/ajrcmb.15.6.8969271.

[273] R. R. Kay, 'Macropinocytosis: Biology and mechanisms', *Cells & Development*, vol. 168, p. 203713, Dec. 2021, doi: 10.1016/j.cdev.2021.203713.

[274] S. Kanno *et al.*, 'Scavenger receptor MARCO contributes to cellular internalization of exosomes by dynamin-dependent endocytosis and macropinocytosis', *Sci Rep*, vol. 10, no. 1, p. 21795, Dec. 2020, doi: 10.1038/s41598-020-78464-2.

[275] S. Dharmawardhane, A. Schürmann, M. A. Sells, J. Chernoff, S. L. Schmid, and G. M. Bokoch, 'Regulation of Macropinocytosis by p21-activated Kinase-1', *Mol Biol Cell*, vol. 11, no. 10, pp. 3341–3352, Oct. 2000, doi: 10.1091/mbc.11.10.3341.

[276] R. C. Orchard and N. M. Alto, 'Mimicking GEFs: a common theme for bacterial pathogens', *Cell Microbiol*, vol. 14, no. 1, pp. 10–18, Jan. 2012, doi: 10.1111/j.1462-5822.2011.01703.x.

[277] J. Augenstreich and V. Briken, 'Host Cell Targets of Released Lipid and Secreted Protein Effectors of Mycobacterium tuberculosis', Oct. 23, 2020, *Frontiers Media S.A.* doi: 10.3389/fcimb.2020.595029.

[278] J. M. Albright, M. J. Sydor, J. Shannahan, C. R. Ferreira, and A. Holian, 'Imipramine Treatment Alters Sphingomyelin, Cholesterol, and Glycerophospholipid Metabolism in Isolated Macrophage Lysosomes', *Biomolecules*, vol. 13, no. 12, p. 1732, Dec. 2023, doi: 10.3390/biom13121732.

[279] T. Kirchhausen, D. Owen, and S. C. Harrison, 'Molecular Structure, Function, and Dynamics of Clathrin-Mediated Membrane Traffic', *Cold Spring Harb Perspect Biol*, vol. 6, no. 5, pp. a016725–a016725, May 2014, doi: 10.1101/cshperspect.a016725.

[280] K. L. Prichard, N. S. O'Brien, S. R. Murcia, J. R. Baker, and A. McCluskey, 'Role of Clathrin and Dynamin in Clathrin Mediated Endocytosis/Synaptic Vesicle Recycling and Implications in Neurological Diseases', *Front Cell Neurosci*, vol. 15, Jan. 2022, doi: 10.3389/fncel.2021.754110.

[281] S. M. Ferguson and P. De Camilli, 'Dynamin, a membrane-remodelling GTPase', *Nat Rev Mol Cell Biol*, vol. 13, no. 2, pp. 75–88, Feb. 2012, doi: 10.1038/nrm3266.

[282] A. E. Y. Engqvist-Goldstein, R. A. Warren, M. M. Kessels, J. H. Keen, J. Heuser, and D. G. Drubin, 'The actin-binding protein Hip1R associates with clathrin during early stages of endocytosis and promotes clathrin assembly in vitro', *J Cell Biol*, vol. 154, no. 6, pp. 1209–1224, Sep. 2001, doi: 10.1083/jcb.200106089.

[283] T. Dallenga *et al.*, 'M. tuberculosis-Induced Necrosis of Infected Neutrophils Promotes Bacterial Growth Following Phagocytosis by Macrophages', *Cell Host Microbe*, vol. 22, no. 4, pp. 519-530.e3, Oct. 2017, doi: 10.1016/j.chom.2017.09.003.

[284] A. Alquraini and J. El Khoury, 'Scavenger receptors', *Current Biology*, vol. 30, no. 14, pp. R790–R795, Jul. 2020, doi: 10.1016/j.cub.2020.05.051.

[285] J. Wang, H. Cao, H. Yang, N. Wang, Y. Weng, and H. Luo, 'The function of CD36 in Mycobacterium tuberculosis infection', *Front Immunol*, vol. 15, May 2024, doi: 10.3389/fimmu.2024.1413947.

[286] Y. Chen, J. Zhang, W. Cui, and R. L. Silverstein, 'CD36, a signaling receptor and fatty acid transporter that regulates immune cell metabolism and fate', *Journal of Experimental Medicine*, vol. 219, no. 6, Jun. 2022, doi: 10.1084/jem.20211314.

[287] M. Febbraio, D. P. Hajjar, and R. L. Silverstein, 'CD36: a class B scavenger receptor involved in angiogenesis, atherosclerosis, inflammation, and lipid metabolism', *Journal of Clinical Investigation*, vol. 108, no. 6, pp. 785–791, Sep. 2001, doi: 10.1172/JCI14006.

[288] I. N. Baranova *et al.*, 'Role of Human CD36 in Bacterial Recognition, Phagocytosis, and Pathogen-Induced JNK-Mediated Signaling', *The Journal of Immunology*, vol. 181, no. 10, pp. 7147–7156, Nov. 2008, doi: 10.4049/jimmunol.181.10.7147.

[289] M. Chen, Y.-K. Yang, T. J. Loux, K. E. Georgeson, and C. M. Harmon, 'The role of hyperglycemia in FAT/CD36 expression and function', *Pediatr Surg Int*, vol. 22, no. 8, pp. 647–654, Aug. 2006, doi: 10.1007/s00383-006-1704-x.

[290] W. Wang, Z. Yan, J. Hu, W.-J. Shen, S. Azhar, and F. B. Kraemer, 'Scavenger receptor class B, type 1 facilitates cellular fatty acid uptake', *Biochimica et Biophysica Acta (BBA) - Molecular and Cell Biology of Lipids*, vol. 1865, no. 2, p. 158554, Feb. 2020, doi: 10.1016/j.bbalip.2019.158554.

[291] O. Neyrolles *et al.*, 'Is Adipose Tissue a Place for Mycobacterium tuberculosis Persistence?', *PLoS One*, vol. 1, no. 1, p. e43, Dec. 2006, doi: 10.1371/journal.pone.0000043.

[292] K. Zhang *et al.*, 'Non-professional efferocytosis of Salmonella-infected intestinal epithelial cells in the neonatal host.', *J Exp Med*, vol. 221, no. 3, Mar. 2024, doi: 10.1084/jem.20231237.

[293] L. M. Stuart *et al.*, 'Response to *Staphylococcus aureus* requires CD36-mediated phagocytosis triggered by the COOH-terminal cytoplasmic domain', *J Cell Biol*, vol. 170, no. 3, pp. 477–485, Aug. 2005, doi: 10.1083/jcb.200501113.

[294] J.-W. Hao *et al.*, 'CD36 facilitates fatty acid uptake by dynamic palmitoylation-regulated endocytosis', *Nat Commun*, vol. 11, no. 1, p. 4765, Sep. 2020, doi: 10.1038/s41467-020-18565-8.

[295] N. Tao, S. J. Wagner, and D. M. Lublin, 'CD36 Is Palmitoylated on Both N- and C-terminal Cytoplasmic Tails', *Journal of Biological Chemistry*, vol. 271, no. 37, pp. 22315–22320, Sep. 1996, doi: 10.1074/jbc.271.37.22315.

[296] L. M. Stuart *et al.*, 'CD36 Signals to the Actin Cytoskeleton and Regulates Microglial Migration via a p130Cas Complex', *Journal of Biological Chemistry*, vol. 282, no. 37, pp. 27392–27401, Sep. 2007, doi: 10.1074/jbc.M702887200.

[297] I. Zani *et al.*, 'Scavenger Receptor Structure and Function in Health and Disease', *Cells*, vol. 4, no. 2, pp. 178–201, May 2015, doi: 10.3390/cells4020178.

[298] J. Furusawa *et al.*, 'Promotion of Expansion and Differentiation of Hematopoietic Stem Cells by Interleukin-27 into Myeloid Progenitors to Control Infection in Emergency Myelopoiesis', *PLoS Pathog*, vol. 12, no. 3, p. e1005507, Mar. 2016, doi: 10.1371/journal.ppat.1005507.

[299] T. Su *et al.*, 'Apigenin inhibits STAT3/CD36 signaling axis and reduces visceral obesity', *Pharmacol Res*, vol. 152, p. 104586, Feb. 2020, doi: 10.1016/j.phrs.2019.104586.

[300] K. M. Wilburn, R. A. Fieweger, and B. C. VanderVen, 'Cholesterol and fatty acids grease the wheels of Mycobacterium tuberculosis pathogenesis', *Pathog Dis*, vol. 76, no. 2, Mar. 2018, doi: 10.1093/femspd/fty021.

[301] P. Agarwal, S. Gordon, and F. O. Martinez, 'Foam Cell Macrophages in Tuberculosis', *Front Immunol*, vol. 12, Dec. 2021, doi: 10.3389/fimmu.2021.775326.

[302] W. Lee, B. C. VanderVen, R. J. Fahey, and D. G. Russell, 'Intracellular Mycobacterium tuberculosis Exploits Host-derived Fatty Acids to Limit Metabolic Stress', *Journal of Biological Chemistry*, vol. 288, no. 10, pp. 6788–6800, Mar. 2013, doi: 10.1074/jbc.M112.445056.

[303] D. G. Russell, P.-J. Cardona, M.-J. Kim, S. Allain, and F. Altare, 'Foamy macrophages and the progression of the human tuberculosis granuloma', *Nat Immunol*, vol. 10, no. 9, pp. 943–948, Sep. 2009, doi: 10.1038/ni.1781.

[304] P. Chandra *et al.*, 'Inhibition of Fatty Acid Oxidation Promotes Macrophage Control of Mycobacterium tuberculosis', *mBio*, vol. 11, no. 4, Aug. 2020, doi: 10.1128/mBio.01139-20.

[305] L. V. Kovtonyuk *et al.*, 'IL-1 mediates microbiome-induced inflammaging of hematopoietic stem cells in mice', *Blood*, vol. 139, no. 1, pp. 44–58, Jan. 2022, doi: 10.1182/blood.2021011570.

[306] L. V. Kovtonyuk, K. Fritsch, X. Feng, M. G. Manz, and H. Takizawa, 'Inflamm-Aging of Hematopoiesis, Hematopoietic Stem Cells, and the Bone Marrow Microenvironment', *Front Immunol*, vol. 7, Nov. 2016, doi: 10.3389/fimmu.2016.00502.

[307] M. ROSENDAAL, G. S. HODGSON, and T. R. BRADLEY, 'Haemopoietic stem cells are organised for use on the basis of their generation-age', *Nature*, vol. 264, no. 5581, pp. 68–69, Nov. 1976, doi: 10.1038/264068a0.

[308] D. Zhong *et al.*, 'The microbiota regulates hematopoietic stem and progenitor cell development by mediating inflammatory signals in the niche', *Cell Rep*, vol. 42, no. 2, p. 112116, Feb. 2023, doi: 10.1016/j.celrep.2023.112116.

[309] D. Zhang *et al.*, 'The microbiota regulates hematopoietic stem cell fate decisions by controlling iron availability in bone marrow', *Cell Stem Cell*, vol. 29, no. 2, pp. 232-247.e7, Feb. 2022, doi: 10.1016/j.stem.2021.12.009.

[310] K. Y. King and M. A. Goodell, 'Inflammatory modulation of HSCs: Viewing the HSC as a foundation for the immune response', Oct. 2011. doi: 10.1038/nri3062.

[311] Y. Nagai *et al.*, 'Toll-like Receptors on Hematopoietic Progenitor Cells Stimulate Innate Immune System Replenishment', *Immunity*, vol. 24, no. 6, pp. 801–812, Jun. 2006, doi: 10.1016/j.immuni.2006.04.008.

[312] D. A. Monlish, S. T. Bhatt, and L. G. Schuettpelz, 'The role of toll-like receptors in hematopoietic malignancies', Sep. 28, 2016, *Frontiers Media S.A.* doi: 10.3389/fimmu.2016.00390.

[313] J. Kleinnijenhuis, M. Oosting, L. A. B. Joosten, M. G. Netea, and R. Van Crevel, 'Innate Immune Recognition of Mycobacterium tuberculosis', *Clin Dev Immunol*, vol. 2011, pp. 1–12, 2011, doi: 10.1155/2011/405310.

[314] I. C. Macaulay *et al.*, 'Single-Cell RNA-Sequencing Reveals a Continuous Spectrum of Differentiation in Hematopoietic Cells', *Cell Rep*, vol. 14, no. 4, pp. 966–977, Feb. 2016, doi: 10.1016/j.celrep.2015.12.082.

[315] M. Feuerer *et al.*, 'Bone marrow as a priming site for T-cell responses to blood-borne antigen', *Nat Med*, vol. 9, no. 9, pp. 1151–1157, Sep. 2003, doi: 10.1038/nm914.

[316] B. J. Hunt, V. Andrews, and K. W. Pettingale, 'The significance of pancytopenia in miliary tuberculosis', *Postgrad Med J*, vol. 63, no. 743, pp. 801–804, Sep. 1987, doi: 10.1136/pgmj.63.743.801.

[317] M. Divangahi *et al.*, 'NOD2-Deficient Mice Have Impaired Resistance to Mycobacterium tuberculosis Infection through Defective Innate and Adaptive Immunity', *The Journal of Immunology*, vol. 181, no. 10, pp. 7157–7165, Nov. 2008, doi: 10.4049/jimmunol.181.10.7157.

[318] F. Altare *et al.*, 'Impairment of Mycobacterial Immunity in Human Interleukin-12 Receptor Deficiency', *Science (1979)*, vol. 280, no. 5368, pp. 1432–1435, May 1998, doi: 10.1126/science.280.5368.1432.

[319] J. A. Vázquez-Boland *et al.*, 'Listeria pathogenesis and molecular virulence determinants', 2001. doi: 10.1128/CMR.14.3.584-640.2001.

[320] S. S. Ahuja, M. R. Brown, T. A. Fleisher, S. K. Ahuja, and H. L. Malech, 'Autocrine activation of hemopoietic progenitor-derived myelo-monocytic cells by IFN-gamma gene transfer.', *The Journal of Immunology*, vol. 156, no. 11, pp. 4345–4353, Jun. 1996, doi: 10.4049/jimmunol.156.11.4345.

[321] O. F. Join-Lambert *et al.*, 'Listeria monocytogenes-infected bone marrow myeloid cells promote bacterial invasion of the central nervous system', *Cell Microbiol*, vol. 7, no. 2, pp. 167–180, Feb. 2005, doi: 10.1111/j.1462-5822.2004.00444.x.

[322] C. Gutiérrez-Jiménez *et al.*, 'Persistence of brucella abortus in the bone marrow of infected mice', *J Immunol Res*, vol. 2018, 2018, doi: 10.1155/2018/5370414.

[323] M. R. Hasanjani Roushan, Z. Moulana, Z. Mohseni Afshar, and S. Ebrahimpour, 'Risk Factors for Relapse of Human Brucellosis', *Glob J Health Sci*, vol. 8, no. 7, pp. 77–82, Nov. 2015, doi: 10.5539/gjhs.v8n7p77.

[324] Ö. Ögredici *et al.*, 'Brucellosis reactivation after 28 years', Dec. 2010. doi: 10.3201/eid1612.100678.

[325] B. J. Farooqui, M. Khurshid, M. K. Ashfaq, M. Ata Khan, U. Hospital, and P. B. J Farooqui, 'Comparative yield of Salmonella typhi from blood and bone marrow cultures in patients with fever of unknown origin', *J Clin Pathol*, vol. 44, no. 3, pp. 258–259, 1991, doi: 10.1136/jcp.44.3.258.

[326] D. Castro-Eguiluz, R. Pelayo, V. Rosales-Garcia, R. Rosales-Reyes, C. Alpuche-Aranda, and V. Ortiz-Navarrete, 'B cell precursors are targets for Salmonella infection', *Microb Pathog*, vol. 47, no. 1, pp. 52–56, 2009, doi: 10.1016/j.micpath.2009.04.005.

[327] L. Dirkx *et al.*, 'Long-term hematopoietic stem cells as a parasite niche during treatment failure in visceral leishmaniasis', *Commun Biol*, vol. 5, no. 1, Dec. 2022, doi: 10.1038/s42003-022-03591-7.

[328] C. S. Lopes, N. Daifalla, B. Das, V. D. Da Silva, and A. Campos-Neto, 'CD271+ mesenchymal stem cells as a possible infectious niche for leishmania infantum', *PLoS One*, vol. 11, no. 9, Sep. 2016, doi: 10.1371/journal.pone.0162927.

[329] A. M. Mirkovich, A. Galelli, A. C. Allison, and F. Z. Modabber, 'Increased myelopoiesis during Leishmania major infection in mice: generation of "safe targets", a possible way to evade the effector immune mechanism.', *Clin Exp Immunol*, vol. 64, no. 1, pp. 1–7, Apr. 1986.

[330] C. Rodríguez-Echeverri, B. L. Gómez, and Á. González, 'Histoplasma capsulatum Activates Hematopoietic Stem Cells and Their Progenitors through a Mechanism Dependent on TLR2, TLR4, and Dectin-1', *Journal of Fungi*, vol. 8, no. 10, Oct. 2022, doi: 10.3390/jof8101108.

[331] C. Rodríguez-Echeverri, B. L. Gómez, and Á. González, 'Histoplasma capsulatum modulates the immune response, affects proliferation and differentiation, and induces apoptosis of mesenchymal stromal cells', *Mycoses*, vol. 66, no. 2, pp. 157–167, Feb. 2023, doi: 10.1111/myc.13537.

[332] C. Rodriguez-Echeverri, J. D. Puerta-Arias, and Á. González, 'Paracoccidioides brasiliensisactivates mesenchymal stem cells through TLR2, TLR4, and Dectin-1', *Med Mycol*, vol. 59, no. 2, pp. 149–157, Feb. 2021, doi: 10.1093/mmy/myaa039.

[333] C. F. Mu *et al.*, 'Targeted drug delivery for tumor therapy inside the bone marrow', *Biomaterials*, vol. 155, pp. 191–202, 2018, doi: 10.1016/j.biomaterials.2017.11.029.

[334] M. Zhao *et al.*, 'N-Cadherin-Expressing Bone and Marrow Stromal Progenitor Cells Maintain Reserve Hematopoietic Stem Cells', *Cell Rep.*, vol. 26, no. 3, pp. 652–669, 2019, doi: 10.1016/j.celrep.2018.12.093.N-Cadherin-Expressing.

[335] A. Verma, A. Ghoshal, V. P. Dwivedi, and A. Bhaskar, 'Tuberculosis: The success tale of less explored dormant Mycobacterium tuberculosis', *Front Cell Infect Microbiol*, vol. 12, Dec. 2022, doi: 10.3389/fcimb.2022.1079569.

[336] W. Shi *et al.*, 'Pyrazinamide Inhibits Trans-Translation in Mycobacterium tuberculosis', *Science (1979)*, vol. 333, no. 6049, pp. 1630–1632, Sep. 2011, doi: 10.1126/science.1208813.

[337] K. D. Bunting, 'ABC Transporters as Phenotypic Markers and Functional Regulators of Stem Cells', *Stem Cells*, vol. 20, no. 1, pp. 11–20, 2002.

[338] F. Tzelepis *et al.*, 'Mitochondrial cyclophilin D regulates T cell metabolic responses and disease tolerance to tuberculosis', *Sci Immunol*, vol. 3, no. 23, May 2018, doi: 10.1126/sciimmunol.aar4135.

[339] H. Takizawa, S. Boettcher, and M. G. Manz, 'Demand-adapted regulation of early hematopoiesis in infection and inflammation', *Blood*, vol. 119, no. 13, pp. 2991–3002, 2012, doi: 10.1182/blood-2011-12.

[340] A. I. Pinto, N. Brown, O. Preham, J. S. P. Doehl, H. Ashwin, and P. M. Kaye, 'TNF signalling drives expansion of bone marrow CD4+ T cells responsible for HSC exhaustion in experimental visceral leishmaniasis', *PLoS Pathog*, vol. 13, no. 7, p. e1006465, Jul. 2017, doi: 10.1371/journal.ppat.1006465.

[341] K. A. Matatall *et al.*, 'Chronic Infection Depletes Hematopoietic Stem Cells through Stress-Induced Terminal Differentiation', *Cell Rep*, vol. 17, no. 10, pp. 2584–2595, Dec. 2016, doi: 10.1016/j.celrep.2016.11.031.

[342] J. Wang, M. Erlacher, and J. Fernandez-Orth, 'The role of inflammation in hematopoiesis and bone marrow failure: What can we learn from mouse models?', *Front Immunol*, vol. 13, Aug. 2022, doi: 10.3389/fimmu.2022.951937.

[343] M. A. Goodell, K. Brose, G. Paradis, A. S. Conner, and R. C. Mulligan, 'Isolation and functional properties of murine hematopoietic stem cells that are replicating in vivo', *J Exp Med*, vol. 183, no. 4, pp. 1797–806, 1996, doi: 10.1084/jem.183.4.1797.

[344] S. Zhou *et al.*, 'The ABC transporter Bcrp1/ABCG2 is expressed in a wide variety of stem cells and is a molecular determinant of the side-population phenotype', *Nat Med*, vol. 7, no. 9, 2001, doi: 10.1038/nm0901-1028.

[345] N. Ganguly, I. Siddiqui, and P. Sharma, 'Role of M. tuberculosis RD-1 region encoded secretory proteins in protective response and virulence', *Tuberculosis*, vol. 88, no. 6, pp. 510–517, Nov. 2008, doi: 10.1016/j.tube.2008.05.002.

[346] J. A. Awuh and T. H. Flo, 'Molecular basis of mycobacterial survival in macrophages', *Cellular and Molecular Life Sciences*, vol. 74, no. 9, pp. 1625–1648, May 2017, doi: 10.1007/s00018-016-2422-8.

[347] J. Fujisaki *et al.*, 'In vivo imaging of T reg cells providing immune privilege to the haematopoietic stem-cell niche', *Nature*, vol. 474, no. 7350, pp. 216–220, Jun. 2011, doi: 10.1038/nature10160.

[348] L. Zou *et al.*, 'Bone marrow is a reservoir for CD4+CD25+ regulatory T cells that traffic through CXCL12/CXCR4 signals', *Cancer Res*, vol. 64, no. 22, pp. 8451–8455, 2004, doi: 10.1158/0008-5472.CAN-04-1987.

[349] J. Fujisaki *et al.*, 'In vivo imaging of Tregs providing immune privilege to the hematopoietic stem cell nice', *Nature*, vol. 474, no. 7350, pp. 216–219, 2011, doi: 10.1038/jid.2014.371.

[350] P. Hernández-Malmierca *et al.*, 'Antigen presentation safeguards the integrity of the hematopoietic stem cell pool', *Cell Stem Cell*, vol. 29, no. 5, pp. 760-775.e10, 2022, doi: 10.1016/j.stem.2022.04.007.

List of Figures

List of Tables

Supplements

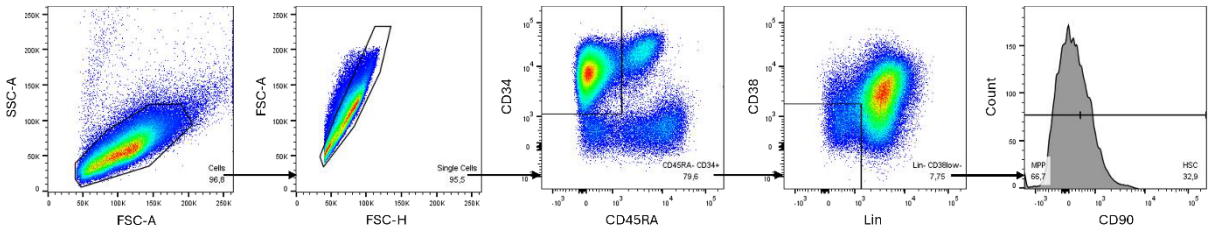

Figure S1: Sorting of human Hematopoietic Stem Cells for Confocal Laser Scanning Microscopy. Hematopoietic progenitor cell cultures from human peripheral blood were infected with *M. tuberculosis* H37Rv DsRed at a MOI of 10. 20 hours post-infection immunofluorescence staining for surface antigens was performed and HSCs were sorted. Cells are gated in FSC-A against SSC-A. Following doublet-exclusion using FSC-H against FSC-A. Human HSCs are identified as $CD34^+$ $CD45RA^-$ Lin^- $CD38^{-/low}$ $CD90^+$ cells. Human MPPs are identified as $CD34^+$ $CD45RA^-$ Lin^- $CD38^{-/low}$ $CD90^-$ cells.

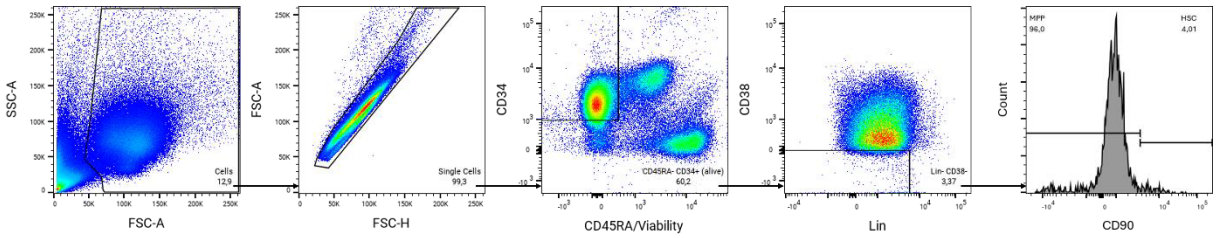

Figure S2: Representative gating scheme to immunophenotypically identify viable human hematopoietic stem cells and multilineage potential progenitors. Cells are gated in FSC-A against SSC-A. Following doublet-exclusion using FSC-H against FSC-A, human HSCs are identified as $CD34^+$ $CD45RA^-$ Live/$Dead^-$ Lin^- $CD38^{-/low}$ $CD90^+$ cells. Human MPPs are identified as $CD34^+$ $CD45RA^-$ Live/$Dead^-$ Lin^- $CD38^{-/low}$ $CD90^-$ cells. Representative gating is shown for a $CD34^+$-enriched human peripheral blood culture after 20 hours of incubation.

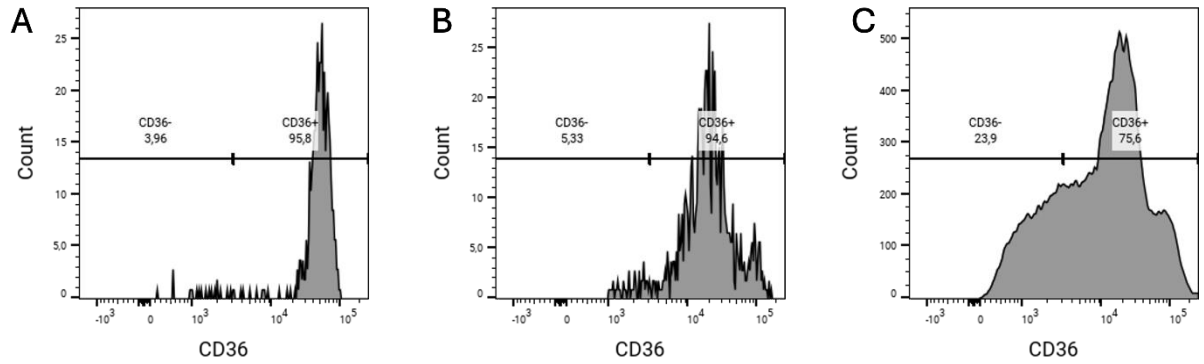

Figure S3: Representative FACS plots to immunophenotypically identify $CD36^+$ HSCs. Human HSCs are identified as $CD34^+$ $CD45RA^-$ Live/$Dead^-$ Lin^- $CD38^{-/low}$ $CD90^+$ cells. Human MPPs are identified as $CD34^+$ $CD45RA^-$ Live/$Dead^-$ Lin^- $CD38^{-/low}$ $CD90^-$ cells. Subpopulations of $CD36^+$ HSCs **(A)** and $CD36^+$ MPPs **(B)** are identified by CD36-FITC fluorescence. **C)** Frequency of all $CD36^+$ cells in the cell culture. Representative gating is shown for a $CD34^+$-enriched human peripheral blood culture after 20 hours of incubation.

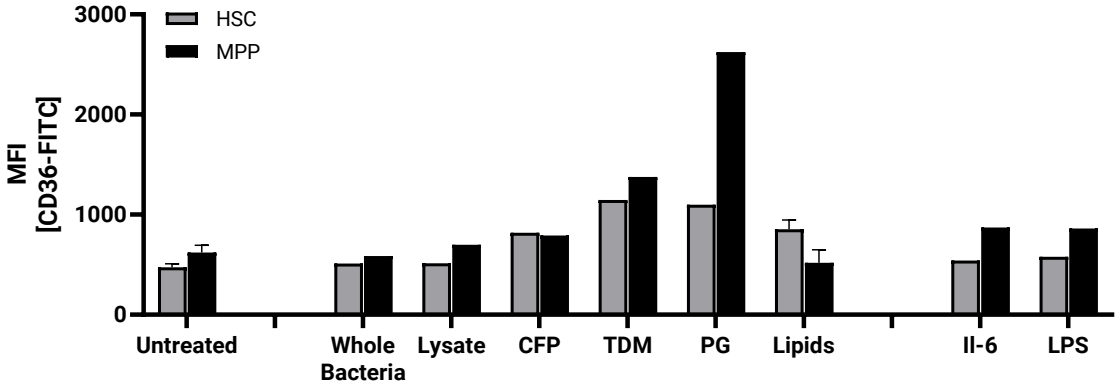

Figure S4: Surface expression of the class B type scavenger receptor CD36 by Hematopoietic Stem Cells from low-baseline donors in response to *M. tuberculosis*-derived pathogen-associated molecular patterns in vitro. Peripheral blood cells from adult human donors were collected and $CD34^+$-cells were enriched. Progenitor-enriched cultures were incubated *M. tuberculosis* H37Rv-derived pathogen-associated molecular patterns for 20 hours: Whole bacteria = γ-irradiated *M. tuberculosis* [20 µg/mL]; Lysate = Whole cell cysates [20 µg/mL]; CFP = Culture filtrate protein [20 µg/mL]; TDM = Trehalose dimycolate [20 µg/mL]; PG = Peptidoglycan [20 µg/mL]; Lipids = Lipids [20 µg/mL]; IL-6 = Interleukin-6 [200 ng/mL]; LPS = Lipopolysaccharide (from *S. Minnesota* R595) [100 ng/mL]. The mean fluorescence intensity (MFI) of CD36-FITC, was quantified using FACS (HSC: $CD34^+$ $CD45RA^-$ Lin^- $CD38^{-/low}$ $CD90^+$; MPP: $CD34^+$ $CD45RA^-$ Lin^- $CD38^{-/low}$ $CD90^-$). Donors were stratified into two subgroups based on the ratio of $CD36^+$ hematopoietic stem cells in untreated samples by k-means clustering (k = 2). Only donors of the identified low-baseline expression group were analyzed. Bars represent the mean ± SD [n=3]. Statistical significance is determined by paired one-tailed t-test. Asterisks indicate p-values (*$p \leq 0.05$; ns $p > 0.05$).

Publications and Presentations

Publications:

Engling P, Schaible UE. **"Hematopoietic Stem Cells as a Niche for *Mycobacterium tuberculosis*: Mechanisms of Internalization and Permissiveness"**. *(Manuscript in preparation)*

Engling P, Schaible UE. "**The Role of the Bone Marrow in Immunity and Infection"**. *(Manuscript in preparation)*

Presentations at conferences:

Engling P, Dallenga T, Linnemann L, Behrends J, Shouxiong H, Hildeman DA, Schaible UE. **"Immune Modulation by Mycobacteria-infected Myeloid Cells in Infection and Immunization"**. 10th BBRS Retreat. Ammersbek, Germany 23.-24.9.2019. *(oral)*

Engling P, Dallenga T, Linnemann L, Behrends J, Shouxiong H, Hildeman DA, Schaible UE. **"Immune Modulation by Mycobacteria-infected Myeloid Cells in Infection and Immunization"**. 11th DGFI Autumn School "Current Concepts in Immunology". Merseburg, Germany, 13.-19.10.2019. *(poster)*

Engling P, Dallenga T, Linnemann L, Behrends J, Shouxiong H, Hildeman DA, Schaible UE. **"Immune Modulation by Mycobacteria-infected Myeloid Cells in Infection and Immunization"**. IRTG1911 Retreat. Heiligenhafen, Germany 23.-24.10.2019. *(oral)*

Engling P, Melchers GF, Hildeman DA, Schaible EU. **"The Stem Cell Niche of *Mycobacterium tuberculosis*"**. 11th BBRS Retreat. Ammersbek, Germany 17-18.8.2020. *(oral)*

Engling P, Melchers GF, Hildeman DA, Schaible EU. **"The Stem Cell Niche of *Mycobacterium tuberculosis*"**. IRTG Virtual Retreat. 15.10.2020. (talk)

Engling P, Melchers GF, Schaible EU. **"Invading the Birthplace of our Immune System – The Stem Cell Niche of *Mycobacterium tuberculosis*"**. LCI Summer school: "Molecular biology of pathogens". 3.-4.6.2021. *(oral – awarded for best talk)*

Engling P, Melchers GF, Schaible EU. **"Invading the Birthplace of our Immune System – The Stem Cell Niche of *Mycobacterium tuberculosis*"**. 12th BBRS Retreat. Ammersbek, Germany 28.-29.9.2021. *(oral)*

Engling P, Melchers GF, Schaible UE. **"The Stem Cell Niche of *Mycobacterium tuberculosis* – At the birthplace of our immune system –"**. NDI3: "New Developments in Immunology, Inflammation, and Infection". Borstel, Germany, 11.-12.11.2021. *(poster)*

Engling P, Melchers GF, Schaible EU. **"The Stem Cell Niche of *Mycobacterium tuberculosis* – At the birthplace of our immune system –"**. DGI-DZIF Joint Annual Meeting. Stuttgart, Germany, 1.-3.6.2022. *(poster)*

Engling P, Melchers GF, Schaible EU. **"The Stem Cell Niche of *Mycobacterium tuberculosis* – At the birthplace of our immune system –"**. ESM 42nd Annual Congress. Bologna, Italy, 26.-29.6.2022 *(poster)*

Engling P, Hildeman DA, Schaible EU. **"The Role of Hematopoietic Stem Cells in the Latency of Tuberculosis"**. Annual Immunology Retreat 2022. College Corner, OH, USA. 6.-7.10.2022. *(oral)*

Engling P, Hildeman DA, Schaible UE. **„Hijacking the Host: The Role of Hematopoietic Stem Cell Infection in the Latency of Tuberculosis"**. Keystone symposium: "Tuberculosis: The Host-Pathogen Interface". Keystone, CO, USA, 24.-27.3.2024. *(poster)*

Acknowledgments

First and foremost, I want to express my gratitude towards my supervisor **Prof. Dr. Ulrich. E. Schaible** for giving me the opportunity to perform my research in his group. His knowledge, guidance, support and trust have been invaluable during my Ph.D. and even more so during the writing process of this thesis. Being available for advice and discussions at any time while supporting the development and pursuit of one's owns ideas, provided the perfect foundation for future projects and a personal future in academia. Both personally and professionally, I regard myself lucky for having had such a great mentor over the last years.

I also want to thank my co-supervisors **Dr. Christoph Hölscher PD** and **Prof. Dr. David A. Hildeman**, for sharing their valuable advice and expertise during our thesis committee meetings. I deeply appreciate the opportunity to perform parts of my research project in Prof. Hildeman's group at the Cincinnati Children's Hospital Medical Center. Not only did this directly connect me with cutting-edge research in the field but also broadened my horizon regarding cultural differences related to working atmosphere and leadership that I hope to assimilate and apply by myself in the future.

I am also grateful to **Jacqueline Eich**, **Kristine Hagens** and **Dr. Lara Linnemann** for their training, assistance, patience and time, especially in the initial phase of my Ph.D. Furthermore, I want to thank Jacqueline Eich and Kristine Hagens for their continuous efforts to keep the laboratory running. Special thanks also go to the whole Hildeman Lab, and especially to **Autumn Ferguson**, **Dr. Ashley Burg** and **Dr. Tiffany Shi** for their practical support and training during my research stay at the CCHMC. Lastly, I want to thank **Prof. Dr. Daniel Lucas** and **Dr. Yanan Sophia Zhang** for sharing their expertise on whole-mount bone marrow microscopy.

I would like to express my appreciation to everyone who still is or was a member of the **Cellular Microbiology** group during my Ph.D. This includes **Jacqueline Eich**, **Kristine Hagens**, **Dörte Grella**, **Ann-Kathrin Lemm**, **Dagmar Meyer**, **Manuel Hein**, **Dr. Tobias Dallenga**, **Dr. Matthias Hauptmann**, **Dr. Natalja Redinger**, **Dr. Uwe Mamat**, **Dr. Christian Alexander**, **Dr. Jessica Ebot-Otang Akoh-Arrey**, **Dr. Lara Linnemann**, **Christoph Leschczyk**, **Claire S. Taylor**, **Celina Prosch**, **Benthe Beu**, **Karen Sichibalo**, **Hawanot Olaitan Tijani** and all the master students and trainees. I am thankful for the great working

environment, the input and discussions in our lab meetings and the funny conversations during centrifugation and incubation periods.

I also want to express my gratitude towards **Prof. Dr. Georg F. Melchers**, **Dr. Peter K. Jani**, **Dr. Pawel Durek** and **Dr. Norbert Reiling PD** for their thought-provoking ideas and recommendations whenever we had discussions about my ongoing research.

I would like to acknowledge the core facilities at the RCB and the CCHMC involved in the acquisition of the presented data. All flow cytometric data were acquired using equipment maintained by either the **Fluorescence Cytometry** facility at the RCB or by the **Research Flow Cytometry Facility** in the Division of Rheumatology at the CCHMC. All microscopic data were acquired using equipment maintained by either the **Fluorescence Cytometry** facility at the RCB or the **Confocal Imaging Core** at CCHMC. Lastly, I want to thank the **animal core facilities** at the RCB and the CCHMC for their support in all animal-experimental work.

I want to thank all volunteers who donated blood for the conducted experiments and especially **Franziska Daduna-Thiessen** for overseeing the blood donation service, as none of the human primary data would have been acquired without them. I am also grateful for the cooperation with **Dr. Verena Boßung PD** and the clinic for gynecology and obstetrics at the university hospital Schleswig-Holstein, in planning and conducting the clinical study on neonatal umbilical cord blood.

I also want to acknowledge the main funding body of this research, namely the DFG for funding the international research training group 1911 **(IRTG1911)**, 'Immune regulation of inflammation in allergy and infection'. This work was also in part supported by the Leibniz Collaborative Excellence Grant **CHROQ-K121/2018**.

I want to express my deepest appreciation to my friends, **Vidhisha**, **Alejandro**, **Claire**, **Lindsay**, **Jessica**, **Emilie**, **Schmaiel**, **George**, **Thalita**, **Simon** and **Annika** for their support and motivation but also reminders to rest when necessary.

Lastly, I cannot put the love, appreciation and gratitude toward my family into words. **Frank, Tim, Jana** and **Elke**, without you I probably would have never come to write these final sentences of this thesis and I'm thankful for every single second we share. Although **Doreen** did not witness me anymore moving north to research tuberculosis, passing on the Robert Koch biography, she read as a child, makes me think she subconsciously knew it all along already. Thank you.